

# Terrapin Rocket Team Project Karkinos

## Team 127 Project Technical Report to the 2023 Spaceport America Cup

Hailu Daniel<sup>\*</sup>, Andrew Bean<sup>†</sup>, Ezra Bregin<sup>‡</sup>, Dasam Gill<sup>§</sup>, Nathan Roy<sup>¶</sup>, Khalid M Jaffar<sup>||</sup>, Garret Alessandrini<sup>\*\*</sup>,  
Michael Mallamaci<sup>††</sup>, Adin Goldberg<sup>‡‡</sup>, Howard Zheng<sup>§§</sup>, Saim Rizvi<sup>¶¶</sup>  
*University of Maryland - Department of Aerospace Engineering, College Park, MD, 20742*

**This document presents the University of Maryland’s 10,000 ft SRAD Motor Category rocket, Karkinos. It is the third time that the team will be attending the Cup in person since 2018, and the current team has built on the lessons learned at the 2022 Cup. The design process for Karkinos is centered around manufacturability and reliability coupled with a rigorous testing process. This report also documents the design of our Air Brake system that actively trims the rocket’s altitude during flight. The CubeSat payload for this rocket will test the release of a vehicle from the rocket during drogue descent.**

---

<sup>\*</sup>Team Leader, Terrapin Rocket Team.

<sup>†</sup>Chief Engineer, Terrapin Rocket Team

<sup>‡</sup>Air Brake Team Leader, Terrapin Rocket Team

<sup>§</sup>Aero-Structures Team Co-Leader, Terrapin Rocket Team

<sup>¶</sup>Payload Team Leader, Terrapin Rocket Team

<sup>||</sup>Air Brake Team Member, Terrapin Rocket Team

<sup>\*\*</sup>Air Brake Team Member, Terrapin Rocket Team

<sup>††</sup>Payload Team Member, Terrapin Rocket Team

<sup>‡‡</sup>Aero-Structures Team Member, Terrapin Rocket Team

<sup>§§</sup>Aero-Structures Team Member, Terrapin Rocket Team

<sup>¶¶</sup>Solid Propulsion Team Member, Terrapin Rocket Team

# Contents

<b>I</b>	<b>Introduction</b>	<b>6</b>
I.A	Academic Program . . . . .	6
I.B	Stakeholders . . . . .	6
I.C	Team Organization . . . . .	6
<b>II</b>	<b>System Architecture Overview</b>	<b>7</b>
II.A	Propulsion Subsystems . . . . .	11
II.A.1	Material Selection and Pressure Vessel Design . . . . .	11
II.A.2	Propellant Characterization . . . . .	15
II.A.3	Full Scale Motor Design . . . . .	17
II.A.4	Motor Manufacturing and Assembly . . . . .	18
II.A.5	Motor Test Stand . . . . .	20
II.A.6	Full Scale Motor Tests and Results . . . . .	22
II.A.7	Mixing Sessions and Motors Made . . . . .	23
II.A.8	Igniters . . . . .	23
II.B	Aero-Structures Subsystems . . . . .	24
II.B.1	Body Tubes and Couplers . . . . .	24
II.B.2	Fins . . . . .	26
II.B.3	Bulkheads . . . . .	31
II.C	Recovery Subsystems . . . . .	33
II.C.1	Recovery Devices and Shear Pins . . . . .	34
II.C.2	Flame Protection . . . . .	34
II.C.3	Recovery Harness . . . . .	35
II.C.4	Recovery Attachment . . . . .	36
II.C.5	Parachute Deployment System . . . . .	37
II.D	Avionics . . . . .	38
II.D.1	Commercial Deployment Computers and Battery Selection . . . . .	38
II.D.2	Commercial Tracking . . . . .	39
II.D.3	SRAD Avionics . . . . .	39
II.D.4	Sled and Mounting . . . . .	42
II.D.5	Avionics Testing . . . . .	43
II.E	Air Brake . . . . .	43
II.E.1	Overview . . . . .	43
II.E.2	Deployment Mechanism . . . . .	44
II.E.3	Air Brake Structure . . . . .	45
II.E.4	Avionics . . . . .	46
II.E.5	State-Estimation . . . . .	49
II.E.6	Controller Design . . . . .	56
II.E.7	Parameter Estimation . . . . .	58
II.E.8	In-Flight Tests and Validation . . . . .	59
II.E.9	Wind Tunnel . . . . .	61
II.F	Payload . . . . .	62
II.F.1	Release Mechanism . . . . .	63
II.F.2	Vehicle Design . . . . .	64
II.F.3	Payload Bay . . . . .	67
II.F.4	Payload Sizing and Mass . . . . .	68
II.G	Full-Scale Test Flights . . . . .	69

<b>III Mission Concept of Operations Overview</b>	<b>73</b>
<b>IV Conclusions and Lessons Learned</b>	<b>75</b>
<b>V Appendix A - System Weights, Measures, and Performance Data</b>	<b>76</b>
V.A Rocket Information . . . . .	76
V.B Predicted Flight Data and Analysis . . . . .	76
V.C Recovery Information . . . . .	77
V.D SRAD Components . . . . .	77
<b>VI Appendix B - Project Test Reports</b>	<b>78</b>
VI.A Recovery System Testing . . . . .	80
VI.B SRAD Propulsion Systems Testing . . . . .	93
VI.C SRAD Pressure Vessel Testing . . . . .	107
VI.D SRAD GPS Testing . . . . .	110
VI.E Payload Recovery System Testing . . . . .	120
VI.F Additional Tests . . . . .	124
<b>VII Appendix C - Hazard Analysis</b>	<b>137</b>
<b>VIII Appendix D - Risk Assessment</b>	<b>139</b>
<b>IX Appendix E - Assembly, Preflight, and Launch Checklists and Procedures</b>	<b>141</b>
<b>X Appendix F - Engineering Drawings</b>	<b>155</b>

## Nomenclature

ABS	Acrylonitrile Butadiene Styrene
CAD	Computer-Aided Design
CFD	Computational Fluid Dynamics
$C_G$	Center of Gravity
CNC	Computer Numerical Control
COTS	Commercial of the Shelf
CP	Center of Pressure
CSV	Comma-separated Values
D	Drag
FEA	Finite Element Analysis
GNSS	Global Navigation Satellite System
GPS	Global Positioning System
GUI	Graphical User Interface
HTPB	Hydroxyl-terminated polybutadiene
I2C	Inter-Integrated Circuit
ID	Inner Diameter
IMU	Inertial Measurement Unit
L/D	Length to Diameter
MDI	Methane Diisocyanate
MDRA	Maryland Delaware Rocketry Association
MEMS	Micro-electro-mechanical Sensors
MPC	Model Predictive Control
OD	Outer Diameter
OLED	Organic Light-Emitting Diode
PCB	Printed Circuit Board
PETG	Polyethylene Terephthalate Glycol
PID	Proportional–Integral–Derivative
PLA	Polylactic Acid
PSRAM	Pseudostatic (Random-Access) Memory
SAC	Spaceport America Cup
SF	Safety Factor
SPI	Serial Peripheral Interface
TWR	Thrust-Weight Ratio
USB	Universal Serial Bus
M	Mach
SRAD	Student Researched and Developed
T	Thrust
UMD	University of Maryland
$g$	Gravitational Acceleration

SF	Safety Factor
$C_p$	Center of Pressure
$C_G$	Center of Gravity
$P_{max}$	Max Operating Pressure
$\sigma$	Stress
$\tau_s$	Shear Stress
$K_n$	Burning Surface Area/Nozzle Throat Area
$P_c$	Chamber Pressure
$C^*$	Characteristic Velocity
$\rho$	Density
$T_s$	Sampling Time
$g_i$	Turn Rate Along Axis $i$
$\alpha$	Tilt Off Vertical Axis
$h$	Height
$v$	Velocity
$\delta$	Flap Deployment Angle
$v_\infty$	Far Field Velocity
$\tau$	Time Constant
$Cd_f$	Coefficient of Drag Of A Flap
$Cd_R$	Coefficient of Drag Of The Rocket Body
$A_f$	Reference Area of a Flap
$A_R$	Reference Area of the Rocket Body
$Q$	Process Covariance Matrix
$F$	State Transition Matrix
$\mathcal{P}(h, v, \alpha, \delta)$	Apogee Predict Function
$R^2$	Coefficient of Determination

## **I. Introduction**

### **A. Academic Program**

The Terrapin Rocket Team is a student organization at the University of Maryland, College Park. The team was established with the goal of providing students hands-on opportunities to learn about rocketry, and to gain experience designing, manufacturing, and testing engineering projects. The team is made up of over 50 undergraduate and 5 graduate members across many disciplines such as Aerospace Engineering, Mechanical Engineering, Computer Science, and Physics. While this team is comprised of several different academic backgrounds, the club is sponsored by the A. James Clark School of Engineering - Department of Aerospace Engineering under the advisement of Dr. Christopher Cadou.

### **B. Stakeholders**

There are two main types of stakeholders for our project - academic and professional. The academic stakeholders are mostly engaged with the development of the team, the members, and the team's reputation. These individuals, with their more complete understanding of rocketry, assist the team through hours of mentorship and explanation of complex topics. These individuals are the ones who provided us the critical feedback during our design reviews and assisted in developing new skills to better design our project. One of the most valuable of these mentors was our Tripoli advisor and President of the Maryland Delaware Rocketry Association (MDRA), Dennis Kingsley, who has been working with the team for the last three years and has been monumental in our success. Scott Szympruch, the former MDRA prefect, has acted as our Solid Propulsion mentor for the Solids Subteam. Additionally, our academic advisor, Dr. Christopher Cadou, has been instrumental in our team's success.

Our professional stakeholders have been those that have helped to ensure our continued success. Their support and engagement are in the form of donations and access to engineering software. These include the A. James Clark School of Engineering, The University of Maryland Student Government Association, Maryland Space Grant Consortium, The Maryland Robotics Center, Glenn L. Martin Wind Tunnel, Boeing, Northrop Grumman, Kratos Space and Missile Defense Systems, Inc., and Blue Origin.

### **C. Team Organization**

TerpRockets is a rocket organization that promotes rocketry and engineering principles. One of the ways we accomplish these goals is by participating in the SAC. The executive board of TerpRockets oversees all of TerpRockets' activities including the hands-on involvement of the SAC team. This team was partitioned into the natural subteams: Aerostructures, Air Brakes, Solids, Recovery, Avionics, and Payload. Aerostructures was tasked with the design, testing, and fabrication of the main rocket body as well as all subsystems not covered by recovery or payload. Air Brakes designed, tested, and manufactured the Air Brake Module. Our Solids Subteam designed and fabricated the solid rocket motor for Karkinos. The Recovery Subteam took responsibility for designing our recovery system and commercial avionics. Avionics developed an SRAD flight computer that behaves as a data logger and broadcasts telemetry. The Payload team was tasked with the design, testing, and fabrication of the payload for Karkinos.

During the 2022-2023 season, we approached SAC 2023 with the goal of flying early and often. This meant following previously proven rocketry techniques and modifying them accordingly for Karkinos. To delegate the workload and ensure rapid testing and flying, we developed a separation between competition-critical systems and non-critical systems for the subteams. A SAC team focused on building and prepping Karkinos for early flights had the ability to work on the competition rocket without relying on the finalized sub-systems. The full breakdown of the team can be shown in Fig. 1.

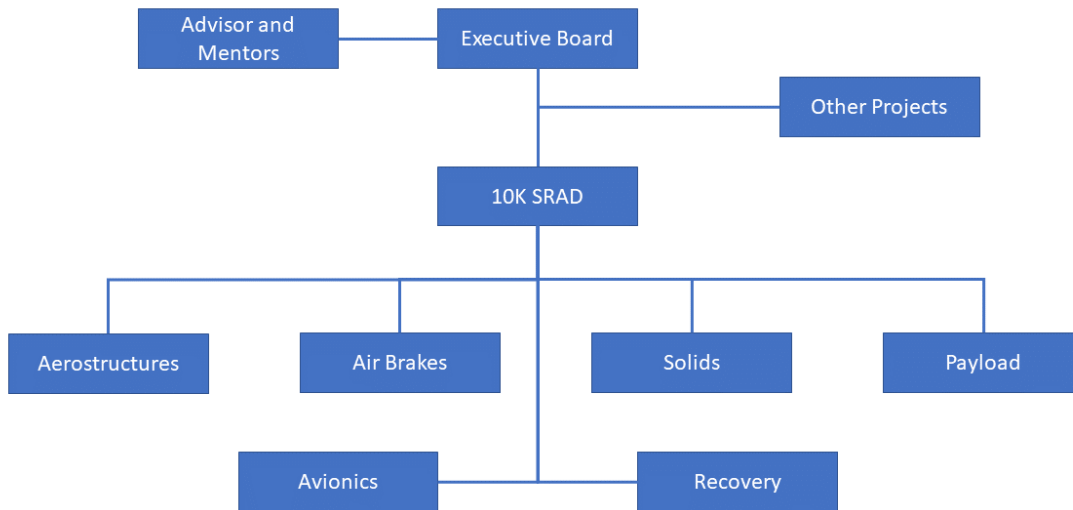


**Fig. 1 Team organization**

## II. System Architecture Overview

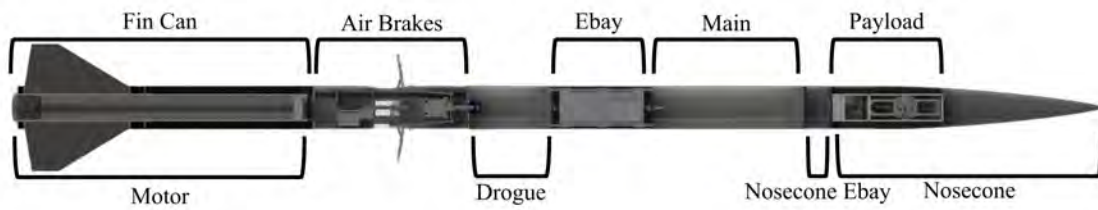


**Fig. 2 Karkinos layout**

Karkinos is composed of 6 separate subsystems: Propulsion, Aerostructures, Air Brake, Avionics, Recovery/Tracking, and Payload. The propulsion subsystem is an SRAD solid rocket motor made by the team. It is a 98 mm motor with approximately 37" of propellant length and 11,500 N-s of impulse designed to take Karkinos to 10,000ft. The Aerostructures subsystem is responsible for the air frame and structural components of the rocket including the fin can, drogue tube, main tube, electronics bays, and nosecone. All external air frames except for the nosecone were made by students from either carbon fiber or fiberglass. Next, the Air Brake system sits directly above the fin can and is designed to trim the rocket's flight to a precise altitude. A variety of sensors onboard allow it to control when to deploy flaps into the air stream to induce drag and slow down the rocket. The SRAD avionics system is within the primary electronics bay and is a custom flight computer collecting data and sending it back to the ground. While it is not deploying any charges, it can transmit the status and location of the rocket to a ground station. Also in the avionics bay are the commercial recovery electronics and GPS trackers. This consists of two Altus Metrum EasyMinis, a Featherweight GPS, and AltusMetrum TeleGPS. Karkinos is a dual break - dual deploy rocket with the drogue parachute directly aft of the electronics bay and the main parachute forward of it. The drogue is deployed at apogee and the main is deployed at 1,000 ft during descent. Directly below the nosecone is a secondary electronics bay with a single

EasyMini and an Eggtimer Wifi Switch. This deploys the nosecone at a set altitude to allow the payload to deploy. The payload is on the top nosecone electronics bay bulkhead and is split up into two sections, a vehicle, and a vehicle release mechanism. The release mechanism is made of an aluminum frame and holds the vehicle during ascent. Once the nosecone is ejected and the release mechanism detects light, the vehicle is pushed out and recovers separately. The vehicle will attempt to control its descent using a flat parachute and moving the shroud lines. The vehicle performance parameters for Karkinos can be found in Table 2. The motor being used for Karkinos is an SRAD 98 mm N2500. Details

**Table 2 Vehicle Parameters**

Predicted Apogee (ft)	10,969
Total Impulse (N-s)	11,548
Peak Thrust (N)	3,620
Takeoff Mass (lb)	82
Takeoff TWR	9.6
Velocity off Rail (ft/s)	92
Max. Velocity (ft/s)	890
Max. Acceleration (g)	9.4
Stability Margin (Calibers)	2.75

about the performance of the motor are listed in Fig. 3 and Table. 3 and further discussed in the propulsion subsection.

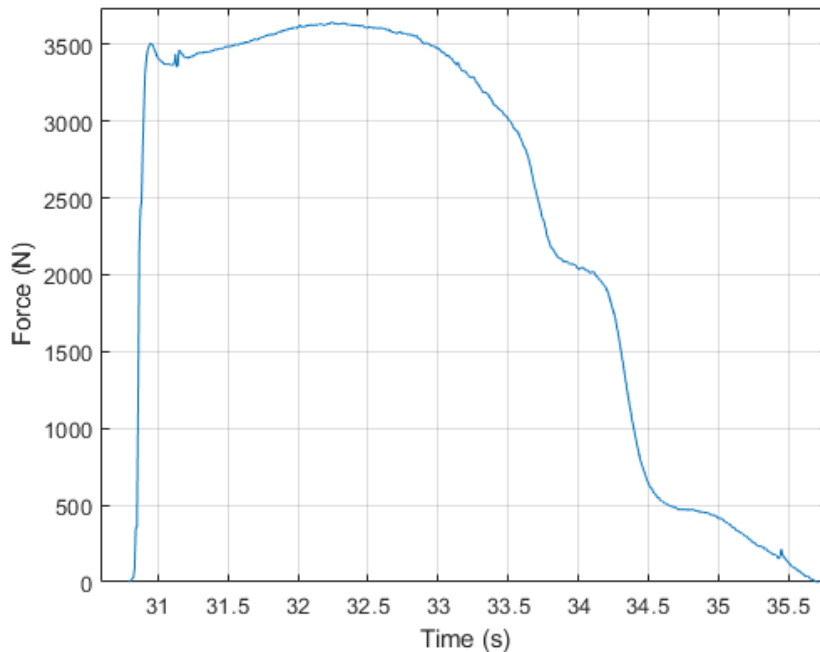


**Fig. 3 TRT N2500 motor characteristics**

**Flight Simulations** Karkinos was primarily simulated in OpenRocket. This program gives us an easy way to design our rocket before detailed design in CAD. It also lets us get fairly accurate weight estimates before building anything, which is important for designing our motor. The base design of Karkinos was based on our competition rocket from 2022, Terpulence II with a few major changes. The primary goals we had were to decrease the weight substantially,

**Table 3 TRT N2500 Motor Characteristics**

Loaded Weight (g)	12,609
Propellant Weight (g)	6,667
Burnout Weight (g)	5,942
Total Impulse (Ns)	11,548
Average Thrust (N)	2,531
Burn Time (s)	4.5

decrease length where possible, and increase the stability margin slightly. The primary weight savings for Karkinos were gained by switching to student-made tubing and removing unnecessary weight. Our custom tubes are around 50%-60% the weight of commercial filament wound fiberglass tubing from Wildman. Especially since we do not have a very demanding flight profile, reducing the load capacity with lighter tubing was worthwhile. This was especially important in the Air Brake module which has a 22” coupler and 10” airframe which added lots of mass to the aft end of the rocket last year. Switching both to custom tubing decreased the weight significantly. We were also able to remove some unnecessary parts that were increasing weight previously. Last year, an extension was added to the fin can so that a longer motor could be accommodated in the middle of the year. This meant another 24” of commercial airframe and 12” of coupler needed to be added since remaking the entire fincan would be excessive. Since we knew what size casing we would need from the start this year, we were able to remove that extension and instead use a single carbon fiber tube that is the proper length. The drogue airframe was also reduced from 32” to 24” while the main tube was increased from 33” to 35” to give more space for the parachute. Weight was also saved throughout the rocket by switching from steel hardware to aluminum hardware. Especially for the multiple threaded rods in both Ebays, switching to aluminum saved an unnecessary weight for little loss in strength. The model was then finalized with the mass of parachutes, harnesses, payload, and estimated epoxy mass.

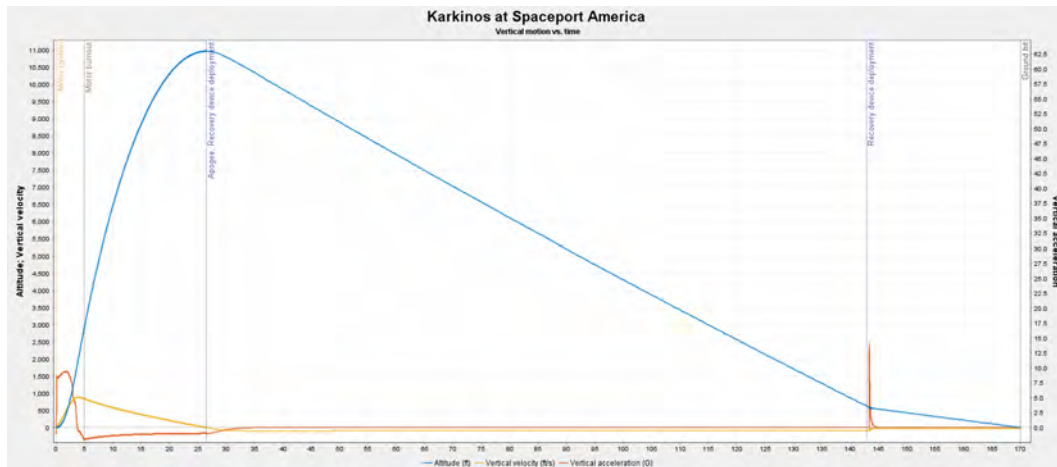


**Fig. 4 OpenRocket simulation for Spaceport America conditions**

Since Karkinos has a fairly high L/D for a rocket, the standard rules of stability are not consistent. While the rocket may have a stability margin above 1, since it is fairly long this may not be adequate. A new rule of thumb for stability that has become more popular in recent years has been to calculate stability in terms of percent of body length. The formula for this value is,

$$SM = \frac{|Cp - Cg|}{L}, \tag{1}$$

where  $Cp$  is the center of pressure,  $Cg$  is the center of mass, and  $L$  is the total length of the rocket. For a stable rocket, this safety margin should be between 8%-18%. This means that a long rocket will have a traditional stability

margin much larger than one and a very short rocket can have a margin below one. The fins were designed around these restrictions and targeted stability on the far end of this margin. Since our air brakes will pull the center of pressure forward when deployed, bringing the center of pressure as far back as possible is important to ensure stability throughout the flight. As seen in 5, Karkinos lifts off with a minimum stability margin of 2.7 calibers, equivalent to 10%. As propellant leaves the rocket, the center of gravity moves forward, and the stability peaks at 5.4 calibers, which is equivalent to 20%.

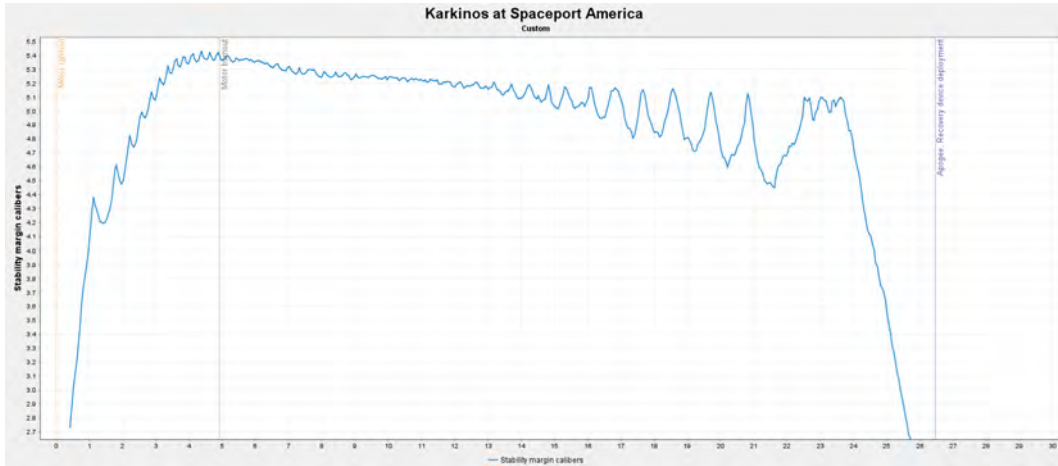


**Fig. 5 OpenRocket simulation of stability over time for Karkinos**

In general, our past simulations in OpenRocket have overpredicted our actual flights. This is for a variety of reasons such as extra protrusions like cameras or bolts outside the rocket as well as not flying perfectly straight. Because of this, the simulation was made to be fairly conservative. Launch conditions were set for Spaceport America with an altitude of 5,000 ft and a rail angle of 2 degrees. Since the rail buttons are spaced 3 ft apart, a rail length of 14ft was used since the buttons can no longer guide the rocket once the first one has left the rail. Since Karkinos contains an air brake module and cannot add any extra thrust, the rocket must overshoot the 10,000 ft target. Theoretically, our air brake can decrease a flight's altitude by up to 1,000 ft. However, it is much easier and less demanding to remove less altitude, so we simulated the rocket to target between 10,200 ft to 11,000ft. Once the rocket was built, the center of gravity and total mass were updated in OpenRocket, and following our third test flight, the surface finish was changed to better match actual flight conditions. Simulation results can be found in 4 below.

**Table 4 Open Rocket Simulation Results**

CG Location (in from tip)	97
CP Location (in from tip)	122
Stability (Caliber)	4.1
Stability (%)	16.3
Takeoff TWR	9.6
Velocity off Rail (ft/s)	92
Max. Velocity (ft/s)	890
Altitude at Max Velocity (ft)	2,000
Max. Altitude (ft)	10,969

### A. Propulsion Subsystems

The motor for Karkinos is a 98 mm SRAD N motor developed and tested by students in the Terrapin Rocket Team. It uses a custom purple propellant called Terple Nebula and is designed to launch Karkinos to 10,000ft at the Spaceport America Cup. Fig.6 shows a cross-section of the motor. It is made up of an aluminum casing from Fisher Research, an aluminum forward closure, a graphite nozzle, and XX phenolic liner. The nozzle and closure are retained on either end with steel snap rings. The motor casing is then slid into the motor mount tube and thrust is transferred from the lip of the case to the thrust plate.

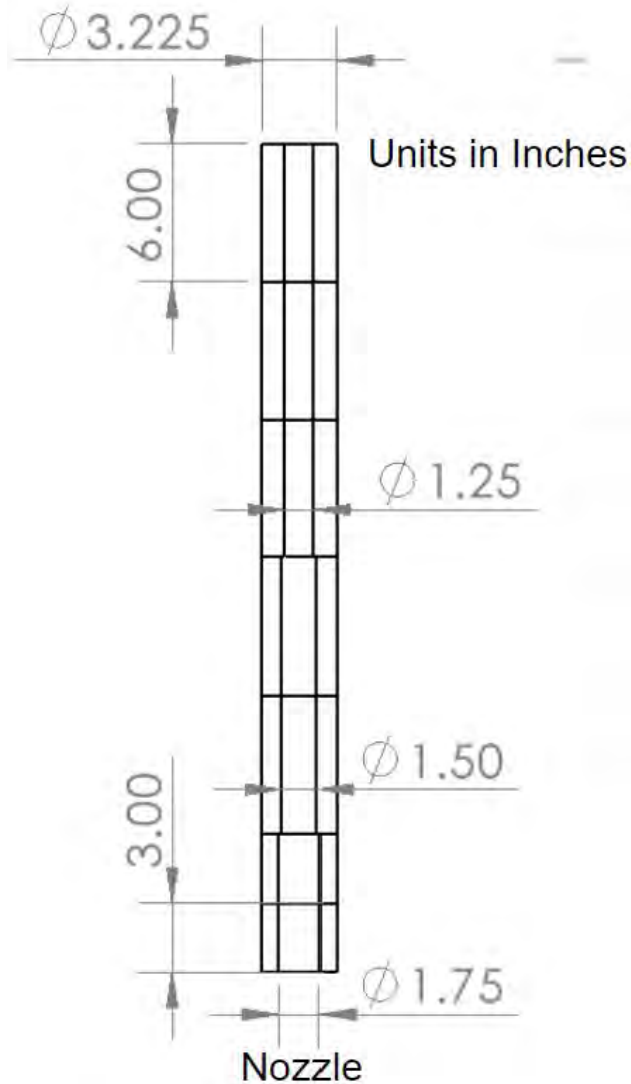


**Fig. 6 Motor Grains Assembly Cross Section**

#### 1. Material Selection and Pressure Vessel Design

Since this is the team's first time making large experimental solids, we wanted to minimize the risk to hardware and our testing timeline. The team completed four full-scale test flights this year; a failure of the motor in testing or flight would lead to a delay of potentially months as new hardware would need to be ordered and the motor redesigned and retested. Because of these requirements, the decision was made to stick to common experimental solid practices

**Table 5 Motor Case Dimensions**

Inner Diameter (in)	3.53
Outer Diameter (in)	3.88
Wall Thickness (in)	0.18
Length (in)	42
Distance from Edge to Snap Ring Groove (in)	0.375

and components. Our motor casing is an aluminum 98-13,000 snap ring casing from Fisher Research. These casings are very common within the hobby and are designed to hold the pressure of standard experimental motors. We also purchased a full graphite nozzle and aluminum forward closure from Fisher shown in Fig.7, also common choices. Steel snap rings retain the nozzle and forward closure on either end and a steel washer is used to distribute the force on the nozzle. On both the nozzle and forward closure, silicone o-rings are used for their good temperature resistance.



**Fig. 7 Nozzles and Forward Closure**

In order to protect the casing from the heat of the motor, we used XX Phenolic Liners from Franklin Fibre. XX liners provide much more protection compared to spiral wound phenolic liners from Always Ready Rocketry, and while our propellant does not run very hot, extra protection is helpful. The propellant is packed into standard cardboard casting tubes and then the grains are glued into the liner before firing, as shown in Fig.8.

Since we are using a commercial casing, we are confident in its ability to hold reasonable pressures, but its failure modes were calculated to determine our burst margins. Table 5 shows the most relevant measurements of our cylindrical casing design.

In order to calculate relevant safety factors, we noted various strength metrics of our chosen material, Aluminum 6061-T6, and recorded them in Table 6. The decreased strength of the material at increased temperatures was also recorded as an addition to the safety factor calculation. The rightmost column in the table takes into account the temperature in the casing at high pressures when the motor is burning (approximated as 392 °F). An additional useful metric for snap ring casing designs is the max allowable thrust for the snap ring itself. This was provided by the manufacturer of the snap ring and is given to be 54,700 pounds. We can also define Max Expected Operating Pressure(MEOP) to be

$$P_{max} = 655psi \quad (2)$$

According to the OpenMotor simulation for the static-tested N motor, the peak chamber pressure was expected to be



**Fig. 8 Glued Test Motors**

**Table 6 Motor case Strengths**

	75° F	392° F
Ultimate Tensile Strength (ksi)	45	19
Yield Tensile Strength (ksi)	40	14.9
Shear Strength (ksi)	30	11.2

about 720 psi. During the completed static fire in January, the pressure transducer data showed an actual peak of about 655 psi, so we used the practical result. For a thin-walled pressure vessel, the hoop stress can be calculated as

$$\sigma_{hoop} = \frac{P_{max}ID}{2t} \quad (3)$$

where ID is the inner diameter of the pressure vessel and t is the wall thickness. This results in a hoop stress of 6,422.64 psi, and to calculate the hoop stress safety factor, we simply divide the yield strength of the material by the hoop stress, or

$$SF_{hoop} = \frac{\sigma_{yield}}{\sigma_{hoop}} \quad (4)$$

The above equation results in a hoop safety factor of 6.23 for a room temperature yield strength, and 2.32 for a yield strength at 392 degrees F. Similarly, the axial stress in a thin-walled pressure can be calculated as

$$\sigma_{axial} = \frac{P_{max}ID}{4t} \quad (5)$$

**Table 7 Motor Case Safety Factors**

	75° F	392° F
Hoop Stress S.F.	6.23	2.32
Axial Stress S.F.	12.45	4.64
Snap Ring Groove Distance S.F.	4.87	1.81

This results in an axial stress of 3211.32 psi, and to calculate the axial stress safety factor, we simply divide the yield strength by the axial stress.

$$SF_{axial} = \frac{\sigma_{yield}}{\sigma_{axial}} \quad (6)$$

The above equation yields in an axial safety factor of 12.45 at room temperature, or 4.64 at 392 degrees F. For snap ring pressure vessel designs, another useful safety metric is the distance from the snap ring groove to the edge. The minimum distance can be calculated as

$$E_{min} = \frac{P_{max}ID}{\tau_s} \quad (7)$$

where  $\tau_s$  is the shear strength of the casing material. Using our values, our minimum distance is 0.08 inches. Our actual snap ring groove distance is 0.375 inches. To calculate the snap ring groove distance safety factor, we simply take the fraction of these numbers as shown.

$$SF_{groovedistance} = \frac{E}{E_{min}} \quad (8)$$

where E is our snap ring groove distance. This safety factor turns out to be 4.87 at room temperature, or 1.81 at 392 degrees F.

The final safety factor calculated was related to the max thrust on the snap ring. The thrust on our snap ring was calculated by taking the MEOP and multiplying it by the cross-sectional area of the casing, or

$$F_{snap} = P_{max}\pi\left(\frac{ID}{2}\right)^2 \quad (9)$$

which results in 6,301.84 lbs. In order to calculate the thrust safety factor, we divide the allowable snap ring force by 6,301.84 as shown.

$$SF_{thrust} = \frac{F_{max}}{F_{snap}} \quad (10)$$

which yields a safety factor of 8.68. Even at relatively high operating temperatures up to 392 degrees F, our stress safety factors stay above 1.81. Each safety factor is about triple its 392-degrees F counterpart assuming room temperatures. The closest point of failure is the snap ring groove shearing axially outwards, but even that is designed to withstand over four times the MEOP.

**Propellant Choice and Formulation** The propellant in the motor powering Karkinos is called Terple Nebula. This is a fairly common experimental propellant that was modified with oxamide in order to slow the burn rate. The chemical proportions and purposes for Terple Nebula can be found in 8.

Since this is the first year that the team is mixing motors, we wanted to have enough time to learn how to properly test motors. By using a preexisting formula, we can have a propellant characterized much faster instead of constantly tweaking the formula. In order to properly characterize this propellant, thermo-chemical values were calculated using a program called ProPep 3. With this program, we could input our chemicals and nominal percentages and receive values such as density,  $c^*$ , and chamber temperature as shown in 9. When calculating our burn rate coefficients, these values are important to find the burn rates at different pressure for each motor.

**Table 8 Terple Nebula Formula**

Ingredient	% of Mixture	Purpose
R45m, HTPB	13	Fuel/Binder
Diocetyl Adipate	2.6	Plasticizer
Castor Oil	0.1	Grain Hardener
Tepanol	0.1	Bonding Agent
Magnesium, 325 mesh	2	Metal Fuel
Strontium Nitrate, 200 $\mu$	15	Secondary Oxidizer
Oxamide	2	Burn Rate Suppressant
Copper Oxide	1	Burn Rate Catalyst
Ammonium Perchlorate, 200 $\mu$	62	Primary Oxidizer
MDI	2.2	Curative

**Table 9 Outputs from ProPep 3**

Density ( $lb/in^3$ )	0.0632
$c^*$ ( $ft/s$ )	4,442
Chamber Temperature (K)	2,368

## 2. Propellant Characterization

Before manufacturing of the full-scale N motors could begin, a set of characterization motors needed to be made to characterize the propellant and determine its burn rate coefficient and burn rate exponent. The planned configuration for the full-scale motor utilized a 98 mm six-grain casing, which has a relatively high length-to-diameter ratio (L/D). High L/D values make it easier for erosive burning to occur, which can cause dangerously high mass fluxes and therefore pressure spikes. It was important to find out if this propellant was prone to these erosive spikes during the characterization phase before the full-scale tests. Therefore, the characterization motor casings had higher L/D ratios as well, roughly in the range of 10.5-13.5.

The set of characterization motors consisted of three 38 mm motors and three 54 mm motors and was tested in configurations that covered a range of possible Kn values that the full-scale motor would experience during its flight. From the OpenMotor simulation, the full-scale motor would reach a peak Kn value of 312. By choosing various case sizes, nozzle throat diameters, and core diameters, a wide range of Kn values and peak pressures can be achieved. Between all six motors, the Kn value varied between 198 and 308, and the peak pressures varied between 369 psi and 723 psi.

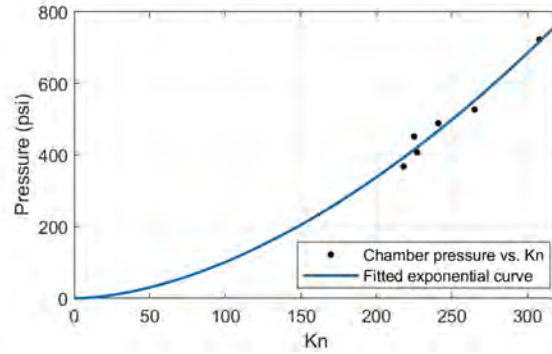


**Fig. 9 Pc vs. Kn curve**

The six characterization motors were tested at the MDRA Sod Farm launch site on September 8th, 2022. For these smaller-scale tests, the team utilized a test stand, pressure transducer, load cell, and DAQ to record pressure and force readings for each of the burns. All test firings were nominal, except for two slight erosive spikes which were not a cause for concern. In order to determine our Kn-Pc and Burn rate relations, the values from the static tests needed to be plotted to find best-fit lines. For the Kn-Pc curve, the known largest Kn from OpenMotor and the largest non-erosive pressure were plotted. The best-fit curve could then be found from these points. To find our burn rate coefficients,  $a$ , and burn rate exponent,  $n$ , for our burn rate Eq. 11, values from the static tests as well as ProPep outputs were used.

$$R_b = ax^n \quad (11)$$

Density and characteristic velocity,  $c^*$ , were found using ProPep. Using the peak Kn and maximum non-erosive pressure, burn rate values were found for each motor. These values were then plotted against pressure in Fig. 10 and a best-fit line was found to model Eq. 11.

$$R_b = \frac{P_{chamber}}{K_n c^* \rho} \quad (12)$$

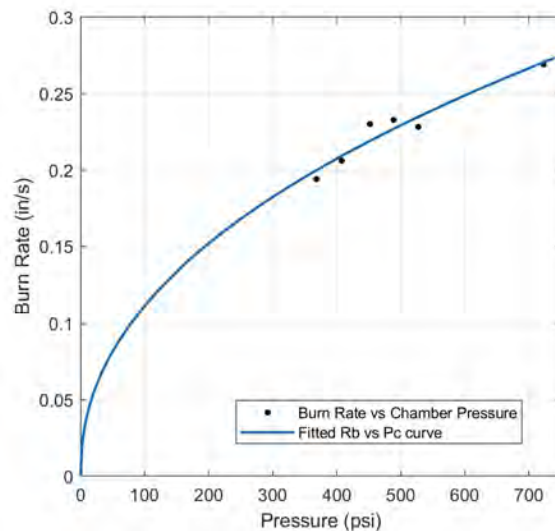


**Fig. 10 Rb vs. Pc curve**

This resulted in a burn rate coefficient  $a$  of 0.013 and a burn rate exponent  $n$  of 0.461. One of the major issues we experienced with characterization was an overestimate of our pressure compared to the static fires. When the

**Table 10 Erosivity Conditions [1]**

Non-Erosive:	
Chamber Pressure (psi)	Maximum Mass Flux (lb/in <sup>2</sup> * s)
400-600	1.0
800	1.75
1400	2.0
Erosive:	
400	2.0
600	2.5
800	3.0

configurations for the motors were originally designed, the nominal propellant length of the case was used. Once the motors were cast and assembled, all of the required grains could not fit into the case. To fix this, the forward grains were shortened to fit, however, their lengths were never measured. This meant that the motors were running at a slightly lower Kn than we were predicting, which meant a lower pressure. While this aspect of the characterization was not accurate, we found that the thrust values from our simulations were fairly consistent with the values from the load cell.

### 3. Full Scale Motor Design

The full-scale motor needs to fulfill multiple requirements for a stable flight and also to satisfy design requirements set by the DTEG, primarily an apogee of 10,000 ft and a rail exit velocity of 100 ft/s. Since Karkinos contains an air brake system, the rocket needs to overshoot its target so that the system can adjust and hit 10,000ft precisely. The team's rocket in 2022, Terpulence II, flew on a Loki N3800 which is a 98 mm snap ring motor with 12,500 Ns of impulse. Since Karkinos is a similar, but lighter rocket due to a much lighter Air Brake system and SRAD tubing, we could target a slightly lower total impulse in a similar casing to reach the desired apogee. Due to these constraints, we chose a Fisher Research 98-13,000 casing that can hold 6 standard 98 mm grains. This casing is slightly longer than the 98-12,500 casing that was used for the Loki N3800 and gave us the option of using spacers if necessary to decrease the amount of propellant if we were overshooting too much.

The second consideration that we had to design for was our rail exit velocity of 100 ft/s. Based on previous experience with rockets of this size, we would need a 10:1 thrust-to-weight ratio. For an 80 lb rocket, this meant we needed 800 lbs of thrust at liftoff, or around 3,500 Newtons. We were also expecting a small erosive spike which would help the rocket get off the pad, so there was some margin in our initial thrust estimates.

The next design requirements were not important for the rocket overall but for the motor itself. Since this is the team's first 98 mm motor, we wanted a fairly conservative design to minimize the destruction of hardware and the rocket. Since we cannot predict erosive burning within OpenMotor, we could follow a few rules of thumb for erosivity. The first is mass flux-based erosive burning, which can become a major problem in motors with higher L/D. Longer motors have much higher mass flows through the aft grains which causes local increases in burn rate. Charles Rogers provides some design criteria for different chamber pressures based on peak core mass flux in his article *Erosive Burning Design Criteria for High Power and Experimental/Amateur Solid Rocket Motors* shown in Table 10.

For a target Kn of 300 and a chamber pressure of 700-800 psi, we aimed to keep the mass flux below the recommended limit of 1.75 lb/sec-in<sup>2</sup>. Since our propellant is fast burning, in a long motor like this, our mass flow rate is going to be fairly high at the aft end of the motor. Since mass flux is mass flow divided by area, by increasing the core diameter of the aft grains where the mass flow is the highest, we could decrease our mass flux. Widening the cores at the aft end also allowed us to increase our initial Kn for a higher initial thrust to get off the pad. However, this also has a few major disadvantages. First, the wider cores decrease our volume loading significantly. We are losing valuable space inside the case for propellant that may be necessary later on. Increasing the core diameter at the aft end also means that since those grains burn out before all of the others, the liner at the aft end will encounter much more heat. This could

**Table 11 Simulated Motor Parameters**

Motor Designation	N2733	Initial Kn	291
Total Impulse (Ns)	11808	Volume Loading (%)	80.37
Motor Class	15% N	Propellant Mass (lb)	14.4
Burn Time (s)	4.3	Propellant Length (in)	36
Peak Pressure (psi)	704	Peak Mass Flux (lb/(in <sup>2</sup> · s))	1.58
Average Pressure (psi)	538	Port Throat Ratio	2.79
Peak Kn	312	Peak Thrust (N)	3700

lead to the remaining casting tubes becoming dislodged and clogging the nozzle or even a liner burn through. However, since our propellant is not very hot and we are not burning for too long, these risks were not especially important to us. The second design constraint in regard to erosivity is the port throat ratio. This is a comparison of the core area of the grains and the throat area of the nozzle. If the port-throat ratio is too small flow can choke within the grains which will locally increase the burn rate. Generally, this value should be above 2:1 in order to prevent major erosive burning. Since we had already increased the core diameter of the aft grains, that also increased our port throat ratio above this limit. After many iterations in OpenMotor, the final configuration decided for the motor is:

- 3 x 6" long 1.25" cores
- 2 x 6" long 1.5" cores
- 2 x 3" long 1.75 cores

Results from OpenMotor using this configuration can be found in table 11.

#### 4. Motor Manufacturing and Assembly

To make predictable, reliable motors, a set procedure, and chemicals from the same batch are important for batch-to-batch consistency. Our mixing procedure was set before mixing the characterization motors and was kept the same for the following two mix sessions. Before mixing, propellant batch quantities were determined based on the total propellant mass desired along with a precautionary extra quantity. These totals could then be input into an Excel spreadsheet that automatically calculates the required quantities of each chemical. During the mixing process, the actual weight was also recorded on this sheet so that any deviations during firing could potentially be traced back to issues during the mixing process. During the 2022-2023 year, the team completed three mixing sessions. The first is for characterization, the second is for two full-scale N motors, and the third is for three full-scale flight motors.

The entire procedure, from mixing to casting, lasts around six to seven hours. The procedure starts with weighing out measuring bowls, recording their mass values, and taring their masses on a scale. Since ingredient quantities for multiple motors were larger than what a single bowl could hold, multiple 20 qt mixers were used to contain fractional batches of propellant. Wearing nitrile gloves, members poured all of the liquid components except the curative as specified by the mix sheet into each bowl one at a time.

Next, the bowls were placed into a 20 qt stand mixer for 20-30 minutes. Special care was taken to scrape any built-up Tepanol on the bottom of the bowl that was not getting picked up by the mixer. Tepanol is a chemical that is used to chemically bind the ammonium perchlorate particles to the HTPB. Tepanol has a shelf life, and if not stored in cold temperature conditions, becomes less effective over time and much more viscous. The Tepanol supply of hobbyists making experimental motors is often a decades-old surplus that has become extremely viscous. This meant that while all the other liquids had already been fully incorporated, the team often had to scrape off the Tepanol from the paddle or bowl to get it mixed. While the liquid components were mixed, the solid powdered components were measured out in clean bowls in a similar fashion to the liquids. Each solid is measured in its own separate bowl, and dry solids are never mixed together. Another ingredient of special note was the Strontium Nitrate, which can absorb moisture and clump together. Before adding to the mixture, the Strontium Nitrate needed to be broken down with a mortar and pestle and pushed through a sieve in order to make sure there were no clumps remaining. Before adding the solids to the liquids



**Fig. 11 Mixing Propellant**

mixture, the mixing bowl was placed under vacuum for ten minutes. This helps get the majority of the air out of the mixture and also gets rid of any water that may have been absorbed. Removing the air leads to a denser propellant and fewer voids, which leads to a more consistent product with a predictable burn rate. After each of the solids is added, the mixture is vacuumed again, then, while wearing solid particulate respirators, the ammonium perchlorate is added. This portion spends the longest under the mixer, so the extra time is used to cut and prepare the casting tubes and mandrels. Once the ammonium perchlorate is mixed in, the batch is put under vacuum one last time and then the curative is added (with organic vapor and solid particulate respirator masks on) and mixed in. Finally, the packing process can begin. While still wearing gloves, the propellant is shaped into elongated clumps that fit evenly around the central mandrel and within the casting tubes. Then, wooden dowels are used to evenly distribute the propellant around the mandrel after each additional amount is added into the casting tube. Once each casting tube is filled, the propellant is left to cure for at least four hours.



**Fig. 12 Liquid Components Under Vacuum**



**Fig. 13 Filled Casting Tubes Curing**

At this point, the grains needed to be cut to size as per the grain schedule in Fig. 6. A hand miter saw was used with a backing block to get straight cuts. Once the grains were prepared, they were then test-fitted with the forward closure and nozzle into the liner and slid into the casing to check for snap ring clearance. Lastly, grains are glued into the liner with silicone caulk. This prevents castings tubes or grains from coming loose and clogging the nozzle. For the final motor assembly, o-rings and the outside of the liner were thoroughly greased, snap ring grooves are checked for



**Fig. 14 Cut Motor Grains**



**Fig. 15 Greasing the Liner**

sharp o-ring damaging burrs, and the assembly is secured in place into the casing by fully seating the snap rings into the casing's grooves.

### 5. Motor Test Stand

To test the solid motor, an SRAD test stand was chosen based on the size of the motor as well as the scale of its thrust output. It also needed to be compatible with the data acquisition setup of our choice, which will be discussed further in this report. This means having a valid location to place the load cell and pressure transducer for each static test. After thorough research, a suitable test stand design was found that was relatively simple to assemble with the materials we had. It also met the criteria of being strong enough to withstand the thrust of the motor to be tested. An assembly of the stand was developed in Solidworks to generate a straightforward bill of materials, which confirmed we had every component necessary to build the stand. The stand was assembled with mechanical fasteners such as spring nuts and bolts.

Figure 16 is the assembled test stand with the motor inserted. The orientation of the stand was chosen to be upright as opposed to horizontal because the downward force from the motor would be absorbed by the ground. This way, the stand simply needed to be stabilized from tipping over, which was done with ratchet straps that were securely staked to the ground. Stakes were also placed along the base of the stand to further secure its orientation and position.

This stand allowed simple placement of the load cell and pressure transducers, shown in Fig. 17. The NPT tee fitting screwed directly onto the forward closure of the casing, and had a flat surface that could be used to push onto the button load cell placed underneath the casing. Two pressure transducers were attached (one on each side of the tee fitting) to confirm the reliability of the pressure data.

An important criterion for choosing a data acquisition device was its ability to connect our computers to the sensors via Ethernet. During the static fire, in order to stay a safe distance away from the motor and collect data, a long-range Ethernet cable was used to provide a direct connection from our computers to the data acquisition device. Ethernet was more reliable than a wireless connection setup and much simpler to put together. For this reason, a Labjack T4 was

chosen, as it provided reliable Ethernet capabilities.



**Fig. 16 Static Fire Setup**

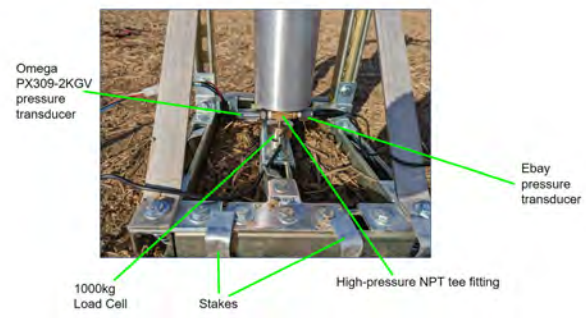


**Fig. 17 Data Acquisition Setup**

A test procedure was developed for the pressure transducer and the load cell to calibrate its readings and confirm they were accurate prior to the static fire. For the pressure transducer, a hydraulic pump was attached to an analog pressure gauge and the pressure transducer. The voltage readings from the pressure transducer were then compared to the pressure readings from the gauge, which allowed us to generate a scaling equation that would convert voltage readings to accurate pressure readings in pounds per square inch.

For the load cell calibration, the load cell was attached to an amplifier that connected to the Labjack T4. Next, we measured and recorded the weights of various aluminum blocks. These blocks were then placed on the load cell via the setup in Fig. 18, and the voltage readings on the load cell corresponded to the amount of weight we placed on it. This allowed us to generate a scaling equation that could convert load cell voltage to weights in pounds for the static test.

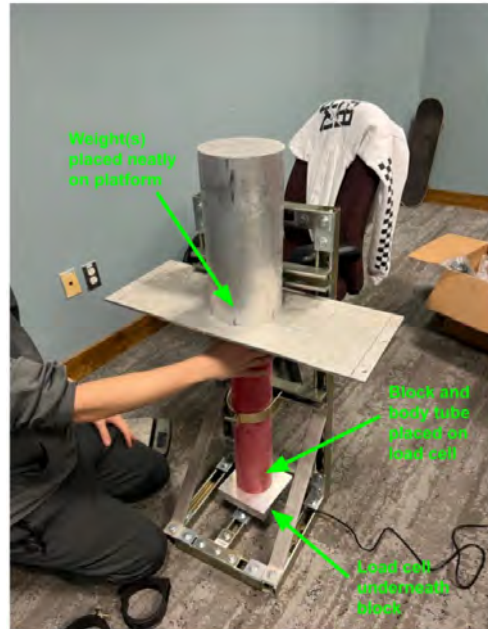


**Fig. 18 Load Cell Calibration Setup**

A problem that was encountered with the load cell was small spikes and choppiness in the data after a static fire. This was caused by low resolution in the data acquisition input port. We changed the port from an analog input to a flexible input/output port on the same Labjack. It is important to note that this port needs to be configured to its analog form (as opposed to digital), or the data will only show in the form of a 1 if a force is applied, or a 0 if no force is applied.

However, this port has a voltage range of 0-2.5 V, so if the load cell output exceeds 2.5 V (which it did according to the static fire data), the Labjack would max out and fail to record data above 2.5 V. Another solution to the choppiness was to increase the sample rate. This would of course increase the file size, but it was worth it to improve the resolution of the data. We decided it was an acceptable trade-off to have minimal spikes in the data to ensure data was collected for the entire thrust range necessary.



**Fig. 19 First Static Fire**

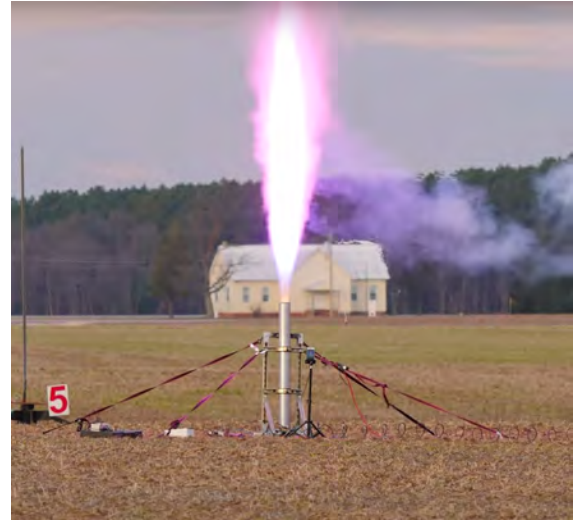


**Fig. 20 Second Static Fire**

### 6. Full Scale Motor Tests and Results

For static testing of the full-scale motor, two motors were manufactured. These would both be ground tested, however, they would have different nozzles. The first motor would have a larger nozzle for a lower  $K_n$  while the second motor would have a smaller throat for the targeted  $K_n$ . This was done in order to verify that there would be no major differences from moving up to 98 mm from 54 mm. By testing at a lower  $K_n$ , the motor would run at a more conservative pressure in case there were any unexpected erosive spikes. For the testing, the motors would each have two pressure transducers being read by entirely separate systems for reliability. These motors were manufactured in November 2022 and were originally planned to be tested in December 2022. Unfortunately, after setting up the test stand and electronics, when assembling the motor the o-rings could not be found and the test firings would have to be delayed until January. During the January testing, setup and assembly of the first motor went nominally. The motor fired without issue, however during review it was found that the data acquisition system did not record force readings. Because of this, the load cell was switched to a different and more proven data acquisition system. This test was also nominal and both pressure and force readings were recorded.

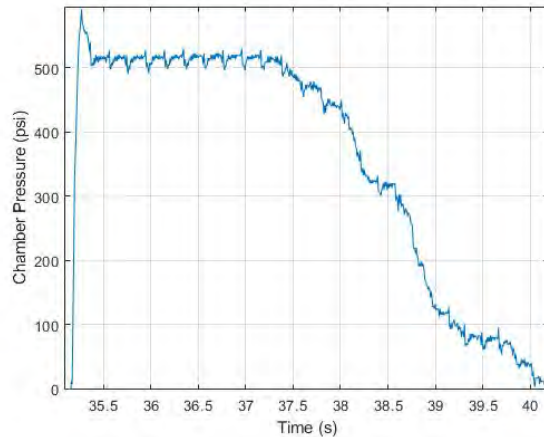


**Fig. 21 Pressure Curve from Static Fire 1**

During the review of the recorded data, the results were fairly close to our expected values. Similar to the characterization motors, the pressure was slightly lower than expected, but the force was similar. There were minor erosive spikes in both motors, but neither was much larger than the normal burning max pressure. The motors also came

up to pressure quickly, even though there were no grain spacer o-rings or concave faces. The force readings for the second motor matched the simulations, with a slightly longer taper toward the end of the burn.

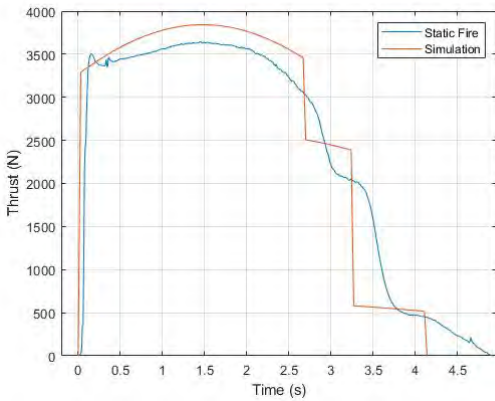


**Fig. 22 Thrust Curve Comparison of Second Static Fire**

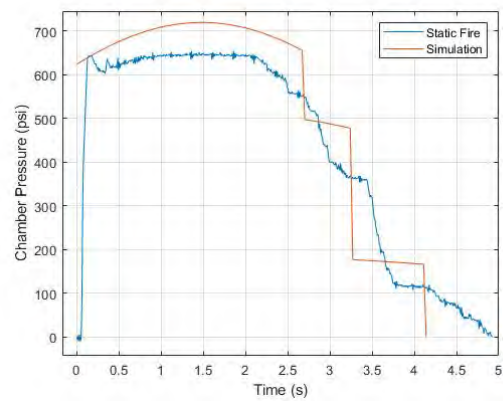


**Fig. 23 Pressure Curve Comparison of Second Static Fire**

### 7. Mixing Sessions and Motors Made

Over the 2022-2023 year, there were a total of three mixing sessions in preparation for the Spaceport America Cup. During the first, six characterization motors were made. Two N motors were made during the second session for ground testing and 3 N motors were made during the third session, two for test flights and one for the competition. During the first full-scale mixing session, everything went nominally, however, we ran into an issue near the end of our casting session. We had oversized the casting tubes so that we could cut the grains to the desired lengths but did not include enough extra in the batch size to accommodate this. We did include 5% for waste, but this was not enough to make up for it. Because of this, we had filled some casting tubes fully while others had 1” remaining. This led to the lengths of the grains changing slightly to accommodate the cast propellant. While some grains ended up shorter and others longer, the simulated thrust curve was not changed too much and the change in Kn was minimal. Since we did not want to retest our motors, we recorded the grain lengths and used those measurements for the flight motors. During the second large mixing session, the excess was increased to 10% and casting tubes were more carefully cut so that there wouldn’t be too much extra.

**Table 12 Mixed Motors Measured Values**

	24 Propellant Mass (g)	Propellant Length (in)
Test Motor 1	6568	36.375
Test Motor 2	6662	36.75
Flight Motor 1	6654	36.125
Flight Motor 2	6690	36.25

### 8. Igniters

For igniting the motors, we have been using QuickBurst ProCast BKnO3. The ProCast is inserted into a straw and then an MJG Firewire igniter is pushed inside. It is then left for the acetone to evaporate from the mixture before being used. Generally, 1.5” to 2” of the mixture is inserted into the straw for the larger N motors. We have used these on many motors from H to N and have had great reliability with ignition. For inserting the igniter into the motor, the wire is

taped to a thin wooden dowel. If the igniter leads are not long enough, they are extended with enough solid core wire to come out of the nozzle. The dowel is then taped to the launch rail so that it cannot fall out and stays at the top of the motor. At the Spaceport America Cup, 2 of these igniters will be used in parallel to ignite the motor.



**Fig. 24 Example BKnO3 Igniter**

## **B. Aero-Structures Subsystems**

The purpose of the Aerostructures subteam is to design and manufacture Karkinos to be lightweight, cost-efficient, and manufacturable. Karkinos is nominally six inches in diameter and stands approximately 12 feet tall. The nose cone and electronics bay coupler are made of wound fiberglass. The recovery section and upper fin can are made of student-rolled fiberglass. The fin can is a student-made hand-rolled carbon fiber airframe and the fins and centering rings are made of G10 fiberglass. The main parachute is housed in the recovery section, whereas the drogue is housed in the upper fin can above the Air Brake. Fiberglass was chosen as the primary structural material as it is lightweight and very strong, which makes it very popular in high-power rocketry. Fiberglass is also transparent to radio frequencies, which is important for receiving telemetry from flight computers. Carbon fiber was chosen for the fin can as it is very strong and stiff while being lightweight. Minimizing weight at the aft end of the rocket is important for stability, and its strength is useful for keeping the rocket together when it touches down.

### *1. Body Tubes and Couplers*

**Airframe Manufacturing** All airframes on Karkinos except the nosecone are student-made fiberglass or carbon fiber tubes. While we have used commercial filament wound tubing in the past, we have found that it is often fairly heavy, and custom-made tubes can be around 50% to 60% the weight of a commercial tube. The process of making a tube starts with the correct mandrel. It is important for the airframes to have the correct inner diameter so that the interface with the couplers is just right. If it is too loose, the airframe will not be rigid and the rocket will bend during flight. If it is too

tight, then assembling the rocket for launch will be difficult and there may be too much interference for the sections to separate in flight. With these constraints in mind, we chose to use a 65" long section of a 6" coupler from Wildman Rocketry. With a piece of Mylar, a clear plastic sheet, over the coupler we can provide adequate tolerances and provide a surface to protect the mandrel from epoxy. The Mylar is then cleaned with acetone and thoroughly coated in epoxy, which for these tubes is Aeropoxy 2032/3665. Fiberglass or Carbon cloth is wrapped around the tube tightly and epoxy is pressed into it using a brush and plastic squeegee. Since carbon is stiffer than fiberglass, we need fewer layers for a tube with similar strength, in this case, we use four wraps of 3k 2x2 twill carbon and six wraps of 6 oz plain weave fiberglass.



**Fig. 25 Layup of carbon fiber airframe**

Once the cloth has been fully wrapped around the tube, a layer of peel ply is pressed into the cloth. This helps fill in the weave and makes it much easier to give the tube a smoother finish. We also attempted to finish a tube with shrink tape for an easier glossy finish but found it difficult to get a consistent wrap and finish. In previous years we had many issues removing the tube from the mandrel. We had tried waxing the mandrel in order to give it a slippery surface, but this was not effective. Instead, this year we coated the mandrel in a dry graphite lubricant. This lets the Mylar slide much easier along the coupler and makes it possible for one person to take it off. Tubes were then cut to size using a hacksaw and the edges deburred with sandpaper.

**Couplers** Karkinos contains six separate coupler connections throughout the rocket. With so many concentric interfaces, it is important to make sure that they are all sufficiently stiff to minimize bending in flight. For a well-fitting coupler, a coupler-airframe overlap of one caliber is generally sufficient. This is the case for all coupler connections except for the one between the nosecone and nosecone Ebay. Since the nosecone is not experiencing any major bending loads, this connection is only 0.5 calibers of overlap. The majority of the couplers in Karkinos are commercial filament wound fiberglass from Wildman Rocketry. However, since we are trying to minimize mass towards the aft of the rocket, the coupler in the Air Brake module was custom-made and is discussed later in this report. When originally made, this coupler was fairly loose in our airframes which led to major bending during fit checks. This was remedied by adding a thin layer of fiberglass on top of the coupler to help fill in the gap and stiffen the connection. Another non-conventional coupler in Karkinos is the forward end of the nosecone coupler. In order to have enough room for the payload to deploy cleanly, a window was cut into the coupler. While this is removing lots of material from the coupler, we have not seen any major decrease in strength or stiffness over three flights in this configuration.

**Nosecone** The nosecone for Karkinos is a commercial 5-1 Von Karman filament wound fiberglass nosecone from Wildman Rocketry. There are not many options for commercial fiberglass nosecones, so this nosecone from Wildman was chosen so that it would be compatible with our couplers. An eyebolt is threaded into the aluminum tip for connection



**Fig. 26 Carbon tube after removal from mandrel**

to the nosecone harness that is connected to the top of the payload. Holes are drilled into the sides for the light sensor on the payload as well as for ambient pressure.

## 2. Fins

**Design** The fins used on Karkinos are similar in proportions to the fins on the team's rocket from the previous year, Terpulence II. Based on the changed dimensions of Karkinos from Terpulence II, the fin shape was altered in Openrocket until the desired stability criteria were met. Stability at lower speeds was less than satisfactory so the span was increased from 4.5" to 6". The larger fin size also meant that the static margin of stability was greater, which is important for keeping the rocket stable while the Air Brake flaps are deployed. The final design consists of four fins with a swept-delta shape and a semi-span of approximately the same width as the airframe. Additionally, the fins include tabs that extend all the way from the leading edge to the trailing edge for maximum through-the-wall attachment length and ease of manufacturing.

**Table 13 Fin Parameters**

Root chord (in)	15
Tip chord (in)	4
Sweep (in)	10
Semispan (in)	6
Thickness (in)	3/16

**Table 14 FinSim Simulation Options**

Altitude	7,000ft ASL
Elastic Axis	0.5
CN-Alpha	NACA TN 4197
Fin Materials	G10 fiberglass, AS H3501 Carbon Fiber

**Flutter Analysis and Construction** The team utilized the aeroelastic fin analysis program AeroFinsim to estimate the flutter speed of the fins on Karkinos. Settings used for analysis can be found in Table 14.

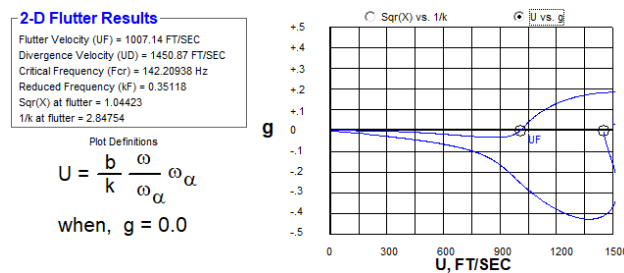


**Fig. 27 Aerofinsim Analysis with G10 fiberglass**

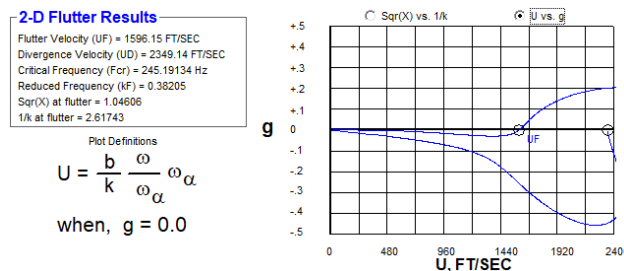


**Fig. 28 Aerofinsim Analysis with H3501 cf**

Using 3/16" G10 fiberglass as the material was problematic initially because the predicted flutter velocity shown in Fig. 34 was very close to the vehicle's max projected velocity of 1000 ft/s. Since the fins should be designed such that neither the divergence nor flutter velocity was reached, the lower of the two was the primary design factor for the fins. Therefore, the composites team performed a carbon fiber vacuum-bag layup over the fins, adding two layers of 3k 2x2 twill carbon fiber to each side of the fin, the first at 45 degrees and the second at 0 degrees. The fin thickness increased from 0.1875" (3/16") to 0.23". Since carbon fiber was now the outer material, the flutter velocity could be computed using this material instead of the G10. Utilizing the carbon fiber composite option that gave the lowest flutter speed, CFRTP AS-4 PEEK, the new fin flutter velocity now reads 2,098 ft/s and the divergence velocity is 3,073 ft/s as shown in Fig. 28. More weight has been added to the rocket's design since the first flutter estimation, so the max velocity

of the rocket has decreased and is currently projected to be 996 ft/s from the OpenRocket simulation, far below the predicted flutter velocity.



**Fig. 29** Cutting the rough shape of the fins on a bandsaw



**Fig. 30** Carbon, peel ply, release film, and breather prepared

The fins for the rocket were initially cut out of 3/16" thick G10 plate on a bandsaw. These were cut with a fairly large margin so that the true fin shape could be more carefully achieved. The fins were then stacked together using alternating layers of painter's tape and super glue. This allowed us to temporarily glue the fins together for sanding. The entire stack could then be sanded down to the desired dimensions using a belt sander. Next, the fins were laid up with carbon fiber in the vacuum-bagging process detailed above. The epoxy was cured to a leathery state and excess carbon was cut using a sharp knife. After the epoxy had fully cured, the fins were finally beveled using a 15-degree chamfer bit on a router table.



**Fig. 31** G10 cores after sanding



**Fig. 32 Fins under vacuum**

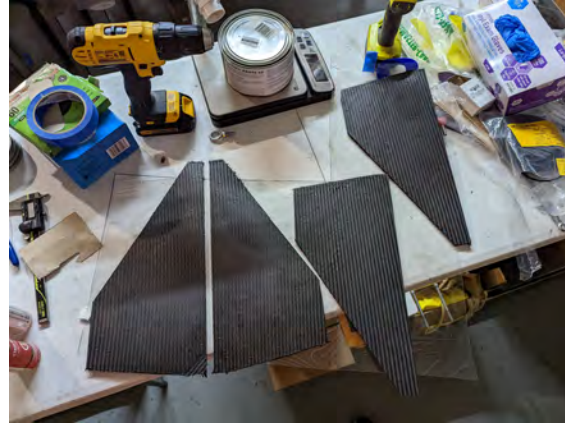


**Fig. 33 Fins after removal from bag and trimming**



**Fig. 34 Fins after bevelling on router**

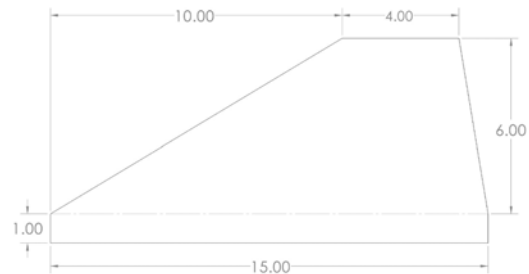


**Fig. 35 Karkinos fin dimensions (in)**

**Fin Can Manufacturing** The fin can for Karkinos must fulfill multiple requirements overall. It must be able to hold the fins rigidly, retain and transfer the thrust of the motor, provide strong recovery attachment, and be built light enough that the rocket's stability margin is not negatively impacted. The airframe is custom-wrapped carbon fiber as discussed in the previous section. The motor tube is a commercial filament wound fiberglass tube that is 23" long and there are three fiberglass centering rings along the motor tube. Two ¼"-20 threaded rods run through the centering rings to help distribute recovery loads. At the top of these rods, there is an eye nut for recovery attachment and the aft ends extend past the end of the airframe to keep the thrust plate secured. A 98 mm Aeropack screw-on retainer is secured to the thrust plate and the thrust plate is retained and held on with the two threaded rods.

Assembly of the fin can begin with the airframe. Fin slots were cut out using a rotary tool with a cutoff wheel. A paper template was taped to the airframe and then the correct markings were drawn on to make sure the cuts would be straight and at the proper angle. These were initially cut undersized and then were test fit with the fins.

The slots were widened with a file until the fins could be pushed through the airframe. This was done to minimize large gaps where epoxy could flow through when making external fillets. Next, the motor mount assembly was made. This assembly is made up of two centering rings forward of the fin and one aft. First, all three centering rings were stacked together and holes were drilled for the threaded rods. This makes sure that each of the holes will be straight and the threaded rods will not have any major twisting. The centering rings were then slid on the tube with the threaded rods with nuts keeping the spacing correct. The forward-centering rings and nuts were then epoxied and set to cure. The aft centering ring remained on the motor mount, however, it was not epoxied on as it would need to be removed. With the motor mount assembly complete, the airframe was prepared for bonding. The inside was sanded with 220 grit,

and then 400 grit sandpaper where the centering rings would interface and then cleaned with acetone. This is also the process that was followed for all bonded surfaces throughout this rocket. Epoxy was then added to the inside of the tube at the forward end only and the motor mount assembly was pushed in. The rocket was then stood vertically, which allowed the epoxy to settle around the perimeter of the centering rings and form a fillet when cured. Once fully cured, the aft centering ring was removed and any threads were taped over to prevent any epoxy from getting on them.



**Fig. 36** Motor mount assembly with forward two centering rings epoxied on

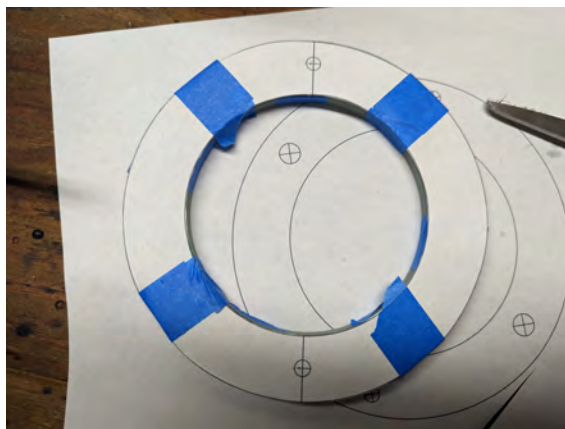


**Fig. 37** Template taped to centering rings prior to drilling



**Fig. 38** Inner diameter of the airframe is sanded for motor mount bonding

Next, each of the fins was tacked into place using Aeropoxy ES6209. In order to make sure that they would each be straight and at the correct angle, two fin guides were cut out of foam board and slid over the airframe. The root edge of each fin was generously coated in epoxy and then pushed onto a motor tube through one of the slots. It is firmly pressed in and wiggled around and then removed. This process is repeated two to three times in order to make sure there is enough epoxy to hold it in. During the final one, epoxy is added to the forward end of the fin tab in order to seal the fin and the centering ring. Once that process has been completed, it is pushed in for the last time and then aligned with the two fin guides. This process is then repeated for each of the four fins giving enough time for the epoxy to cure. After each of the fins is tacked on, internal fillets are made with Aeropoxy 2032/3665. The epoxy is thickened with colloidal silica and then poured into a syringe. The syringe is used to inject the epoxy from the aft end along the root of the fin tab. Two internal fillets are done at once and the entire fin can be rocked back and forth to evenly distribute the epoxy. This was then repeated for each of the fins taking care to make sure the epoxy was not leaking where it should not have been. External fillets were then done using Aeropoxy ES6209, however, this was thickened with colloidal silica and dyed black. The aft centering was then secured with nuts on the threaded rods and epoxied into place. Finally, the thrust plate was added and secured with two nuts and thread lock. Once completed, the entire fin can be wet sanded up to 1000 grit and then clear coated in order to give it a glossy carbon look.



**Fig. 39** A small fillet is formed when the fin is tacked



**Fig. 40** All fins tacked on with fin guides

**Airframe Finishing** In order to give the airframe a smooth finish for both aerodynamic and aesthetic reasons, a few methods were used to complete the airframes. For the carbon fin can, both the airframe and fins were sanded smooth with sandpaper. A thin coat of laminating epoxy was then applied to the surface to fill in any major surface imperfections. This was then sanded down again to remove bumps. A clear coat was then used to give the surface a smooth glossy finish. For the fiberglass airframes, they were first given a coat of high-build spray primer. This helps fill any small divots and also makes imperfections visible. Spot putty was then used to fill the major gashed and then the entire airframe was sanded smooth. This process was repeated until there were minimal imperfections visible. The airframes and nosecones were then given a coat of gloss white spray paint and finished with two coats of gloss clear coat.

### 3. Bulkheads

**Electronics Bay Bulkheads** The electronics bay (Ebay) bulkhead shown in Fig. 42 is a circular plate manufactured from aluminum 6061-T6. The overall dimensions of the bulkhead are as follows: the outer diameter is 5.998" and the total thickness is 1/4". The bulkhead is separated into two layers with a 1/8" thick and 5.998" diameter outer lip and a 1/8" thick and 5.82" diameter ribbed pattern to strengthen the bulkhead while minimizing weight. Three sets of holes were cut from the bulkheads: two 0.386" clearance holes for a 3/8" u-bolt located at the center, two 0.323" clearance holes for two 5/16" threaded rods located 2.50" from the center, and two 0.164" holes for wiring of ejection charges. Two Ebay bulkheads enclose the electronics bay and are fixed together with the two threaded rods. A waterjet

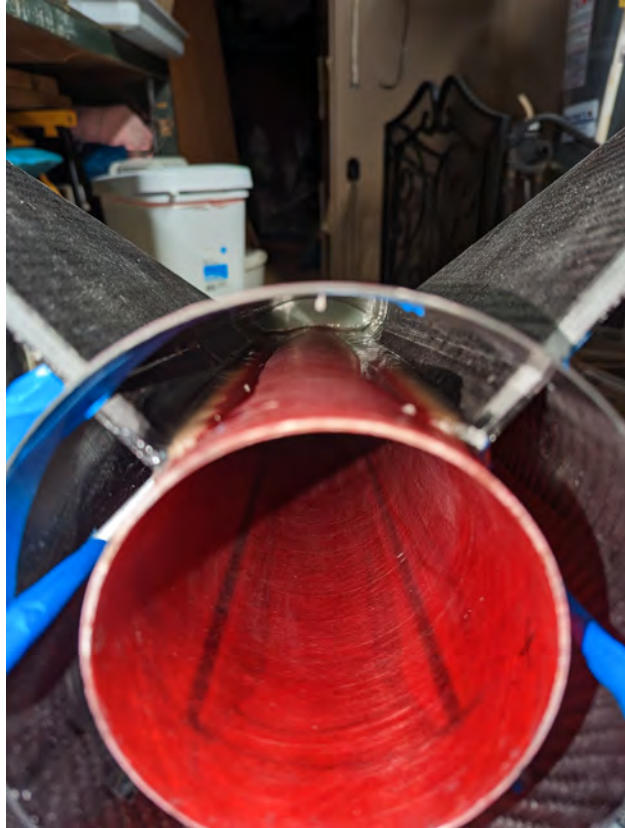


**Fig. 41 Internal fillets**

was selected as the fastest and cheapest means of manufacturing. The outer lip and inner ribbing were manufactured separately and joined together using the u-bolts and threaded rods; no adhesive was used. Fig. 42 shows a CAD of the bulkhead and Fig. 43 shows a FEA of the bulkhead.

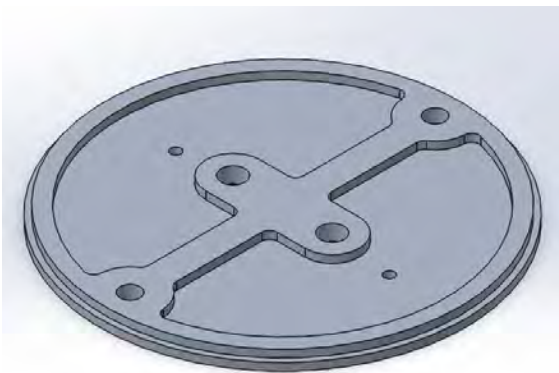


**Fig. 42 CAD of Ebay bulkhead**

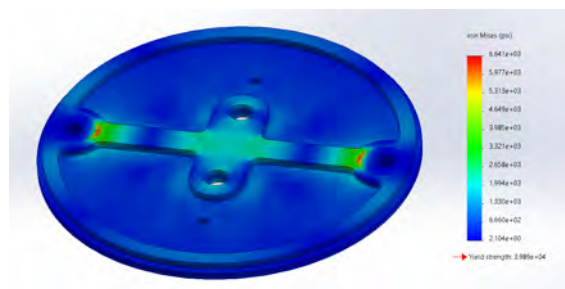


**Fig. 43 FEA of Ebay bulkhead**

Finite Element Analysis (FEA) was conducted on the Ebay bulkhead. The bulkheads experience the largest loads at two points during the flight, apogee deployment, and main deployment. The force at apogee is primarily from the jerking of the recovery harness as it separates. For Karkinos, this is minimized by having a very long harness and z-folding the lines. During the main deployment, as the parachute fully inflates, it also induces a jerk on the rocket.

The main lines are also z-folded and the way the parachute is packed leads to a more gradual opening to minimize this effect. Based on accelerometer data collected from last year’s test flights, the peak loading condition was discovered to be approximately the weight of the rocket from main parachute deployment. Given that the structural design of our rocket underwent few changes this year, it can be reasonably assumed that the maximum force applied is the weight of the rocket which is about 83 lbf. The analysis shown in Fig. 44 progressively increased the element density around high-stress locations. The results show a maximum stress value of approximately 6.7 ksi. Aluminum 6061-T6 has a yield strength 40 ksi and an ultimate strength of 45 ksi. Thus, the bulkheads have a safety factor of 5.97 and will have no issue handling the peak loading condition. During our test flights this year, the bulkheads performed as expected with no deformation visible after the flight.

**Thrust Plate** At the very aft end of Karkinos is the thrust plate and motor retainer. Standard high power rockets transfer their motor thrust through the motor tube which then goes through the fins, then centering rings, and finally into the airframe. With a thrust plate, this force is not only put through the motor tube but also directly into the airframe. The thrust plate also provides a convenient way to attach the Aeropack 98mm screw on retainer. The 12 holes can be difficult to drill accurately by hand, so these are cut with a CNC machine and then tapped by hand. Since the thrust plate is secured using two ¼” nuts, it can be easily removed and switched between rockets as well. We have flown with this thrust plate multiple times, even with a motor that has almost 5000N of peak thrust and has not seen any deformation or issues.

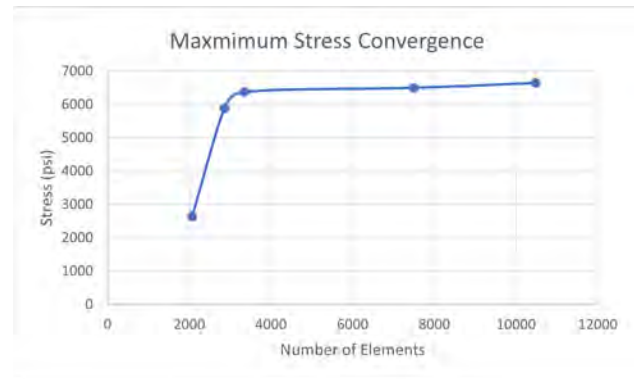


**Fig. 44** Convergent analysis through refinement of mesh around concentrated stress loads



**Fig. 45** Thrust plate attachment



**Fig. 46** Interface between Retainer, thrustplate, and motor mount tube

### C. Recovery Subsystems

Recovery is one of the most important parts of the flight, and often the hardest to get right. For this reason, our recovery system is made to be as simple and as reliable as possible. We are using techniques that are proven not only by the high power rocketry community but also from many test flights by our own team. We conducted four successful flights with this setup in 2022, two successful L3 certifications, and four successful flights this year with this combination of parachutes, recovery harnesses, and ejection charges with a very low failure rate. This experience and simplicity

allow the recovery system to be integrated quickly and easily and allow the focus to go to other more complicated parts of the rocket.

### *1. Recovery Devices and Shear Pins*

Parachutes for Karkinos were chosen based on manufacturer-rated descent rates, packing volume, and previous experience by the team. After burnout, Karkinos weighs approximately 67 lbs. The team has used Recon Recovery and Skyangle Cert3 chutes in the past and is very familiar with folding and packing them into 6 in. airframes. For this burnout weight, the Cert3XXL from Skyangle was the best fit for a safe descent. This parachute is sized for a rocket weighing between 60 and 130 lbs for a safe descent of 17-25 ft/s [2]. With our rocket on the low end of this scale, Karkinos lands at a speed of 20 ft/s, however this will be slightly faster at the higher altitudes at Spaceport America. This was the same parachute that was used for our competition rocket in 2022, and we knew from experience that it could fit in the 6" diameter by 18" space of our main recovery tube. This parachute is also readily available and more economical compared to others in its size class, which is especially important if it needs to be replaced. For our drogue parachute, the team selected a 24" parachute from Recon Recovery. We have used this parachute as a drogue on multiple large 6" rockets including our competition rocket from last year as well as two L3s. Previously we have found rockets to descend around 90 ft/s with this parachute, and that is consistent with this year's flights. It is important that the rocket descends at a high speed under drogue to minimize drift. This makes recovery much easier, especially on the east coast where trees can be an issue.

During flight, Karkinos has three separate separation/ deployment events. At apogee, the rocket separates in half and deploys the drogue parachute. At 1,700 ft, the nosecone of the rocket is ejected and the deployable payload is released five seconds later. Finally, at 1,000 ft the main parachute is deployed. Each of these sections are held together with shear pins to prevent premature deployment both during descent and ascent. Between the drogue section and primary Ebay there are four 4-40 nylon shear pins. Not only could the drag on the fin can cause premature separation at burnout, but our Air Brake system is also producing up to 150 lbs of drag in a worst-case scenario, so it is necessary to retain these sections together. Each 4-40 shear pin provides around 50 lbs of shear force, which means 200 lbs of force total are required to separate that section. The nosecone is held together with two 4-40 shear pins. This section does not have much force trying to separate it in flight, so it is held together with the minimum amount of shear pins. Having only one shear pin could cause the coupler to jam in the airframe, so two are used to keep the forces symmetric. While smaller shear pins could have probably been used here, it is simpler to keep everything the same across the rocket to minimize the number of unique parts necessary and streamline assembly. The nosecone Ebay is held to the main airframe tube using six 4-40 shear pins, for a required total shear force of around 300 lbs. Because of the heavy 9 lb payload in this section, these shear pins keep the inertia from separating the Ebay if the drogue line snaps taught.

### *2. Flame Protection*

Since the black powder is being used for deployment events, the parachutes, harnesses, and electronics need to be protected from the high heat of the charges. All of our harnesses are made from kevlar, which is naturally flame resistant. It can withstand many ejection charges without weakening like a nylon harness. Since our parachutes are made primarily of nylon, they require extra protection to prevent melting or burning. This is done by wrapping the parachute in a nomex blanket. The drogue parachute uses a 24" x 24" blanket while the main uses a 30" x 30" blanket. Both parachutes are wrapped like a burrito, which protect the parachute and shroud lines entirely and allows it to slide easily into the airframe. Once deployed, the blanket easily unravels and lets the parachute inflate.

Both electronics bays are protected primarily by the bulkheads on either end, but there are pass-through holes for charges as well. These holes are partially sealed by the e-match wires, and the remaining space is covered with a piece of electrical tape. This prevents the hot gas from passing through the ebay, potentially damaging the electronics and venting the pressure leading to no deployment. In the nosecone, since there isn't a coupler interface with the top bulkhead, there needed to be an alternative way to seal the payload from the ejection charge. The top bulkhead has a layer of adhesive foam around the outer edge. When the nosecone is slid over the coupler, the foam is compressed sealing the top of the nose cone from the rest of the compartment. The charge that is wired in this section is similarly

sealed with electrical tape.



**Fig. 47 Main parachute wrapped in nomex with lines Z-folded**

### *3. Recovery Harness*

Karkinos has four sets of recovery harnesses throughout the rocket. Starting from the aft end, two 7 ft sections of 7/16" tubular kevlar rated for 3,600 lbs [3] are connected to the forward centering ring of the fin can form a y harness. These cords are routed through the Air Brake via two carbon tubes and then figure eight knots are tied at each end. A quick link connects both of these to the primary drogue harness. The drogue harness is made up of two 35 ft 7/16" 5300 lb tubular kevlar sections from OneBadHawk in series [4]. There are multiple reasons our drogue shock cord is so long, primarily because of the very heavy nosecone. When the drogue charges fire at apogee, we want to avoid the nosecone coming out too fast and snapping the shock cord taught. This shock can cause the nosecone Ebay shear pins to break, deploying the main at 10,000ft. A longer shock cord lets drag slow down both sections of the rocket, greatly reducing the forces of the shock. A long shock cord also helps keep the sections of the rocket further away during descent which minimizes the chance of sections hitting each other and causing damage. The final reason for a long shock cord is an issue specific to East Coast flying. While MDRA has a fairly large recovery area, there are multiple large patches of trees surrounding the launch site. Especially if there are high winds, which is common for the eastern shore of Maryland, our rocket can end up drifting out of the recovery area and into trees. This occurred for 3 out of our four test flights this year and two of those times our long shock cord let us recover the rocket from the trees. Unfortunately, even a long shock cord can not always help and the recovery of our third test flight required hiring tree climbers to cut the harness and recover the rocket. These kevlar harnesses have three loops, and the drogue parachute is connected to the middle loop on the forward harness. The main harness is made up of one 7/16" 35 ft. harness from OneBadHawk. This is connected from the forward end of the Ebay to the aft of the nosecone Ebay bulkhead. The main parachute is connected to the end of the cord instead of the middle of the cord here. We have found on test flights that letting the main parachute be the top of all the sections falling prevents it from tangling during descent. The final section of the shock cord is between the top of the payload and the nosecone tip. The nosecone needs to separate so that the payload can be deployed, but everything needs to stay together so that another section does not need to be tracked. These two sections are connected by 15 ft of 1/4" tubular kevlar rated for 3,000 lb. This section does not encounter any major recovery forces and the goal is to get the nosecone away from the rocket so that the payload can deploy cleanly without tangling.

When packing the drogue and main into the rocket, both harnesses are z-folded together. This is accomplished by making multiple bundles throughout the shock cord and using painter's tape to hold them together as seen in 47. This makes packing it into the airframe much cleaner and also helps provide some shock absorption by ripping the tape off.



**Fig. 48 Karkinos descending under its main parachute**

#### *4. Recovery Attachment*

Recovery mounting for Karkinos starts in the fin can. There are two 1/4-20 steel threaded rods running through the three centering rings and out the aft end of the rocket. These threaded rods are tightened with nuts to each centering ring and then epoxied in place. On the forwardmost centering ring, a 1/4-20 steel eye nut rated for 3750 lbs was then screwed on and epoxied in place on top of both threaded rods [5]. While these eye nuts are rated for much higher loads than other components, they were the only ones with a small enough form factor that could fit between the motor mount and airframe without interference. Last year's competition rocket used much larger "eye nuts" instead which made it very difficult to connect and disconnect the Y harness. This is necessary to do if the kevlar becomes damaged and needs to be replaced. The Y harness then connects to the eye nuts using 1/4" steel quick links rated for 1,200 lbs [6]. These quick links are connected to the y harness with a Figure-8 knot. We have used this knot many times over multiple rockets

and have found it to be very resilient. While we have not found it to have a tendency to untie itself during flight, it is wrapped a few times in electrical tape to keep it all together. After passing the Y harness through the Air Brake module, Figure-8 knots are tied on that end and a 5/16" steel quick link rated for 1,700 lbs is used to connect the Y harness to the drogue harness [7]. Since the drogue harness is made up of two 35 ft. lengths, both sections are connected with another 5/16" quick link. A 1/4" quick link is used to connect the drogue parachute and nomex blanket at the middle loop of the forward drogue harness, and then the end is connected to the aft end of the electronics bay with another 5/16" quick link. Both electronics bays in this rocket have " U bolts rated for 1,075 lbs on their bulkheads for recovery attachment [8]. The main follows the same pattern of quick links and U bolts as the drogue harness with the exception of the nosecone e bay and main switching which loop they are connected to. At the top of the payload frame, there is an adapter plate. A 1/4" eyebolt is secured to the middle here and a 1/4" quick link connects it to the payload shock cord. On the other end, another 1/4" eyebolt is secured to the nosecone tip and kept in place with high strength threadlock.



**Fig. 49 Y harness mount in fin can**

### *5. Parachute Deployment System*

All deployment events on Karkinos are done using 4F black powder charges. The team has lots of experience with black powder and it is by far the easiest and simplest method to deploy parachutes. Charge sizing for Karkinos was primarily based on charge sizes from our 2022 competition rocket, which had similar ejection volumes. They were then adjusted based on our four test flights. The charge sizes for this rocket are the following:

- Main Primary: 6g Swiss 4F Black Powder
- Main Backup: 7g Swiss 4F Black Powder
- Drogue Primary: 7g Swiss 4F Black Powder
- Drogue Backup: 8g Swiss 4F Black Powder
- Nose cone: 2g Swiss 4F Black Powder

The charges are made using nitrile glove fingers and electrical tape. The black powder is first measured and placed into a gloved finger and then an ematch with leads shunted is inserted. The glove is then twisted around the ematch wire and secured with a piece of electrical tape. More electrical tape is then tightly wound around the glove radially and axially until it is hard and cannot be squeezed. We have flown to 10,000 ft with these charges multiple times and have not had any issues with parachute deployment. Since the rocket is not at a very high altitude, the black powder can fully combust, producing gases that pressurize the air frame sufficiently to overcome the shear pins.



**Fig. 50 Charges prepared for flight**

## **D. Avionics**

### *1. Commercial Deployment Computers and Battery Selection*

Karkinos uses three Altus Metrum EasyMinis in total, two for the main and drogue parachute and one to deploy the nose cone. These were primarily chosen based on the team's familiarity with them. They have been the default choice for many of our certification and test flights for two years and have been very reliable for us. They are very simple and low profile so integrating them into an electronics bay is easy and leaves lots of room for other components such as GPS or custom avionics. However, one of the major disadvantages of the EasyMini is that it only contains a barometer for data collection during flight. This does not provide nearly enough information that we would like for post-flight analysis such as tilt angle, acceleration measurements, and roll rate which can be very helpful to not only take an in-depth look at our flight but also tweak our various other flight computers on the rocket. In previous years, we solved this by using an Altus Metrum TeleMega. In theory, this flight computer has all the sensors and features that we are looking for, however, we have found its reliability to be very questionable. In the 2021-2022 year, we flew two TeleMegas in our rockets. At some point, the first one became unusable as the accelerometer stopped working and would not calibrate. The second TeleMega flew in our competition rocket three times flawlessly, and then at SAC 2022, its barometer completely failed and deployed the drogue parachute a few seconds after motor burnout. In addition to our own issues with the TeleMega, we have also heard from multiple other teams and individuals about their own issues with the flight computer and as a result have stopped using them. Instead, we decided it would be safer to use two simpler, more reliable flight computers and develop a separate avionics system instead which will be discussed later. All of the EasyMinis on Karkinos use 400 mAh batteries specifically made for Altus Metrum flight computers. EasyMinis are very simple flight computers and do not draw lots of current, which makes small batteries perfect for them. While we have not tested the full battery life of an EasyMini on this battery, we have found it to be more than enough for launch operations. On our second flight,

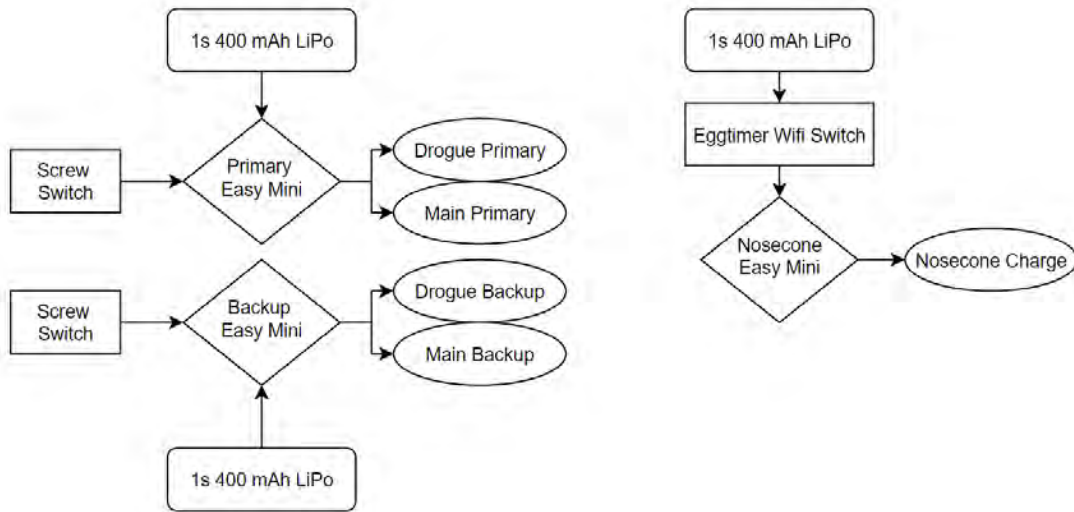


**Fig. 51 Wiring diagram for COTS flight computers**

our EasyMinis were still beeping 3-4 hours after launch until we were able to pull the rocket out of a tree to turn them off. We have also flown the same batteries without charging them between flights as the voltage on the battery had not decreased much from nominal. Our Featherweight GPS trackers also run on 400 mAh batteries. This is the size that comes in stock from Featherweight, and according to their website can last up to 16 hours on one charge. The TeleGPS uses an 800 mAh battery made for AltusMetrum devices. Since the power draw on the TeleGPS is likely higher than the EasyMini due to radio transmissions, it was decided to use the next largest battery size for this device.

## 2. Commercial Tracking

GPS tracking on Karkinos is completed by a Featherweight GPS and AltusMetrum TeleGPS. The deployable payload also has its own Featherweight GPS so that it can be found once it lands. The tracking solutions for Karkinos have changed drastically over the year. Originally, we had planned to use TeleGPSs on our rocket and payload for our primary tracking and a ComSpec radio beacon as a backup. Unfortunately, both of these products became very difficult to obtain. AltusMetrum has had major supply chain issues with many of its products leading to redesigns. While other units with GPS such as the Telemega and Telemetrum came back in stock, there has been no news about new TeleGPSs. Luckily we still have one, but with no way to replace it, we needed other options. We had planned to use ComSpec radio beacons because of their simplicity and robustness. There is no need for a GPS lock or complicated telemetry, it just needs a battery and then it works. The person running ComSpec retired earlier this year and stopped producing trackers and receivers. While there are other radio beacons on the market, such as the LL Electronics XLF series, they are much more expensive and you can instead buy a Featherweight GPS for \$10 more. We also attempted a flight with a BigRedBee 70cm GPS unit, however, its large size and difficult user interface meant it was abandoned in favor of the Featherweight GPS. Our multiple test flights with the Featherweight GPS have worked very well and we have received good tracking data throughout the entire flight.

## 3. SRAD Avionics

The goal of the SRAD avionics board is to be able to perform the telemetry and data logging for the flight that a COTS flight computer and GPS can normally perform and is added to the rocket as a redundant flight system for data logging and telemetry. A system overview is pictured below in Fig. 53.

Device	TeleMega	version 1.9.9	serial 8193
Flight	2		
Date/Time	2022-04-02	20:18:36 UTC	
Maximum height	2401.8 m	7880 ft	
Maximum GPS height	2376.0 m	7795 ft	
Maximum speed	239.2 m/s	785 fps	Mach 0.7
Maximum boost acceleration	103.6 m/s <sup>2</sup>	340 ft/s <sup>2</sup>	10.56 G
Average boost acceleration	71.5 m/s <sup>2</sup>	235 ft/s <sup>2</sup>	7.30 G
Ascent time	3.6 s boost	18.8 s coast	
Drogue descent rate	27.7 m/s	91 ft/s	

**Fig. 52 Flight summary from our third test flight**

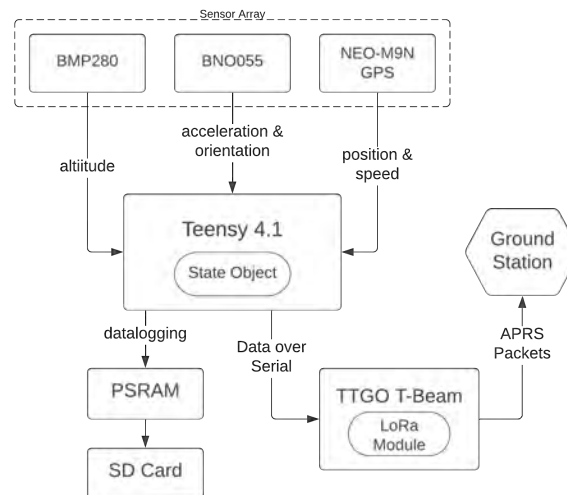


**Fig. 53 System overview of the different parts of the SRAD Avionics**

**Sensor Array** A variety of sensors and other components are used to collect data for the rocket’s flight. An Adafruit BMP280 barometer breakout board is used as an altimeter, which gives the altitude by measuring air pressure and converting it into height. The Adafruit BNO055 breakout board is then used as a 9-DOF sensor that is used as an accelerometer and gyroscope and transmits data over the  $I^2C$  protocol. These breakout boards were chosen due to their relative reliability in measuring accurate data, as well as for their ease of integrating into the system, due to the standards and documentation Adafruit provides.

In order to receive GPS positional data, a Sparkfun NEO-M9N GPS breakout board is implemented into the flight computer. This breakout board is centered around the u-blox M9 engine GNSS receiver chip. We chose this GPS because with it being based on a NEO-M9N chip, it can be configured to be in Airborne mode, preparing it for the high-velocity situation of a rocket launch, as well as for giving high-accuracy position details. This board has a 1 Hz refresh rate for checking if it has received a full NMEA sentence from its satellites, which is then simplified to UBX data to avoid transmitting NMEA noise over  $I^2C$  to the microcontroller. This packet is then parsed and extracted for data on fixed quality, satellites in use, latitude, longitude, velocity, and time, which is then recorded or transmitted by

the PSRAM and the radio module.

A Teensy 4.1 is used as the main microcontroller for the computer to handle all this sensor input, estimate the rocket's state, and then feed the data to the radio module for transmission. The Teensy was chosen for the large number of pins it provides that can be used to handle the sensor data, as well as for its processing capabilities as a micro-controller, helping to avoid backlogging and delays.

### PCB Overview

To combine all the sensors with the microcontroller we decided to create a custom PCB, which was done for the benefits it has. A custom PCB simplifies electrical assembly and allows for better organization of breakout boards, as well as reduces the space taken up by physical connections. In addition, a PCB is more reliable than wired connections and minimizes assembly error. An electrical schematic of the final PCB is shown below in Fig. 54.

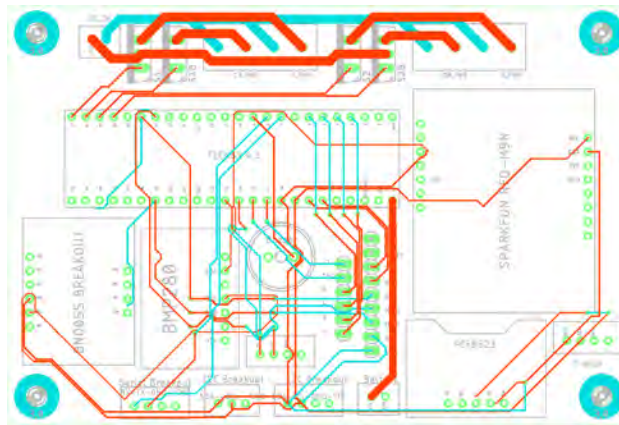


**Fig. 54 Schematic of routes and pads for the PCB**

### Data Storage

In order to store data collected by the sensors, an 8 MB PSRAM chip is used for short-term storage during the flight, with the data then being offloaded to a Micro SD card for persistent storage. Since writing data directly to the SD card is relatively slow and may be blocking to the sensors, it's first transmitted to the PSRAM chip where the data is stored in a buffer until the board detects that the rocket has landed or it has been 20 minutes from launch, whichever comes first, at which point it will transmit the data to the SD card through the SDIO protocol where it is stored in a CSV file for retrieval. The rocket's state is recorded and written to the PSRAM every 100 milliseconds, so as to be often enough to have a good data set, yet not so often that it is storing redundant data or is blocking the execution of the sensors. In order to prevent meaningless pre-launch data from filling up the PSRAM, a rolling buffer is used to hold 10 seconds worth of data, which is then dumped to the PSRAM upon launch.

### Battery

The Tenergy 4.8 V battery pack was selected as the power source for the flight computer due to voltage, runtime, and ease of use. Each of the main components of the flight computer that this battery would power are listed in Table 15 below. This battery pack runs at 4.8 V, which meets the operational requirements for all our components, and has 2 Ah of charge, which will provide around 15 hours of runtime on standby and around 9.5 hours of runtime when in use, which meets the needs of the flight computer.

### Telemetry

For telemetry transmission from the rocket, we selected the TTGO Meshtastic T-Beam V1.1, primarily because it uses a SX1278 LoRa module and has an integrated battery holder. The SX1278 allows the module to transmit in the Ham radio frequency range using the LoRa (Long Range) protocol, which is capable of longer range than other methods

**Table 15 SRAD Avionics Components Current Draw**

<b>Parts</b>	<b>Idle Operating Current (mA)</b>	<b>Max Operating Current (mA)</b>	<b>Idle Power Consumption (mW)</b>	<b>Max Power Consumption (mW)</b>	<b>Operating Voltage (V)</b>
Teensy 4.1	100	100	500	500	5
BNO055	0.4	1.23	1.44	4.43	3.6
Sparkfun NEO-M9N GPS	31	100	116.6	360	3.6
BMP280 Barometric Pressure Sensor	0.325	7.20	7.2	7.2	3.6
<b>TOTAL</b>	<b>131.9</b>	<b>209.0</b>			

while using low power. The radio module itself is running custom firmware that takes in data from the flight computer over a standard Serial connection using a custom packet-based protocol for minimal overhead. It then formats this data for APRS transmission and sends it to the SX1278 over SPI using separate third-party libraries. The module is set to transmit on 433.775 MHz with 20 dBm transmit power, a spreading factor of ten, a 125 kHz signal bandwidth, and a coding rate of 4/5, all of which were chosen to optimize transmission range. The custom firmware is also capable of quickly changing frequencies or other settings in case of a conflict with other teams. The radio module is powered using a 18650 3700 mAh Lithium-ion battery. Based on an average power draw of ~55 mA measured by the AXP192 power management chip on the radio module, the radio should have over 67 hours of battery life.

Data from the radio module onboard the rocket is first received by a separate TTGO Meshtastic T-Beam V1.1 on the ground. We chose this board for the ground station receiver because, since it is the same as the transmitter, we were already familiar with it. This board is connected to a 70 cm Yagi antenna to improve signal range and reliability over the included antenna for longer distances. Once it receives a transmission, the module then deconstructs the APRS message using the same third-party library used for encoding, and the data is sent to a connected computer over USB Serial using the same custom packet-based protocol used by the onboard radio module and the flight computer. A custom ground station application programmed in Node.js and running on the computer is connected to the receiver’s Serial port and saves the received data to a CSV file on the computer. It then displays the data in a GUI that includes live altitude, speed, heading, stage, and position data, along with a live graph of altitude and speed, and a map with a marker that represents the rocket’s current position. If there is an issue with the GUI, the program also has a text-based output for the data, and the radio displays transmissions on the attached OLED.

**Test Flight Results**

The entire SRAD avionics system has been test flown twice, with the second test flight being a successful one where the system was proved to work. During this test flight, radio transmissions stayed in contact throughout the duration of the flight, effectively range testing the radio up to 9,800 ft, with the distance between the radio transmitter and ground station at its maximum at apogee (9,570 ft in altitude and 2090 ft along the ground). The onboard sensor array also yielded useful data for characterizing the rocket’s flight. As seen by the plot of altitude and vertical acceleration versus time in Fig. 55, key moments can be identified as to represent stages in the rocket’s flight, which is then leveraged by the onboard sensor-detection code. The initial peak in acceleration represents the transition from powered ascent to coasting, the zero acceleration occurs at apogee, and the spike in acceleration and change in velocity indicates main deployment.

*4. Sled and Mounting*

All electronics are mounted to a 3D-printed PETG sled. This sled has guides for the two threaded rods to keep it stationary within the electronics bay. The flight computers are mounted with brass standoffs to the sled and batteries have printed enclosures to keep them from moving. The screw switches are mounted to the sides of the sled on shelves and also have their own standoffs. The switches are placed so that they are close to the coupler wall and they are easy to turn on once the rocket is on the pad. PETG was chosen for the sled as it is more temperature resistant than PLA and we have seen PETG work well for rockets in high-temperature environments. In order to fit both the commercial and

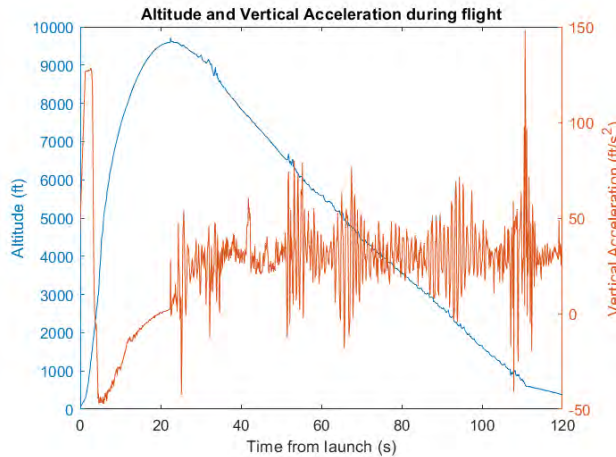


**Fig. 55 Plot of SRAD board recorded altitude and acceleration during a Karkinos test flight**

custom avionics within the electronics bay, the sled had to be made in two parts in order to fit on our 3d printer. Since the sled is not a structural component of the rocket, its strength is not critical. One of the major difficulties with this sled is spacing the various radios properly. During the first iteration of the sled, the SRAD avionics antenna and BigRedBee antenna were basically on top of each other on opposite sides of the sled. Since they are both on the 70 cm band, major interference meant we did not get good telemetry during the flight. This was fixed by moving the devices around and they are not on completely opposite sides of the sled pointing in opposite directions, which has worked well during our testing.

### 5. Avionics Testing

While avionics were primarily tested via flight tests, the EasyMinis were also tested on the ground to verify functionality after potential damage. During the third flight of Karkinos, the rocket landed in a tree and could not be recovered by the team from the ground. A tree climber needed to be hired to recover it which took about a week from the launch. During this time there were some rain showers, so we wanted to confirm that the flight computers still worked properly. Both EasyMinis were turned on and placed in a vacuum chamber. The vacuum was then turned on, held for five seconds, and released. We then confirmed that the "flights" on the altimeter recorded a pressure change and "fired" the charges.

### E. Air Brake

Karkinos comes equipped with an Air Brake module to increase its performance to reach a desired apogee. The module is a drag-modulating closed-feedback system to vary the drag of Karkinos to allow it to reject the many uncertainties that cannot be accounted for in simulation such as motor thrust uncertainties, tilt angle off of the pad, and wind conditions.

This project was started during the 2021-2022 academic year and has continued up until the 2023 SAC. Much of the development was discussed in the 2022 Terrapin Rocket Team Technical Report, "Team 9 Project Technical Presentation to the 2022 Spaceport America Cup". The only items discussed in this report are the current year's development and analysis as well as items deemed critical to the understanding of the system.

#### 1. Overview

The Air Brake is designed as a separate module in order to minimize the complexity while integrating it with the rest of the rocket. Taking inspiration from traditional Ebays the Air Brake's casing is a 10" long 6" airframe tube and a 22" in length 6" coupler. This design was chosen over the lighter design of building the Air Brake into the frame of the rocket for two main reasons. First, due to its complexity, there was a significant chance that part or all of the Air Brake



**Fig. 56 Air brake module**



**Fig. 57 External CAD of the Air Brake module.**



**Fig. 58 Internal CAD of the Air Brake module.**

would not be certified as flight ready. In this scenario, it was important to have a contingency plan to allow Karkinos to still compete at the 2023 SAC without Air Brakes. Since it is designed to be modular a boilerplate with the appropriate fairings would be able to be manufactured very quickly to get Karkinos to be flight ready in time for the competition. Secondly, this multi-year project will outlive the specific competition rocket that it flies on. To reduce the manufacturing time and cost a modular design allows us to fly with the Air Brake on a much wider array of rockets. In fact, the current Air Brake has flown on three different rockets this past year.

There are two common designs for the control surfaces of Air Brakes: the first are plates that extend out of the rocket body perpendicular to the airflow, and the second are flaps that start parallel to the rocket body and rotate upwards into the flow. Although the first design is usually smaller and less massive, we chose the second design since it is considered to be safer. The aerodynamic forces on the second design will force the flaps into the inert position thereby reducing the chances of undesired external moments on the rocket.

## *2. Deployment Mechanism*

The deployment is achieved by a stepper motor. The motor displaces an actuator disk which is connected to four threaded rods. The actuator disk has two channels that restrict the disk to only move in the vertical direction. The rods are connected on their other end to a control horn connected to the flaps. As the disk is displaced down it rotates the flaps into the airflow. The entire assembly is coupled so that the flaps are mechanically locked to each other and are

therefore guaranteed to deploy to the same angle; figs. 59 to 61 shows various deployment configurations.

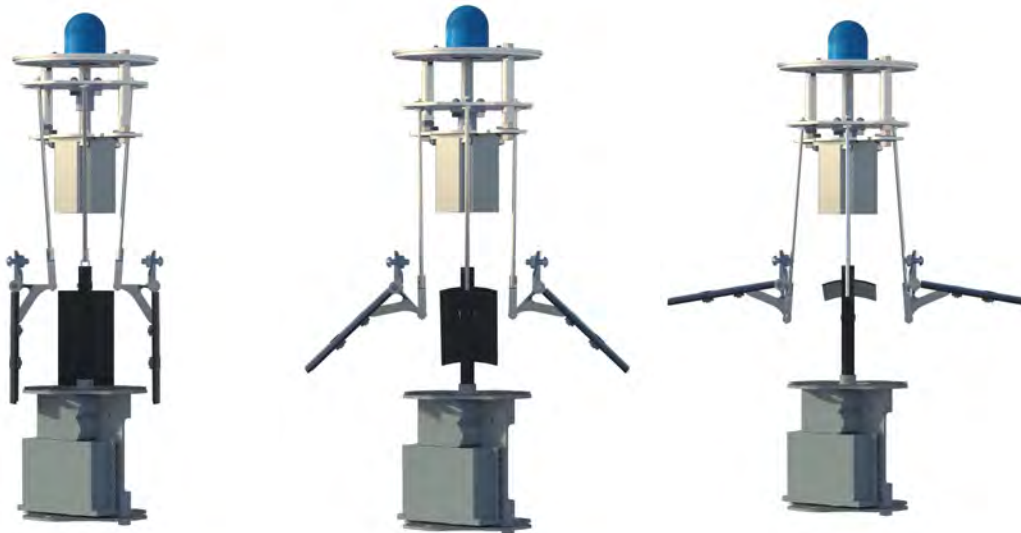


**Fig. 59 Flaps fully retracted**    **Fig. 60 Flaps deployed to 45°**    **Fig. 61 Flaps fully deployed**

### 3. Air Brake Structure

The structure of the Air Brake module is inspired by standard electronic bays in high-powered model rockets. The Air Brake frame is, similar to the construction of the main body tube and couplers, a student-made, hand-rolled fiberglass airframe, made by rolling seven layers of fiberglass cloth and epoxy resin, shown in Fig 64. Fiberglass was chosen because it is very strong and stiff while being lightweight and inexpensive. To make the Air Brake coupler, a section of the Air Brake frame was sliced the length of the tube, shown in Fig 62 and squeezed inside the airframe section. A strip of fiberglass was epoxied on the seam, and another layer of fiberglass cloth was added to the coupler to ensure a better fit in the Air Brake frame. Two  $\frac{1}{4}$ " aluminum rods connected to bulkheads placed at the top and bottom of the module provide an anchor for the various systems. The cuts in the switch band which house the flap and screw holes for the upper section of flap assembly were cut on a manual mill using an indexing head to allow for precise radial cuts. This switch band then acted as a guide for the cutouts on the coupler which were cut using a Dremel. The external and internal bulkheads were cut from  $\frac{1}{8}$ " aluminum stock using a water jet. There are also two carbon fiber tubes that run the length of the Air Brake. These are to allow passage of the recovery shock cords to run from the fincan to the electronics bay. We wanted the force of the recovery events to bypass the Air Brake but also need the shock cords to not tangle with any of the hardware of the Air Brake. Lastly, we have a few 3D-printed bulkheads and tubes to help with cable management. There are a lot of cables that pass close to moving parts so we designed and added barriers to ensure nothing gets tangled.

The flaps on the previous Air Brake design were manufactured with a high-strength carbon fiber-infused plastic. During one of the flight tests, a flap broke due to the large aerodynamic drag forces right after burnout. To remedy this failure the flaps were redesigned. The hinge and clevis rod are 3D printed out of stainless steel and the flaps are cutouts of a fiberglass SRAD airframe section. The flaps are then fixed to the clevis rod with a pair of screws. To test the strength of the new design a tensile test was performed. A luggage scale was hooked into a slit in the flap and then the pressure was applied to the luggage scale. We managed to apply 100 lbs of force on the flap and it remained undamaged. This is a minimum factor of safety of three but in reality, it is probably much greater.



**Fig. 62** Cutting airframe from coupler



**Fig. 63** Rolling of fiberglass and epoxy resin

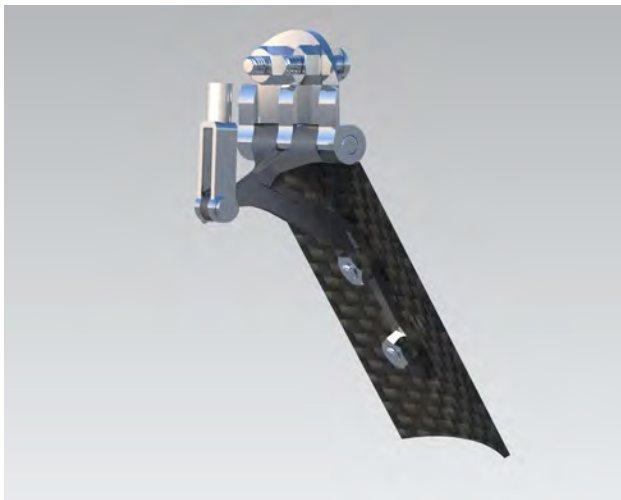


**Fig. 64** Back view of redesigned flaps



**Fig. 65** Front view of redesigned flaps

#### 4. Avionics

**PCB Overview** The Air Brake's printed circuit board measures 3.5" by 2.5", and routes signals between the system's various sensors and computation boards. These components are mounted on one side for easy prototyping, convenience, and because space was not a large concern. Four 0.112" diameter holes interface with the printed eBay via screws. A silk screen outlines the orientation and nameplates for the placement of each component. A local ground and power plane reduce noise and extraneous power from spreading inside the circuit. Our PCB uses two Teensy 4.1 microcontrollers.

This choice was considered based on our ground tests, which saw single microcontroller use as not ideal. Using just one microcontroller substantially strains the processing capabilities since stepper motors constantly require pulsed signals, and we also need computation for vital functions: data collection, state estimation, apogee prediction, and feedback control. By using the primary microcontroller to only process data and send the actuation angle to the secondary Teensy, the Air Brake computer can process data using one microcontroller and actuate continuously through the other. Both microcontrollers communicate via the TX and RX channels.

The main microcontroller collects data from a barometric pressure sensor and IMU. The IMU is oriented along the Y axis of the board, where it will remain near the rocket's axis of symmetry, reducing the measurement of centrifugal forces. While most of the processing components rest on header pins for replacement and convenience, the motor microcontroller is directly soldered to the board. This compromise is necessary to access the flash and SD ports of each microcontroller. Initial flight tests provided more noise than previous boards, which may have been due to interference between each trace signaling. As a result, all traces are now isolated with a 0.015" tolerance between each other. The PCB went through multiple iterations, each reflective of the change in Air Brake priorities. In the future, the team aims to reduce Air Brake complexity and eventually outline an algorithm that facilitates one microcontroller use.

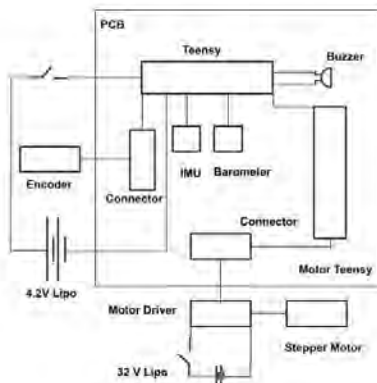


**Fig. 66 Schematic of airbrake computer and actuator**



**Fig. 67 Circuit board, assembled**

### Sensor Data Overview

- Data from the LSM9DS1 (IMU) provides acceleration and gyroscopic data
- Data from the BMP388 (Barometric Pressure Sensor) reports height estimates
- Data from the Encoder allows us to confirm that the position of the flaps matches exactly with our expectations. It also allows us to do error correction after the initial actuation if the flaps are not in the desired position

**Data Storage Overview** To store data from our sensors along with other diagnostic information, we utilize a PSRAM chip for short-term storage and an SD Card for long-term storage. While testing, we noticed that the process of writing to an SD Card is quite slow, but writing to the PSRAM was significantly faster. To take advantage of this finding, we write the flight data to the PSRAM before copying the data to the SD Card after the flight computer determines the recovery event has occurred. The data on the SD Card is in a CSV format for easy importing into MatLab and Microsoft Excel for analysis.

**Offloading of Actuation** Along with data collection, the Teensy is tasked with using the sensor measurements to determine how much actuation is required for the Air Brake flaps. While we could actuate from the Teensy directly, the process of stepping the motor causes a critical slowdown in sensor collection, we therefore use a second Teensy 4.1 to step the motor driver. The actuation information is transmitted as the number of motor steps away from the desired actuation and is communicated through a Serial connection.

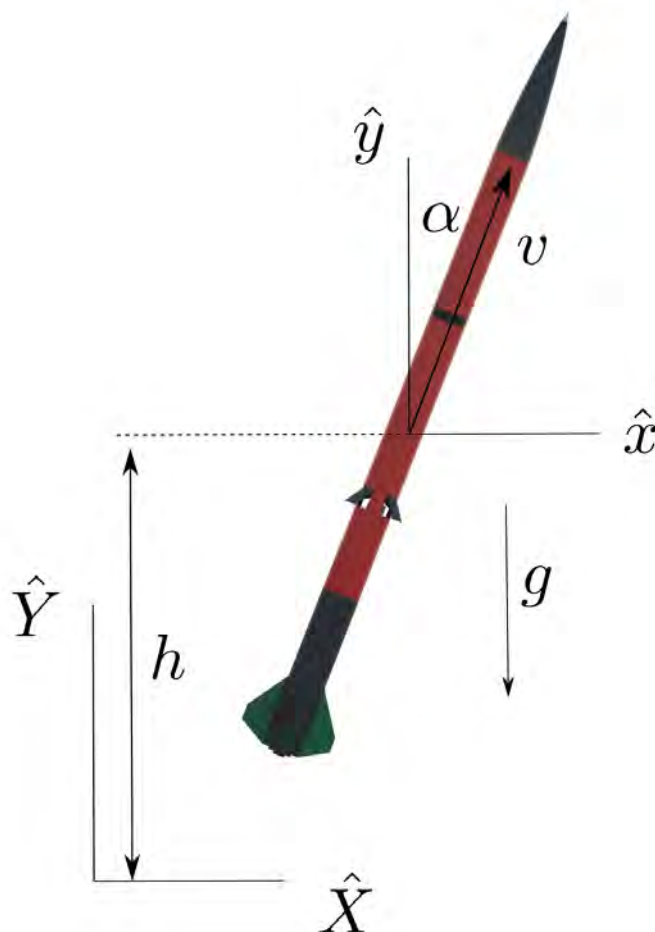


**Fig. 68** The relevant states: height,  $h$ , velocity along body-axis,  $v$  and tilt off the vertical-axis,  $\alpha$  of the closed-loop altitude control system and inertial axis

**Main Computer Code Breakdown** On the main Teensy, the code consists of a setup process that initializes and calibrates the sensors as well as a control loop that repeatedly polls data that feeds into a state machine. A block diagram of our system is in Figure 66.

Before launch, sensor data will be written directly to the SD Card until our pre-programmed launch conditions are met. Once the launch condition is met, sensor data will be written to our PSRAM chip instead, and we will calculate the desired actuation angle for transmission to the Teensy actuation controller. We will also watch for a pre-programmed condition to determine when the first recovery event has occurred. Once triggered, the contents in PSRAM will be copied to the SD Card. Sensor data will continue being written to the SD Card until the power is turned off.

**Actuation Controller Code Breakdown** The Teensy actuation controller operates in a loop of polling for desired actuation angles from the primary Teensy. When the motor Teensy actuation controller receives a number of motor steps away from the desired actuation, it will actuate accordingly. Not all steps are completed in one sequence, so the desired actuation can change mid-sequence and the controller will account for that. The number of steps received from the primary Teensy is based on the desired actuation and encoder values, so the secondary Teensy can be sure that the data

received is the exact number of steps from our desired actuation. We also send the value multiple times to prevent issues related to data corruption along the Serial transmission line. If the primary Teensy detects any off-nominal behavior it will command the Teensy to fully retract the flaps and remain closed.

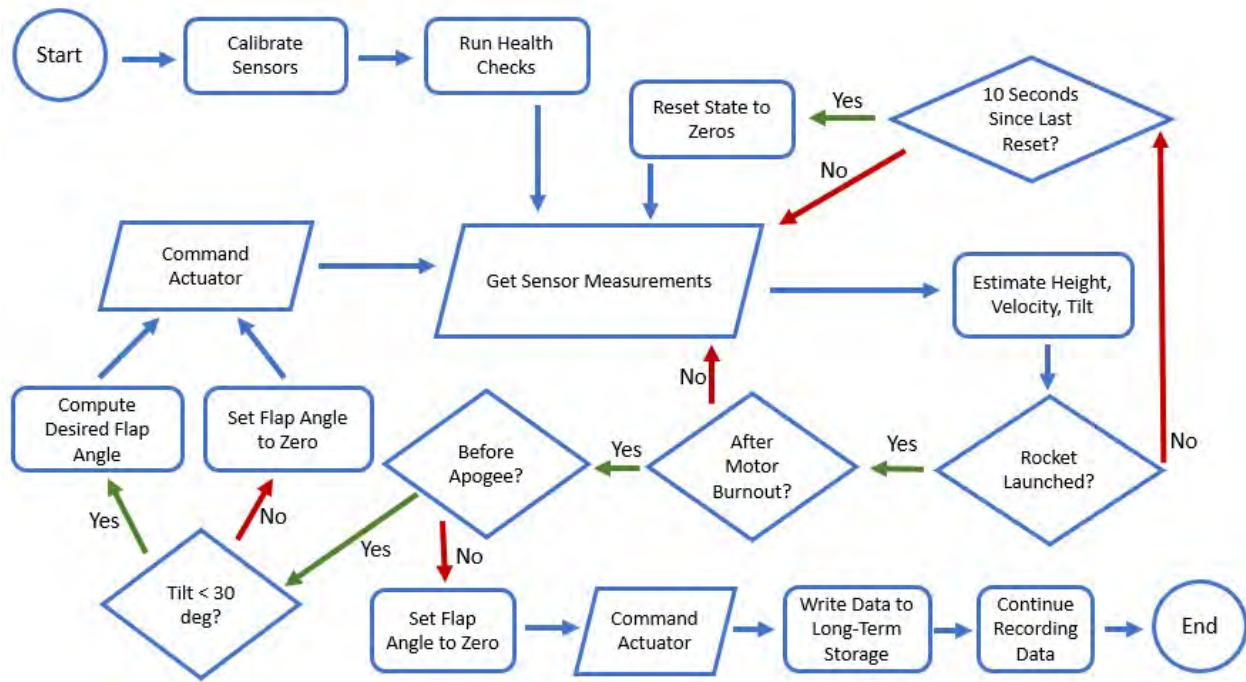


**Fig. 69 State machine flow chart of the Air Brake flight computer**

Figure 69 shows a flow chart of the main parts of the flight computer process.

### 5. State-Estimation

**Kalman Filter** An important aspect of a closed-loop control system is obtaining *state-feedback*. In our case, the state  $\mathbf{x} = [h, v]^T$ , where  $h$  is the height of the rocket and  $v$  is its velocity along its longitudinal axis. To this effect, we use a Kalman filter (KF) as our state estimator. A Kalman Filter serves a dual purpose — estimating state feedback and filtering sensor noise.

The Kalman filter comprises of two steps: *predict* and *update*. It uses the system’s process model and prior state to *predict*, and sensor measurements to *update* the prediction, obtaining a "filtered" estimate of the state. The filter is a linear, discrete-time, optimal estimator that assumes uni-modal Gaussian noise. In practice, with proper parameter-tuning, Kalman filters are sufficient for most systems with micro-electro-mechanical sensors (MEMS).

Sensor data obtained from the accelerometer ( $a_m$ ) and barometer ( $h_m$ ) are used to drive the process model. The tilt of the rocket,  $\alpha$  is estimated in a separate process, as described in the subsequent section. The Kalman Filter assumes the tilt to be already estimated and uses it as one of the inputs. The state variables are as illustrated in Fig. 68, and the corresponding state equations in discrete time are as follows:

*Process model:*

$$\begin{bmatrix} h \\ v \end{bmatrix}_{k+1} = \begin{bmatrix} 1 & T_s \cos \alpha_k \\ 0 & 1 \end{bmatrix} \begin{bmatrix} h \\ v \end{bmatrix}_k + \begin{bmatrix} \frac{T_s^2}{2} (a_m \cos \alpha_k - g) \\ T_s (a_m - g \cos \alpha_k) \end{bmatrix} + \omega_k \quad (13)$$

$$\mathbf{x}_{k+1} = \mathbf{F}_k \mathbf{x}_k + \mathbf{u}_k + \omega_k$$

*Measurement model:*

$$\begin{aligned} \begin{bmatrix} h_m \end{bmatrix}_k &= \begin{bmatrix} 1 & 0 \end{bmatrix} \begin{bmatrix} h \\ v \end{bmatrix}_k + \mathbf{v}_k \\ \mathbf{z}_k &= \mathbf{H}_k \mathbf{x}_k + \mathbf{v}_k \end{aligned} \quad (14)$$

where,  $T_s$  is the sampling time,  $a_m$  is the component of the acceleration along the axis of symmetry of the rocket, measured from the accelerometer,  $g$  is the acceleration due to gravity, and  $k$  indicates the time-instance.  $\omega$  and  $v$  are normal-distributed Gaussian noise with covariance matrices  $Q$  and  $R$  respectively.  $R$  is a scalar and  $Q$  is defined as [9],

$$Q = q^2 \begin{bmatrix} \frac{T_s^2}{2} & \frac{T_s^3}{3} \\ \frac{T_s^3}{3} & \frac{T_s^4}{4} \end{bmatrix} \quad (15)$$

where  $q$  is the random noise in the accelerometer. In practice, both  $R$  and  $q$  were tuned with flight data. The actual Kalman filter algorithm can be found in many common textbooks.

**Tilt Estimation** Although the tilt should ideally be implemented into the aforementioned state estimator and incorporate all nine measurements from the IMU (three each from gyroscope, accelerometer, and magnetometer), a more simple scheme was tested and shown to work for our specific application.

The body-fixed frame  $\mathcal{B}$  of the rocket can be described in terms of a  $ZYX$  rotation from the inertial frame,  $\mathcal{I}$  using a rotation matrix,  $R_{zyx}$ . The yaw, pitch, and roll rates are measured from the gyroscope in the IMU. For small angles, we can formulate the propagation of the rotation matrix as,

$$R^{k+1} = R_{zyx}(g_z T_s, g_y T_s, g_x T_s) R^k, \quad (16)$$

where  $g_i$  is the measured angular-rate about axis- $i$ ,  $T_s$  is the sampling time, and  $k$  is the time-instance. Since we can initialize the rotation matrix to the identity matrix on power up, this enables us to fully describe the orientation of the rocket at any given time. From the rotation matrix, we can compute the rotation angles,  $\theta_1$  and  $\theta_2$ , about the two axes perpendicular to the rocket as [10],

$$\theta_1^k = -\sin^{-1}(R_{13}^k) \quad \theta_2^k = \tan^{-1}\left(-\frac{R_{12}^k}{R_{11}^k}\right) \quad (17)$$

Where  $R_{ij}^k$  is the  $i$ - $j$ th component of  $R$  at time  $k$ . Note that this is only valid as long as  $\alpha < 90^\circ$ . This is not a limitation since when  $\alpha$  is close to  $90^\circ$ , the flight is past a nominal flight so the Air Brake will have already been triggered to an inert state. We can then compute the tilt as

$$\alpha^k = \sin^{-1}(\sqrt{\sin^2 \theta_1^k + \sin^2 \theta_2^k}). \quad (18)$$

**Calibration** The only additional calibration is a *bias-correction* for each of the measurements. After powering up, we first dump a few hundred measurements as we wait for the sensors to reach a steady state. We then average the next few hundred measurements and use this quantity for correcting the bias in the subsequent measurements. Due to simplifying assumptions such as zero-mean Gaussian noise, linear process model, etc., and other unmodelled disturbances, the estimated states are expected to drift while on the pad. To counteract this effect, the computer resets the state to zero every ten seconds if it does not detect a launch.

Fig 70 shows the estimated state as Karkinos sits on the pad ready for launch. The drifts in the estimated height and velocity are deemed low enough for our feedback-loop requirements. The drift in the tilt starts at 0.06 degrees per second and becomes almost 0.3 degrees per second close to motor ignition. This is presumed to be caused by the (small) "random-walk" drift of the gyroscope readings. However, due to the periodic *zeroing-out*, the maximum drift we

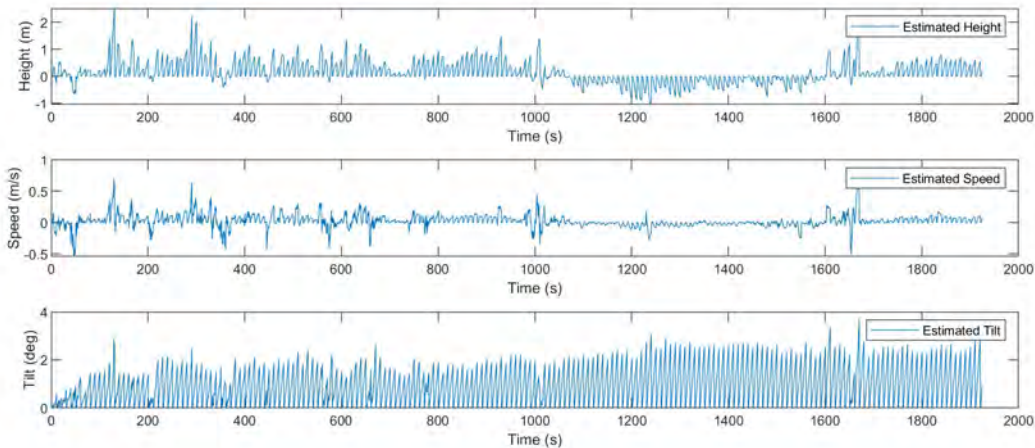


**Fig. 70** The estimated state of Karkinos as it sits on the pad. A small drift is apparent in the state estimator. The estimator resets the state to zero every 10 seconds if it does not detect a launch.

encounter is  $3^\circ$ . In the future, we plan to explore dynamic calibration to counteract this effect.

**Verification And Validation** The calibration and estimator were first synthesized and developed in MATLAB using simulated data. Once we were satisfied with the preliminary results, we took raw sensor data from a few flights on small-scale rockets and post-processed them with our Matlab implementation. Finally, we ran the estimator onboard during the flight and saved the estimated states. Post-launch, we compared these *in-flight* estimates to Matlab post-processing on the raw data and demonstrated that, within precision bounds, they match.

To validate our estimator design, we compared our estimated state to those of some commercial flight computers that flew onboard the rocket as well, figs. 71 to 73 show various flight-curves from our estimated states compared against those estimated by commercial flight computers.

**Barometric Error Correction** One of the many challenges to the feedback-control design of Air Brakes is the fluctuations in barometric pressure around the rocket as the flaps are deployed. Since the altitude measured using the barometer is hugely significant to the Kalman filter, large non-zero-mean noises considerably degrade the estimator’s performance. Figure 75 shows the barometric height from the SRAD flight computer and the commercial flight computer that was housed in the Ebay during a flight with flap deployment. It is evident that when the flaps open they cause a decrease in pressure around the Air Brake sensor-suite, and therefore cause an increase in the raw height measurements. The figure also shows that there is a monotonic positive relationship between the flap angle and the “overestimated” height from the barometer.

We observe this behavior in the commercial flight computer too, but to a lesser extent since the commercial flight computer is located much farther away from the flaps. This error is especially concerning since this will cause instability in the controller performance. The flaps will initially deploy if it predicts an overshoot. This will cause the measured height to increase and then the controller will predict an even higher apogee, deploying them farther, thus resulting in a catastrophic positive feedback loop.

Due to the requirement for an expedient, minimum viable solution to this problem, a data-driven heuristic was explored. Though usually an error correction is applied directly to the barometric pressure, we attempt to correct the reported height instead. We model the measured height at any given time as,

$$h_r = h + f(h, v, \delta), \quad (19)$$

where  $h$  is the true height,  $h_r$  is the height as reported from the barometer, and  $f(h, v, \delta)$  is the error in the height

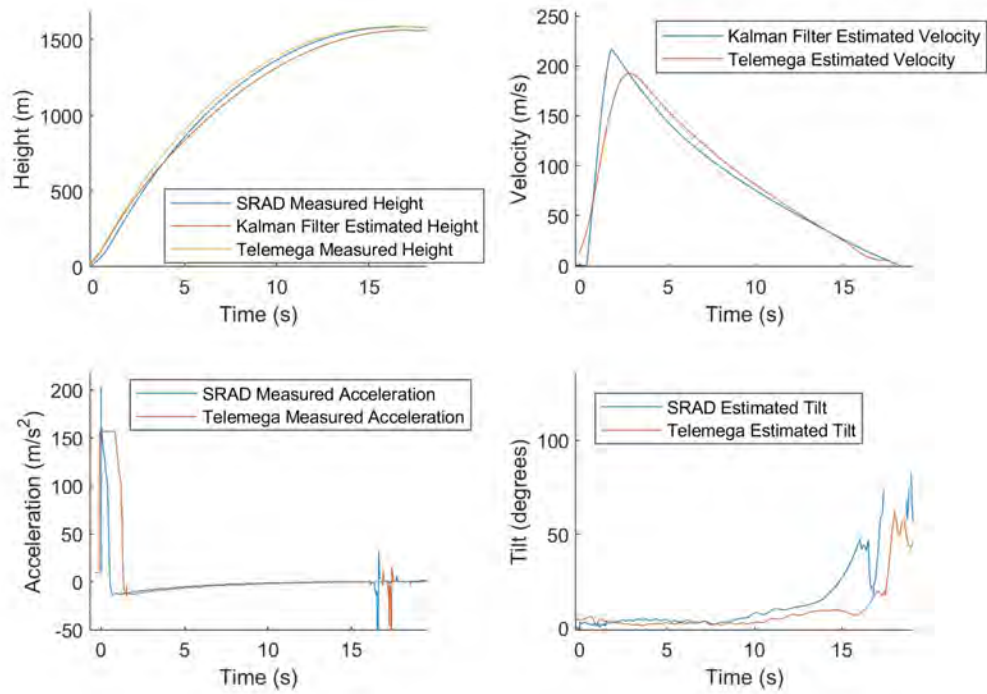


**Fig. 71** The estimated states from the flight computer compared to a commercial flight computer (Telemega) for the Blue Rocket. (Launch date: 3/5/23)

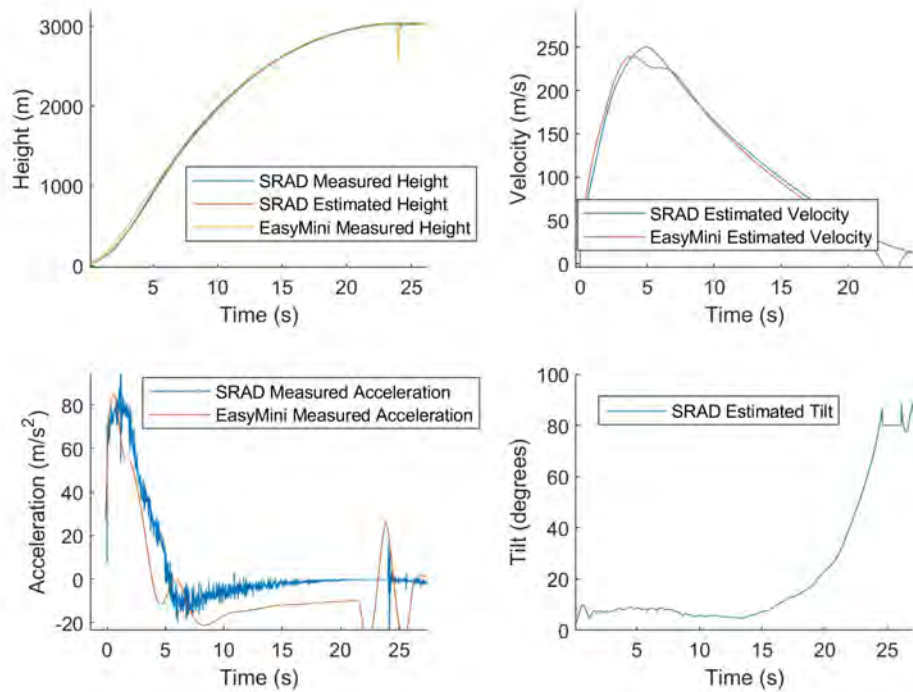


**Fig. 72** The estimated states from the flight computer compared to a commercial flight computer (EasyMini) for the Icarus Rocket. (Launch date: 4/2/23)

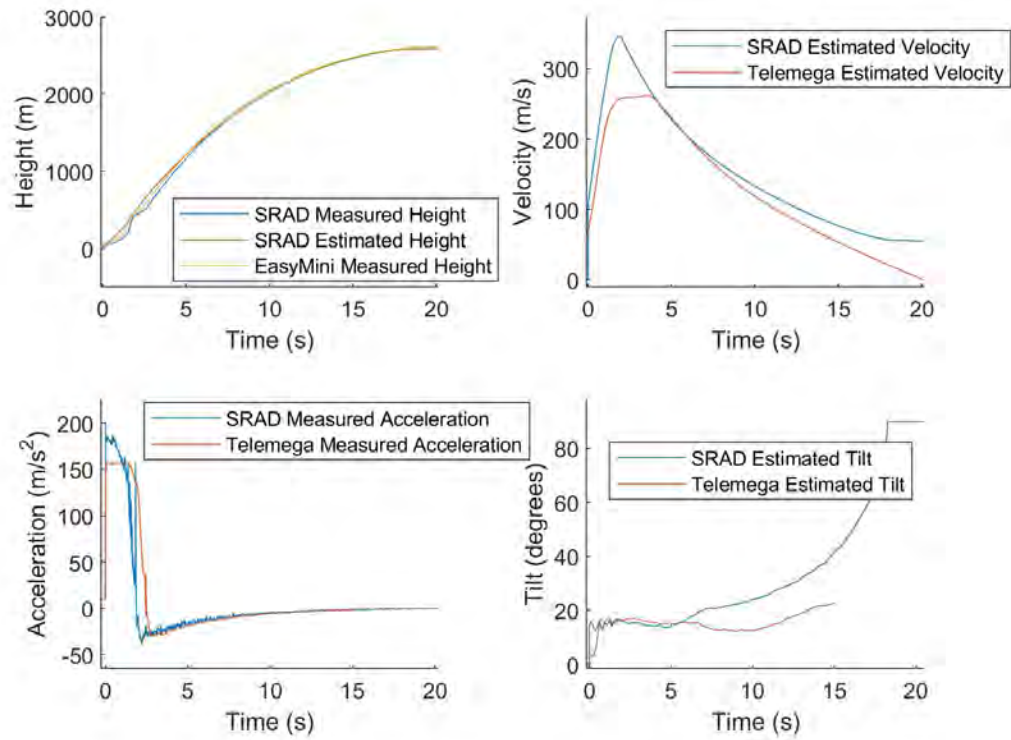


**Fig. 73** The estimated states from the flight computer compared to a commercial flight computer (EasyMini, Telemega) for the Blue Rocket. (Launch date: 4/2/23)



**Fig. 74**  $\delta$  is defined as the flap deployment angle

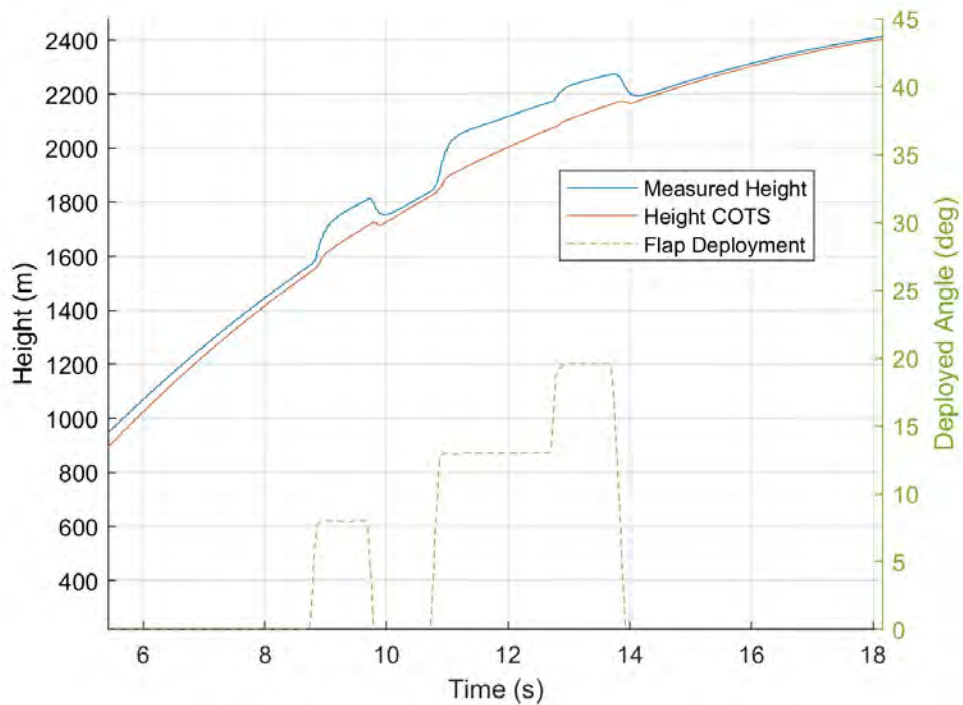


**Fig. 75 Barometric sensor reading error while flaps are deployed**

measurement and is a function of true height, velocity, and flap deployment angle. Deployment angle  $\delta$ , is illustrated in Fig. 74.

Figure 76 shows a *wind-tunnel test* with  $v_\infty = 50 \text{ m/s}$  plotting the reported height from the barometer that was housed inside the Air Brake module. The average pressure in the wind tunnel did not change significantly during the test but the local pressure near the barometer was clearly decreasing as the flaps opened. Figure 77 illustrates all of the wind tunnel tests with the reported error as a function of deployment angle.

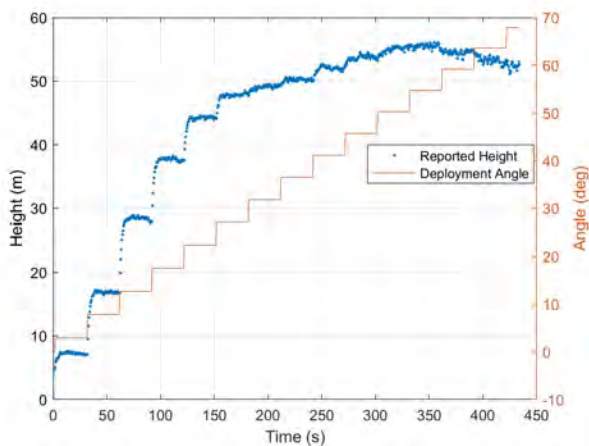


**Fig. 76 Barometer height reading while in the wind tunnel with  $v_\infty = 50 \text{ m/s}$**

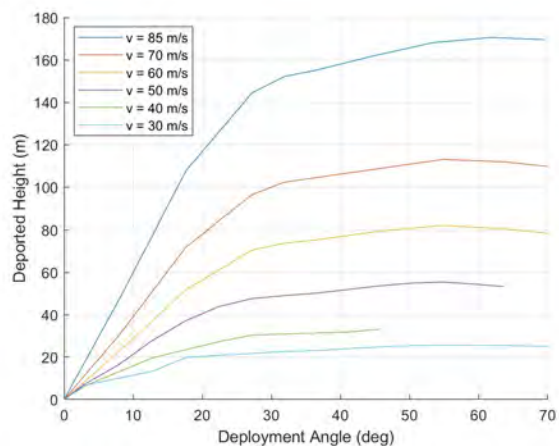


**Fig. 77 Height error curves from all wind tunnel tests**

Upon careful inspection of the data and trying out a few error models, the following error model gave us the best

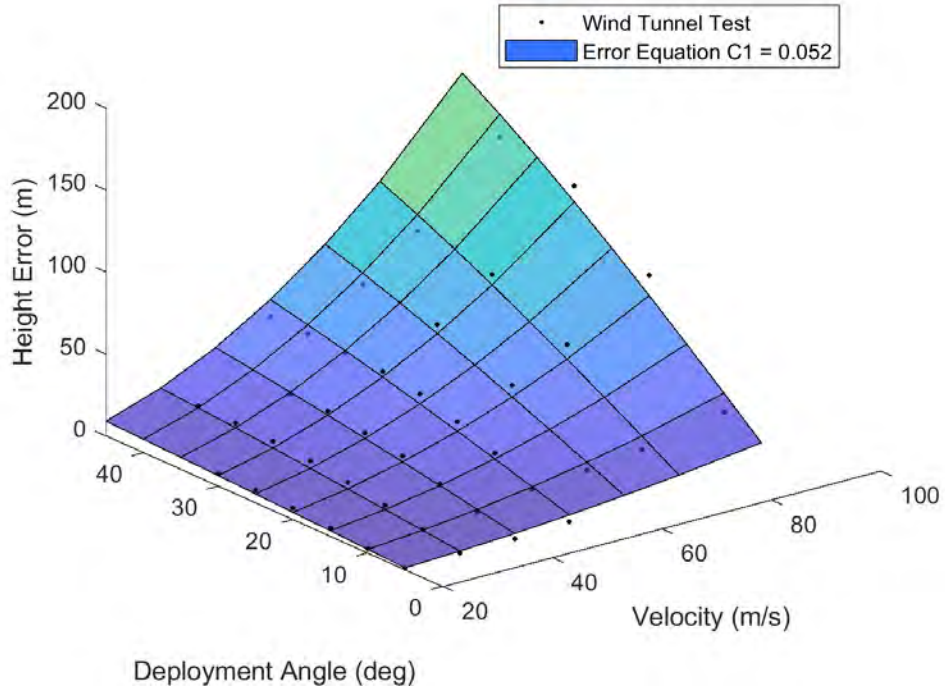


**Fig. 78 Surface fit of our error function to the wind tunnel barometer height recordings**

function fit without overfitting,

$$f(h, v, \delta) = \begin{cases} cq \sin \delta & \delta < 45^\circ \\ cq \sin 45^\circ & \delta \geq 45^\circ \end{cases} \quad (20)$$

where  $q = \frac{1}{2}\rho v^2$  is the dynamic pressure and  $\delta$  is the flap deployment angle. We identify the parameter coefficient,  $c$  by fitting this error function to data from wind tunnel tests. Using a standard least square method, we estimate  $c = 0.052$  with an  $R^2 = 0.97$ . Figure 78 shows the wind tunnel data used for fitting and the surface plot using Eq. 20 with  $c = 0.052$ .

Using this error model, we first correct the height error before sending it to the Kalman filter. Figure 79 shows the reported height as well as the height after the error correction using Eq. 20. It is clear from the plot that although the steady state corrected height is usable there is a transient time that is significant and Eq. 20 does not capture it. The assumption is that there are some complicated aerodynamic effects that take time to settle. A low pass filter was chosen as a candidate to pseudo-capture these effects. The simple time-independent low-pass filter does not work since the bandwidth of the filter is dependent on the sampling time and in our case, it is the underlying physics that we are trying to capture. With this consideration, we choose a filter defined as,

$$\Delta_{k+1} = (1 - \alpha)\Delta_k + \alpha f(h, v, \delta)_k \quad (21)$$

$$\alpha \equiv \frac{T_s}{T_s + \tau} \quad (22)$$

where  $\Delta_k$  is the value subtracted from the reported height at time  $k$ ,  $T_s$  is the sample time, and  $\tau$  is the time constant.  $\tau$  is then tuned using flight data and a value of  $\tau = 0.15$  is chosen. Figure 80 shows the flight with the corrected error using this low-pass filter. **To reiterate the novelty of this method, we are able to correct for the complicated aerodynamic effects on a commercial barometer with just two tunable parameters:  $c$  and  $\tau$ .**

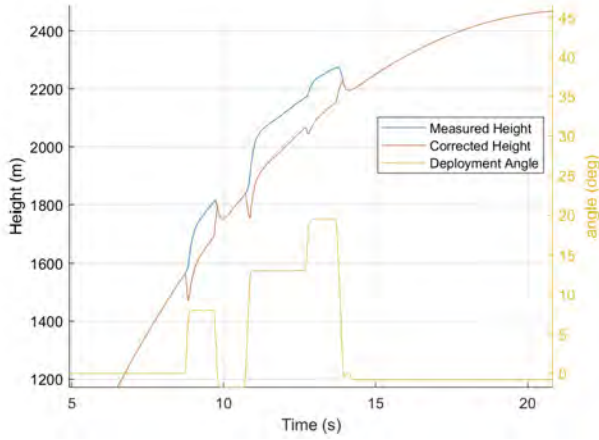


**Fig. 79 Height error correction without the low-pass filter**

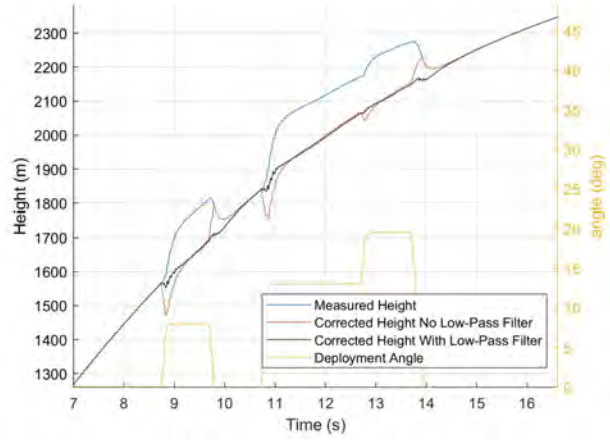


**Fig. 80 Height error correction with and without the low-pass filter**

This error correction scheme was implemented on the full-scale flight test of Karkinos. Figure 81 shows both the height and speed estimated states. The measured height is extremely perturbed due to the change in pressure around the rocket after flap deployment. The blue solid curve is the estimated height if we did not run any error correction on the reported height and only used our Kalman filter. It is clear that this estimation has a significant error and our controller would most probably have failed and would have saturated very quickly. The increased performance using the low pass filter as defined in Eq. 21 does perform better but the standard Kalman filter is able to mostly correct for the transient period.

## 6. Controller Design

A few different control schemes were considered but a simple form of Model Predictive Control (MPC) was chosen. Since the Air Brake has a limited control domain, a controller that is able to capture much of the flight dynamics is attractive. Model-free PID controllers were seriously considered but behaved poorly in simulation. Another major benefit of our MPC-based control is that it has few parameters and no gains to be tuned. The Air Brake is expensive to full-scale test so getting sufficient flight data sets to properly tune gains is not feasible.

The planning horizon of the MPC is chosen in the velocity space instead of the standard time domain. The MPC plans until velocity goes negative, indicating apogee. To simplify the planning optimization, a static control angle constraint is applied to the planning algorithm. At each controller iteration, the MPC predicts the apogee for various sample flap angles assuming that the Air Brake will hold that sampled flap angle for the rest of the flight, and chooses the best flap angle that will get the rocket closest to the desired apogee.

There are three main assumptions about the dynamics of the rocket. First, the angle of attack is always zero; second, the rocket's flight is constrained to a plane; and third, the drag of the rocket body and flaps are decoupled. The second assumption is valid from rocketry experience and the third from wind tunnel tests. With these assumptions, the equation of motion during the rocket's coast phase is,

$$m\ddot{\mathbf{r}} = -\frac{1}{2}\rho(4C_{d_f}A_f(\delta) + C_{d_R}A_R)\dot{\mathbf{r}}^2\hat{\mathbf{r}} - mg\hat{\mathbf{y}}, \quad (23)$$

where  $m$  is the mass of the rocket,  $\mathbf{r}$  is the position vector,  $\rho$  is the local air density,  $C_{d_f}$  is the coefficient of drag of the flaps,  $A_f(\delta)$  is the effective surface area of the flaps and is a function of the flap angle,  $C_{d_R}$  is the coefficient of drag of the rocket body,  $A_R$  is the reference area of the entire rocket, and  $g$  is the acceleration due to gravity. The constant '4' appears in the equation since there are four flaps in our Air Brake.

Note that  $\dot{\mathbf{r}}^2 = \dot{\mathbf{x}}^2 + \dot{\mathbf{y}}^2$ . Using the three assumptions mentioned before and further assuming that  $\rho$  is locally

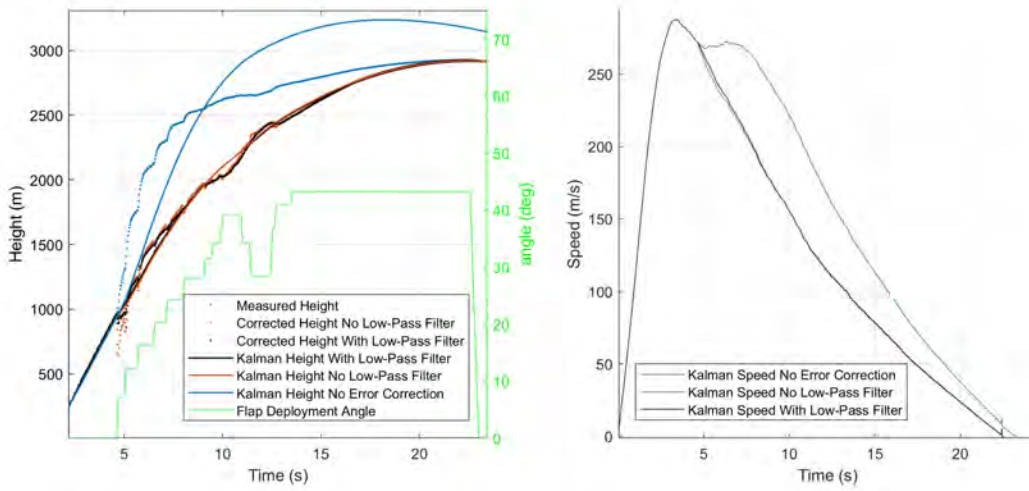


**Fig. 81** Estimated states from the Kalman filter with various type of measured height inputs — uncorrected/corrected, with/without low-pass filter

constant, we can write out the equations of motion as,

$$\ddot{\mathbf{y}} = -\frac{1}{2m}\rho(4Cd_fA_f(\delta) + Cd_RA_R)\dot{\mathbf{y}}\sqrt{\dot{\mathbf{x}}^2 + \dot{\mathbf{y}}^2} - g, \quad (24)$$

$$\ddot{\mathbf{x}} = -\frac{1}{2m}\rho(4Cd_fA_f(\delta) + Cd_RA_R)\dot{\mathbf{x}}\sqrt{\dot{\mathbf{x}}^2 + \dot{\mathbf{y}}^2}. \quad (25)$$

At any point in the flight, we can forward integrate Eq. 24 and 25 with the initial conditions being the current state to obtain apogee-predictions. The initial conditions are computed from the state estimates obtained using Kalman filter,

$$\begin{bmatrix} \mathbf{x} \\ \dot{\mathbf{x}} \\ \mathbf{y} \\ \dot{\mathbf{y}} \end{bmatrix}_0 = \begin{bmatrix} 0 \\ v \sin \alpha \\ h \\ v \cos \alpha \end{bmatrix} \quad (26)$$

where  $h$ ,  $v$  and  $\alpha$  are the estimated height, velocity, and tilt of the rocket at the current time. Using this formulation we can define an apogee predict function  $\mathcal{P}$ ,

$$h_{max} = \mathcal{P}(h, v, \alpha, \delta) \quad (27)$$

The function takes in height, velocity, tilt, and a flap deployment angle and integrates Eq. 24 and 25 until  $\dot{\mathbf{y}} \leq 0$  (descent-phase). Recall that  $\mathcal{P}$  assumes a constant  $\delta$ . It returns  $\mathbf{y}(h_{max})$  at the time instance when  $\dot{\mathbf{y}}$  first becomes negative as the predicted apogee. Equation 27 was implemented with a second-order Runge-Kutta integrator since it gave a sub-meter precision compared to the more standard fourth-order but runs a bit faster on the resource-limited flight computer.

Using  $\mathcal{P}(h, v, \alpha, \delta)$ , the MPC-based planner determines the *optimal* flap-angle,  $\delta$  that will result in  $h_{max}$  being close to the desired apogee. We use a binary search method with a  $5^\circ$  resolution to search over the space of control inputs (flap-angles). To verify the veracity of  $\mathcal{P}$ , we flew the flight computer on a rocket without actuating the flaps and computed the predicted apogee during the coast phase assuming  $\delta = 0$ . Figure 82 is the flight of Karkinos from March 5th, 2023. It was Karkinos in its full configuration with the flaps of the Air Brake turned off. The yellow curve is the output of Eq. 27 during the coast phase. Figure 88 is the error of the predicted apogee function compared to the actual apogee.

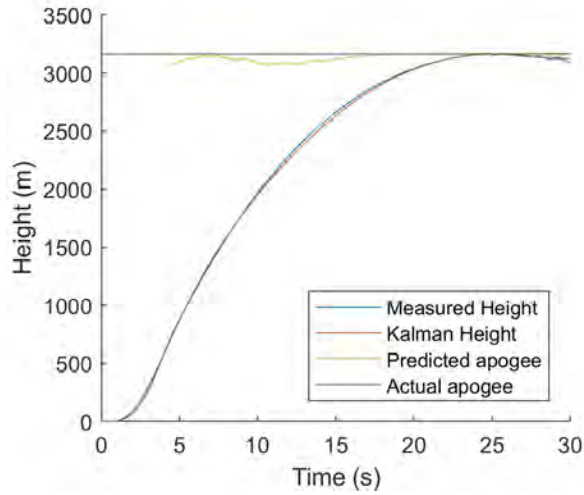


**Fig. 82** Estimated height and predicted apogee in time on the Karkinos flight of March 5th

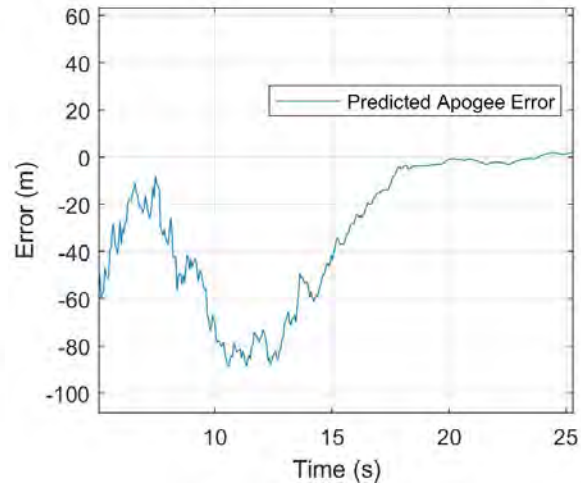


**Fig. 83** Error in the predict apogee function of the controller

### 7. Parameter Estimation

The predict function,  $\mathcal{P}$ , requires the estimation of constants:  $m$ ,  $C_{d_f}$ ,  $A_f(\delta)$ ,  $C_{d_R}$  and  $A_R$  – the mass and drag characteristics of the rocket and the flaps.  $m$  is simply the empty mass of the rocket. It is calculated as the measured wet mass minus the expected propellant mass. Next, consider  $C_{d_R}$  and  $A_R$ . We can obtain estimates of these values from our OpenRocket model but OpenRocket does not have all of the details of the rocket such as surface finish and various exposed hardware. Another option is using a CFD tool to estimate  $C_{d_R}$  but this has the same downside as OpenRocket with the additional issue that our usage of the simulation software is not validated. Lastly, we can use our wind tunnel tests to estimate  $C_{d_R}$ . There are two problems with using the wind tunnel tests: the measured drag includes the model mount and we were unsure how to accurately subtract it out and second, wind tunnel tests are expensive and logistically complicated. So it was determined to not be a long-term solution as rockets designs can change much more rapidly than our ability to run wind tunnel tests. Our solution was to estimate these constants *in-flight* using onboard sensors. The acceleration due to drag without flap deployment is considered. It can be written as,

$$a_D = \frac{1}{2m} \rho C_{d_R} A_R v^2. \quad (28)$$

$a_D$  is precisely what the IMU measures while the rocket is in the coast phase. Given the fact that  $C_{d_R}$  and  $A_R$  only ever appear as a product in our controller equations, we can readily estimate it from Eq. 28 as,

$$C_{d_R} A_R = \frac{2ma_D}{\rho v^2}. \quad (29)$$

In practice,  $a_D$  is generally noisy, so we take the mean of  $C_{d_R} A_R$  over one second of measurements after motor burnout and before any flap deployment. This method was found to be within 15% of the value obtained from OpenRocket.

The drag characteristics of the flaps:  $C_{d_f}$  and  $A_f(\delta)$ , were determined from wind tunnel tests with the assumption that,

$$A_f(\delta) = A_0 \sin \delta, \quad (30)$$

where  $A_0 = 10in^2$  is the approximate surface area of each flap, and  $\delta$  is flap-deflection angle. Using the standard drag

**Table 16 Coefficient of drag of the rocket assuming a 29.9in<sup>2</sup> reference area**

	Wind Tunnel	OpenRocket	In flight sensors	CFD
$C_{dR}$	0.71	0.51	0.58	0.66
Drawback(s)	Includes mount	Missing rocket features	Noisy measurements	Low fidelity model and simulation tool complexities

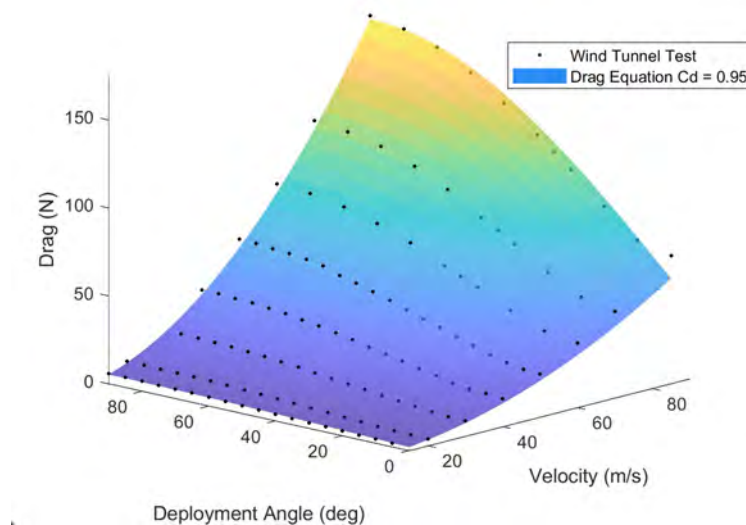


**Fig. 84 Wind tunnel test and resultant fit of the drag equation**

equation and assuming the drag of the rocket and flaps are decoupled, we can write the equation for the total drag as,

$$D = \frac{1}{2}\rho(4C_{d_f}A_0 \sin \delta + C_{d_R}A_R)v^2. \quad (31)$$

This equation was fit using a linear least square method to the data from wind tunnel tests. This method resulted in estimated  $C_{d_f} = 0.95$  with a  $R^2 = 0.996$ . Figure 84 shows the data points as well as the contour fit of Eq. 31 using  $C_{d_f} = 0.95$ .

### 8. In-Flight Tests and Validation

Karkinos had two full integration tests. One on March 5th and the second on April 2nd. We disabled the Air Brake deployment and enabled them on the latter flight. The first flight reached an apogee of 3,164 m or 10,381 ft. For the second flight, we turned on the Air Brake and set the desired apogee to 2,900 m or 9,514 ft. **On the second flight, Karkinos achieved an apogee of 2,922 m or 9,588 ft, an apogee error of just 74 ft!**

To validate our process model, we integrated the rocket state from just after motor burnout according to Eq. 23. We integrated considering the flap deployment profile as recorded on the April 2nd flight and another assuming zero flap deployment. We then compared these two curves with the two actual flight profiles. Figure 85 shows these four curves. **It is clear that the process model is close to the true rocket dynamics and that we shaved off nearly 800 ft to reach our desired apogee!** We assume that the red curve divergence at the beginning of the flight is due to the limitations of our barometric error correction.

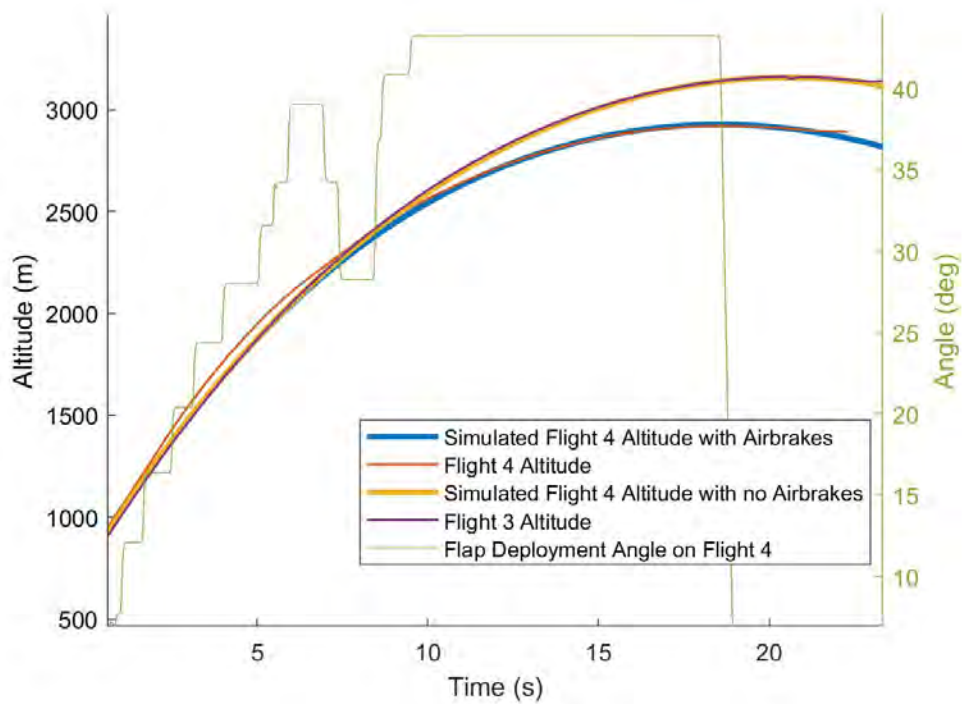


**Fig. 85** The blue and orange curves are the integration of the initial condition of the rocket (flight 4) just after motor burnout. The blue takes into account the drag from the deployed flap angle and the orange assumes no flap deployment. These curves are compared to actual flight 4 (red) and actual flight 3 (purple). Note that flights 3 and 4 were nearly identical except for flight 3 having the Air Brakes disabled.



**Fig. 86 Terrapin Rocket Team members standing near the turbine in the Glenn L. Martin Wind Tunnel**

### *9. Wind Tunnel*

The primary motivation to test Karkinos in a wind tunnel is to properly characterize the drag profile of the flaps and validate our dynamics model. The Model Predictive Control algorithm we use relies heavily on an accurate process model. There are constants in the model that need to be estimated. Furthermore simplifying assumptions such as the body drag and flap drag are decoupled, and  $Cd_f$  doesn't change with flap angle  $\delta$  need to be validated. We were graciously gifted a day in the wind tunnel by the University of Maryland Glenn L. Martin Wind Tunnel. The tunnel test section is approximately 2.5x2.5x6 meters and velocity ranges from 10 m/s to close to 100 m/s.

We first worked with the wind tunnel staff to design and build a mount to install Karkinos in the tunnel. The mount we designed is very similar to a motor mount. It is a hand-rolled fiberglass tube and water jet cut G10 fiberglass centering rings. A COTS fiberglass tube was glued to the centering rings and interfaced with a stinger supplied by the wind tunnel staff. Various components were added/removed from the internal of the rocket to achieve a center of mass near the sting interface. This  $C_G$  was forward of the center of pressure so the rocket was stable in the tunnel.

We set up a test matrix to test various flap angles at varying speeds. We started our test at low speeds to ensure that if damage were to occur we would still have usable data. After obtaining a minimum viable set of data, we ran some smoke tests to obtain nice visuals of the aerodynamics of the flaps. After these initial runs and as time permitted we increased our data set by increasing  $v_\infty$  and deploying to various flap deployment angles.



**Fig. 87** Observation room in the wind tunnel



**Fig. 88** Karkinos mounted in the wind tunnel

### F. Payload

The T.E.R.P payload (Testbed for Ejecting Research Payloads) is a test bed system for releasing objects from the rocket during drogue descent. In addition, this test bed is releasing an experimental system designed to test the controlled movement of a circular parachute. For this document, "vehicle" will refer to all components that are released from the rocket, "release system" will refer to all components involved in integrating the vehicle into the rocket and releasing it at the right altitude, and "payload" or "payload assembly" will refer to the assembly of both of these systems.



**Fig. 89** Payload assembly with a mass stand in vehicle



**Fig. 90** Backside of the payload assembly and connecting bulkheads, with Ebay cover panel removed

### 1. Release Mechanism

**Overview** The goal of the 2022-2023 payload was to develop a system capable of releasing a wide array of vehicles from the rocket to allow for the deployment of more complicated systems in the future. The use of a dedicated releasing system was selected for two reasons. The first and primary reason was to reduce the required weight of the released vehicle, as a lower mass system increases safety and reduces complexity. The second reason was to reduce the complexity of integrating the vehicle into the rocket. A system that bolts in place removes the need for extra payload supports and allows for vehicle integration days prior to the launch, reducing the number of tasks that need to be completed directly before the launch.

The release mechanism was designed under the following constraints: does not use pyrotechnics to release the vehicle, is low profile to maximize the available vehicle footprint within the cubesat standard, is easy to reset, allows for easy integration into the rocket, and works with a wide range of vehicle geometries. The latter most requirement ensures that the system would be compatible with future vehicle designs without knowing what they may look like. It was also necessary as the 2023 vehicle structure had not been finalized by the completion of the release mechanism.

**Mechanical design** To fulfill these requirements, a servo-actuated pin and retention line system was developed. The vehicle is held in place by two lines, each of which connects to a pin at one end. These pins were connected to servo motors, such that turning the motor would pull the pin, releasing one side of each line, and freeing the vehicle. The pins are held in place by pre-tensioned springs to prevent premature release, as seen in Fig. 91. The thin profile of the pin system leaves an 8 cm x 8 cm x 25 cm volume for retaining the vehicle.



**Fig. 91 Pin release system. Left: Pin in standard configuration. Right: Pin mechanism exploded**

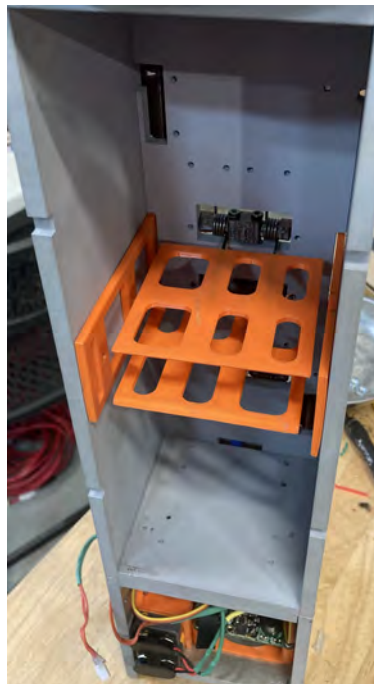


**Fig. 92 Vehicle retention section with torsion springs at zero deformation (note retention lines not present)**

Torsion springs were selected to give the vehicle some distance from the release system given their low profile and better temperature resistance than an elastic system. The springs are mounted such that at zero deformation they extend 8 cm from the back wall of the release system, as seen in Fig. 92. When deformed a total of 90° they provide 4 lbs of force. 4 lbs was selected to ensure the springs were strong enough

to move the vehicle, without putting excessive stress on the retention lines. These springs had the added benefit of tensioning the straps to reduce vibrations. To further prevent lateral movement, shims were added to provide contact with the release system walls. These have the added benefit of providing a gap for the retention lines on both sides of the payload. The retention straps were fabricated out of fishing line, selected for its diameter-to-strength ratio. To ensure the straps could hold the weight of the vehicle and tension from the torsion springs, 8lb line was used. Between the two lines, this provides a safety factor of four. A high safety factor was selected as lateral forces on the vehicle during launch are unknown.

**Avionics** A Teensy 4.1 microcontroller was selected to standardize controller use across the payload, air brake, and avionics teams. A BMP280 pressure sensor provides altitude data to ensure the vehicle is released at the correct point. A BH1750 light sensor was added to ensure the vehicle would not be released should the nose cone fail to separate (nose cone separation is discussed in the Payload Bay section). A BNO055 accelerometer was added to provide more information on the orientation of the nose cone when the vehicle is released. The release system Teensy also has a power and I2C connection to the vehicle avionics, which allows the release system to turn on the vehicle and ensure it is functioning normally. This connection was selected to streamline powering on payload components, as it is difficult to access a switch on the vehicle through the nose cone wall. To aid in processing the data collected by the previously mentioned sensors, a PCF8523 real-time clock was added to provide timestamps. Finally, a buzzer was added to provide audio verification that the system turned on properly. These components are mounted on a custom PCB for ease of wiring. Power is provided by two 9v batteries wired in parallel. These were selected for ease of use, as they can simply be replaced as needed. A 6v linear regulator is used to lower this voltage to a usable level. The release system avionics are mounted with the servo motors below the vehicle retention section of the release system, as seen in Fig. 93. This configuration was selected to provide more room for the vehicle and to raise the release section out of the coupler to better clear the nose cone shoulder.

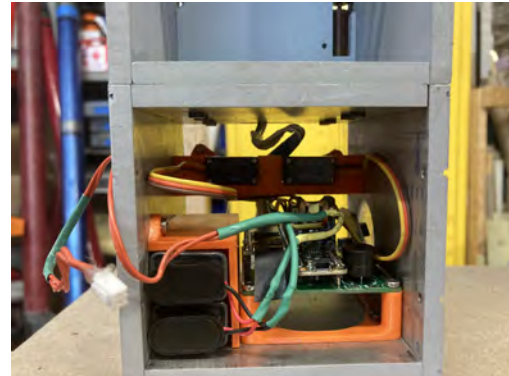


**Fig. 93 Release system Ebay**

**Manufacturing** The structure of the release system was assembled from 1/4" thick 6061 aluminum plates secured by countersunk M3 bolts. This arrangement was proved effective by last years payload; it allows for direct integration into the rocket without the need for external support and helps to meet the weight requirements. To aid in construction, plates were cut on a water jet and holes were drilled and tapped on a drill press with a jig to ensure proper alignment.

## 2. Vehicle Design

**Overview** The primary goal of the vehicle is to act as a repeater station between the rocket and the ground station to aid in receiving telemetry after the rocket leaves line of sight. As the vehicle descends slower than the rocket, it will remain airborne longer and will be able to relay GPS coordinates after the rocket touches down. The secondary goal of the vehicle is to act as a test bed for a drift minimization system, as described later in this section. A diagram of what a basic vehicle separation looks like can be seen in Fig. 95.

**Deployment** To ensure that the vehicle parachute deploys correctly, it is not restrained by the vehicle itself. The parachute is held up against the vehicle by the release system retention lines, on the side of the vehicle that faces the opening. Releasing the vehicle from the rocket also releases the parachute, ensuring that the vehicle either releases with its parachute deployed or does not release at all. As the parachute is released before the vehicle, it will help to pull the vehicle out of the release system. To ensure this added force does not cause the vehicle to jam, the parachute risers connect in the middle of the vehicle. Given the low altitude at which the vehicle is released (under 2,000 ft, just before

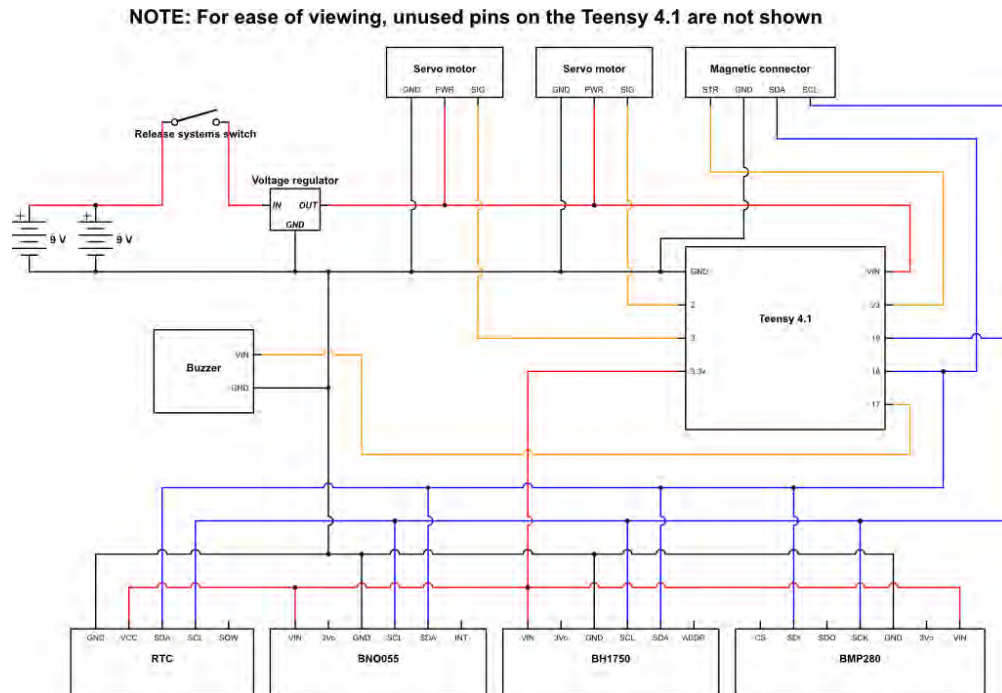


**Fig. 94 Release system wiring diagram**

the deployment of the rocket's main parachute), a two-stage recovery system is not required, allowing for immediate deployment of a single parachute.

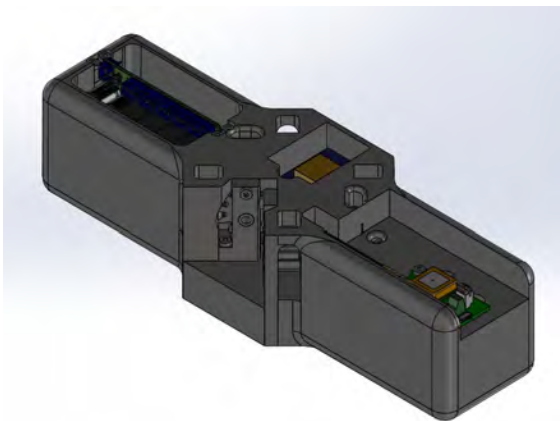


**Fig. 96 Vehicle CAD assembly**

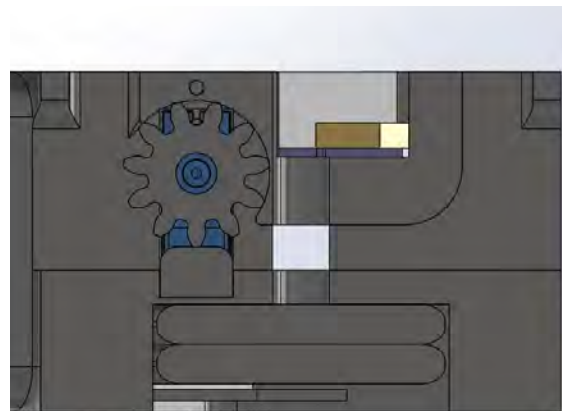


**Fig. 97 Vehicle drift minimization cross section**

**Parachute adjustment** The drift minimization system was based on research by [11], who proved that the descent path of an object of a circular parachute could be adjusted by changing the length of the parachute risers. A similar system was used in the vehicle to aid in recovery. A circular parachute system was selected over a parafoil to reduce the total flight distance should a system fail. A 25" diameter parachute was selected for compatibility with an IRIS 3.1" test rocket. The expected vehicle weight of roughly 1.3 lb resulted in a descent rate of roughly 20 ft/s, which was deemed to be acceptable for providing adequate flight time while still limiting drift without the mitigation system.

The parachute used has four pairs of risers, and opposing sets were connected to each other, forming two loops that cross over in the middle. Each loop runs through a channel in the vehicle frame, and around a drive wheel, as seen in Fig.

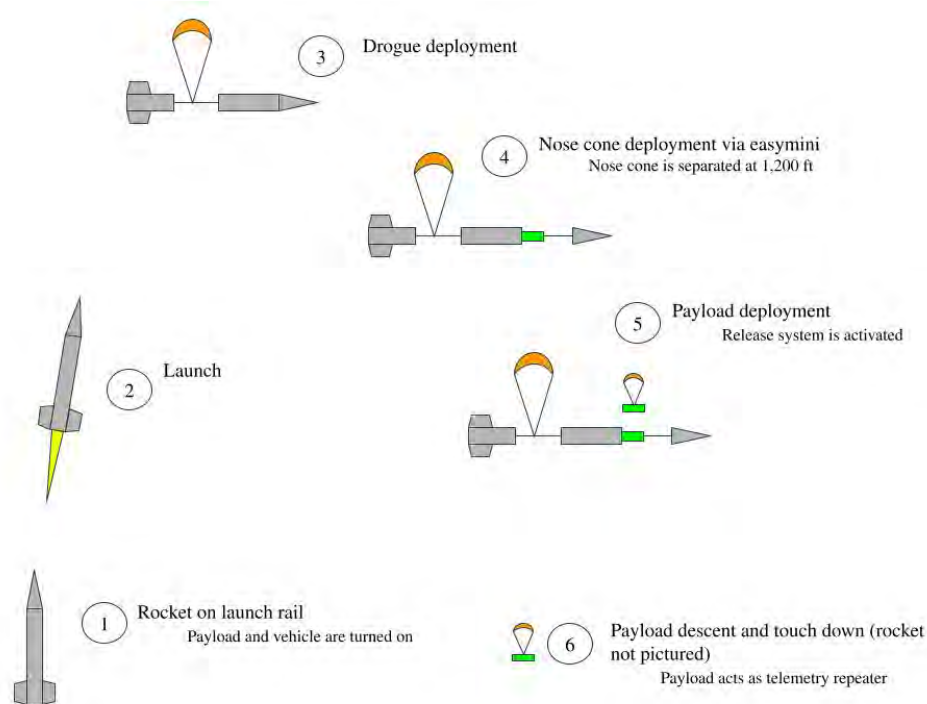


**Fig. 95 Vehicle CONOPS**

97. The drive wheels are powered by continuous rotation servo motors, which allow the vehicle to bias the riser loops in one direction or another. As the two loops are perpendicular to each other, a full range of movement in a 2D plane can be accomplished. The use of loops was selected over actuating each individual riser pair to reduce the force on the servos, as they only need to account for the imbalance in load between the risers, which reduces the required motor power.

**Electronics** Like the release system, the vehicle is controlled by a Teensy 4.1. IMU data is provided by a BNO055, altitude by a BME280, and GPS by a PA1616S breakout. A buzzer is again used to provide an audio cue at power on. The aforementioned parachute system uses two servo motors, the grounds of which are wired through a N-channel mosfet. This allows the motors to be turned off when not in use to save power. The vehicle PCB also has a connection point for a LORA digipeater used with the SRAD telemetry system. This is a purely power connection, as no data is sent to the repeater from the vehicle. Power is provided by two single cell 2000 mAh lipo batteries wired in series. This output is then sent through the same voltage regulator as on the release system before reaching the Teensy and servo motors. The vehicle has 2 N-channel mosfets between the ground of the voltage regulator and the batteries; one is triggered by the release system through the magnetic connector, the other by the vehicle Teensy. In the future this system will be used to turn the vehicle on using a signal from the release system. However, the vehicle is currently turned on with a screw switch prior to the assembly of the rocket to allow the GPS to get a fix. As a result we are currently not using the two N-channel mosfets.

The release system also has a Featherweight GPS module to provide telemetry to aid in recovering the vehicle. The Featherweight module has the added advantage of acting as a relay for Featherweight modules in the rocket, providing a redundant system to the SRAD telemetry. The Featherweight is powered by a 400 mAh battery, and uses an internal switch. Like the vehicle, the Featherweight module is powered on before the nose cone is placed over the release system to gain a GPS fix.

**NOTE: For ease of viewing, unused pins on the Teensy 4.1 are not shown**

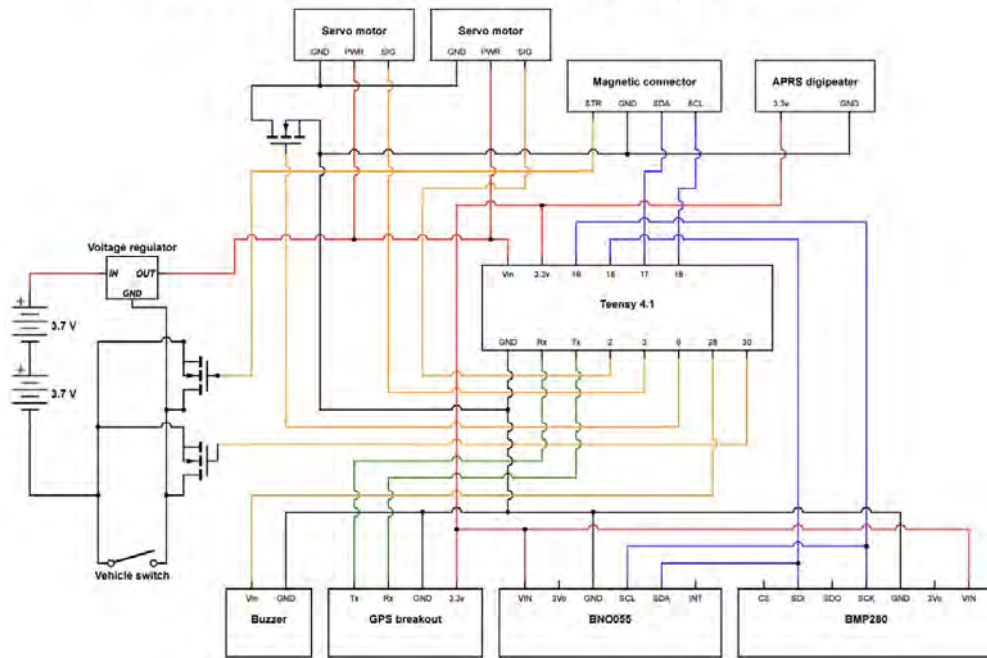


**Fig. 98 Vehicle wiring diagram**

**Control software** As the design of the movement system has yet to be proven, the control system is rather rudimentary. Using position data taken from the GPS, the vehicle determines its distance from a predefined target point in the x and y axes. These axes are based off the riser lines that connect to the parachute and turn with the vehicle; a line passing through two diagonal risers forms an axis. If the distance along a given axis is greater than 20 ft, the system will deform the parachute to move toward the target point along said axis. The vehicle will not stop moving until it is within 10 ft of the target point along the defined axes. When attempting to move, the parachute will be deformed to its fullest extent, where one riser is roughly 3.5" longer than the opposing one. This value was scaled to our parachute size from the deformation used by [? ]. A on/off movement scheme was selected for three reasons. The first is simplicity, as removing complexities was necessary given time constraints. The second was to provide as clear a separation as possible between when the vehicle is actuated and when it is not. This is useful in analysing motion post launch to determine the effectiveness of the system. Third, as the point of the motion system is primarily to counter drift, precision accuracy is not necessary, allowing for a less complicated control scheme.

**Manufacturing** Due to the complex geometries associated with the movement system, the vehicle was 3D printed in two parts and screwed together with M3 bolts. PETG was selected for its better heat tolerance when compared to PLA and ease of printing when compared to ABS. The vehicle PCB fits into a slot in the vehicle frame and is held in place by 3D printed brackets. To ensure the 3D print would not break due to layer separation, parts were printed so that the perimeters run the length of the vehicle.

### 3. Payload Bay

The payload is mounted within the nose cone. While the rocket descends under its drogue parachute, the nose cone is ejected by electronics independent from the payload, exposing the release system and allowing the vehicle to clear the rocket. While black powder was selected for ease of use, it requires independent electronics given payloads cannot use pyrotechnics. These independent electronics are mounted in an Ebay below the release system in a coupler (referred to as the nose cone coupler) between the nose cone and the body tube containing the main parachute.



**Fig. 99** Top down view of the nose cone Ebay



**Fig. 100** Top bulkhead mounted to the release system

The nose cone Ebay, pictured in Fig. 99, holds an easy mini flight computer (used to trigger a 1g black powder charge), an Egg timer wifi switch (used to turn the easy mini on once the rocket is raised on the launch rail), and two switches (used to power on the release system and wifi switch/easy mini). The bottom of this Ebay connects to the main parachute shock cord line via a U-bolt and quick link. The top of this ebay is connected to the bottom of the release system through four 1/4" bolts. The bulkheads connect to each other through two 1/4" threaded rods, which hold the bulkheads against a lip inside the coupler. This lip is made of a smaller diameter fiberglass tube epoxied in place, providing a strong connection to the coupler wall. This mounting method was chosen for its ease of construction when compared securing a bulkhead to the fiberglass tube with bolts. The coupler is connected to the nose cone via two shear pins and the main parachute tube via 6 shear pins. A 1" thick band on the outside of the coupler prevents the assembly from falling into the main tube should the shear pins fail prematurely.

The top of the release system is connected to an upper bulkhead through four 1/4" bolts, as seen in Fig. 100. Directly connecting bulkheads to the release system was selected to remove the excess weight of supporting hardware. The outer edge of this bulkhead is covered in a thin layer of foam, which seals against the nose cone wall. The ejection charge for the nose cone is placed on top of this bulkhead, so that when fired the pressure is kept away from the sensors below. This upper bulkhead also has an eyebolt, which connects to a shock chord that runs to the tip of the nose cone. This arrangement ensures that the nose cone remains connected to the rest of the rocket for easier recovery.

#### *4. Payload Sizing and Mass*

The payload follows the 4U size constraints. This layout was selected to maximize available space for the vehicle in the release system. Roughly 2.5U is allocated to holding the vehicle, 1U to the release system electronics, and 0.5U for ballast. The release system weighs 8.5 lbs and the vehicle weighs 1.3 lbs, for a total weight of 9.8 lbs.

## G. Full-Scale Test Flights



**Fig. 101 Liftoff of Karkinos on a Loki M3464**



**Fig. 102 Karkinos after flight**

Karkinos had a total of 4 test flights during the 2022-2023 season. Since our local high-altitude field is only open from December to early April, it is very important for us to begin flying as early as January so that we can fully test all of our subsystems. Our first test flight occurred on January 7th, 2023 at the MDRA Higgs Farm. Karkinos had been built over the previous months, but still had a few components that were not ready including a section of airframe and the Air Brake module. On this first flight, a commercial tube was used instead and the Air Brake flew without being turned on. This flight was primarily a test to make sure that the fin can and recovery systems would work as expected. Karkinos flew on a Loki M3464 to 8,400 ft. Both the drogue and main deployed nominally and the rocket landed without damage over a tree.

The second test flight of Karkinos took place a month after the first, this time on an M2500 to 8000 ft. This flight had the same airframes as the first, but also included a working Air Brake module. As the rocket left the rail, it turned slightly into the wind which is likely due to the lower thrust of this motor. The Air Brakes were able to deploy on the way up, however the Air Brake stepper motor had stalled partway through. Drogue deployment was nominal, however the main never deployed and the rocket landed in a group of trees.

The nosecone hit a branch, shattering the fiberglass and the payload electronics inside. Once we walked up to the rocket to recover it, it was evident that one of the Air Brake flaps was missing. We could not find it near the landing site, and video review of the flight showed the rocket tumbling near apogee. This behavior would be consistent with the asymmetric drag of a missing flap. We concluded that a flap was lost during the rocket's ascent.



Fig. 103 Members in front of Karkinos before flight



Fig. 104 The second flight of Karkinos on an M2500

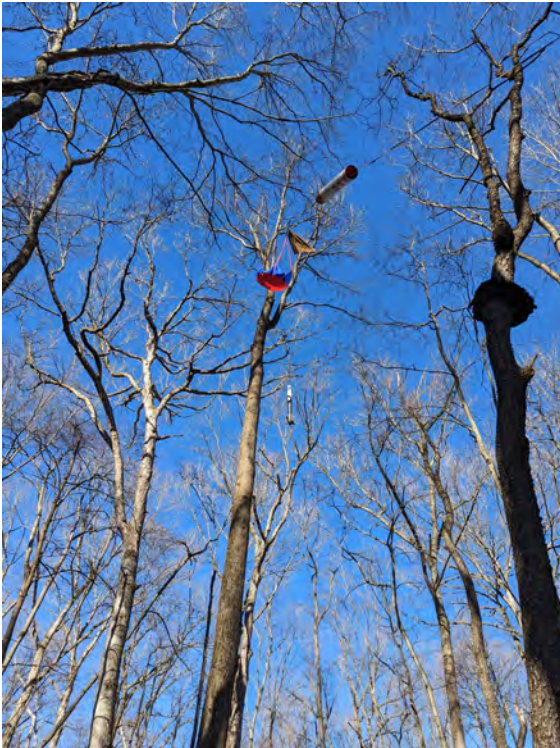


Fig. 105 The main airframe and fin can in a tree



Fig. 106 Attempting to pull the rocket out of the tree



**Fig. 107 The third flight of Karkinos on an EX N2500**

The third flight of this rocket was the first on our SRAD N2500. This flight included the full payload, Air Brakes, and SRAD avionics system onboard as well as an AltusMetrum EasyMotor on the forward closure of the motor. The motor worked as expected, but the Air Brakes did not end up deploying in flight and it reached an altitude of 10,500 ft. While they did not deploy, this flight gave us a benchmark to update our simulation with flight results. Drogue deployment, nosecone deployment, and main deployment were nominal and as far as we can tell the payload deployed as well. The payload landed in a group of trees along with the rocket and could not be found after extensive searching. This time, the rocket could not be pulled out of the trees and a tree climber was hired to recover it. Karkinos spent around a week outside, including some rain, but no evidence of water damage could be found. The EasyMotor also did not record any pressure data from the motor during this flight. Poor antenna management in the electronics bay also meant that GPS telemetry was spotty, but the rocket was within visible range for almost the entire flight.



**Fig. 108 The fourth flight of Karkinos on an EX N2500**



**Fig. 109 A close up view of liftoff**

Karkinos' fourth flight took place on April 2nd at MDRA's Red Glare. This flight was also on the team's SRAD N2500 and the flight contained the same electronics as the last, except the payload would not be deploying. The motor worked nominally and the Air Brake deployed on the way up. The target apogee for this flight was 9,500 ft and the Air Brake was able to bring the rocket to 9,574 ft. Both the drogue and main deployed nominally, and for the first time, the rocket landed in an open field and was recovered with minimal damage.

### III. Mission Concept of Operations Overview

Karkinos's mission profile will be that of a standard two-break dual deploy high power rocket. The use of a smaller drogue and a larger main minimizes drift from the launch site and makes recovery easier. The concept of operations for Karkinos can be found below along with the phases on a simulation plot.

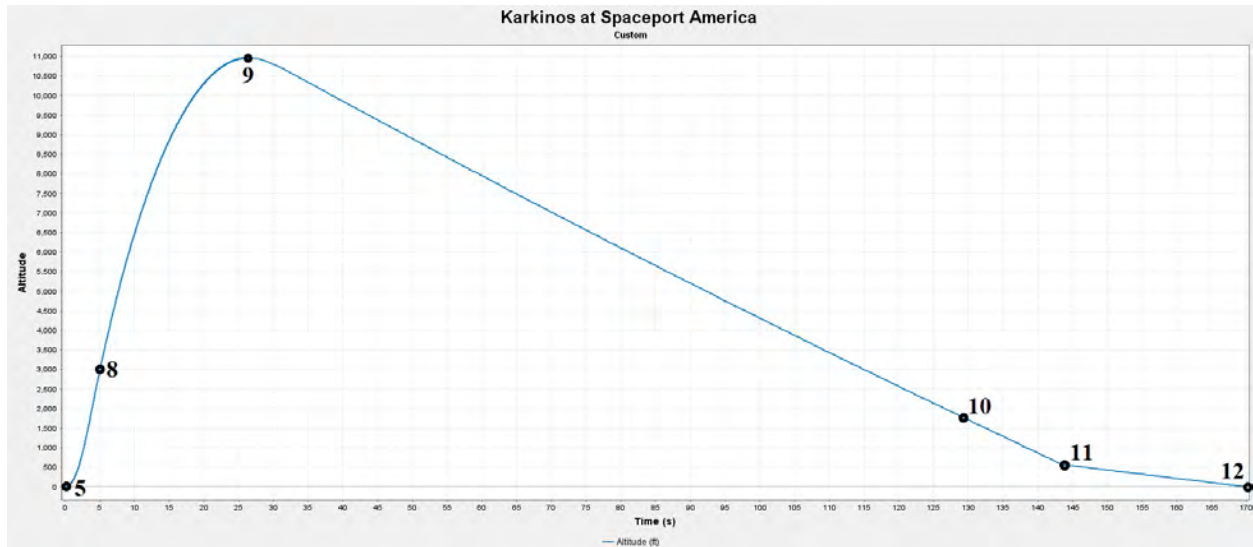


**Fig. 110** *Karkinos* Concept of operations

- 1) Phase 1: Preflight Preparation  
During the week leading up to the flight, the motor is assembled, the electronics are mounted in the electronics bay, and the Air Brake and payload modules are prepped for flight.
- 2) Phase 2: Preflight Assembly  
The motor is integrated, charges are connected to the electronics, and the rocket is assembled. Recovery parachutes and shock cord is packed into the recovery tubes. Shear pins and bolts are used to connect the tubes together.
- 3) Phase 3: Launch Pad Integration  
The rocket is slid onto the rail and payload WiFi switch is turned on. The rail is raised vertical and locked.
- 4) Phase 4: Arming  
Air brake computer is powered on. Flight computers are powered on. Cameras are powered on. Continuity on all E-matches is confirmed via auditory cues from computers. Telemetry is checked for GPS lock. Unnecessary personnel are cleared from the area and the motor igniter is installed.
- 5) Phase 5: Ignition (t = 0.00 s)  
Current is sent through the igniter and the motor is lit. Smoke is seen coming out the aft end of the motor.
- 6) Phase 6: Lift-off (t = 0.01 s)  
The motor begins to produce thrust and vertical motion is visible.
- 7) Phase 7: Powered Ascent (t = 0.3 s)  
The rocket accelerates upward under motor power. This phase lasts approximately 4.5 seconds, at which point the rocket is 2800 ft above the ground.
- 8) Phase 8: Unpowered Ascent (t = 5 s)  
The rocket coasts to apogee. After motor burnout, the Air Brakes deploy as needed in order to reach 10,000 ft accurately. This occurs from 5 seconds into flight and continues until apogee.
- 9) Phase 9: Apogee, Drogue Deployment, and Descent (t = 26 s)  
At apogee, the primary EasyMini fires its drogue charge followed by the backup EasyMini on a two second delay. The booster separates from the electronics bay and the six shear pins break. The two halves of the rocket

separate and the drogue parachute inflates and the rocket falls at a rate of 90 ft/s.

10) Phase 10: Nosecone and Payload Deployment (t = 130 s)

Once the nosecone EasyMini detects an altitude of 1,700 ft during descent, the nosecone charge fires and separates the nosecone. The payload detects an increase in light and deploys the payload 5 seconds later.

11) Phase 11: Main Deployment and Descent (t = 143 s)

When the primary EasyMini detects an altitude of 1,000 ft, the main charge fires. This is followed by the backup EasyMini which is set to deploy its charge at 800ft. The nose cone Ebay is separated from the rocket and the main parachute inflates, slowing it to a safe descent velocity.

12) Phase 12: Ground Recovery (t > 170s)

The rocket has hit the ground and the flight has ended. A recovery team will be sent to locate the rocket using GPS data received from the Featherweight GPS. Once recovered, electronics are powered off and the rocket is taken back to the judges for post-flight evaluation. Flight, Payload, Avionics, and Air Brake data is then downloaded and analyzed.

## **IV. Conclusions and Lessons Learned**

This year will be our third time attending SAC. We previously competed in 10,000 COTS Solid Divisions at SAC 2022 and SAC 2018. The competition rocket in 2022 showed great promise prior to the competition. At the competition, our COTS flight computer malfunctioned and deployed our drogue parachute upon ascent. This led to an early end to the flight and a disappointing data review. In 2018, our rocket took flight but was never recovered.

Prior to SAC 2022, we flew our competition rocket four times. The fourth time was at full configuration with all sub-systems fully integrated and working. In comparison, other teams at SAC launched their competition rockets once or twice. Our rapid testing and launching led to a swift safety inspection of the rocket with little concern from the inspectors. On the first day of launches, we were the 7th team to be on the pad and launch our rocket. This was all possible because of our previous flight experience with the competition rocket and utilizing simple designs that worked.

Although our performance at SAC has not been what we hoped, we have developed great confidence and support in our methodology. With this in mind, we entered the 2022-2023 season with a laser-sharp focus on testing and flying often. MDRA provides a local launch site that our team has flown at for many years. They host launch events once a month and have been a great support to the team. Whether we are launching our own competition rocket or personal rockets, we make it a habit to attend each launch and develop a close relationship with MDRA and its members.

One of the areas the team made many mistakes was with the new solid propulsion team. It was the first year that the team was attempting anything like this, and mistakes were expected. There was no team knowledge for many of the processes and we had to depend on the advice of our mentors and those online. This meant lots of different procedures for everything from mixing procedures to determining burn rate. Plenty of mistakes were made along the way including slightly inaccurate burn rate values, a complete failure of our data collection system during a full scale test fire, and not preparing enough propellant to fill our casting tubes. However, due to the team's cautious approach this year, the impact of these mistakes was minimized. Especially by choosing to use well-known commercial components, risk could be minimized where safety was absolutely critical. A failure of the motor casing would not only be catastrophic to our hardware but could potentially hurt someone on the team or at the launch. By purchasing these components, we could focus on other parts of the motor and make sure they would be safe instead of designing and manufacturing our own. All of these lessons learned this year are now allowing us to chase much more ambitious goals next year. Now that we know how to properly characterize a propellant, we can spend time designing and tweaking our own custom propellant. We have found what works and what doesn't for data collection during a static fire and can change our procedures to make those systems much more reliable. Now that we have made some very large motors, we can try to manufacture our own casings, closures, and nozzles. Working up in complexity lets us solve issues at a much more reasonable rate and still meet our timeline.

We have faced issues in the past with a lack of knowledge transfer, lack of high-power rocket experience, or falling victim to design paralysis by making overly complicated designs. We have witnessed the impact of members earning their high power certifications and noted the positive difference in work production. The motivation to have members earn their certifications is to further build our knowledge of dual-deployment, recovery, solid rocket motors, and general launch operations and manufacturing techniques. As of recent records, we have over 20 L1s, 4 L2s, and 2 L3s. These are the most certifications in the team's history. The ability to understand the fundamentals of rocketry will push our team to further heights with more technical projects in the future.

We have learned that offering multiple projects outside of SAC has kept our members engaged and curious about the field of rocketry. These projects include a 2-stage high-power rocket model, a minimum diameter rocket, a liquid-powered rocket, and a hybrid-powered engine testing. There are a variety of skills and interests that university students have. By offering projects that meet their interests, we have been able to recruit and retain our members much better.

## V. Appendix A - System Weights, Measures, and Performance Data

### A. Rocket Information

**Table 17 Overall Rocket Parameters**

Airframe Length (in)	155
Airframe Diameter (in)	6
Fin-Span (in)	6
Vehicle Weight (lb)	57.3
Propellant Weight (lb)	14.7
Payload Weight (lb)	10
Liftoff Weight (lb)	82
Number of Stages	1
Strap-on Booster Cluster	No
Propulsion Type	Solid
Propulsion Manufacturer	Terrapin Rocket Team

**Table 18 Propulsion System**

Propulsion Type	Solid
COTS, SRAD, or Combo	SRAD
Propulsion Manufacturer	Terrapin Rocket Team
Motor	N2500
Motor Classification	N
Average Thrust (N)	2531
Total Impulse (N-s)	11543
Motor Burn Time (s)	4.55

### B. Predicted Flight Data and Analysis

**Table 19 Flight Predictions**

Launch Rail	ESRA Provided Rail
Rail Length (ft)	17
Liftoff Thrust-Weight Ratio	9.6
Launch Rail Departure Velocity (ft/s)	92
Minimum Static Margin During Boost	2.75
Maximum Acceleration (G)	9.43
Maximum Velocity (ft/s)	890
Target Apogee (ft AGL)	10,000
Predicted Apogee (ft AGL)	10,980

**C. Recovery Information**

**Table 20 Recovery Information**

COTS Altimeter	AltusMetrum EasyMini
Redundant Altimeter	AltusMetrum EasyMini
Drogue Primary & Backup Deployment Charges (g)	7 & 8 of black powder
Drogue Deployment Altitude	Apogee
Drogue Decent Rate (ft/s)	90
Nosecone Deployment Altitude	1,700
Nosecone Deployment Charge (g)	1
Main Primary & Backup Deployment Charges	6 & 7 of black powder
Main Deployment Altitude (ft)	1,000
Main Descent Rate (ft/s)	20
Shock Cord Length (ft)	8 (Y harness), 70 (drogue), 35 (main),15 (nose)

**D. SRAD Components**

**Table 21 SRAD Components**

Component	SRAD/COTS	Material
Thrust Plate	SRAD	Aluminum
Fin Can Tube	SRAD	Carbon Fiber
Fins	SRAD	G10/Carbon Fiber
Centering Rings	COTS	G10
Air Brake Airframe	SRAD	Fiberglass
Air Brake Coupler	SRAD	Fiberglass
Air Brake Bulkheads	SRAD	G10/Aluminum
Drogue Airframe	SRAD	Fiberglass
Ebay Coupler	COTS	Fiberglass
Switch Band	SRAD	Fiberglass
Ebay Bulkheads	SRAD	Aluminum
Main Tube	SRAD	Fiberglass
Nosecone Ebay Coupler	COTS	Fiberglass
Nosecone Ebay Bulkheads	SRAD	Aluminum
Payload	SRAD	Mutiple
Nosecone	COTS	Fiberglass

## VI. Appendix B - Project Test Reports

**Table 22 Outline of Tests**

Date	Type	Description	Status	Comments
9/10/2022	Ground	Motor Characterization	Successful	Burned six motors to find burn rate values
10/6/2022	Ground	Payload drop test 1	Successful	Dropped a prototype vehicle from a parking garage to prove the concept
10/8/2022	Flight	Payload drop test 2	Failure	Launched the prototype vehicle on a 3" test rocket
1/5/2023	Ground	Test Stand Calibration	Successful	Calibration of pressure transducer and load cell for static test stand.
1/7/2023	Ground	Full Scale Motor Static Tests	Successful	Static tested 2 full scale motors
1/7/2023	Ground	Full Scale Rocket Ejection Testing	Successful	Ground testing of ejection charges for full scale rocket
1/7/2023	Flight	Full Scale Rocket Flight 1	Successful	First full scale flight on M3464 to 8,500 ft.
1/7/2023	Flight	Payload Data Flight 1	Failure	First attempt at recording a IMU and altitude dataset from the competition rocket
1/31/2023	Ground	Motor Case Hydrostatic Test	Successful	Hydrostatic testing of motor case to 1000 psi
2/4/2023	Flight	Full Scale Rocket Flight 2	Partial Failure	Second full scale flight on M2500 to 8,000 ft. No main deployment
2/4/2023	Flight	Payload Data Flight 2	Failure	Second attempt at recording an IMU and altitude dataset from the competition rocket
2/12/2023	Ground	Air Brake PCB Test	Successful	Structural test of air brake flaps
2/17/2023	Ground	Avionics Ground Test	Successful	Ground test of the SRAD avionics board.
2/22/2023	Ground	Wind Tunnel Air Brake Testing	Successful	Full rocket in wind tunnel to characterize Air Brake system.
2/24/2023	Ground	Avionics Ground Range Test	Partial Failure	Ground test of SRAD telemetry.
3/3/2023	Ground	Air Brake Flap Tensile Test	Successful	Ground test of the release system to verify proper vehicle separation
3/3/2023	Ground	Payload Release Mechanism Verification	Successful	Ground test of the release system to verify proper vehicle separation
3/5/2023	Flight	Blue Rocket Flight 1	Successful	Test flight of Air Brake computer on K1100 to 6,000 ft.
3/5/2023	Flight	Full Scale Rocket Flight 3	Successful	Third full scale flight on EX N2500 to 10,500 ft

Date	Type	Description	Status	Comments
3/5/2023	Flight	Avionics Flight Test 1	Failure	First test of SRAD telemetry and datalogging
3/5/2023	Flight	Payload Release Flight 1	Successful	First test of releasing a vehicle from the competition rocket
4/2/2023	Flight	6" Test Rocket Flight 1	Partial Failure	Flight on M1939 to 10,000 ft to test Air Brake deployment. Air Brakes did not deploy, otherwise nominal flight.
4/2/2023	Flight	Blue Rocket Flight 2	Successful	Test flight of Air Brake computer on L1090 to 8,500 ft
4/2/2023	Flight	Full Scale Rocket Flight 4	Successful	Fourth full scale flight on EX N2500 to 9,500 ft
4/2/2023	Flight	Avionics Flight Test 2	Successful	Second test of SRAD telemetry and datalogging
4/2/2023	Flight	Payload vehicle retention flight	Failure	Launched a vehicle in the payload system to test retention under launch loads
5/6/2023	Flight	6" Test Rocket Flight 2	Partial Failure	Test flight of test rocket to 3,000 ft on M1500. Testing Air Brake deployment, payload deployment, and SRAD avionics
5/6/2023	Flight	Payload Release Flight 2	Successful	Second test of releasing a vehicle from the competition rocket

**A. Recovery System Testing**

(As found on the following page)

# Karkinos Ejection Testing

TerpRockets | Andrew Bean | MDRA Higgs Farm | January 7, 2023

## Test Objective:

This is a test of the drogue ejection charge for Karkinos. Since the airframe volumes, parachutes, and shear pins are similar to our 2022 competition rocket, the same charge sizes are being used as a baseline.

This test is primarily to see if the drogue charge can be made smaller, in this case 5 grams instead of 7 grams. Since the Main section is identical to last year's rocket, it is not being ground tested. The first flight of the rocket will confirm that the charge sizes will reliably separate the sections of the rocket. Each deployment even has redundant charges, with an extra gram of black powder. The flight contains 2 independent flight computers with separate batteries and power switches.



Karkinos set up for ejection testing

## Test Procedure:

For Ground Testing:

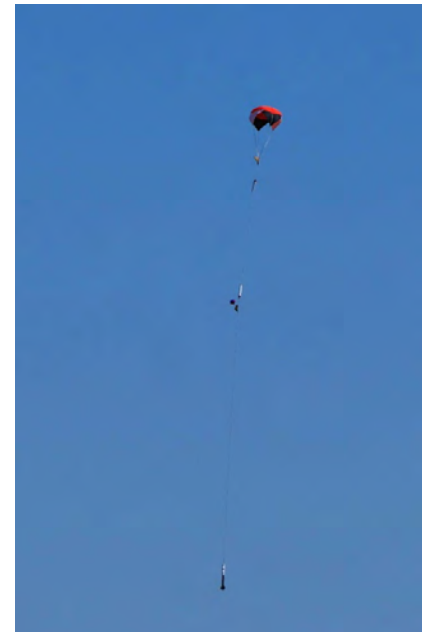
1. Assemble the rocket as it would be for launch. This includes any bolted sections, shear pins, parachutes, recovery hardware, and motor.
2. Guide ejection charge wires through bulkhead and out of vent hole
3. Set up rocket at A rack, parallel to flight line on stands
4. Connect ematch leads to launch control system
5. LCO ignites charge, rocket should separate

For Flight Testing:

1. Assemble rocket for flight, verify all charges are connected to correct terminals
2. Launch rocket
3. Track rocket visually and confirm apogee and main deployment
4. Recover rocket

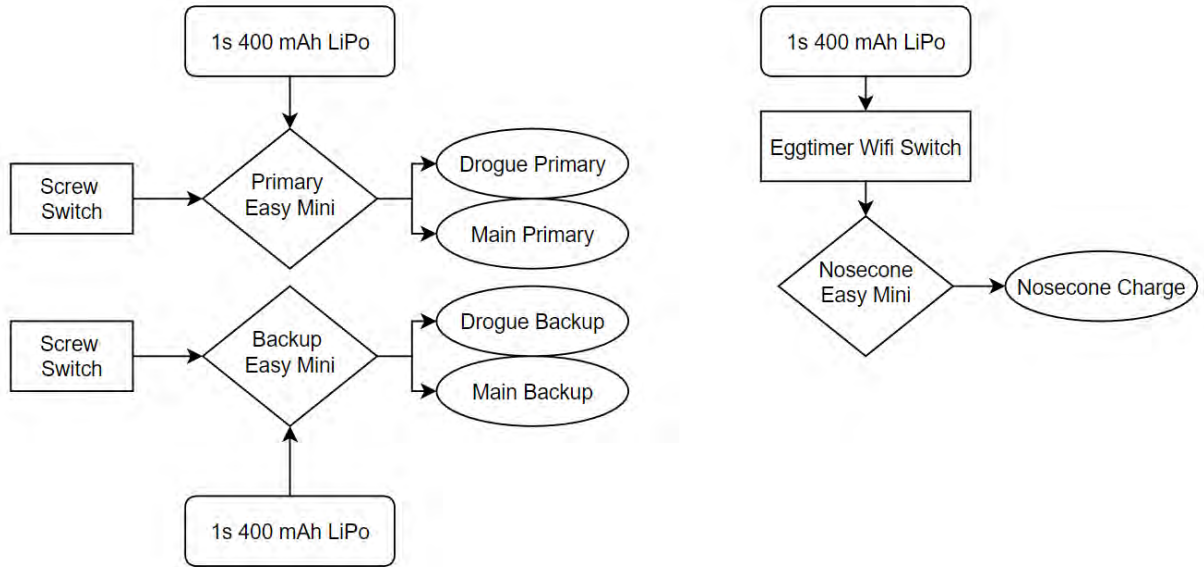
## Test Results:

Since this test was primarily an attempt to see if charge sizes could be decreased, success was not very likely. Once the charge was set off, the shear pins on the rocket broke but it did not separate very much. Since we knew that this size of charge could separate the booster with the new amount of shear pins, it was brought back up to the original quantity of 7 grams for the flight. During the following flight, both sections of the rocket separated and the parachutes inflated nominally.



Karkinos descending under its main parachute





Each flight computer has its own 400 mAh 1s lipo battery, screw switch, and set of charges. The backup EasyMini is configured to activate its apogee charge on a two-second delay. The main charge deploys at 800 ft instead of 1000ft.

Event and Success Criteria		
Shear Pins break (Ground)	PASS	1/7/2023
Clean Separation (Ground)	FAILURE	1/7/2023
Drogue Separation and Deployment (Flight)	PASS	1/7/2023
Main Separation and Deployment (Flight)	PASS	1/7/2023
<b>System Analysis</b>	<b>SUCCESS</b>	1/7/2023



# Karkinos Flight 1 Test Report

TerpRockets | Andrew Bean | MDRA Higgs Farm | January 7, 2023

## Test Objective:

This is the first flight of the full scale competition rocket for the 2023 competition year. The rocket will be flying on a Loki M3464 and will verify the integrity of the new airframe and also familiarize members with launch procedures. While this flight includes the airbrake module, it was not turned on during flight.

This flight also had payload electronics in the nosecone for data collection. This flight also used the electronics bay, main tube, and nosecone from the 2022 competition rocket since all the tubes necessary weren't complete.

Electronics onboard:

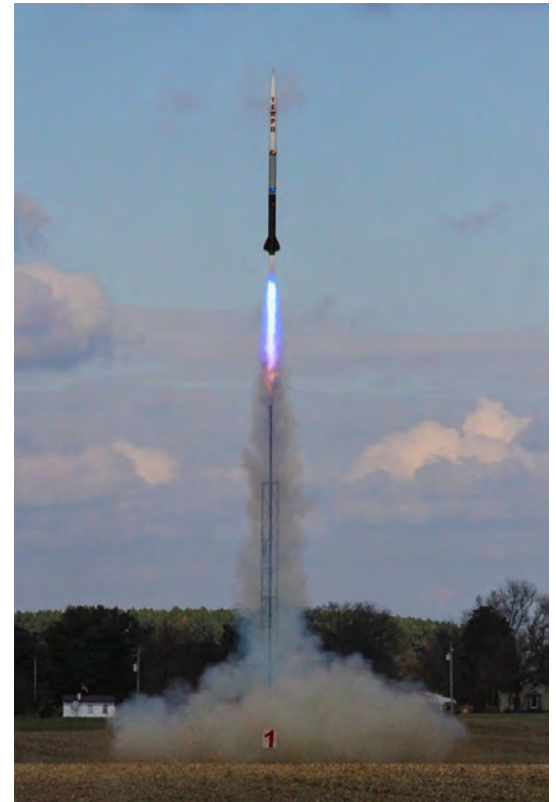
1. Telemega
2. EasyMini
3. ComSpec radio beacon

## Test Procedure:

1. Follow the launch procedure checklist for preparing the rocket for flight
2. Once the rocket is vertical on the rail, turn on deployment electronics. Verify 3 beeps from each for continuity of both charges
3. Verify telemetry is still working for both trackers onboard
4. Insert igniter and clear the pad
5. Make sure 2 people are assigned to track the rocket with the antennas
6. Once the rocket has landed, find using the receivers and turn off all flight computers

## Test Results:

Karkinos left the pad very straight without any turning or weather cocking. However, there was a slight wobble due to the loose Air Brake couplers. Both the drogue and main parachute deployed nominally without any tangling or major delays and the rocket came down softly at the edge of the property. The rocket landed across an irrigation ditch and over a tree. Members had to disconnect harnesses and pull the rocket down to recover it. Telemetry was maintained until touchdown, however the rocket was visible so the GPS coordinates were not used during recovery.



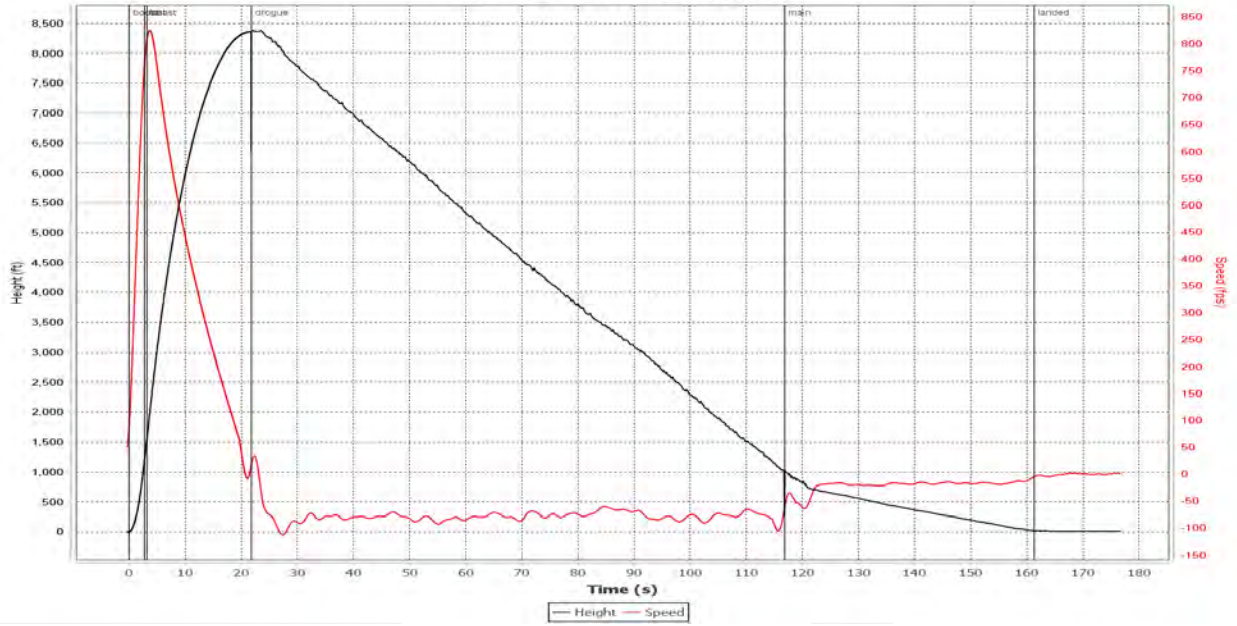
Karkinos at Liftoff



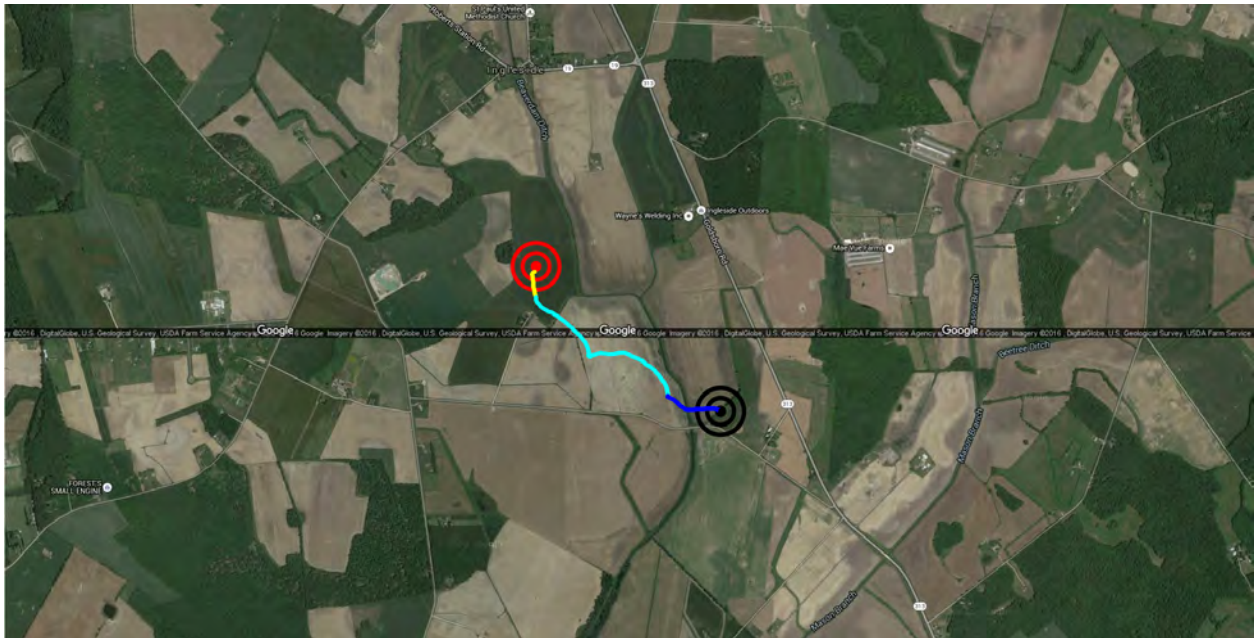
Karkinos during recovery



### TeleMega-v5.0 8349 flight 1



Altimeter data from Flight 1



GPS track of flight



<b>Event and Success Criteria</b>		
Motor Ignition and Nominal Boost	PASS	1/7/2023
Drogue Deployment	PASS	1/7/2023
Main Deployment	PASS	1/7/2023
Maintained Tracking During Flight	PASS	1/7/2023
<b>System Analysis</b>	<b>SUCCESS</b>	1/7/2023



# Karkinos Flight 2 Test Report

TerpRockets | Andrew Bean | MDRA Higgs Farm | February 4, 2023

## Test Objective:

This is the second flight of Karkinos for the 2023 Spaceport America Cup. This flight is on an Aerotech M2500 motor and is meant primarily to test the airbrake and payload subsystems. The airbrake will attempt to deploy on this flight and the payload will be turned on and collecting data for future flights. This flight also used commercial tubing for the main tube since the SRAD tubing was not ready yet.

Electronics onboard:

1. Telemega
2. EasyMini
3. ComSpec radio beacon

## Test Procedure:

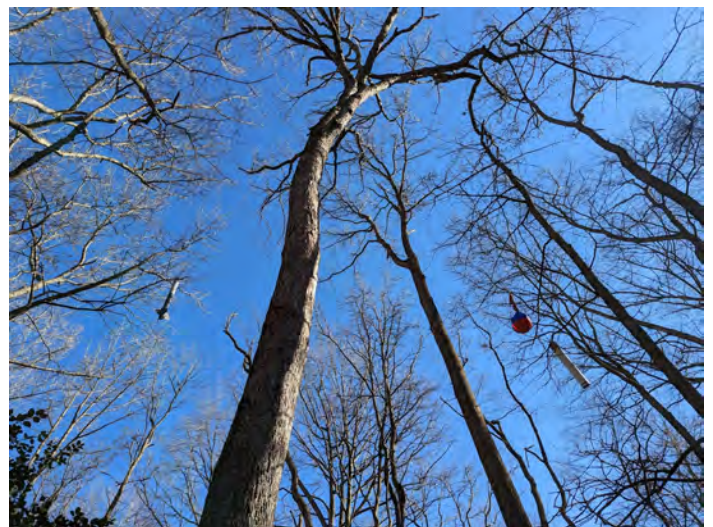
1. Follow the launch procedure checklist for preparing the rocket for flight
2. Once the rocket is vertical on the rail, turn on deployment electronics. Verify 3 beeps from each for continuity of both charges
3. Verify telemetry is still working for both trackers onboard
4. Insert igniter and clear the pad
5. Make sure 2 people are assigned to track the rocket with the antennas
6. Once the rocket has landed, find using the receivers and turn off all flight computers



Karkinos at Liftoff

## Test Results:

This launch of Karkinos occurred on a very cold day. Temperatures were below freezing all day long which caused multiple human and physical errors. The largest issue with this flight was the fact that our main parachute did not deploy. There are a few reasons we believe this happened including poor packing of ejection charges, poor parachute packing, and poor ebay sealing. Since it was cold, packing both the charges and parachute was rushed to minimize time in the cold. It is possible mistakes were made here that affected the flight. The bulkheads were also very dirty from the previous flight, which meant the electrical



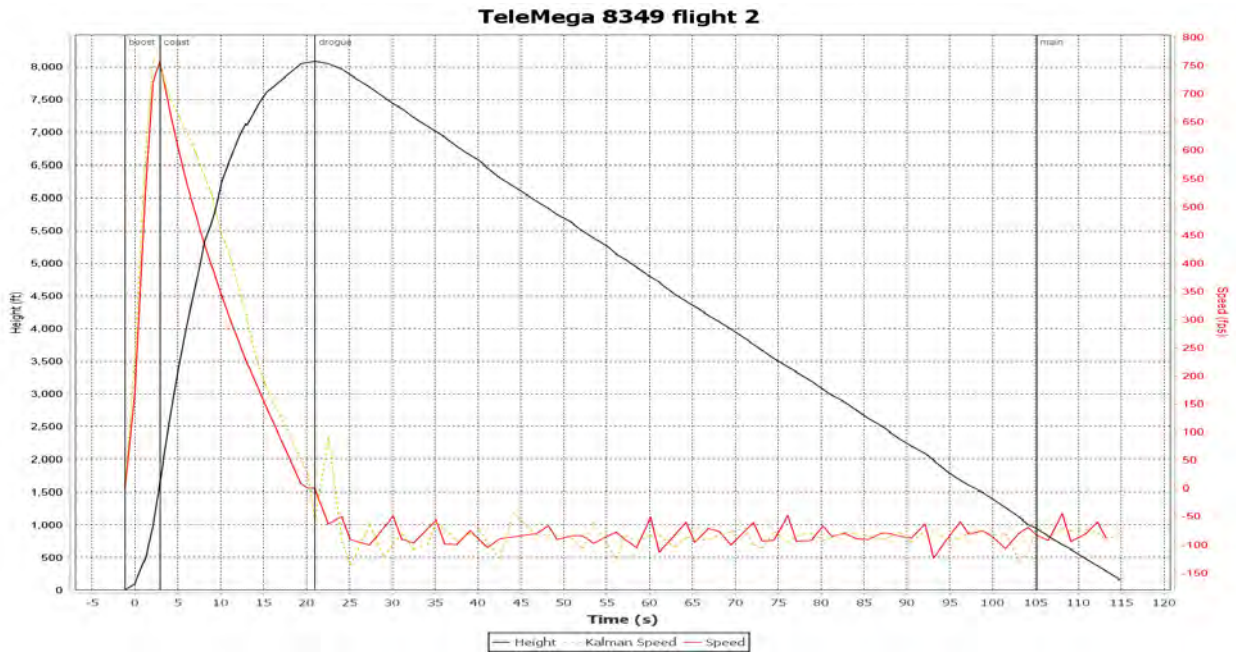
Karkinos hanging from trees after flight



tape we used to seal wire holes was not sticking very well. We attempted to wash it off, but this in addition to the cold probably meant that the bulkheads were not sealed well and gasses were vented through the ebay instead of pushing the parachute out. Since the main did not deploy, the rocket came down very fast. It fell over a group of trees and the nosecone impacted a branch and shattered. This led to a loss of the prototype payload electronics onboard. Since it landed in trees, it was also difficult to recover and took approximately 2 hours to get everything down. The second major fault with this flight was an airbrake breaking off. During the video, the rocket begins to do loops near apogee, and once recovered we found a flap was missing. After this flight, the Air Brakes were upgraded with fiberglass and steel to prevent this from happening again.



Missing airbrake after flight



Telemetry data for flight 2



<b>Event and Success Criteria</b>		
Motor Ignition and Nominal Boost	PASS	2/4/2023
Drogue Deployment	PASS	2/4/2023
Main Deployment	FAILURE	2/4/2023
Maintained Tracking During Flight	PASS	2/4/2023
Airbrake Deployment	PARTIAL FAILURE	2/4/2023
<b>System Analysis</b>	PARTIAL FAILURE	2/4/2023



# Karkinos Flight 3 Test Report

TerpRockets | Andrew Bean | MDRA Higgs Farm | March 5, 2023

## Test Objective:

This is the third test flight of Karkinos and the first in its full competition configuration. This flight is on the team's SRAD N2500 motor developed for the competition and also has the payload set up to deploy and come down on its own.

Electronics onboard:

1. EasyMini 1
2. EasyMini 2
3. BigRedBee 70cm GPS
4. ComSpec Tracker (Payload)

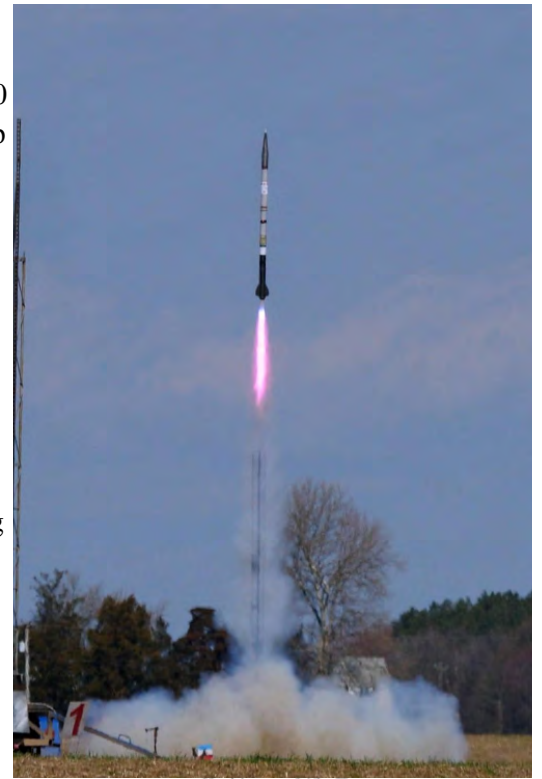
## Test Procedure:

1. Follow the launch procedure checklist for preparing the rocket for flight
2. Once the rocket is vertical on the rail, turn on deployment electronics. Verify 3 beeps from each for continuity of both charges
3. Verify telemetry is still working for both trackers onboard
4. Insert igniter and clear the pad
5. Make sure 2 people are assigned to track the rocket with the antennas
6. Once the rocket has landed, find using the receivers and turn off all flight computers

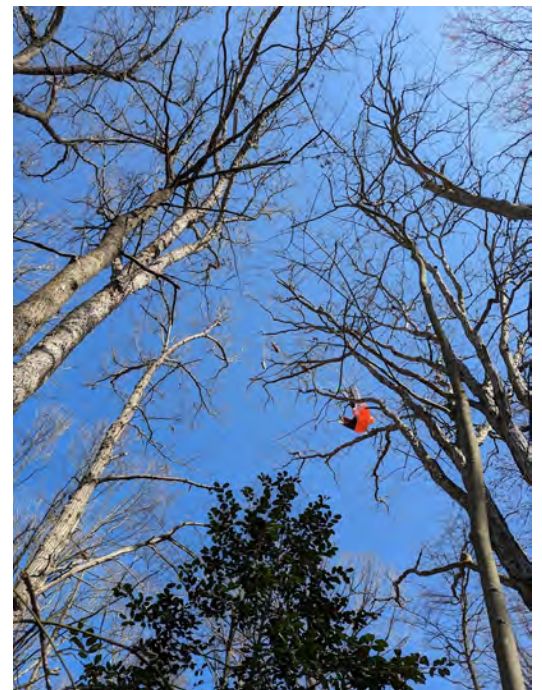
## Test Results:

Karkinos left the pad very straight without any turning or weather cocking. Both the drogue and main parachute deployed nominally without any tangling but the rocket did land in trees for a third time. Unfortunately this time, the rocket could not be pulled out from the ground and tree climbers had to be hired to recover it.

The payload also deployed as expected, however since it was above a group of trees, it could not be found even with the tracker. The Air Brakes failed to deploy on this flight, but it did give us a reference to adjust our simulations to be more accurate to the flight in New Mexico.

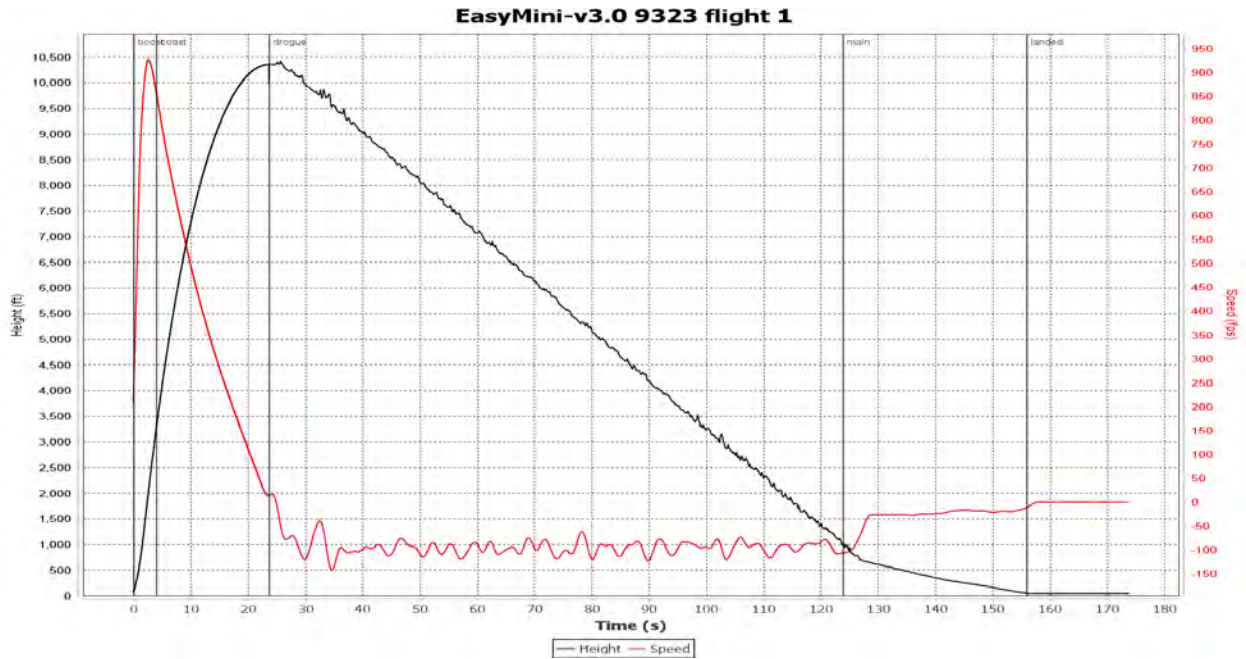


Karkinos at Liftoff



Karkinos during recovery





Altimeter data from Flight 3

Event and Success Criteria		
Motor Ignition and Nominal Boost	PASS	3/5/2023
Drogue Deployment	PASS	3/5/2023
Main Deployment	PASS	3/5/2023
Maintained Tracking During Flight	PASS	3/5/2023
Airbrake Deployment	FAILURE	3/5/2023
Payload Deployment	PASS	3/5/2023
Payload Recovery	FAILURE	3/5/2023
<b>System Analysis</b>	<b>SUCCESS</b>	3/5/2023



# Karkinos Flight 4 Test Report

TerpRockets | Andrew Bean | MDRA Higgs Farm | April 2, 2023

## Test Objective:

This is the fourth and final test flight of Karkinos before the Spaceport America Cup in June. This flight is in basically the same configuration as it will be at the competition and is meant to verify some remaining systems. While the payload will not be deploying this flight, it will be riding along and gathering data. The avionics system has also been moved to minimize interference and the ground station has switched to a yagi instead of a rubber duck antenna. The Air Brakes are also set to deploy on this flight and trim the altitude to 9,500 ft.

Electronics onboard:

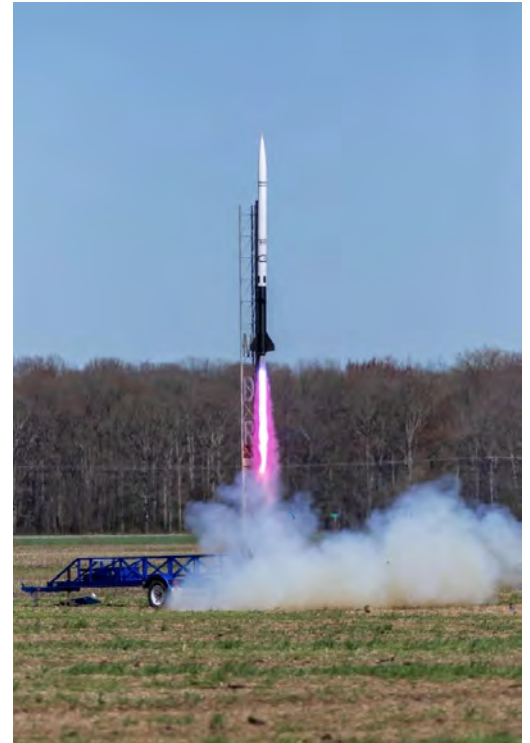
1. EasyMini 1
2. EasyMini 2
3. Featherweight GPS
4. Altus Metrum TeleGPS

## Test Procedure:

1. Follow the launch procedure checklist for preparing the rocket for flight
2. Once the rocket is vertical on the rail, turn on deployment electronics. Verify 3 beeps from each for continuity of both charges
3. Verify telemetry is still working for both trackers onboard
4. Insert igniter and clear the pad
5. Make sure 2 people are assigned to track the rocket with the antennas
6. Once the rocket has landed, find using the receivers and turn off all flight computers

## Test Results:

Karkinos took off and flew very straight off the pad. The Air Brakes deployed in flight and trimmed the altitude to 9,574 feet, only 74 ft off the target altitude. Telemetry was also maintained with the SRAD avionics throughout the flight as well as the Featherweight GPS. Recovery was nominal and the rocket landed in an open field not too far from the launch site. There was minimal damage to the airframe, however the 3D printed electronics bay sled did break slightly when the rocket hit the ground.

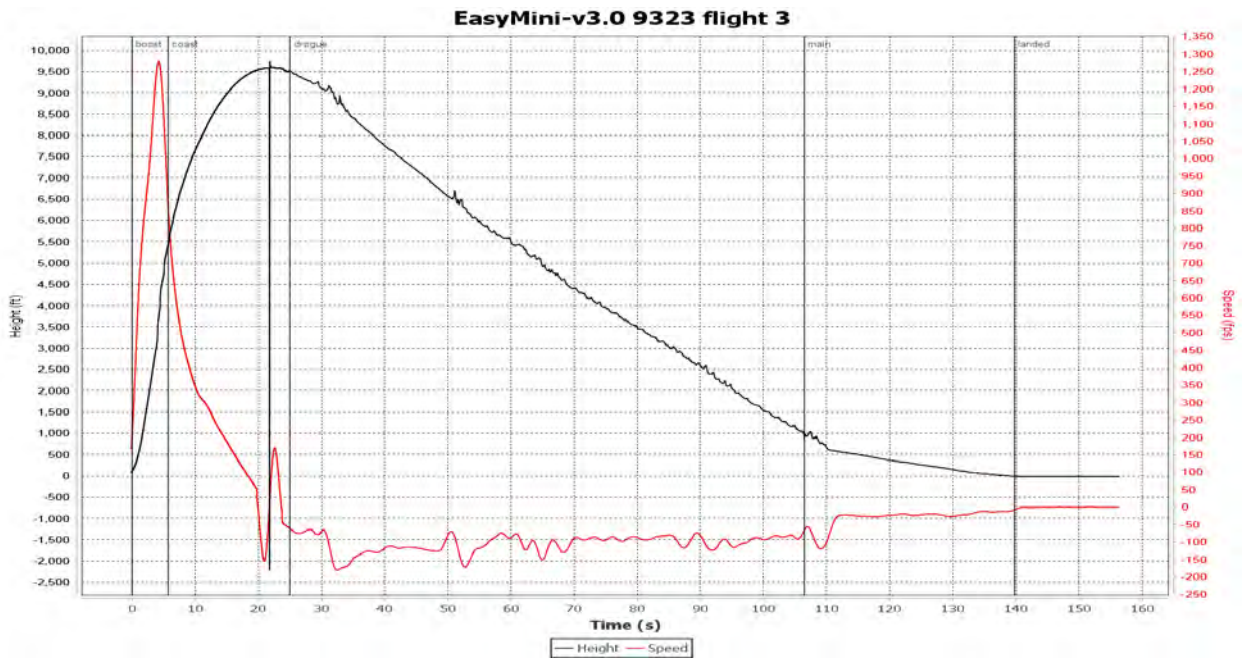


Karkinos at Liftoff



Karkinos during recovery





Altimeter data from Flight 4

Event and Success Criteria		
Motor Ignition and Nominal Boost	PASS	3/5/2023
Drogue Deployment	PASS	3/5/2023
Main Deployment	PASS	3/5/2023
Maintained Tracking During Flight	PASS	3/5/2023
Airbrake Deployment	PASS	3/5/2023
System Analysis	SUCCESS	3/5/2023



**B. SRAD Propulsion Systems Testing**

(As found on the following page)

# Characterization Motor Firings

Solid Propulsion | Adin Goldberg, Jackson Diaz, Andrew Bean | MDRA Sod Farm Launch Site |  
9/10/2022

## Test Objective:

These test-firings were conducted to get empirical data on the new experimental propellant, Terple Nebula. By firing a Kn-varied range of 38mm and 54mm motors, experimental-found chamber pressures can be plotted and fit to the Kn vs Chamber Pressure (Pc) curves and the Burn Rate vs Pc curves. Both curves can be fitted to an exponential model parameterized by a burn rate coefficient and a burn rate exponent. By test-firing motors in the Kn range of the full-scale model's projected Kn value, a value for chamber pressure of the full-scale motor can be determined via interpolation of the Kn vs Pc curve. In addition, points can be plotted on a burn-rate vs chamber pressure chart to be fitted to the burn rate exponential curve, thereby numerically solving for the burn rate coefficient and exponent.

## Burn rate equation

$$R_b = P_c / K_n \cdot \rho^* (c^*)$$

(c\* and density of propellant provided by PROPEP)

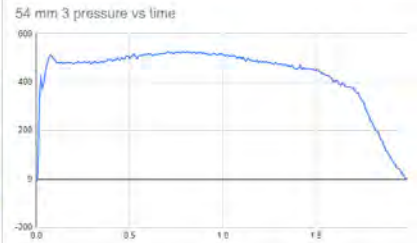
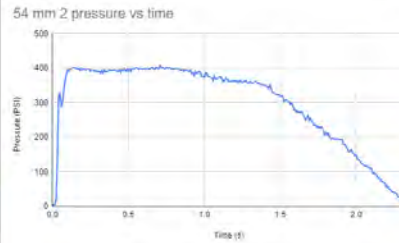
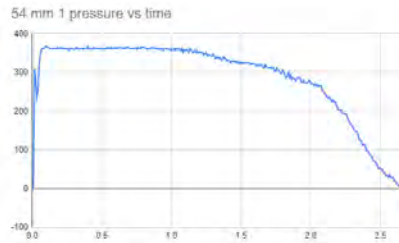
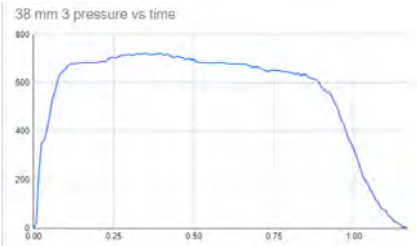
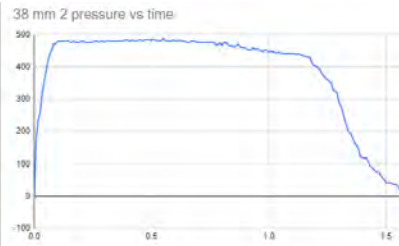
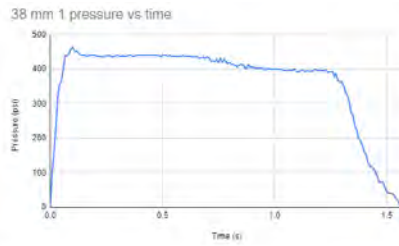
## Test Procedure:

1. Insert fasten in motor into the test stand out at the launch racks
2. Insert igniter into test motor
3. Start load cell and pressure transducer data recordings from laptop.
4. Fire motor
5. Verify that the data has been recorded and end recording.
6. Repeat steps 1-5 for all (5) test motors

## Test Results:

Other than small erosive spikes upon startup for some of the motors, all firings performed nominally and data was recorded successfully. From the pressure readings, the burn rate vs Kn and Kn vs Chamber Pressure plots were able to be fitted to exponential curve models.





Event and Success Criteria		
38mm Motor 1	PASS	9/10/2023
38mm Motor 2	PASS	9/10/2023
38mm Motor 3	PASS	9/10/2023
54mm Motor 1	PASS	9/10/2023
54mm Motor 2	PASS	9/10/2023
54mm Motor 3	PASS	9/10/2023
Data collection	PASS	
<b>System Analysis</b>	<b>SUCCESS</b>	9/10/2023



# Load Cell & PT Calibration

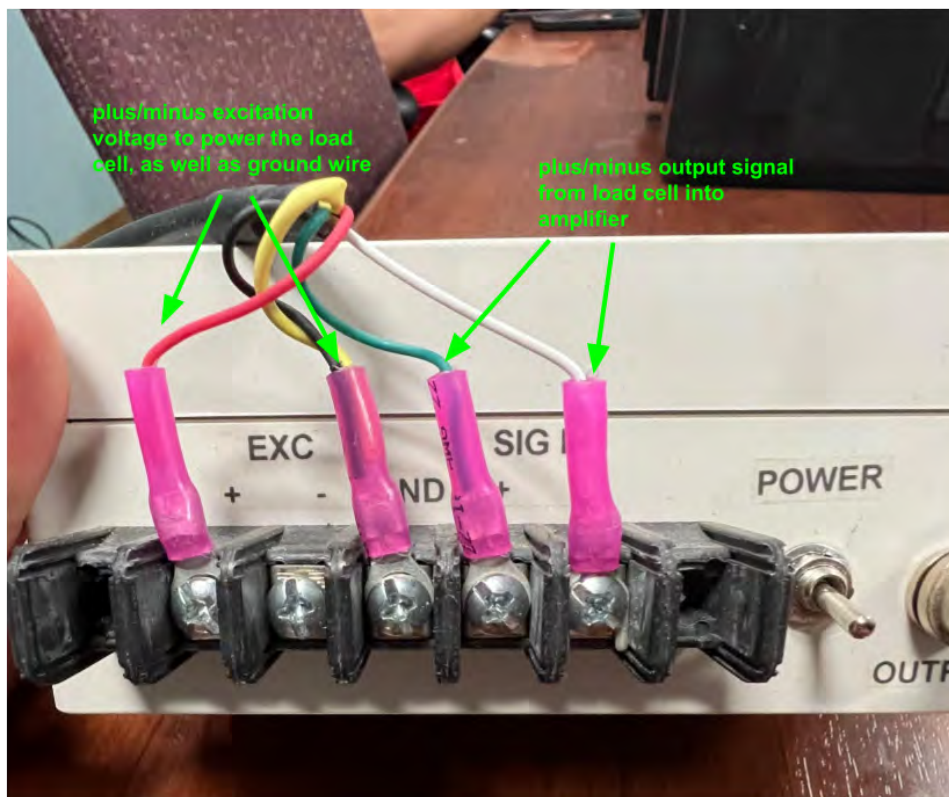
Solids | Saim Rizvi, Andrew Bean, Adin Goldberg | Cypress Building, UMD | Dec. 12, 2022

## Test Objective:

Calibrate the load cell and pressure transducer such that the voltage readings they produce can be converted via a scaling equation to pounds and pounds per square inch, respectively. This allows us to get relevant thrust and chamber pressure data from our motor static fires to use when thinking about incorporating the motor into our competition rocket.

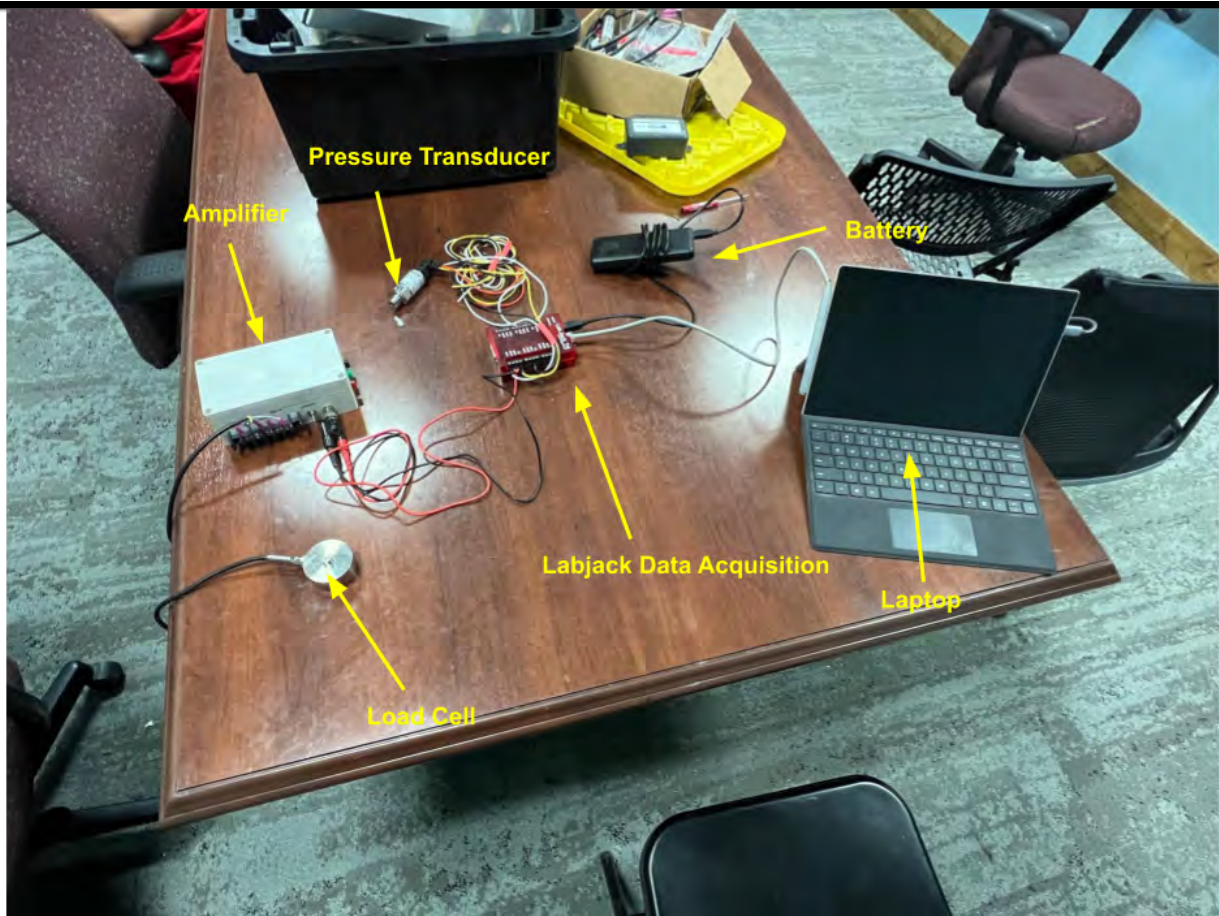
## Test Procedure:

1. Wire electronic components
  - a. Take 1000kg button load cell and connect it to signal amplifier



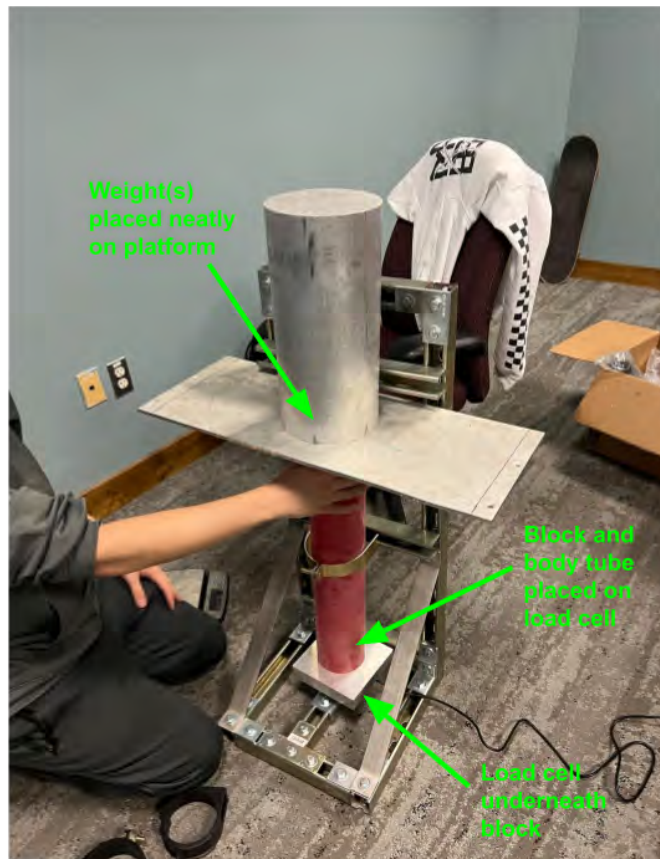
- b. Connect amplifier to an analog input port on the Labjack T4
    - c. Connect the Labjack to a power source (for the sake of our calibration test, we used a USB connection from the Labjack to a laptop)





2. Open necessary software to record data. We used LJStreamM, a high speed data logging software designed for the Labjack data acquisition
3. Prepare the various objects to be used as weights
  - a. We gathered various aluminum blocks and sand buckets, and measured their weights with a digital scale
  - b. We recorded these weights and noted with object they corresponded to
4. Prepare test stand setup
  - a. With the test stand in a vertical orientation, we placed the load cell on the bottom of the stand so that it is concentric with the circular brackets on the stand that would hold the motor casing in place
  - b. A fiberglass rocket body tube was placed in the brackets on the stand to mimic the casing for the actual static fire, and a small aluminum block was placed in between the button of the load cell and the bottom of the body tube in order to create a flat surface that would press the load cell
    - i. Because the aluminum block and body tube were not heavy enough to show a reading on the load cell, we did not use their weight as a data point in the calibration, but their weights were added to the total value
  - c. A flat sheet of metal was placed on the top end of the body tube to create a platform for the known weights to sit on



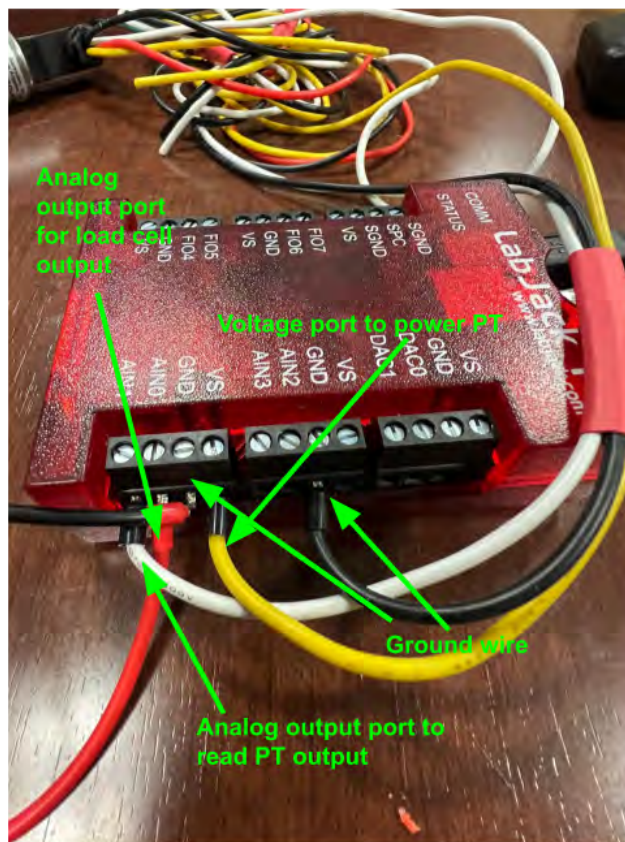


5. Place the first aluminum block with a known weight on the setup, and record the output voltage shown from LJStreamM, as well as the current weight that is pushing on the load cell. This is data point #1
6. Repeat step 5, adding more and more weight incrementally, and recording the voltage reading as well as how much weight is on the load cell for each reading. Collect at least 4 data points and try to get as much weight as possible (safely!) on the load cell to broaden the range of data points
7. Record your data points in an Excel spreadsheet or any software that can generate a linear fit to the data points (most load cells have a linear relationship between voltage output and corresponding force units)
8. Generate a linear function that converts voltage to the force unit used to measure the weights, and input this equation into the LJStreamM software so that future voltage readings are automatically converted to the force unit of choice during static tests

### **Pressure Transducer Procedure Steps**

9. Wire electronic components
  - a. Take pressure transducer and wire it to an analog input port on the Labjack T4





- b. Connect the Labjack to a power source (for the sake of our calibration test, we used a USB connection from the Labjack to a laptop)
- 10. Open necessary software to record data. We used LJStreamM, a high speed data logging software designed for the Labjack data acquisition
- 11. Prepare Hydraulic pump setup
  - a. Connect long high pressure line to hydraulic pump from one end and NPT cross on the other end
  - b. On the NPT cross, you should connect one of each at the ports: analog pressure gauge, bleed valve, pressure transducer
    - i. You may need an adapter for the pressure transducer if it is a smaller thread size.
- 12. Begin pumping hydraulic pump, and mark the voltage reading for its corresponding pressure valve reading. Collect 5-10 data points ranging from 100 psi to at least 1000 psi (depending on the rating of the pressure transducer)
- 13. Record your data points in an Excel spreadsheet or any software that can generate a linear fit to the data points

Generate a linear function that converts voltage to the pressure unit used to measure the pressure, and input this equation into the LJStreamM software so that future voltage readings are automatically converted to the pressure unit of choice during static tests

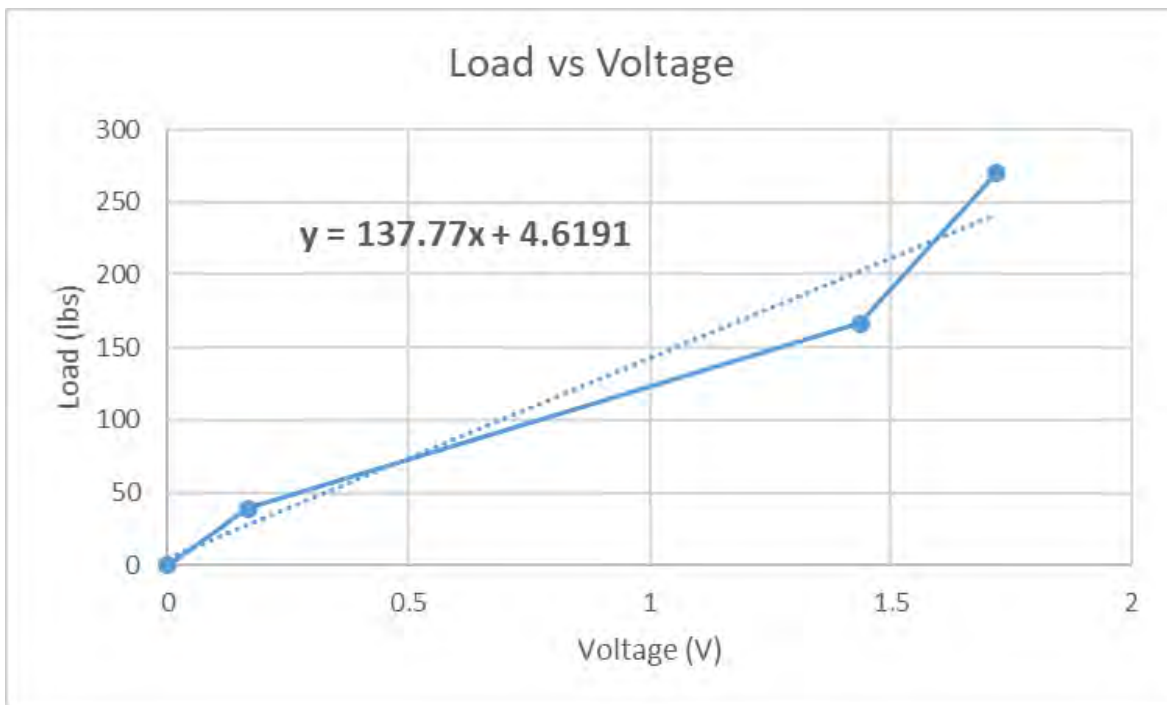


### Test Results:

For the load cell, the following data points were collected. These were then plotted in excel to show a relationship between load and voltage readings.

Voltage (V)	Load (lbs)
0	0
.166	39.1
1.437	166.7
1.719	270.4

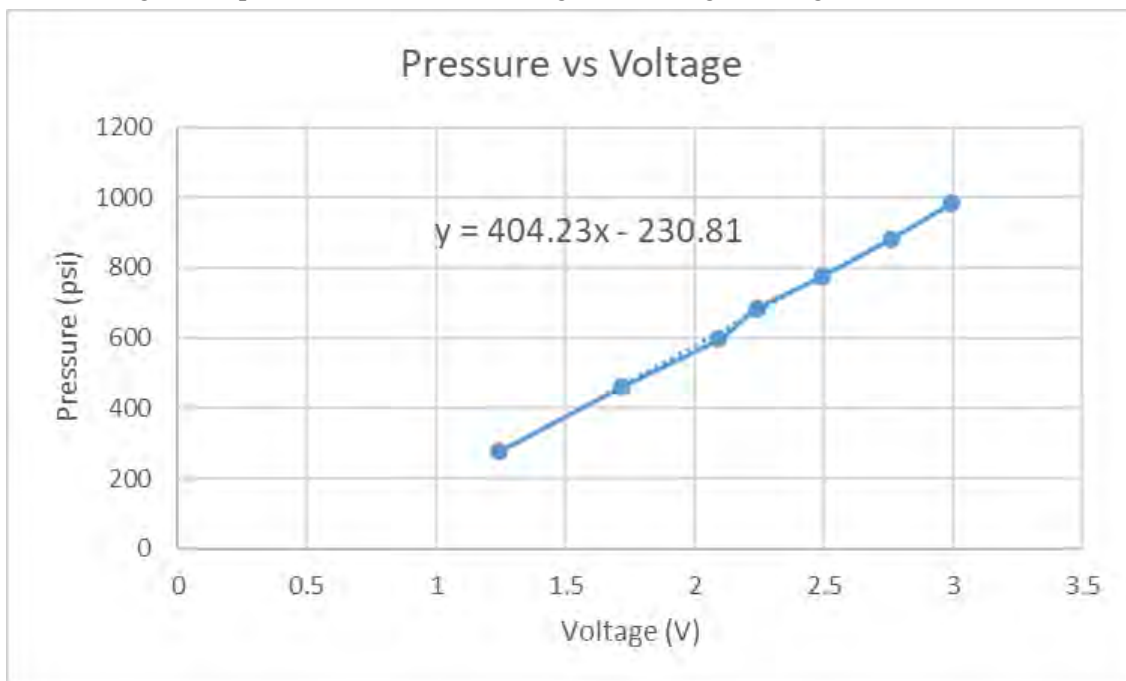
The load cell calibration data resulted in a line of best fit as shown below. The 4.6191 term accounts for the fact that there is some slight noise in the load cell. As a result, it shows a small negative voltage reading even when there is no load being applied. This equation fixes that by giving a y value (load) of 0 when x (voltage) gives that small negative value.



The pressure transducer calibration produced the following data points.

Voltage (V)	Pressure (psi)
1.24	277
1.72	462
2.09	597
2.24	685
2.49	775
2.76	883
2.99	983

Plotting this data in Excel resulted in the following linear function that relates voltage to pressure. The y-intercept of -230.81 serves the same purpose as in the load cell function. When there is negligible static pressure acting on the pressure transducer, it still gives a voltage reading due to noise.



These linear functions are then plugged directly into the data acquisition software of choice, and immediately convert the voltage readings to more useful engineering units (in our case, pounds and pounds per square inch).



<b>Event and Success Criteria</b>		
Load Cell Calibration	PASS	12/12/2022
Pressure Transducer Calibration	PASS	12/12/2022
<b>System Analysis</b>	<b>SUCCESS</b>	<b>12/12/2022</b>



# Full Scale Static Motor Testing

Solid Propulsion | Andrew Bean, Adin Goldberg, Saim Rizvi | MDRA Higgs Farm | January 7, 2023

## Test Objective:

This test will be a series of two static fires of our full scale 98mm motors, first a low Kn static fire and then a static fire at the target Kn. This is being done to make sure that there are not any major differences as we scale up from 54mm motors. The motor will be retained in the team's static test stand and will be fired vertically. Pressure readings will be taken during the test using two separate pressure transducers to two separate data acquisition systems. Force readings will be taken via a 1000kg load cell connected to one of the data acquisition systems. This will also be a test of our BK<sub>n</sub>O<sub>3</sub> igniters to confirm proper sizing as well as reasonable startup timing.

## Test Procedure:

### Test Stand Setup

1. Move horizontal bars to appropriate locations for the length of the motor being tested
2. Bring the test stand out at an appropriate distance for motors being tested.
3. Verify ignition leads can reach test stand
4. Set stand up vertically and secure base with stakes.
5. Connect ratchet straps at top corners and go outwards diagonally in 4 directions
6. Secure end of ratchet strap into ground with stake.
7. Begin tightening ratchet straps. Go slowly and make sure that you are not pulling the stand in any direction.
8. Once all straps have been tightened sufficiently, ensure that the test stand will not move easily.



Motor #2 secured in test stand

### Motor Setup

1. Make sure the motor has been assembled following the proper assembly procedures
2. If not already, lightly pack pressure transducers with grease. Also pack the tee and empty spots with grease.
3. Make sure to use teflon tape on any new NPT connections
4. Verify there is enough clearance with the pressure transducers to fully seat the forward closure and get the snap rings on.
5. Slide motor clamps onto casing, but do not tighten.
6. Bring the motor and igniter out to the motor test stand. Slide the motor and clamps onto the horizontal rails.
7. Center the motor and make sure that the tee will be able to press on the load cell.
8. Tighten clamps, but not all the way. The motor should be able to slide through them slightly.
9. AFTER DAQ SETUP: have non essential members clear the area and insert the igniter. Connect leads to the launch control system and leave area.



## DAQ Setup

1. Lay out ethernet cable from test stand to LCO table (or as far as it will go)
2. Open load cell amp and check voltage of batteries, replace if necessary
3. Check charge on portable battery for DAQ, plug in DAQ with USB cable
4. Connect load cell amp to DAQ
5. Connect pressure transducer cable to DAQ
6. Turn on load cell amp
7. Connect laptop to ethernet cable, verify that DAQ is recognized and is reading sensors
8. Move electronics away from stand as much as reasonable

## Firing Procedure

1. Make sure LCO is aware of intent to test fire, tell them that you need to start recording before they start
2. Before countdown, start recording on DAQ and confirm with LCO.
3. Start camera recordings
4. LCO Ignites motor
5. After firing, verify that sensors worked and stop recording. Make sure the file is saved.
6. Once the range is clear, approach the motor and begin to prepare for the next test or pack up.
7. The motor will still be hot, so proceed with caution.

## Test Results:

Both static fires went nominally. Both burns started and stopped fairly smoothly and there were no signs of overpressure or thermal failure. During the first static fire, we used a load cell connected to our own data acquisition system. While we had tested the load cell readings with a smaller 38mm motor the previous month, changes that we had made to the system since then meant that we received no force readings during the static test. Because of this, we decided to switch out our load cell for our mentor's load cell for the second test. During the second test, pressure and force readings were collected and were within the range that we were expecting.

Towards the end of the second static fire, a portion of the casting tube was ejected through the nozzle. Since this was during the end of the burn, the resulting pressure spike was not significant. However, if this occurs earlier in the burn, it could lead to an over-pressure or even crack the nozzle. The cause of this was found to be the way the grains were glued to the liner. Elmers Glue All Max, a low foaming glue recommended for gluing the grains in Aerotech and Cesaroni, was used for gluing the grains for both of these motors. Commercial motors generally have tighter tolerances between the casting tube and liner which means a thinner glue works well. Since our casting tubes and liners are from two separate companies, the gap between them is slightly larger and the glue did not work as well as it should have. After these tests, based on advice from Scott Kormier at Loki Research, we switched to



Motor #2 during static test

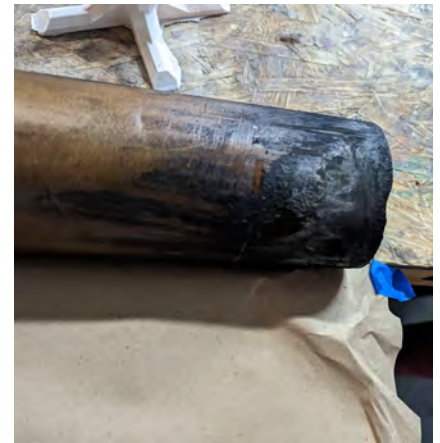


Motor #2 ejecting a casting tube during static test

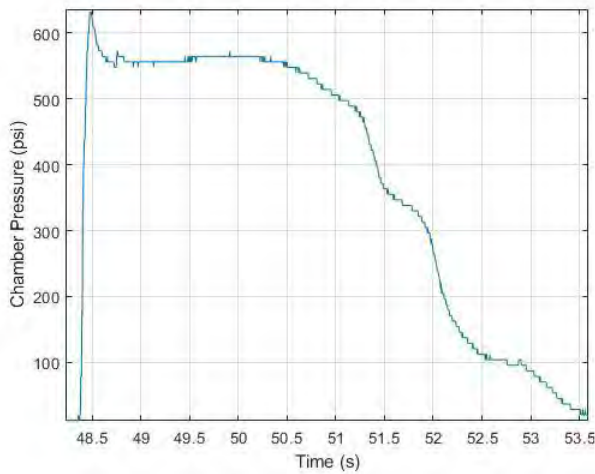


100% silicone caulk instead. This is much thicker, which is able to fill the gap better, and is more flexible compared to the All Max which is much more brittle.

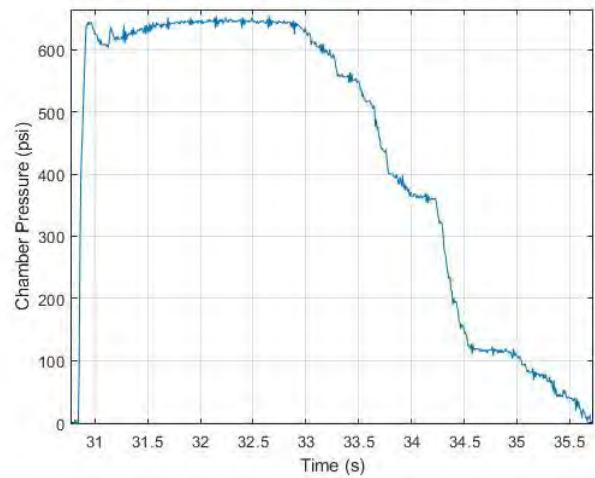
After taking the motor apart after the test, it was noted that a flame was able to pass by the forward closure shoulder and outside of the liner. This led to some of the flame touching the case at the forward end. While slightly charred from the grease, no deformation or bubbling was seen on the casing. Following motors will have a liberal amount of grease added the exterior of the forward liner as well as the forward closure shoulder to minimize the flame front traveling around and potentially damaging the casing.



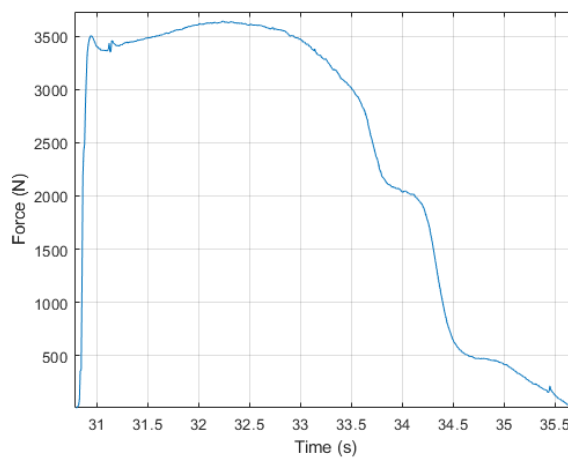
Forward end of liner after second motor test



Pressure vs Time for N Motor 1



Pressure vs Time for N Motor 2



Force vs Time for N Motor 2



<b>Event and Success Criteria</b>		
Motor 1 Ignition	PASS	1/7/2023
Motor 1 Burn	PASS	1/7/2023
Motor 1 Data Acquisition	PARTIAL FAILURE	1/7/2023
Motor 2 Ignition	PASS	1/7/2023
Motor 2 Burn	PASS	1/7/2023
Motor 2 Data Acquisition	PASS	1/7/2023
<b>System Analysis</b>	<b>SUCCESS</b>	1/7/2023



**C. SRAD Pressure Vessel Testing**

(As found on the following page)

# Motor Case Hydrostatic Test Report

Solid Propulsion | Andrew Bean, Adin Goldberg, Saim Rizvi | UMD | January 31, 2023

## Test Objective:

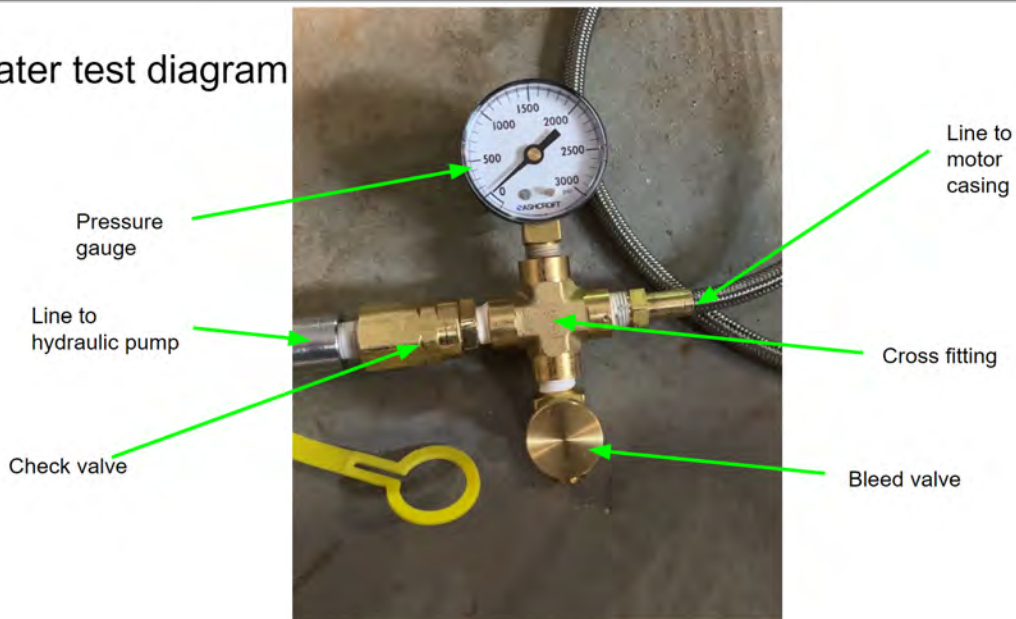
As per Spaceport Requirements, the motor casing for the SRAD motor needs to be hydrostatically tested to 1.5 times its Maximum Expected Operating Pressure (MEOP). The SRAD motor that the solid propulsion team had designed is expected to have an operating pressure of 650 psi, so to round up the casing needed to be tested to approximately 1000 psi for at least twice the duration of the firing time. Since the casing was commercially procured, it was expected that the casing would pass the test with no issues as long as the casing was filled and sealed properly.

## Test Procedure:

1. Hook up all testing components
  - a. Hydraulic Pump
  - b. Long High Pressure Line
  - c. Pressure Gauge
  - d. Check valve (prevents backflow)
  - e. Bleed valve
  - f. Cross Fitting
2. Connect hose to the NPT tap closure of the motor casing
3. Connect other end of hose to check valve on cross fitting
4. Fill casing and hose with water from open end of the casing
  - a. Make sure to move the casing around to allow as much air as possible to come out
  - b. Slightly open bleed valve to allow air to come out of casing/hose assembly
  - c. Once water begins to come out of bleed valve and casing/hose assembly is full of water, close bleed valve fully
5. Close open end of casing with second closure and snap ring
6. Make sure to set up casing away from any people. Around the corner of a building or with a blast shield in between.
7. Turn on the camera to watch both the pressure gauge and casing.
8. Begin pumping until pressure begins to rise.
  - a. Each pump afterwards should raise the pressure in the system. If it does not, the case might be yielding.



## Water test diagram



- b. If this is happening at a not super high pressure, there are two possible options
  - i. Check for leaks at the connections. Make sure there are no leaks anywhere.
  - ii. Air could be compressing inside the casing, if so it is safe to keep pumping since the casing should not yield.
9. Pump incrementally up to 1.5x Max Expected Operating Pressure (MEOP) (650 psi x 1.5)
10. Wait twice the expected motor burn time at 1.5x MEOP
11. Use bleed valve to relieve pressure slowly

### Test Results:

When pumping up from atmospheric pressure to 1000psi, the gauge seemed to stop increasing once 500psi was reached. The connection points between the fittings were thoroughly checked, but no leakages were found. The same casing was test fired twice before at 650psi so there was little concern about the casing yielding during this static test, so pumping to 1000psi continued. After reaching 1000 psi, the casing stayed at this pressure for over a minute before depressurizing. There were no cracks or yielding detected in the casing after the test.

Event and Success Criteria		
Ability to go to 1.5x MEOP	PASS	1/31/2023
Hold pressure for twice the burn time	PASS	1/31/2023
<b>System Analysis</b>	<b>SUCCESS</b>	<b>1/31/2023</b>



**D. SRAD GPS Testing**

(As found on the following page)

# SRAD Avionics Ground Test

Avionics | Varun Unnithan | University of Maryland | February 17, 2023

## Test Objective:

The SRAD avionics flight computer was assembled with all its components to test if the system worked. The goal would be to test whether an altered version of the flight computer, one with code suited for an on-the-ground test, would turn on completely, as well as record and report the desired data.

## Test Procedure:

1. Set up the board, adding in headers and the necessary components
2. Alter the stage code to not rely on in-flight indicators of changing stages
  - a. Replace it with code that waited a set amount of time before changing stages
3. Connect the board to a laptop to see real-time output from the computer
4. Turn on the board and verify that all parts are powered and running
5. Verify that the ground station radio is receiving transmitted packets from the transmitter
6. Verify that the NEO-M9N GPS received a fix and sensors are receiving data
7. Turn the board off
8. Verify that data was recorded and dumped to the SD Card

## Test Results:

This test proceeded as expected, with the board turning on and it being indicated, via serial transmissions to the connected laptop, that the Teensy microcontroller had turned on and all sensors had been properly set up. After a few seconds of setup, the radio module indicated that it was able to successfully receive sensor data from the microcontroller and turn it into an APRS packet for it to transmit. The receiver module and the ground station program associated with it was able to receive the transmitted packets and decode it successfully. Initially, the GPS did not receive a lock onto any satellites, and thus was not able to get any data, but after a few minutes and going into a more clear area, the GPS received a fix and was able to report longitude and latitude data. It initially picked up nine satellites to receive data from, but at times was in contact with up to seventeen satellites to receive better data from. Both the accelerometer and the altimeter were able to give accurate readings that seem to have matched the motion of the board as well. After the board was turned off, the SD Card was extracted, where it was found that the sensor data was successfully recorded and offloaded.



<b>Event and Success Criteria</b>		
Board turned on	PASS	2/17/2023
Radio was transmitting APRS packets	PASS	2/17/2023
Ground Station was receiving APRS packets	PASS	2/17/2023
GPS received a fix and position data	PASS	2/17/2023
Accelerometer recorded accurate data	PASS	2/17/2023
Altimeter recorded accurate altitude data	PASS	2/17/2023
SD Card held recorded data	PASS	2/17/2023
<b>System Analysis</b>	<b>SUCCESS</b>	2/17/2023



# SRAD Avionics Ground Range Test

Avionics | Varun Unnithan | University of Maryland | February 24, 2023

## Test Objective:

The goal of this test was to assess the radio transmitter and radio receiver in isolation to see how far, on the ground, the system can reliably transmit data, and if the receiver and transmitter can stay in contact the entire time.

## Test Procedure:

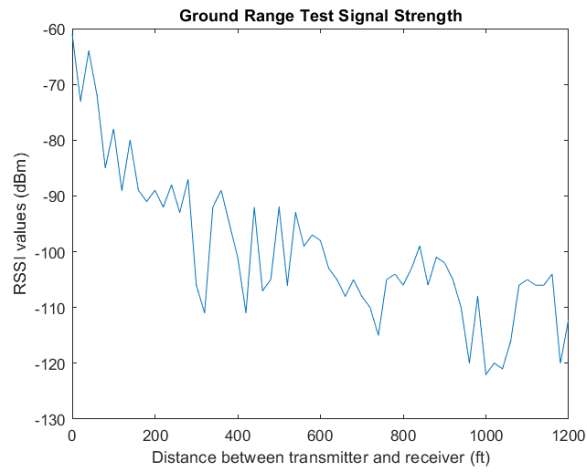
1. Modify the radio transmitter code to transmit pre-recorded data
  - a. To avoid issues due to sensor or Teensy errors
2. Set up the radio receiver and the ground station to be ready to receive packets
3. Have one person hold the transmitter, and start with the transmitter being next to the receiver
4. Turn on the transmitter, and begin to walk away from the receiver
  - a. Walk in a straight line over flat land that has a line of sight to the receiver
5. Continue walking until the end of the area is reached, before returning to the receiver
  - a. We used McKeldin Mall at the University of Maryland, which has a length of 1200 ft
6. Turn off the transmitter and turn off the receiver and ground station and collect data generated by the ground station

## Test Results:

The radio transmitter and the receiver both turned on fine and were able to get a connection between them where APRS packets were transmitted and received. The receiver was able to successfully transmit these packets to the ground station, where it was able to decode the packets correctly and yielded the expected data points. The initial issue that was noticed was that even when the transmitter and receiver were next to each other, low RSSI values were being recorded, around -60, indicating a lower signal strength than we expected and had seen when in closed rooms, a fact attributed to the fact we were outside. As the transmitter was moving away from the receiver, the RSSI decreased rapidly, as seen below on the graph.

As the distance to the receiver increased, the RSSI decreased at a lower rate, making the relationship between distance and RSSI values roughly follow an exponential decay. However, throughout, the RSSI values were lower than expected and by the time the transmitter had reached the end of the 1200ft, the RSSI value was around -110, a value much higher than desired if we wanted the range to extend much further than this distance. So despite the transmitter and receiver staying in contact the entire time, the low signal strength makes this test a partial failure.





Event and Success Criteria		
Radio transmitter and receiver turned on and initially connect	PASS	2/24/2023
Ground station correctly decodes the APRS packets received	PASS	2/24/2023
Ground Station was receiving APRS packets	PASS	2/24/2023
Receiver and transmitter remained in contact	PASS	2/24/2023
RSSI values remained high	FAILURE	2/24/2023
<b>System Analysis</b>	<b>PARTIAL FAILURE</b>	2/24/2023



# Avionics Flight Test 1

SRAD Avionics | Joseph Hauerstein, Varun Unnithan | MDRA Higgs Farm | March 5, 2023

## Test Objective:

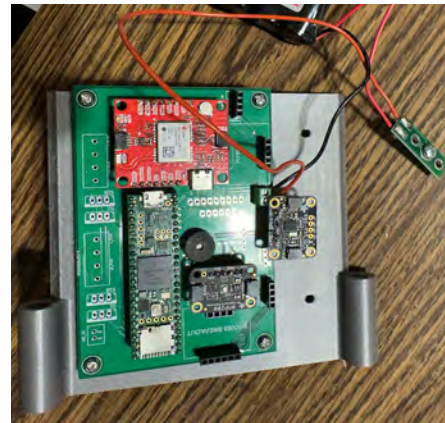
The goal of this event is to test how the flight computer performs when put on an actual rocket in terms of telemetry and datalogging. The SRAD avionics flight computer is to be mounted onto the sled in the electronics bay of the Karkinos rocket, and upon launch of the rocket, the flight computer should relay data to the ground station and record it to the SD card. This test has the goal of testing to see if the radio is able to transmit packets throughout the flight, and if an accurate data set about the flight can be obtained.

## Test Procedure:

1. Mount the avionics flight computer onto the electronics bay sled using screws
2. Turn on the radio transmitter, ensuring that the light indicating power blinks
3. Insert the sled into the rocket, ensuring that the screw switch can be accessed from the outside
4. When the rocket is on the pad, screw in the screw switch, turning on the Teensy and the rest of the avionics board
5. Set up the radio receiver and the ground station, and verify that the APRS packets are being received
6. Monitor the rocket via the ground station throughout the launch and flight, checking to ensure that data is being received
7. Once the rocket has landed, recover it and unscrew the screw switch, turning off the board
8. Turn off the radio transmitter
9. Remove the SD card and collect data from the SD card and the logs from the ground station
10. Verify that the data matches up with what is expected



Back of the sled with the radio module mounted



Front of the sled, with the complete board mounted

## Test Results:

The test began with turning on the radio module and the avionics board, both of which went well and were ready for the rocket's launch. After turning on the avionics board on the pad, and returning to the ground station, it could be seen that the radio receiver and ground station were receiving APRS packets, indicating that the radio module was transmitting. However, the data in these packets included faulty data, as the GPS longitude and latitude information was not being reported. Later examinations of the code



would reveal that this issue was due to a bug in the GPS code, as it was written to work when it was directly connected to a laptop or computer, as it looked to transmit serial data to such to report its fixes, however, when operating standalone with just the microcontroller, this code caused the GPS to fail. In addition, upon launch, the radio receiver immediately stopped receiving APRS packet transmissions, deeming this criteria as only a partial success. This was also due to a similar bug that emerged when code detecting the rocket's launch was triggered. There was also an issue with retrieving the data from the flight, as the SD card did not properly record the sensor data from the flight. This is believed to be due to the fact that since the rocket sat on the pad a while before launch, the PSRAM filled up with stationary data, thus preventing the actual flight data from having space to be stored. A remedy for this would be to implement a buffer for pre-launch flight data. These issues caused this flight test to be a failure.

<b>Event and Success Criteria</b>		
Radio transmitter and flight computer board turns on	PASS	3/4/23
Radio transmitter transmits packets to the ground station	PARTIAL FAILURE	3/4/23
GPS obtains a fix and relays position data	FAILURE	3/4/23
Accelerometer relays data	PASS	3/4/23
Altimeter relays data	PASS	3/4/23
SD card records flight sensor data	FAILURE	3/4/23
Data matches what was expected	FAILURE	3/4/23
<b>System Analysis</b>	<b>FAILURE</b>	3/4/23



# Avionics Flight Test 2

SRAD Avionics | Varun Unnithan | MDRA Higgs Farm | April 2, 2023

## Test Objective:

The goal of this test is to assess how the flight computer performs in an actual flight, and to see if it is capable of recording and transmitting reliable data about the rocket's flight. The updated board containing bug fixes and a buffer for the SD card data storage will be flown on Karkinos to see if these fixes can remedy the issues found in the previous flight test, and to see if a reliable dataset can be acquired. In addition, a Yagi antenna is used in connection with the radio receiver to see if improved telemetry connections and ranges can be established.

## Test Procedure:

1. Mount the avionics flight computer onto the electronics bay sled using screws
2. Turn on the radio transmitter, ensuring that the light indicating power blinks
3. Insert the sled into the rocket, ensuring that the screw switch can be accessed from the outside
4. When the rocket is on the pad, screw in the screw switch, turning on the Teensy and the rest of the avionics board
5. Set up the ground station and the radio receiver, connecting the Yagi antenna to the receiver
6. Verify that the APRS packets are being received by the ground station
7. Monitor the rocket via the ground station throughout the launch and flight, checking to ensure that data is being received
8. Once the rocket has landed, recover it and unscrew the screw switch, turning off the board
9. Turn off the radio transmitter
10. Remove the SD card and collect data from the SD card and the logs from the ground station
11. Verify that the data matches up with what is expected

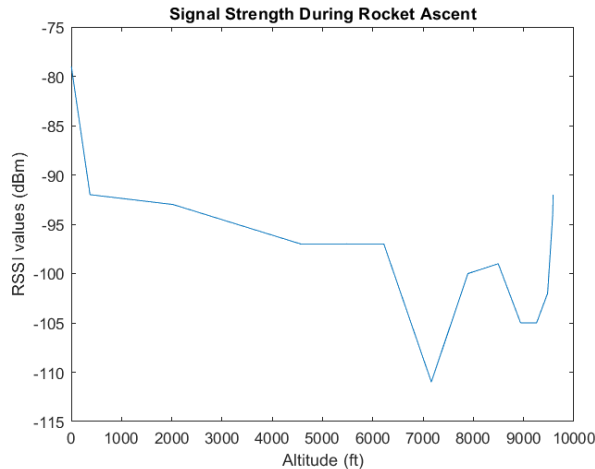
## Test Results:

This test flight went well, with the transmitter and board correctly turning on when the button is pressed and the screw switch was tightened, as indicated by the buzzer on the avionics board. The radio transmitter module transmitted APRS packets that were picked up by the receiver module and were able to be decoded by the ground station. Altitude, orientation and GPS position data were all reported by the sensor array through the radio transmissions, indicating that these transmissions were successful at providing this data in real-time. As the rocket launched, the radio transmissions relayed live data of the rocket's altitude, speed, and position, which continued throughout the duration of the rocket's flight, indicating that the radio transmitter was able to stay within range. In addition, upon landing, the SD card and flight computer were able to be recovered, where it was then found that the data was able to be effectively stored.

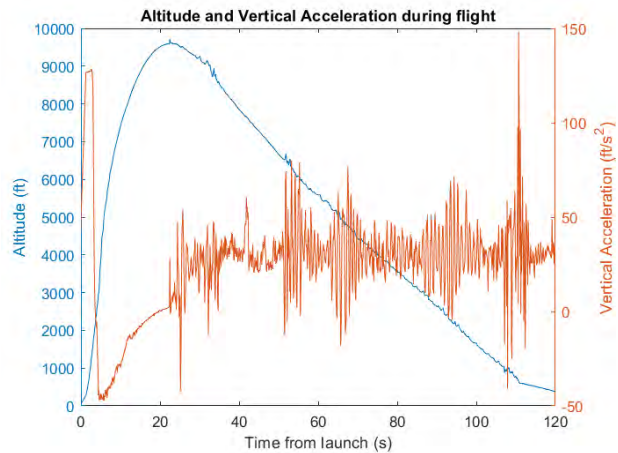
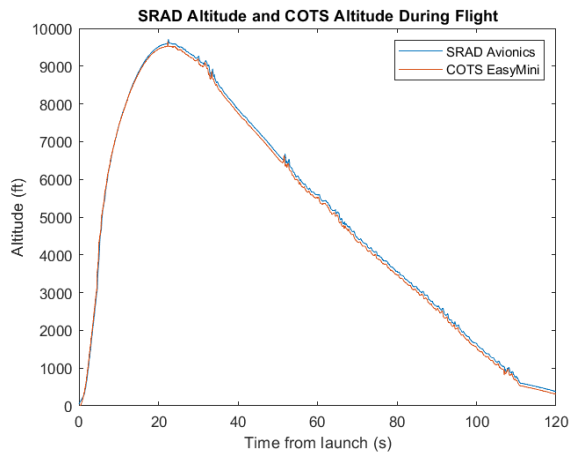
During the flight itself, the live radio transmissions gave flight data for altitude and speed that matched what would be expected by the flight, which was corroborated by the data obtained from the SD card. This test flight was also to be used as a range test for the radio, and by staying in contact for the duration of the flight, the radio's range was tested for distances up to its furthest point. This would be at apogee, at around 9570 ft above the ground, at which point the rocket was also 2090 ft away from the ground station along the ground. Thus, the radio's range was successfully tested to a distance of up to about 9800 ft, which is a little short of two miles. The radio transmission's RSSI values over the duration of the rocket's



ascent can be seen in the figure below, with a lower RSSI value corresponding to a weaker signal. Since a directional antenna was used, spikes in the graph may be due to human inaccuracy in following the rocket with the antenna, which would help explain why, at apogee, the RSSI values increased, as since the rocket was slowing down and more visible, it was easier to track. Throughout the flight, the RSSI values stayed at around -100 or below, which is successful considering the lower limit threshold for reliable data as -120.



The SD card's buffer system worked as well, holding only 10 seconds worth of pre-flight data. It was also able to record reliable and accurate data for other flight parameters, thus succeeding in its goals. The plots of the rocket's recorded altitude over time, as well as its vertical acceleration are shown below. The altitude curve follows what is expected and what was recorded by the commercial flight computers onboard, recording an apogee of around 9580 ft. The rocket's descent data is more noisy than ideal, however, and this is something that can be improved for future flights through the use of an effective Kalman filter or other filtering system. In addition, the altitude data combined with the recorded data for the rocket's vertical acceleration shows the stages of flight for the rocket, with the data matching what is predicted. The peak in acceleration four seconds after launch matches with the rocket's powered ascent and then coasting, with the acceleration also being zero at apogee and spiking when the main parachute is deployed, all of which occurs at the expected periods, indicating that the recorded data is reliable and accurate.



<b>Event and Success Criteria</b>		
Radio transmitter and flight computer board turns on	PASS	4/2/23
Radio transmitter transmits packets to the ground station	PASS	4/2/23
Radio transmissions stay in range throughout the flight's duration	PASS	4/2/23
GPS obtains a fix and relays position data	PASS	4/2/23
Accelerometer relays data	PASS	4/2/23
Altimeter relays data	PASS	4/2/23
SD card buffer works	PASS	4/2/23
SD card records flight sensor data	PASS	4/2/23
Data matches what was expected	PASS	3/4/23
<b>System Analysis</b>	<b>SUCCESS</b>	3/4/23



**E. Payload Recovery System Testing**

(As found on the following page)

# Release Mechanism Verification

Payload | Nathan Roy | University of Maryland | March 3, 2023

## Test Objective:

Release an object from the release mechanism.

## Test Procedure:

1. Load an inert vehicle into the release system
2. Trigger the release mechanism using the light sensor
3. Evaluate the ability of the release system to overcome internal forces and eject the vehicle

## Test Results:

The release system successfully released when triggered, and pushed the vehicle out of the mechanism.

Event and Success Criteria		
The release pins trigger off the light sensor	PASS	3/3/2023
The vehicle clears the mechanism	PASS	3/3/2023
<b>System Analysis</b>	<b>SUCCESS</b>	<b>3/3/2023</b>



# Release Flight 1

Payload | Nathan Roy | MDRA Higs Farm | March 5, 2023

## Test Objective:

Release an object from the rocket during descent under drogue.

## Test Procedure:

1. Load an inert vehicle with a radio beacon into the release system
2. Load the release system into the rocket with the nose cone ebay
3. Set the nose cone separation easy mini to fire a 1g black powder charge at 4000ft
4. Set the release system to deploy the vehicle 30 seconds after nose cone separation is detected
5. Turn on the nose cone electronics
6. Launch the rocket
7. Separate the nose cone
8. Deploy the vehicle
9. Recover the vehicle
10. Evaluate the release mechanism post-launch to ensure vehicle separation was intentional and not the result of structural failure

## Test Results:

The release system successfully released the vehicle through the pin system following nose cone separation. However, the rocket landed in a forested area, which prevented locating the vehicle with the radio beacon.

Event and Success Criteria		
Release the vehicle	PASS	3/5/2023
Recover the vehicle	FAILURE	3/5/2023
System Analysis	SUCCESS	3/5/2023



# Release Flight 2

Payload | Nathan Roy | MDRA Sod Farm | May 6, 2023

## Test Objective:

Recover a vehicle deployed from the rocket and test telemetry via.

## Test Procedure:

1. Load the vehicle into the release system
2. Power on the Featherweight GPS establish a GPS fix
3. Power on the jolly logic parachute release mechanism
4. Establish a connection with the APRS repeater
5. Load the release system into the rocket with the nose cone eBay
6. Set the nose cone separation easy mini to fire a 1g black powder charge at 1700ft
7. Set the release system to deploy the vehicle 5 seconds after nose cone separation is detected
8. Turn on the nose cone electronics
9. Verify Featherweight connection while on the launch rail
10. Launch the rocket
11. Separate the nose cone
12. Deploy the vehicle
13. Read telemetry data off the Featherweight
14. Recover the vehicle



## Test Results:

The payload successfully separated and was recovered from the rocket. Due to a calibration issue with the light sensor, the vehicle was released earlier than expected, but this did not impact the flight or recovery. The Featherweight GPS provided telemetry throughout the flight and was not impeded by interference due to the launch rail. The parachute release helped with vehicle recovery, as the vehicle descent rate was slower than expected. A picture of the descending vehicle and rocket can be seen to the right.

Event and Success Criteria		
Recover the vehicle	PASS	5/6/2023
Read GPS data off the Featherweight GPS	PASS	5/6/2023
<b>System Analysis</b>	<b>SUCCESS</b>	<b>5/6/2023</b>



**F. Additional Tests**

(As found on the following page)

# Payload Drop Test 1

Payload | Nathan Roy, Michael Mallamaci | University of Maryland | October 6, 2022

## Test Objective:

To determine the effectiveness of adjusting the length of parachute risers to cause drift in a given direction on the scale of a 36in parachute.

## Test Procedure:

1. Hold the motion system prototype (pictured to the right) from the top of a parking garage by the parachute
  - a. The riser control lines should be set up such that 2 neighboring servos are in the up position and 2 in the down
2. Release the parachute
3. Visually determine drift in the system



## Test Results:

As the system descended it began to drift forward, although spin caused the system to spiral, preventing any net lateral movement.

Event and Success Criteria		
Motion towards to actuated servos	PASS	10/6/2022
<b>System Analysis</b>	<b>SUCCESS</b>	<b>10/6/2022</b>



# Payload Drop Test 2

Payload | Michael Mallamaci | MDRA Sod Farm | October 8, 2022

## Test Objective:

To determine the effectiveness of adjusting the length of parachute risers to cause drift in a given direction from a higher altitude, and with greater mass.

## Test Procedure:

1. Connect the motion system device to the shock cord of a 3” test rocket
2. Launch the rest rocket
3. As the rocket descends, actuate the servo motors for 10 seconds, then reset
4. Visually determine whether a change in drift occurred due to the motion system

## Test Results:

During the deployment of the motion system from the rocket, the parachute became tangled, preventing it from opening. Furthermore, it was determined afterward that the servo motors were too weak to adjust the parachute risers to the full length required.

Event and Success Criteria		
Observe movement	FAILURE	10/8/2022
System Analysis	FAILURE	10/8/2022



# Air Brake, Data Collection, and Controller Tests

Air brake | Ezra Bregin, Sunjum Mehta, Matthew Chou | MDR, Higgs Farm |  
January 7th, February 4th, March 5th, April 2nd, and May 6th 2023

## Test Objective:

Test the various Air Brake subsystems.

## Test Procedure:

### *Prelaunch*

1. Assemble the Air Brake as defined in the Air Brake Manual
2. Integrate the Air Brake in the rocket

### *Launch*

1. Turn on the power switch

### *Post Launch and Data Analysis*

1. Unload the SD card and download the data into Matlab
2. Process data

## Test Results:

	Objective	Result	Date
Flight 1	Obtain sensor data	PARTIAL FAILURE (data corrupted)	1/7/2023
Flight 2	Obtain flight data	SUCCESS	2/4/2023
	Deploy flaps to waypoints	SUCCESS	2/4/2023
Flight 3	Obtain flight data	SUCCESS	3/5/2023
	Test tilt algorithm	SUCCESS	3/5/2023
	Deploy flaps to waypoints	FAILURE (Unknown Failure)	3/5/2023
Flight 4a	Obtain flight data	SUCCESS	4/2/2023
	Test Controller	SUCCESS (Apogee error of 74 ft)	4/2/2023
Flight 4b	Obtain flight data	SUCCESS	4/2/2023
	Test Controller	FAILURE (Bad Actuator Batteries)	4/2/2023
Flight 5	Obtain flight data	SUCCESS	5/6/2023
	Test additional ground health checks	SUCCESS	5/6/2023
	Test deployment error correction	PARTIAL FAILURE (limited correction)	5/6/2023





# Data Collection Flight 1

Payload | Nathan Roy | MDRA Higgs Farm | January 7, 2023

## Test Objective:

To collect an altimeter and accelerometer data set for use in Kalman filter development, and to test the ability of a magnetic connector to withstand the forces of a launch.

## Test Procedure:

1. Load a PCB with the required sensors and magnetic connector into the rocket with a boilerplate payload
2. Turn on the PCB
3. Launch the rocket
  - a. During the launch the PCB records altimeter and accelerometer data, as well as reads if the magnetic connector is still intact
4. After the rocket lands, write recorded data to an SD card
5. Recover the PCB after launch, and read the collected data off an SD card

## Test Results:

Unaccounted power drain through the magnetic connector state detection system and extended time on the launch pad resulted in the system dying before recorded data could be dumped to the SD card, preventing the recovery of data. The magnetic connector stayed connected throughout the whole flight, verifying its ability to withstand the required forces.

Event and Success Criteria		
Evaluate the connector	PASS	1/7/2023
Collect data	FAILURE	1/7/2023
System Analysis	FAILURE	1/7/2023



# Data Collection Flight 2

Payload | Andrew Bean | MDRA Sod Farm | February 4, 2023

## Test Objective:

To collect an altimeter and accelerometer data set for use in Kalman filter development.

## Test Procedure:

1. Load a PCB with the required sensors into the rocket with a boilerplate payload
2. Turn on the PCB
3. Launch the rocket
  - a. During the launch the PCB records altimeter and accelerometer data
4. After the rocket lands, write recorded data to an SD card
5. Recover the PCB after launch, and read the collected data off an SD card

## Test Results:

The rocket landed in a tree, causing the nose cone to swing into the trunk, damaging the PCB and preventing data from being recorded to an SD card.

Event and Success Criteria		
Collect data	FAILURE	2/4/2023
System Analysis	FAILURE	2/4/2023



# Printed Circuit Board Testing

Airbrake | Ezra Bregin, Garrett Alessandrini, Matthew Chou | Cypress Building | February 12th

## Test Objective:

The printed circuit board routes signaling between all the air brake's components. Each circuit board has been designed through Fusion 360 and is sent to PCBWay for manufacturing. This process may take up to three weeks with each order requiring a minimum purchase of five boards. There were a total of three main PCB iterations with two smaller designs for separate rocket testing. The goal of PCB testing is to establish proper current continuity and for the system to perform aboard a test flight.

## Test Procedure:

### Development

1. Solder header pins according to the PCB silk screening.
2. Solder buzzer, JST connectors, and Molex connectors to PCB, also following silk screening.
3. Plug-in data sensors and microcontrollers.

### Testing Stages

1. Plug in USB-C to power up the Main Teensy. A power test is successful if all components light up.
2. Upload test program and await connection message from TeensyDuino console. A connection test is successful if all components are found by the program.
3. Data outputted from the test program must make sense. A successful data test has values consistent with the motion of the circuit board sensors.
4. Launch the PCB aboard a test rocket. A successful flight test has values consistent with the motion of the circuit board sensors.

## Test Results:

*Main Iteration 1:* Failed at the first test, the power improperly wired, components must fit on one side

*Main Iteration 2:* Failed at the third test, TX and RX lines must be connected to their opposite pin

*Main Iteration 3:* Passed all four tests

*Test Rocket Iteration 1:* Fails at the second test. Same issue as *Main Iteration 2*

*Test Rocket Iteration 2:* Fails at the third test. Sensor lines may be creating interference.

Event and Success Criteria					
PCB	Power	Connection	Data	Flight	Date
Main 1	FAILURE	-	-	-	
Main 2	PASS	PASS	FAILURE	-	
Test 1	PASS	FAILURE	-	-	
Test 2	PASS	PASS	-	-	
Main 3	PASS	PASS	PASS	PASS	



# Wind Tunnel Test

Air brake | Ezra Bregin, Andrew Bean | Glenn Martin Wind Tunnel | February 22nd, 2023

## Test Objective:

Determine the coefficient of drag with respect to wind tunnel speed and flap deployment angles. From this data, we will be better able to tune the Kalman Filter and project our altitude and respective flap deployment. A smoke test would also be performed for visualization and photography purposes.

## Test Procedure:

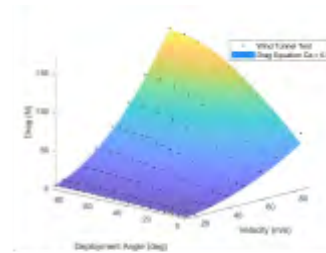
### Test

1. Run the wind tunnel from the following velocities (m/s) [15, 20, 30, 40, 50, 60, 70, 85]
  - a. With each velocity, span the angles [0-90]
2. A smoke test at 30 m/s was conducted using a smoke machine placed at the tip of the rocket

### Post Launch and Data Analysis

1. Pull data from onboard SD card and from Wind Tunnel data files
2. Process data and upload visuals

## Test Results:



(Left) Wind Tunnel with mounted rocket. (Right) CD processing with MATLAB

Run	Velocity (m/s)	Flap (deg)	Smoke	Success
1	15	[0,90]	-	
2	20	[0,90]	-	
3	30	[0,90]	-	
4	15	[0,90]	Yes	
5	40	[0,90]	-	
6	50	[0,90]	-	
7	60	[0,90]	-	
8	70	[0,90]	-	
9	85	[0,90]	-	



# Airbrake Flap, Tensile Test

Airbrakes | Ezra Bregin, Kyle Kingsberry, Matthew Chou | Cypress Building | March 1st, 2024

## Test Objective:

The air brake's flaps are the fins that induce drag upon the rocket. Initial test flights demonstrated flap failure under induced drag. This testing would look into the feasibility of differing materials, drawing comparisons between plastic and carbon fiber composites versus fiberglass. Testing would be carried out using a luggage scale and fiberglass flap with an interfacing slot.

## Test Procedure:

### Development

1. 3D print a flap template with an outer diameter equal to the inner diameter of a 6-in diameter tube
2. Clean print of impurities.
3. Remove four sections of a 6-in-diameter fiberglass body tube using a dremel and clamps. Ensure the cross-section is larger than the flap template.
4. Trace the dimensions of the printed template along the fiberglass's body. This was done by using a strong source of light and fiberglass's opaque complexion to distinguish the template perimeter.
5. Dremel off the extra fiberglass beyond the traced perimeter. When trimming for precision, sand the fins along a piece of sandpaper taped onto a flat surface.

### Testing

1. Remove a rectangular hole from the now complete test flap.
2. Slide in a luggage scale, making sure the hook is secure in the hole
3. Have two individuals pull on both ends, measuring with a luggage scale. The drag test is successful once flaps can operate under 150 lbs of force.

## Test Results:



Fig 1: Luggage scale to flap interface



Fig 2: Tension testing flap system

Event and Success Criteria		
Event 1	PASS	3/1/23



# Blue Rocket, Data Collection Test

Air brake | Ezra Bregin, Sunjum Mehta, Matthew Chou | MDR, Higgs Farm | March 5th and April 2nd 2023

## Test Objective:

The Blue Rocket is an alternative L3 rocket used by Terrapin Rockets to test fly preliminary systems. In this test, our goal was to collect and analyze the quality of the flight sensor data, specifically the IMU and barometric outputs.

## Test Procedure:

### Prelaunch

1. Plug USB-C into PCB and power up, test if the connection to all components exist
2. Flash PCB with flight testing parameters
3. Assemble the air brake according to the checklist
4. Load onto Blue Rocket

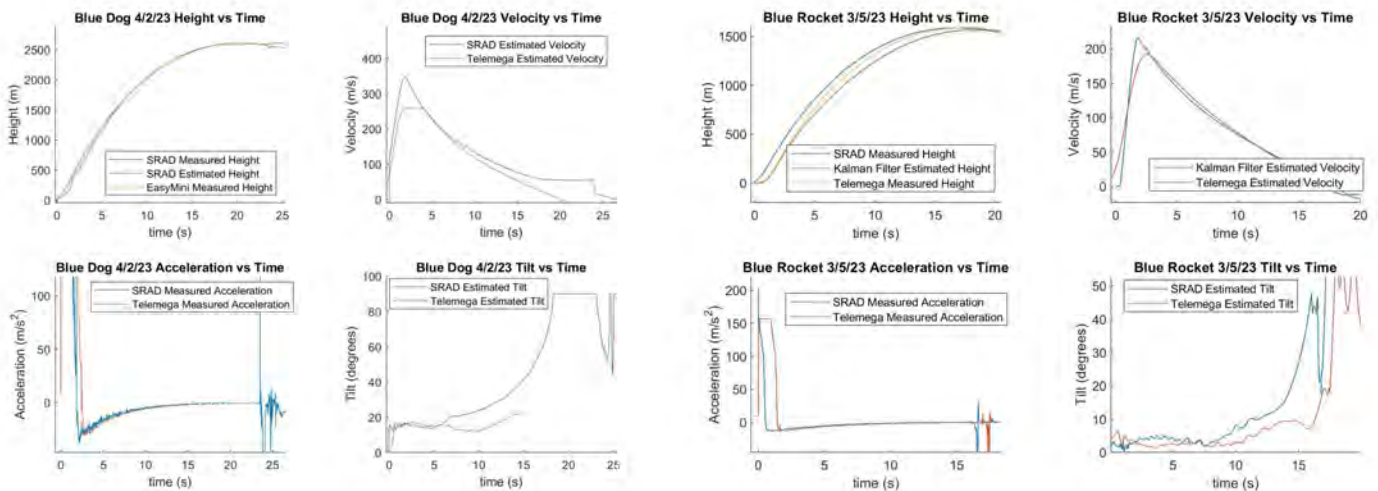
### Launch

1. Turn on the power switch

### Post Launch and Data Analysis

1. Unload the SD card and download the data into Matlab
2. Process data
3. Match apogee and accelerations with predictions

## Test Results:



Event and Success Criteria*		
Flight 1	PASS	3/4/23
Flight 2	PARTIAL FAILURE	4/2/23
System Analysis	SUCCESS	5/6/23

*\*Note, there were other test flights excluding Blue Rocket*



# Vehicle Retention Flight

Payload | Andrew Bean | MDRA Higgs Farm | April 2, 2023

## Test Objective:

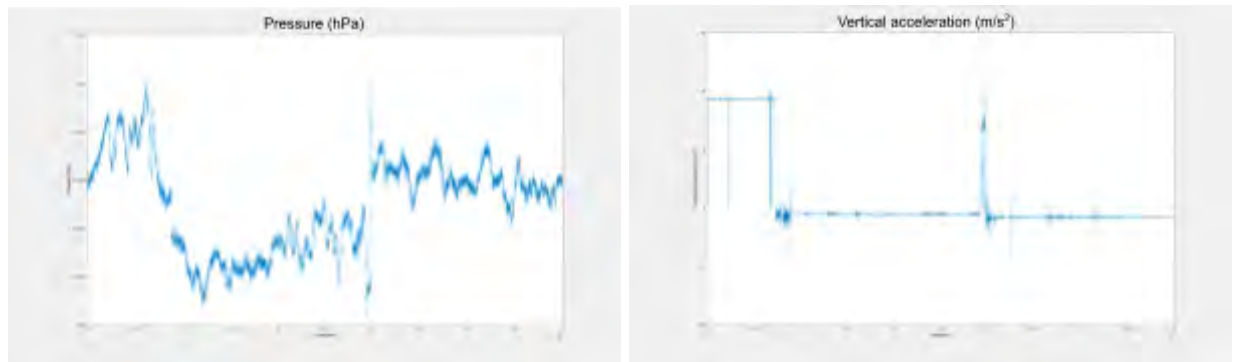
Ensure that the mass of the vehicle will not cause premature separation during the launch, and collect a data set for use in Kalman filter development.

## Test Procedure:

1. Load a 1.5lb mass stand in into the release system.
2. Load the release system into the rocket without the nose cone ebay electronics
3. Turn on nose cone electronics
4. Launch the rocket
5. Record data directly to the SD card
6. After recovering the rocket, verify that the release mechanism properly retained the mass stand in

## Test Results:

While the pin system succeeded in retaining the mass, the incorrect fishing line was used, which resulted in the retention lines fraying and breaking. This did not impact the function of the rocket, as the mass was still retained by a backup cover. A dataset was recovered, although as the nose cone was not separated, pressure data did not represent the actual flight. Furthermore, as data was written directly to the SD card, there are places in the data where the lack of connection due to launch vibrations caused a reset.



Event and Success Criteria		
Collect data	PASS	4/2/2023
Retain the mass stand in	FAILURE	4/2/2023
System Analysis	FAILURE	4/2/2023



THIS PAGE IS INTENTIONALLY LEFT BLANK

**VII. Appendix C - Hazard Analysis**  
(As found on the following page)

**Table 23 Hazard Analysis**

Hazardous Material	Storage	Handling	Transportation	Risk of Mishap	Mitigation (Process/Design)	Risk of Injury after Mitigation
Black Powder	Stored in a dry cabinet away from any flammable substances.	When used, avoid any heat and ignition sources. Use Black Powder vials to measure and load. Do not touch directly. Wear safety glasses of face shield.	Kept in original packaging until used.	Low	Restricted access to individuals who are experienced and familiar with the material and handling procedures.	Very Low
Fuel Grains	Ensure fuel grains remain in plastic bags. Keep stored in a flame locker.	Keep fuel grains in original packaging until ready to be loaded into casing. Loading should only be done by certified individuals. Once in the casing, the motor is handled carefully to prevent fracturing the grains or nozzle.	Keep in original packaging out of the sun and somewhere cool and dry.	Low	Only individuals whom hold certifications for given rocket motor (or are in the process of obtaining) are authorized to handle fuel grains.	Very Low
Lipo Batteries	Keep in cool dry places. Ensure in a flame retardant battery case. Stored at "storage voltage".	LiPo batteries should be stored in safe places until ready for use. Avoid sharp objects and high temperature areas.	Batteries should only be transported in the authorized LiPo battery transportation bags per safety instructions.	Low	Ensure battery charging is done correctly with multi cell battery charger. Charging only prior to launch/test events. Inspect batteries before/after use for punctures or any other signs of damage.	Very Low
E-Matches Igniters	Stored in a dry flame locker. Keep away from any ignition sources or energetics.	Careful when handling to ensure circuitry doesn't prematurely detonate. Leads are twisted or shunted when not connected to flight computer	Transport in a separate container from energetics and ignition sources	Low	Circuit switches will be switched off and flight computers will only be powered on once the vehicle is on the pad ready for the flight to prevent premature ignition.	Very Low

**VIII. Appendix D - Risk Assessment**  
(As found on the following page)

Risk Assessment					
Hazard	Possible Causes	Risk of Mishap and Rationale	Mitigation Approach	Risk of Injury After Mitigation	Overseeing Division
Explosion of solid-propellant rocket motor during launch with blast or flying debris causing injury	Cracks in propellant grains, incorrect assembly of motor	Low	Grains will be inspected before assembly and the motor will be assembled only by those certified following the proper procedure..	Low	Propulsion
Rocket deviates from nominal flight path, comes in contact with personnel at high speed	Rocket has low rail exit velocity, is unstable, or fins have broken off	Low	Simulate rocket in Open Rocket to calculate stability caliber, calculate fin flutter for expected speeds. Rocket has been test flown multiple times to verify simulation results.	Low	Aerostructures
Recovery system fails to deploy, rocket or payload comes in contact with personnel	Flight computers fail to fire charges, charges are undersized	Low	Redundant independant flight computers, batteries, and charges. Ground and flight testing of ejection and separation systems.	Low	Recovery
Recovery system partially deploys, rocket or payload comes in contact with personnel	Parachutes become tangled, main does not deploy	Medium	Parachutes carefully packed to ensure clean exit from body tube and easy inflation. Test flights to check for correct packing of recovery system and charge sizing.	Low	Recovery
Recovery system deploys during assembly or prelaunch, causing injury	Flight computers are turned on while loading and packing the rocket. E-matches are accidentally shorted	Low	Flight computers are powered off while connected to igniters and charges. Computers are only powered on once on the pad and ready for launch. Igniters are twisted or shunted until connected to flight computers. Personell handling energetics are minimized and wearing proper safety equipment	Low	Recovery
Main parachute deploys at or near apogee, rocket or payload drifts to highway(s)	Incorrect wiring to flight computers, heavy nosecone seperates due to drogue ejection forces	Medium	Flight computer connections are checked by multiple team members to verify correctness. Long drogue lines and extra shear pins in nosecone are in place to prevent early separation	Low	Recovery
Rocket does not ignite when command is given (“hang fire”), but does ignite when team approaches to troubleshoot	Igniter incorrectly inserted, not following manufacturer specifications	Low	Make sure igniter is inserted all the way into the motor. Tape dowel to launch tower to prevent it from falling out.	Low	Propulsion
Rocket falls from launch rail during prelaunch preparations, causing injury	Rail buttons fall off	Low, Rail buttons tightly secured	Rail buttons are tightened into nuts in airframe. Rocket is raised by the rail buttons to make sure they are on properly.	Low	Aerostructures
Power loss	Batteries not charged, wired disconnected during flight, flight causes a switch to flip	Low	Batteries are charged/replaced prior to flight. Only switches used are those that will not turn off during flight	Low	Recovery
Fail to detonate at decoupling event altitude	Power loss due to severed wires or flipped switch. Insufficient ejection force to break shear pins. Bad e-match.	Medium	Redundant independant flight computers, batteries, and switches. Ground testing of ejection and separation. Switches used cannot be turned off by flight forces. E-matches are checked with multimeter to check continuity before connecting to computers.	Low	Recovery

**IX. Appendix E - Assembly, Preflight, and Launch Checklists and Procedures**  
(As found on the following page)

**Assembly, Preflight, and Launch Checklists**

<b>Project Terpulence Karkinos</b>			<b>June 2023</b>
<b>Step</b>	<b>Division</b>	<b>Task</b>	<b>Completed?</b>
<b>ASSEMBLE MAIN RECOVERY SECTION</b>			
1.0	Recovery	Fold main tightly and burrito wrap in nomex blanket	<input type="checkbox"/>
1.1	Recovery	Verify nosecone is connected to second loop from the top and the main parachute to the top loop	<input type="checkbox"/>
1.2	Recovery	Verify all quick links are connected to shock cords and tightened	<input type="checkbox"/>
1.3	Recovery	Insert packed main parachute into recovery airframe	<input type="checkbox"/>
1.4	Recovery	Carefully z fold shock cord with blue tape and insert behind main parachute	<input type="checkbox"/>
1.5	Recovery	Slide nosecone into main airframe and align marks for shear pins (make sure payload is ready first)	<input type="checkbox"/>
1.6	Recovery	Stand section vertically and insert 6 4-40 shear pins into nosecone	<input type="checkbox"/>
<b>ASSEMBLE PAYLOAD SECTION</b>			
2	Payload	Bolt the payload to the middle bulkhead, aligning the black stripe	<input type="checkbox"/>
2.1	Payload	Run the payload switch wire through the middle bulkhead and seal the hole with tape	<input type="checkbox"/>
2.2	Payload	Run a 1g black powder charge through the top and middle bulkheads, and seal the top hole with electrical tape	<input type="checkbox"/>
2.3	Payload	Place the payload in the coupler, aligning the release hole with the cutout	<input type="checkbox"/>
2.4	Payload	Connect the payload switch, easy mini switch, and black powder charge to their respective points on the nose cone sled	<input type="checkbox"/>
2.5	Payload	Load the nose cone sled into the coupler	<input type="checkbox"/>
2.6	Payload	Bolt the sled down	<input type="checkbox"/>
2.7	Payload	Bolt the bottom bulkhead to the coupler (ensure the bulkheads sit flush against the inner coupler)	<input type="checkbox"/>
2.8	Payload	Bolt the payload to the upper bulkhead (use nuts as spacers)	<input type="checkbox"/>
2.9	Payload	Connect the shock cord from the nose cone tip to the eye bolt on the top bulkhead	<input type="checkbox"/>
2.1	Payload	Turn on the vehicle featherweight GPS and verify connection to groundstation	<input type="checkbox"/>
2.11	Payload	Turn on the vehicle	<input type="checkbox"/>
2.12	Payload	Turn on the jolly logic parachute release and set it to 300ft	<input type="checkbox"/>
2.13	Paylaod	Connect the nose cone to the coupler with 2 shear pins, ensuring the top bulkhead seals correctly	<input type="checkbox"/>
<b>ASSEMBLE DROGUE RECOVERY SECTION</b>			
3	Recovery	Fold drogue tightly and burrito wrap in nomex blanket	<input type="checkbox"/>
3.1	Recovery	Verify all knots and quick links are tightened	<input type="checkbox"/>
3.2	Recovery	Assemble air brake module (see section 6)	<input type="checkbox"/>
3.3	Recovery	Feed Y harness lines through airbrake module	<input type="checkbox"/>
3.4	Recovery	Secure airbrake module using 2 1/4"-20 screws on foward and aft ends	<input type="checkbox"/>
3.5	Recovery	Connect Y harness to drogue harness and slide drogue tube onto airbrake	<input type="checkbox"/>
3.6	Recovery	Carefully fold shock cord lines with painters tape	<input type="checkbox"/>
3.7	Recovery	Push drogue harness and folded drogue parachute into airframe. Push it all the way in.	<input type="checkbox"/>
<b>ASSEMBLE AVIONICS BAY</b>			

4.0 Recovery	Make sure main power switches are turned off and batteries are disconnected	<input type="checkbox"/>
4.1 Recovery	Locate four 3ft ematches and verify continuity with multimeter. Twist leads to shunt	<input type="checkbox"/>
4.2 Recovery	Pack charges using 4F black powder to the following amounts: main 6g/7g, drogue 7g/8g	<input type="checkbox"/>
4.3 Recovery	feed charges through bulkheads and secure into proper terminals	<input type="checkbox"/>
4.4 Recovery	lightly tug each wire to make sure it is secure in the screw terminal	<input type="checkbox"/>
4.5 Recovery	use electrical tape to seal wire holes on both bulkheads	<input type="checkbox"/>
4.6 Recovery	plug in batteries	<input type="checkbox"/>
4.7	Plug in batteries for GPS units. Turn on switch if necessary. Verify lock and telemetry	<input type="checkbox"/>
4.8 Avionics	Press the small button near the usb port on the SRAD TTGO radio transmitter and release - light should turn on	<input type="checkbox"/>
4.9 Recovery	slide aft bulkhead onto threaded rods and align sled with screw switch holes	<input type="checkbox"/>
4.10 Recovery	on each threaded rod add a washer and two 5/16" nuts. Tighten each with a wrench.	<input type="checkbox"/>
4.11 Recovery	Verify quick links have been connected to U-bolts and tightened	<input type="checkbox"/>
4.12 Recovery	Align electronics bay with marks on main recovery airframe. Secure with two 1/4" 20 screws	<input type="checkbox"/>
4.13 Recovery	Align electronics bay on booster section, stand rocket vertically	<input type="checkbox"/>
4.14 Recovery	insert 4 4-40 shear pins into booster - electronics bay connection. Wrap completely with tape	<input type="checkbox"/>

### ASSEMBLE MOTOR SECTION

- |                |   |                          |
|----------------|---|--------------------------|
| 5.0 Propulsion | Glue grains to liner at least 24 hrs before launch  | <input type="checkbox"/> |
|                | Run nail along snap rings to find any burrs. Use sandpaper to remove and sharp edges. Clean snap ring grooves and o ring grooves of any debris. | <input type="checkbox"/> |
| 5.1 Propulsion | Verify both the forward closure and nozzle each have two greased orings   | <input type="checkbox"/> |
|                | Stand liner on top of nozzle and grease thouroughly. Slide casing over liner.   | <input type="checkbox"/> |
|                | Insert forward closure and nozzle washer. Insert snap rings and verify that they are fully seated.  | <input type="checkbox"/> |
| 5.2 Propulsion | Insert motor into motor tube and secure with aeropack retainer  | <input type="checkbox"/> |
|                | Tape igniter to thin dowel rod. Tape multiple dowels together if necessary.   | <input type="checkbox"/> |
| 5.3 Propulsion |   | <input type="checkbox"/> |
| 5.4 Propulsion | do not insert igniter until on pad and electronics have been turned on  | <input type="checkbox"/> |

### Assemble Air Brake Module

- |               |   |                          |
|---------------|---|--------------------------|
| 6.0 Air Brake | Charge both 4s Lipo Batteries                     | <input type="checkbox"/> |
| 6.1 Air Brake | Insert fresh 9V Battery                           | <input type="checkbox"/> |
| 6.3 Air Brake | Install air brake electronics bay into module     | <input type="checkbox"/> |
| 6.4 Air Brake | Flash arduino test code and test configuration    | <input type="checkbox"/> |
| 6.5 Air Brake | Turn off arduino                                  | <input type="checkbox"/> |
| 6.6 Air Brake | Turn linear screw until flaps are fully retracted | <input type="checkbox"/> |
| 6.7 Air Brake | Install linear screw guard                        | <input type="checkbox"/> |

### PREFLIGHT CHECKLIST

#### Nominal Procedure

- |               |  |                          |
|---------------|--|--------------------------|
| 7.0 N/A       | Carry rocket out to launch pad   | <input type="checkbox"/> |
| 7.1 N/A       | Install rocket on rail   | <input type="checkbox"/> |
| 7.2 Avionics  | Turn on nose cone electronics  | <input type="checkbox"/> |
| 7.3 N/A       | Lift launch rail vertically  | <input type="checkbox"/> |
| 7.4 Avionics  | Turn on nose cone easy mini via wifi switch                            | <input type="checkbox"/> |
| 7.5 Air Brake | Turn on Airbrake flight computer                                       | <input type="checkbox"/> |
| 7.6 Air Brake | Plug in Lipo Batteries   | <input type="checkbox"/> |
| 7.7 Avionics  | Turn on SRAD avionics  | <input type="checkbox"/> |
| 7.8 Avionics  | Turn on Primary EasyMini switch and verify continuity on both charges  | <input type="checkbox"/> |
| 7.9 Avionics  | Turn on Backup EasyMini and verify continuity on both charges          | <input type="checkbox"/> |
| 7.1 Avionics  | Verify GPS systems are still transmitting                              | <input type="checkbox"/> |
| 7.2 N/A       | Clear area of personnel and insert motor igniter. Tape to Launch rail. | <input type="checkbox"/> |

#### Off-nominal Procedure

- |                     |  |                          |
|---------------------|--|--------------------------|
| 7.0A Safety Officer | Remove igniter   | <input type="checkbox"/> |
|                     | Turn off recovery electronics followed by cameras, airbrakes, SRAD | <input type="checkbox"/> |
| 7.1A Safety Officer | avionics, and payload.   | <input type="checkbox"/> |
| N/A                 | Remove rocket from rail  | <input type="checkbox"/> |

### LAUNCH CHECKLIST

#### Nominal Procedure

- |                |   |                          |
|----------------|---|--------------------------|
| 8.0 Propulsion | Ignite motor                            | <input type="checkbox"/> |
| 8.1 All        | Track rocket visually and via telemetry | <input type="checkbox"/> |

#### Off-nominal Procedure

- |                     |  |                          |
|---------------------|--|--------------------------|
| 8.0A All            | Take cover until given all clear to approach rocket or rocket wreckage | <input type="checkbox"/> |
| 8.1A Safety Officer | Turn off flight computers if necessary                                 | <input type="checkbox"/> |
| 8.0A Safety Officer | Disconnect charges from flight computers                               | <input type="checkbox"/> |
| 8.1A Safety Officer | Remove any LiPo batteries that may be damaged                          | <input type="checkbox"/> |

**RECOVERY CHECKLIST**

- |              |  |                          |
|--------------|--|--------------------------|
| 9.0 Avionics | Turn off flight computers, payload, airbrake, and avionics                   | <input type="checkbox"/> |
| 9.1 Avionics | Turn off cameras   | <input type="checkbox"/> |
| 9.2 Avionics | Verify all charge have fired. If not cut wires and remove powder from charge | <input type="checkbox"/> |
| 9.3 Avionics | Turn off both GPS units after opening electronics bay                        | <input type="checkbox"/> |
| 9.4 All      | Verify all sections of the rocket have been accounted for                    | <input type="checkbox"/> |

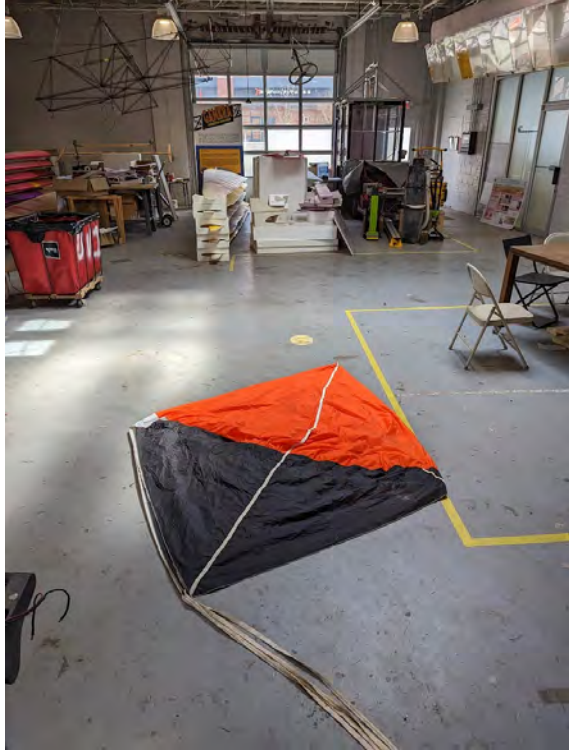
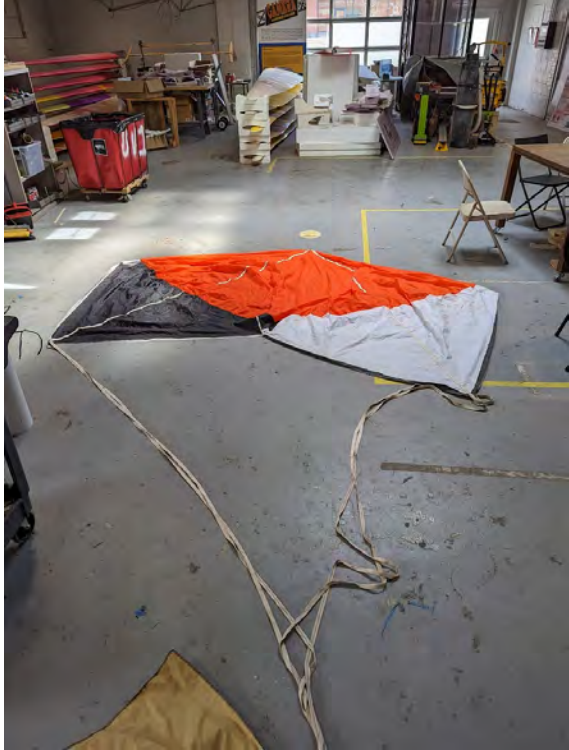
# Parachute Packing Procedure

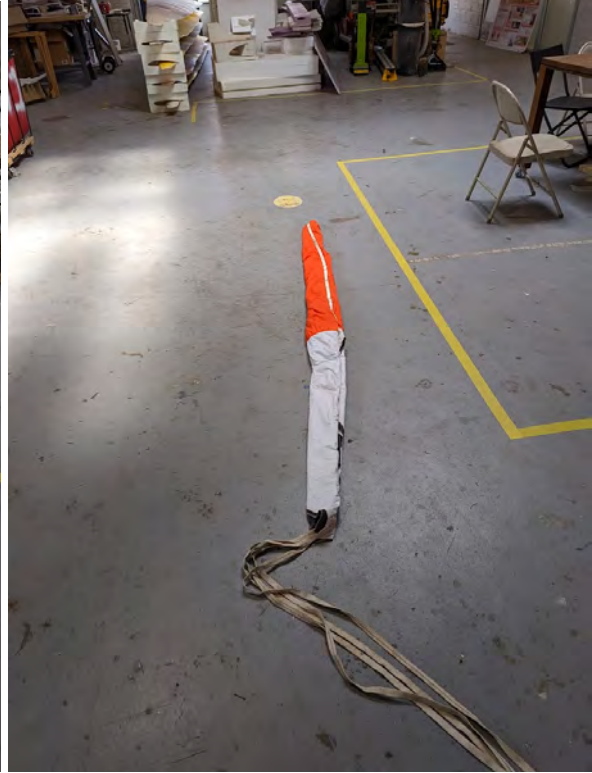
Andrew Bean

This procedure is made for packing parachutes and harnesses for the Terrapin Rocket Team competition rocket, but is applicable to many other rockets. These pictures are using a Skyangle Cert3XXL parachute with a 30"x30" nomex blanket, but works for smaller and larger parachutes.

1. Lay the parachute out on the ground and align the corners. Make sure it is flat and completely spread out. Begin to fold it in half lengthwise, for this parachute it is done 4 times. Make sure to push as much air out of the parachute as possible in between each fold.
2. Begin to fold the parachute widthwise. For this parachute, it is done three times. Just like the initial folds, make sure to push out the air for each fold. Once in the final folded position, it is helpful to push your knee on top to push air out and keep it folded.
3. Place the folded parachute on the corner of the nomex connected with the quicklink.
4. Lightly place the shroud lines in front of the parachute on the nomex.
5. Begin to roll the nomex over the blanket. Make sure to keep it tight and try not to let extra air into the parachute.
6. Once you are slightly less than halfway up the nomex, fold the sides into the middle, like a burrito. Make sure the sides of the nomex are angled slightly inwards or straight, not outwards.
7. Continue rolling until the end, keeping the wrap tight. It should be able to fit in the airframe. If not, repeat the process.











# Motor Assembly Procedure

Andrew Bean

## Gluing the Grains:

1. Make sure liner is cut to correct size - test fit into casing without grains
  - a. Make sure there is good overlap with the shoulders on both the nozzle and forward closure
  - b. Make sure the snap rings can be fully seated with the nozzle and closures on. Ensure there is just enough play that you can still get the pliers into the snap ring for removal.
  - c. Square ends are very helpful. Using the same jig to cut grains to cut the liner works well. If you have one end that's less square, use that as the nozzle end. The sealing is more important at the forward end.
2. Insert grains into the liner and make sure closures can still fit, if not cut the top grain. Make sure to record the new length and weight.
3. Remove grains and stack them up vertically. The nozzle end should be on the table.
4. Using wide packing tape, carefully wrap the seam once with a little overlap. Try to minimize wrinkles as this will make it harder to get the liner on.
  - a. Have a second person push down on the top grain while it is being taped.
5. Once the full stack has been taped together, do another dry fit of the motor and make sure everything still fits. If not, remove the appropriate amount from the top grain and record the change.
6. Put the nozzle on the table and cover with a piece of cellophane. Make sure it is large enough to cover the entire shoulder with the liner on
7. Using a paper towel, make sure the inside of the liner is free of any dust.
8. With the grain stack standing upright, begin to apply adhesive
  - a. 100% silicone caulk works very well and was recommended by Scott Kormier at Loki.
    - i. Make sure you are doing this in a well ventilated area and use respirators with organic cartridges. You do not want to breathe in the fumes.
    - ii. You will have a short working time with this. It is useful to have an extra person on hand to start a timer and call out every fifteen seconds. Try to get the entire thing coated in 1-2 minutes. Any longer and you risk not being able to get the liner on.
  - b. If you choose to use something else, make sure it is NON FOAMING or MINIMAL FOAMING. Elmers Glue All Max is recommended for Aerotech motors, but we have spit casting tubes in our EX motors with it.
9. Apply glue evenly over the entire grain stack. Make sure not to get and glue on the exposed grain faces.
10. Once fully covered, slide the liner down the grain stack. Use a paper towel to wipe up extra glue that collects at the bottom. Wipe off any glue on the sides of the liner as well so that it can still fit into the casing.
11. Lay the stack horizontally and push the nozzle into the aft end. Make sure the cellophane is covering the nozzle.

12. Stand it back up and let it cure vertically at least overnight. Make sure the grains are fully pushed down and inspect for any foaming that may push the grains outwards (foaming is not an issue with silicone)
13. Once cured, you can leave the cellophane on the nozzle as this will help seal the grains from humidity. If there is too much, cut away the cellophane so that it cannot touch the orings.

#### **Final Motor Assembly:**

14. Prepare 4 silicon -338 O-rings. Lightly grease (Super Lube) your fingers and pull the O-Rings through your fingers to lubricate them.
15. Once greased, put the O-rings onto both the nozzle and forward closure (2 each)
16. Stack the grains and liner back onto the nozzle and liberally grease the outside of the liner (don't be afraid to use more than you think)
17. Grease nozzle washer and nozzle snap ring
18. Make sure snap ring grooves are clean and free of any grime or debris. Run your fingernail across the snap ring grooves to check for burrs. These can cut your orings and are important to check for. Use a small piece of sandpaper to remove these.
19. Slide casing down over liner and nozzle, wipe away excess grease at the bottom.
20. At the forward end of your casing, add a good amount of grease to the case wall right above the liner.
21. Lay casing horizontally and push the nozzle past the snap ring groove. Insert the greased washer and snap ring.
22. Bring the stack back vertical. Apply a coat of grease to the inside of the liner above the grains (where the closure shoulder will interface). Also apply more grease to the casing wall above the liner.
23. Make sure any fittings are securely connected to the forward closure, and push it into the casing fully. Insert the forward snap ring.
24. Make sure to verify that both snap rings are FULLY seated

#### **Post Firing Disassembly:**

25. After firing, try to disassemble the motor while it is still warm (not hot). The grease will seize if allowed to cool, making disassembly much more difficult.
26. Remove snap rings and washer. Be careful as the graphite will retain heat much longer than other parts of the motor.
27. Using a wooden dowel (or similar) push on the forward closure until the liner slides out (this may take a decent amount of effort).
  - a. If the motor has fully cooled, take a spare closure and rubber mallet and hit the forward end of the motor. Once it is deep enough, you can use a thick dowel to transfer the force.
28. Remove o-rings from nozzle and forward closure. Make sure to clean O-ring and snap ring grooves.
29. Inspect casing for any bulging or discoloration. If there is any, the casing can no longer be used.

# Air Brake Inspection Checklist – Assembly, Preflight, Launch

## Disassembling:

Section	Task	Completion
0.1	Unscrew two nuts	
0.2	Pull off bulkhead and retaining ring	
0.3	Pull out front PLA ring	
0.4	Unscrew two nuts	
0.5	Pull off EBay	
0.6	Pull out back retaining ring	
0.7	Unplug 3.7V, two 32Vs, battery to encoder connection, battery to Stepper motor connection, and two encoder Molexes	
0.8	Remove four pins and four pin clips	
0.9	Pull out air brake skeleton	

## Reassembling:

Section	Task	Completion
0.10	Slide shell onto air brake skeleton, aligning bulkhead “4” with shell “4”	
0.11	Check hull to see if wires flow smoothly	
0.12	Rotate motor screw, until air brake clevis meets flap	
0.13	Slide in four pins and four pin clips	
0.14	Test if flaps are flush (ref. Troubleshoot)	
0.15	Feed wires into circular PLA ring and push to end of Air brake	
0.16	Connect three charged batteries to Air brake	
0.17	Plug in two Molexes and remaining cables	
0.18	Slide in EBay	
0.19	Slide in front retaining ring, with proper orientation	
0.20	Put on two bolts to hold the EBay system in place	
0.21	Turn on switch to system check	
0.22	Put on metal retaining rings	
0.23	Screw on nuts	
0.24	Turn on switch to system check	

## Troubleshoot:

### Flaps not flush:

Section	Task	Completion
-	Rotate frame 180 degrees, only two possible alignments	
-	Check clevis screws are tight and aligned to center	

### System not turning on:

Section	Task	Completion
-	Follow disassembly until only the back retaining ring is in Air brake	
-	Check continuity of all wires	
-	Replace broken system	
-	Follow reassembly	

## Day Prior\*:

Section	Subteam	Task	Completion
---------	---------	------	------------

1.1	Airbrake	Turn on switch	
1.2	Airbrake	Flash Teensy(s) with simulation code	
1.3	Airbrake	Test actuation	
1.4	Airbrake	Reflash Teensy with flight code	
1.5	Airbrake	Check continuity and cables	
1.6	Airbrake	Turn off switch	
1.7	Airbrake	Push in electronic module	
1.8	Airbrake	Attach bulkheads	
1.9	Airbrake	Attach nuts	
1.10	Airbrake	Screw on driver protection shaft	
1.11	Airbrake	Charge Lipo batteries to 4.2V	
1.12	Airbrake	Package all components into a yellow box and Ezra's box	

Assumptions: Blue Dog is prepped. Air brake starts disassembled in normal operations.\*

### Pre-pad:

Section	Subteam	Task	Completion
2.1	Airbrake	Check all electronics are charged	
2.2	Blue Dog	<i>Check screw switch orientation</i>	
2.3	Blue Dog	<i>Check Feather Weight GPS is on</i>	
2.4	Blue Dog	<i>Align eyebolts onto threaded rods</i>	
2.5	Airbrake	Components are in	
2.6	Airbrake	Load airbrake below sponsor sheet, above fin can	
2.7	Airbrake	Screw pins	
2.8	Airbrake	Check for 1 beep initialization	

### On the pad:

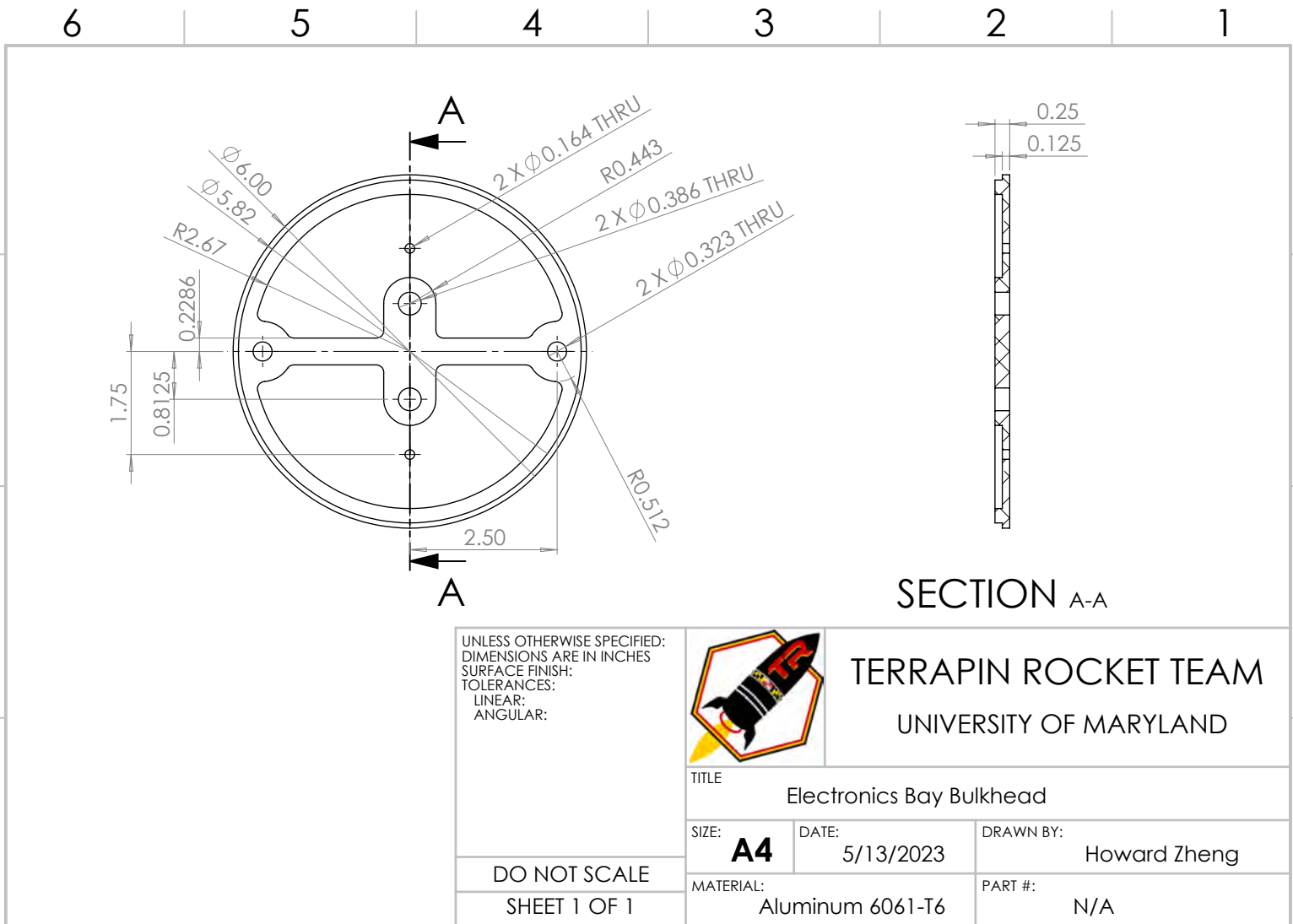
Section	Subteam	Task	Completion
3.1	Airbrake	Turn switch	
3.2	Airbrake	Check for 1 beep initialization, 1 beep/10 sec	
3.3	<i>Blue Dog</i>	<i>Both Easy Minis are beeping, beep initialization, 3 beeps/2 sec</i>	
3.4	<i>Blue Dog</i>	<i>Check Feather Weight GPS status</i>	
3.5	<i>Blue Dog</i>	<i>Turn on Airbrake</i>	
3.6	<i>Blue Dog</i>	<i>Arm Easy Minis</i>	
3.7	<i>Blue Dog</i>	<i>Plant igniter</i>	

### Recovery:

Section	Subteam	Task	Completion
4.1	Airbrake	Turn off airbrake immediately	
4.2	Airbrake	Measure smaller Lipo, swapping out if necessary	
4.3	Airbrake	Measure larger Lipo, swapping out if necessary	
4.4	Airbrake	Once at camp, upload data from SD card	

**X. Appendix F - Engineering Drawings**

(As found on the following page)



SECTION A-A

UNLESS OTHERWISE SPECIFIED:  
 DIMENSIONS ARE IN INCHES  
 SURFACE FINISH:  
 TOLERANCES:  
 LINEAR:  
 ANGULAR:

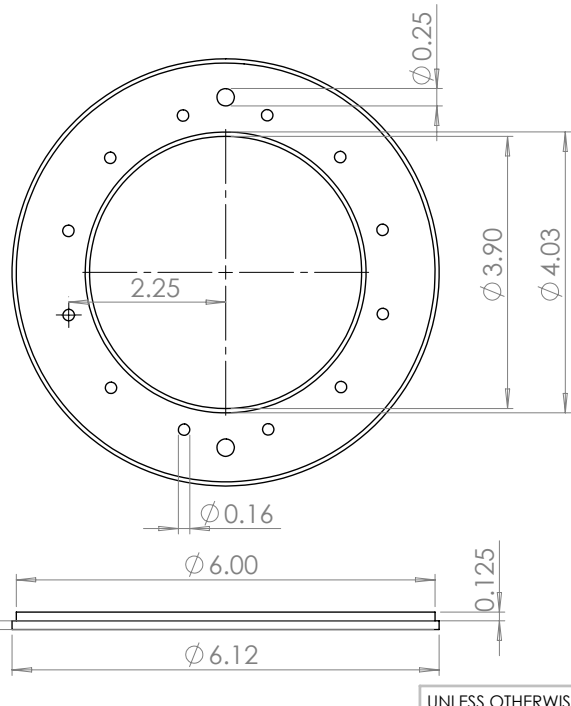


TERRAPIN ROCKET TEAM  
 UNIVERSITY OF MARYLAND

TITLE		
Electronics Bay Bulkhead		
SIZE:	DATE:	DRAWN BY:
<b>A4</b>	5/13/2023	Howard Zheng
MATERIAL:	PART #:	
Aluminum 6061-T6	N/A	

DO NOT SCALE  
 SHEET 1 OF 1

6 5 4 3 2 1



UNLESS OTHERWISE SPECIFIED:  
 DIMENSIONS ARE IN INCHES  
 SURFACE FINISH:  
 TOLERANCES:  
 LINEAR:  
 ANGULAR:

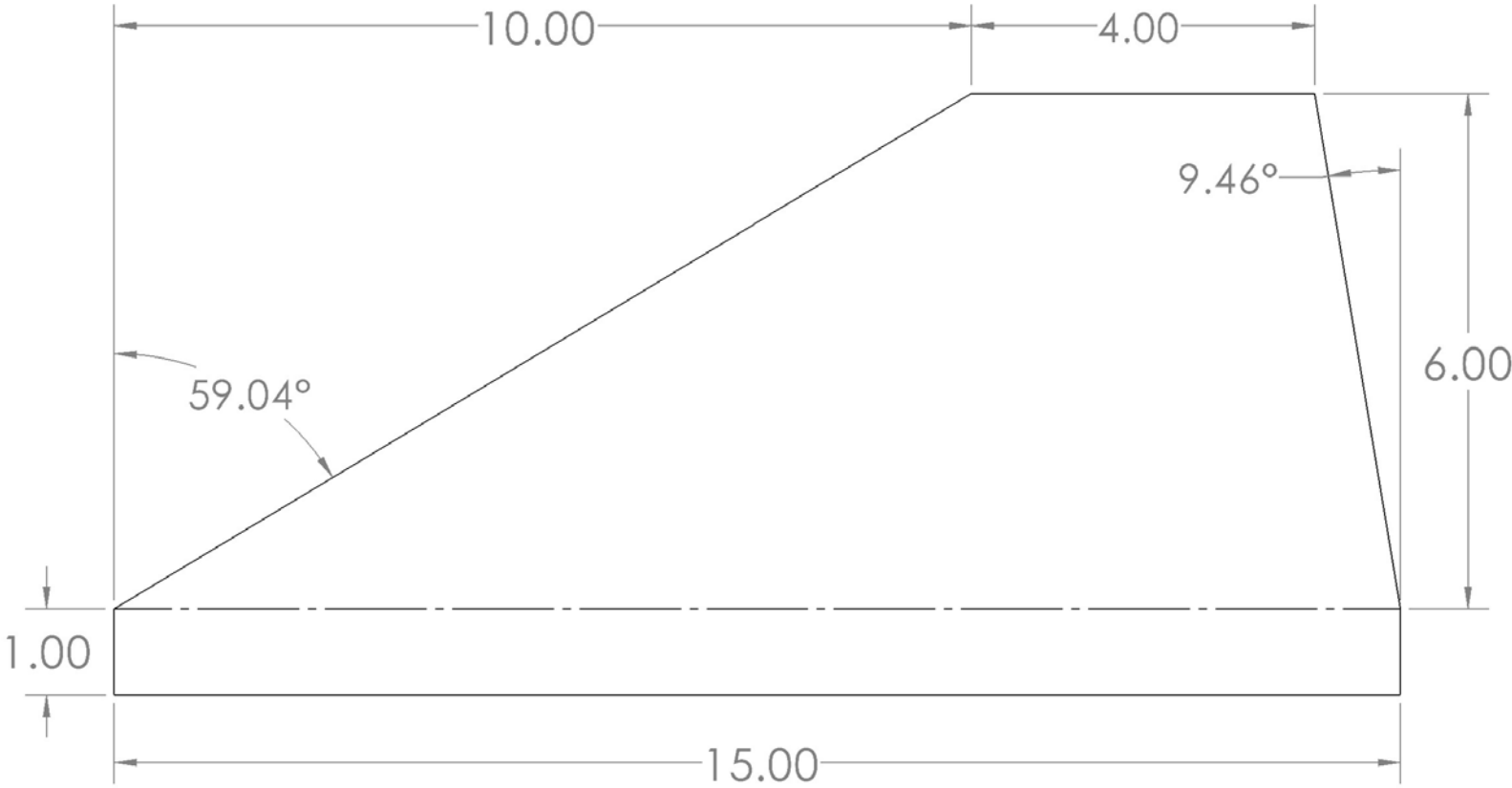


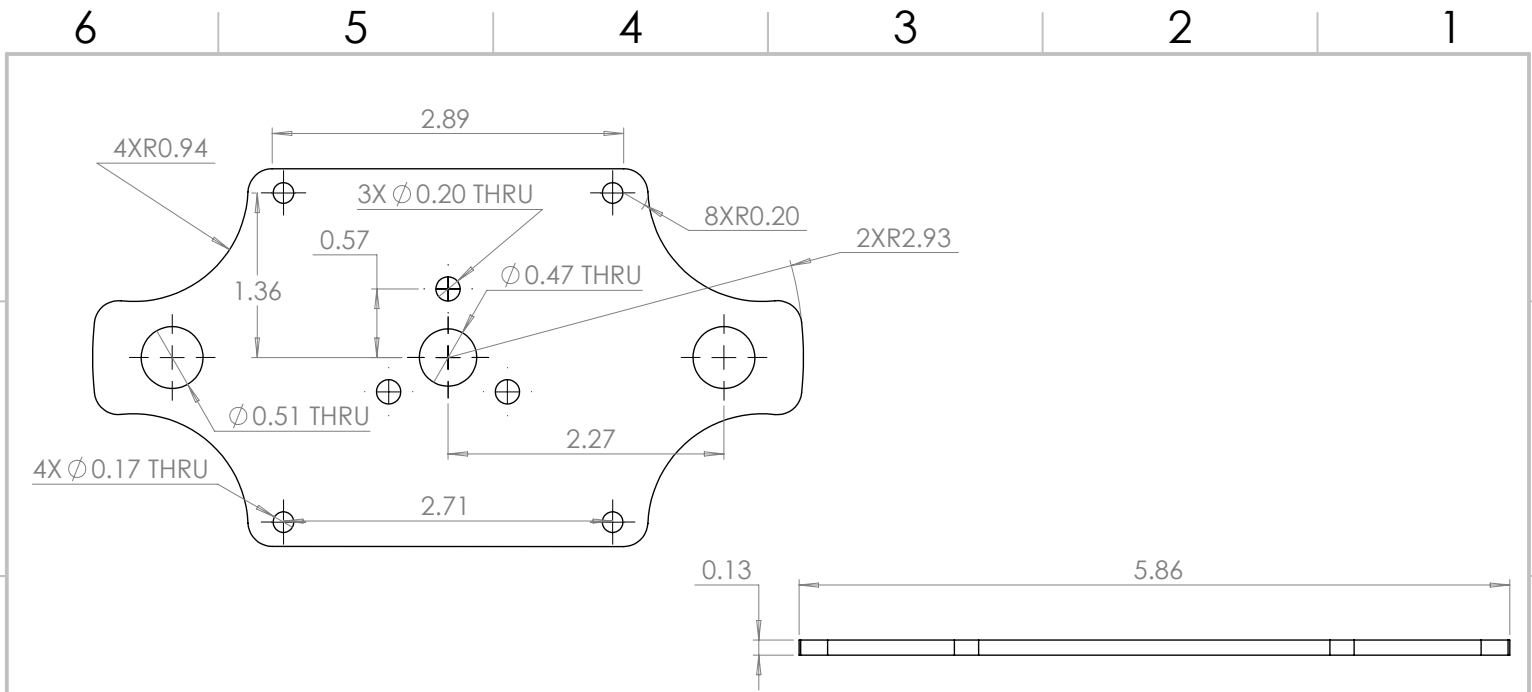
TERRAPIN ROCKET TEAM  
 UNIVERSITY OF MARYLAND

TITLE Thrust Plate		
SIZE: <b>A4</b>	DATE: 5/13/2023	DRAWN BY: Andrew Bean
MATERIAL: 1/4" 6061 Aluminum		PART #: N/A

DO NOT SCALE  
 SHEET 1 OF 1

6 5 4 3 2 1





UNLESS OTHERWISE SPECIFIED:  
DIMENSIONS ARE IN INCHES

SURFACE FINISH: ✓

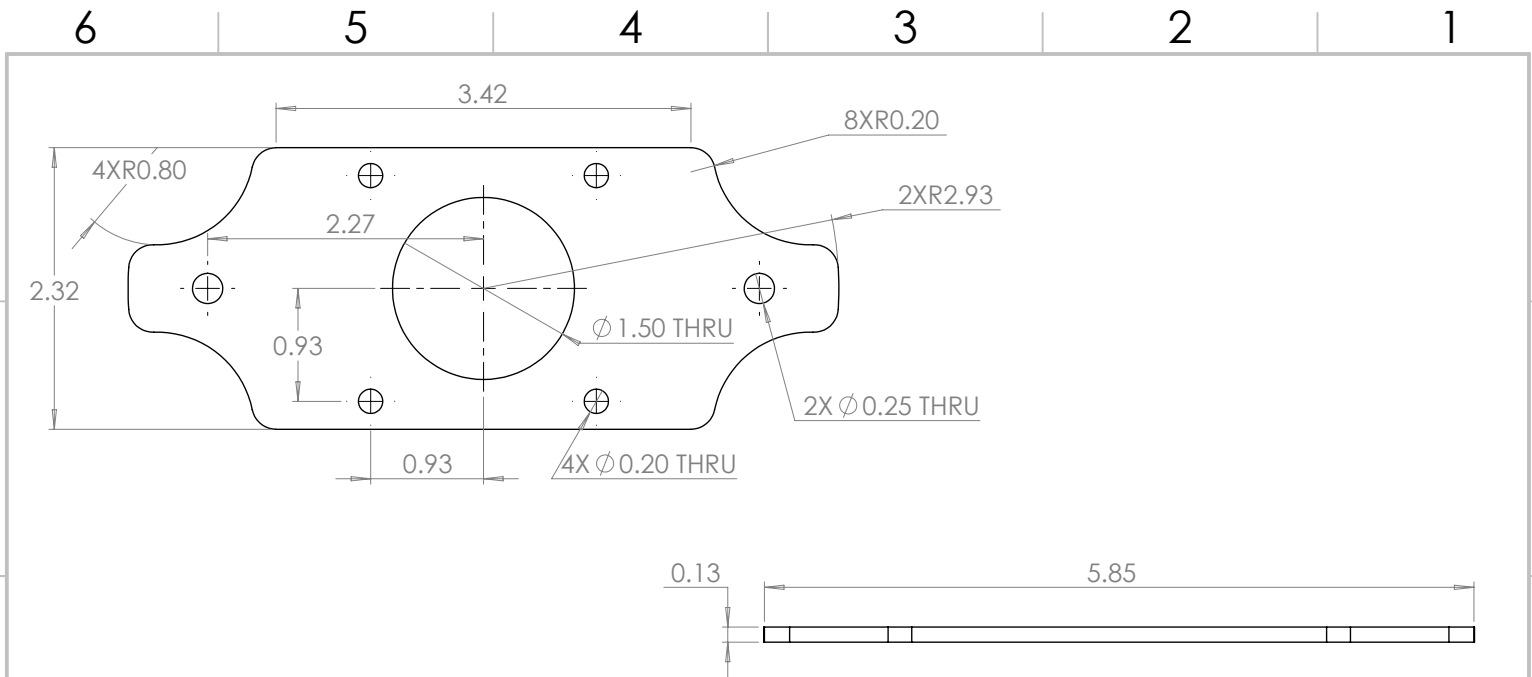
TOLERANCES:  
± 7.87 mil

DO NOT SCALE  
SHEET 1 OF 1



TERRAPIN ROCKET TEAM  
UNIVERSITY OF MARYLAND

TITLE Actuator Disk		
SIZE: <b>A4</b>	DATE: 4/29/2023	DRAWN BY: Jeyadave NK
MATERIAL: Aluminum 6061-T6		PART #: INSERT PART #



UNLESS OTHERWISE SPECIFIED:  
DIMENSIONS ARE IN INCHES

SURFACE FINISH:

TOLERANCES:  
± 7.87 mil

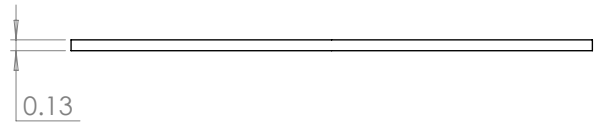
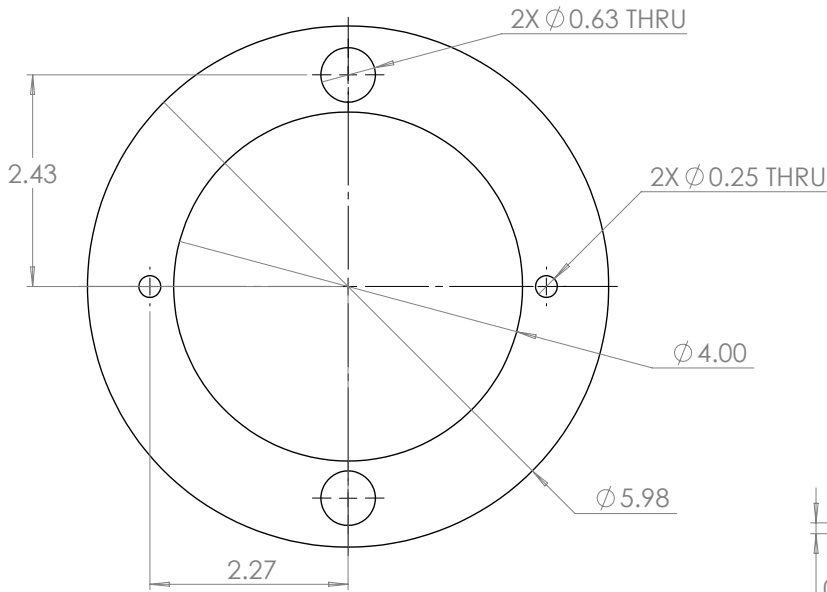
DO NOT SCALE  
SHEET 1 OF 1



TERRAPIN ROCKET TEAM  
UNIVERSITY OF MARYLAND

TITLE Actuator Mounting Plate		
SIZE: <b>A4</b>	DATE: 4/29/2023	DRAWN BY: Jeyadave NK
MATERIAL: Aluminum 6061-T6		PART #: INSERT PART #

6 5 4 3 2 1



UNLESS OTHERWISE SPECIFIED:  
DIMENSIONS ARE IN INCHES

SURFACE FINISH:

TOLERANCES:  
 $\pm 7.87$  mil

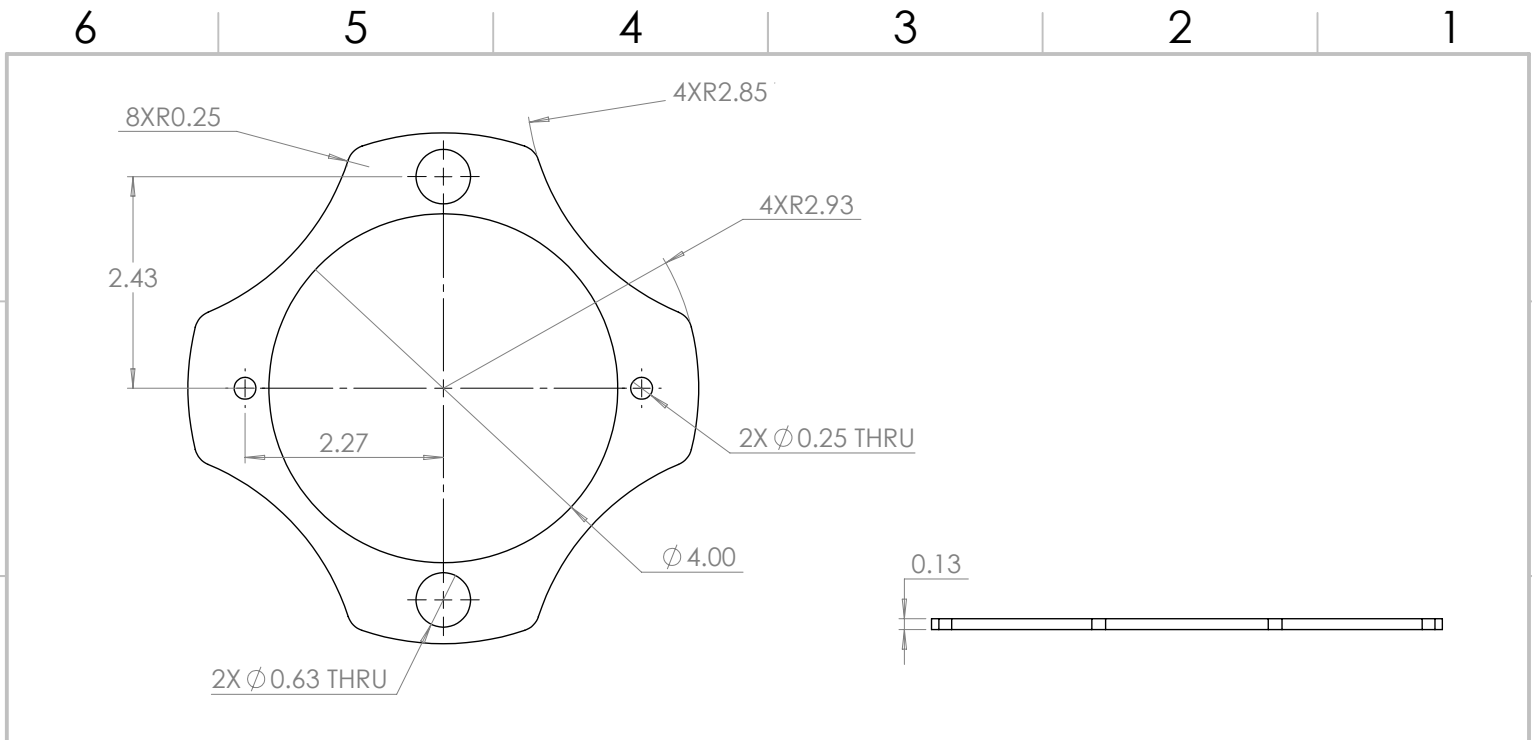
DO NOT SCALE  
SHEET 1 OF 1



TERRAPIN ROCKET TEAM  
UNIVERSITY OF MARYLAND

TITLE Lower Bulkhead Bottom		
SIZE: <b>A4</b>	DATE: 04/29/2023	DRAWN BY: Jeyadave NK
MATERIAL: Aluminum 6061-T6		PART #: INSERT PART #

6 5 4 3 2 1



UNLESS OTHERWISE SPECIFIED:  
DIMENSIONS ARE IN INCHES

SURFACE FINISH: ✓

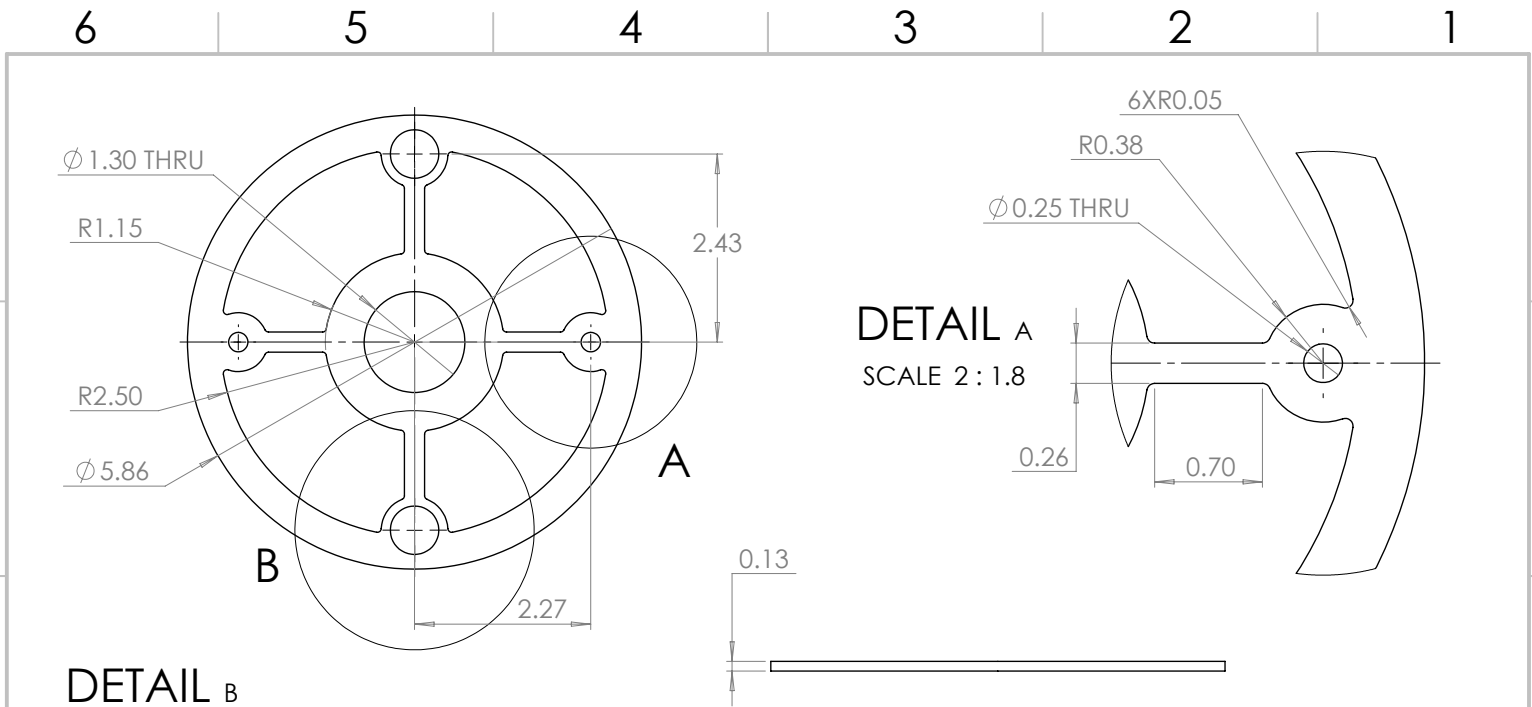
TOLERANCES:  
± 7.87 mil

DO NOT SCALE  
SHEET 1 OF 1

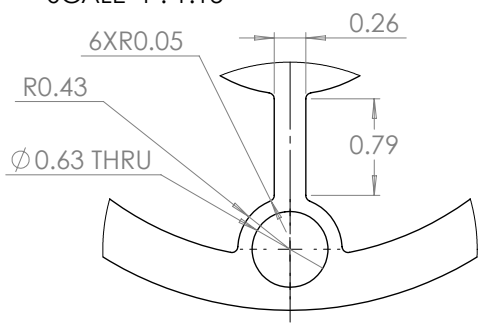


**TERRAPIN ROCKET TEAM**  
UNIVERSITY OF MARYLAND

TITLE Lower Bulkhead Drawing		
SIZE: <b>A4</b>	DATE: 4/29/2023	DRAWN BY: Jeyadave NK
MATERIAL: Aluminum 6061-T6		PART #: INSERT PART #



**DETAIL B**  
SCALE 1 : 1.15



UNLESS OTHERWISE SPECIFIED:  
DIMENSIONS ARE IN INCHES

SURFACE FINISH:  ✓

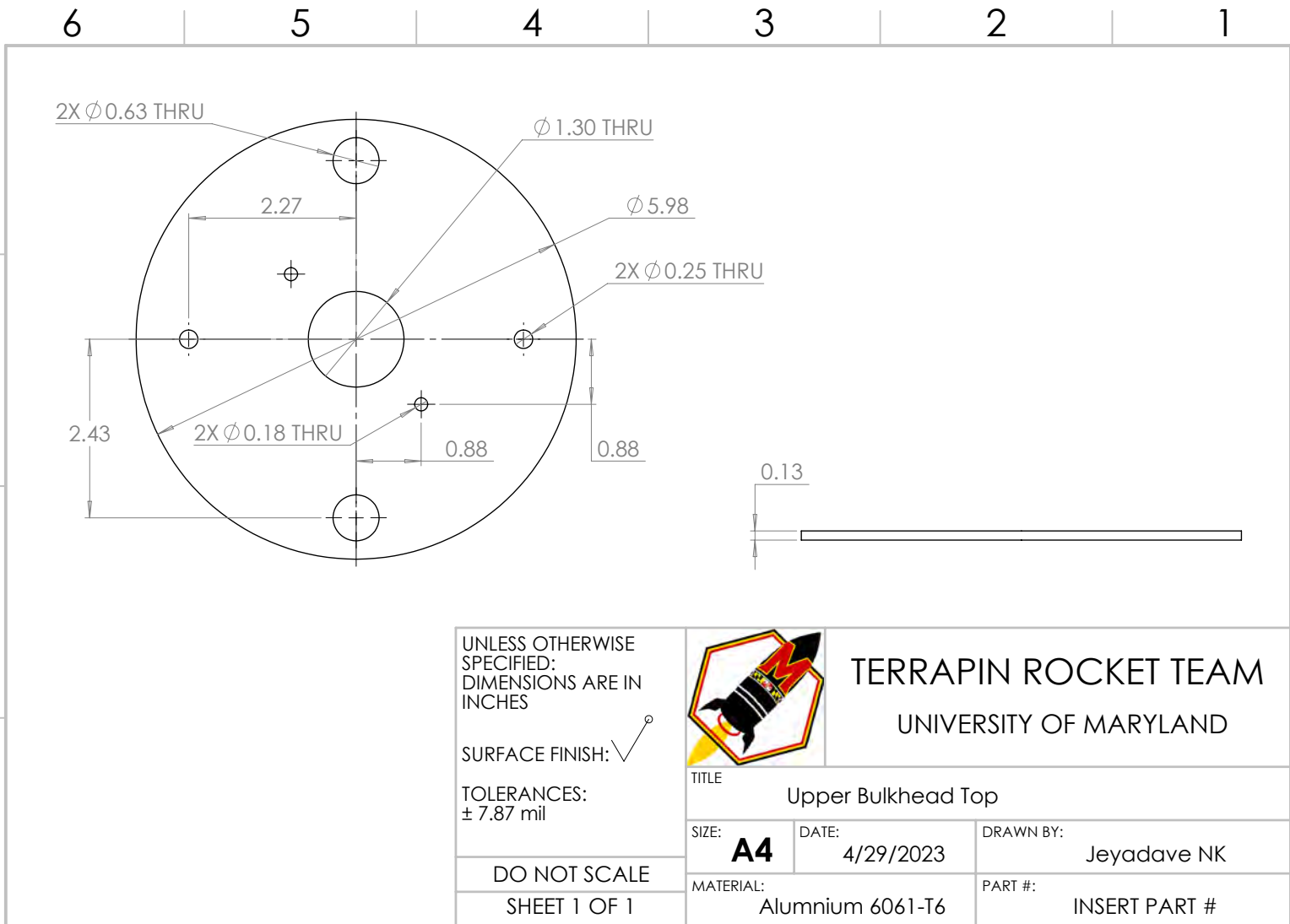
TOLERANCES:  
± 7.87 mil

DO NOT SCALE  
SHEET 1 OF 1



**TERRAPIN ROCKET TEAM**  
UNIVERSITY OF MARYLAND

TITLE Upper Bulkhead Bottom		
SIZE: <b>A4</b>	DATE: 4/29/2023	DRAWN BY: Jeyadave NK
MATERIAL: Aluminum 6061-T6		PART #: INSERT PART #



UNLESS OTHERWISE SPECIFIED:  
DIMENSIONS ARE IN INCHES

SURFACE FINISH:

TOLERANCES:  
 $\pm$  7.87 mil

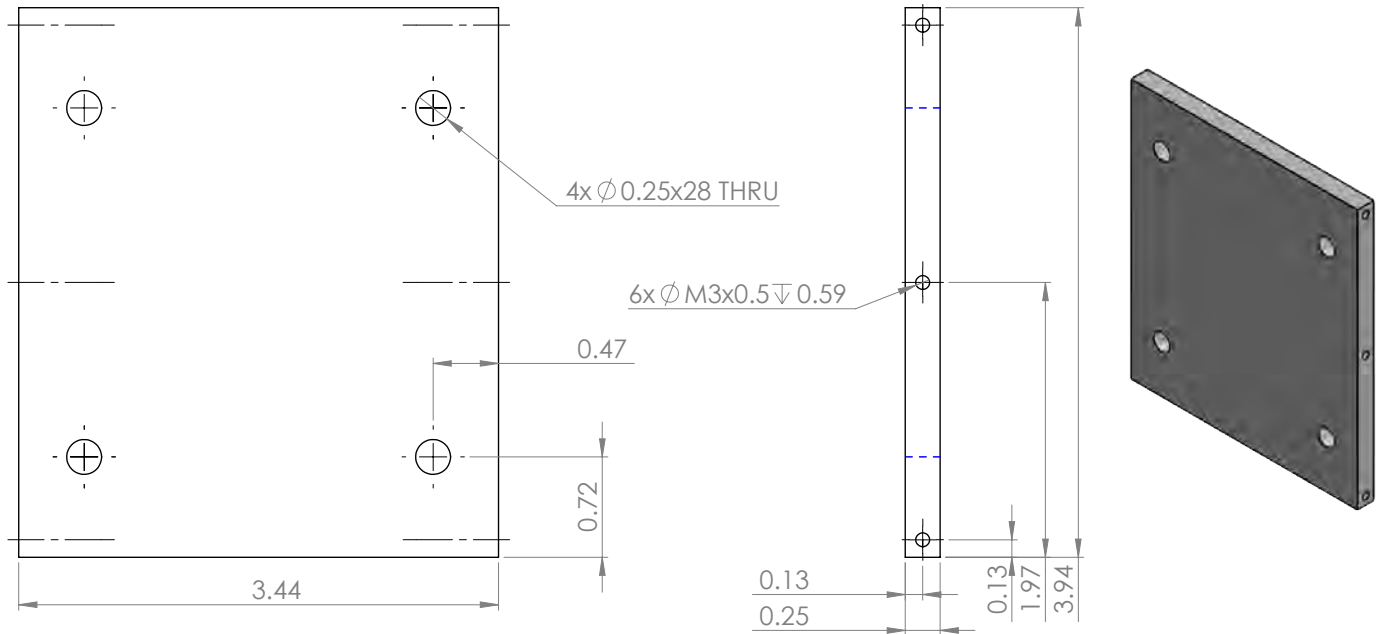
DO NOT SCALE  
SHEET 1 OF 1



TERRAPIN ROCKET TEAM  
UNIVERSITY OF MARYLAND

TITLE Upper Bulkhead Top		
SIZE: <b>A4</b>	DATE: 4/29/2023	DRAWN BY: Jeyadave NK
MATERIAL: Alumnum 6061-T6		PART #: INSERT PART #

6 5 4 3 2 1



UNLESS OTHERWISE SPECIFIED:  
 DIMENSIONS ARE IN INCHES  
 SURFACE FINISH:  
 TOLERANCES:  
 LINEAR:  
 ANGULAR:

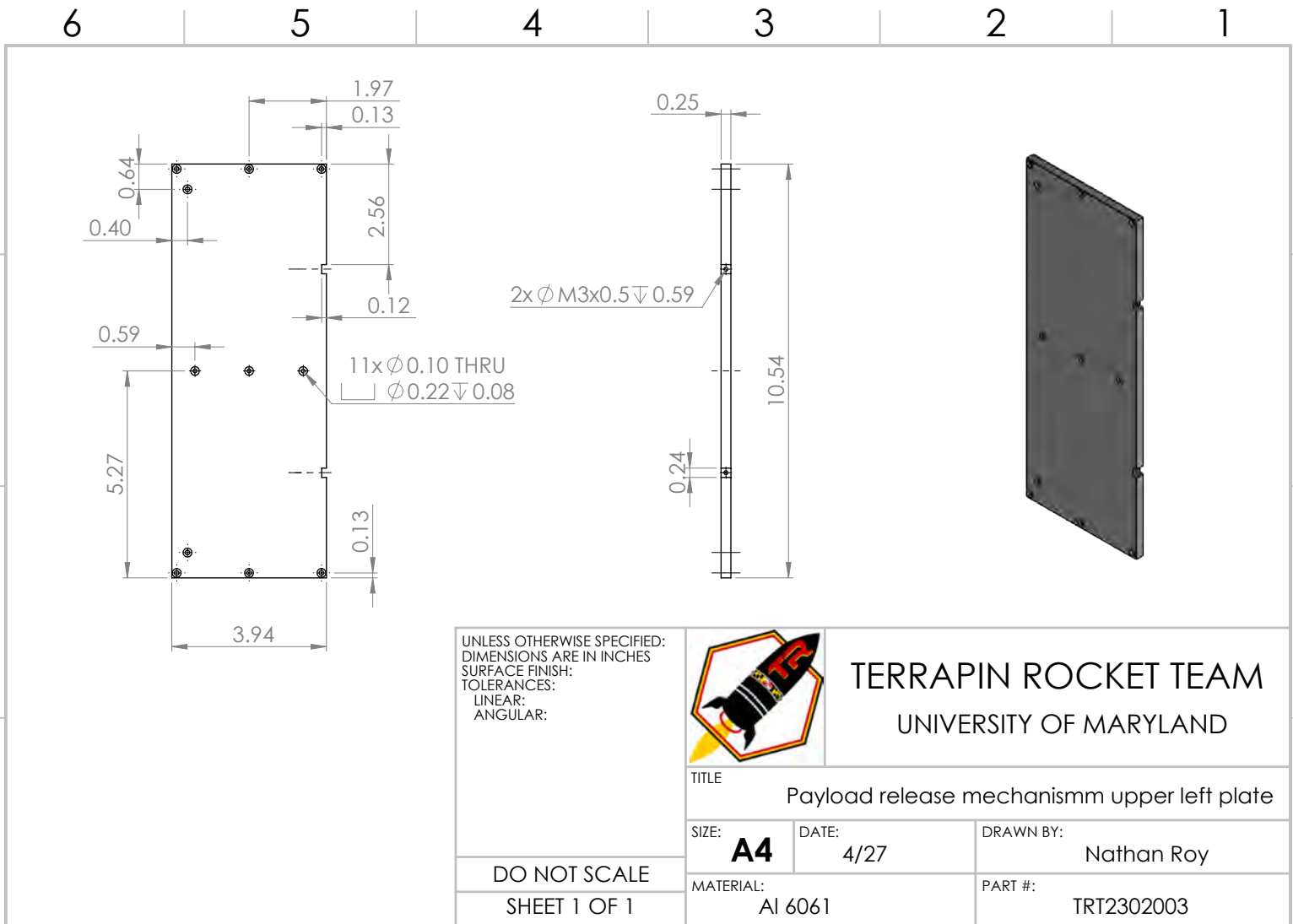


TERRAPIN ROCKET TEAM  
 UNIVERSITY OF MARYLAND

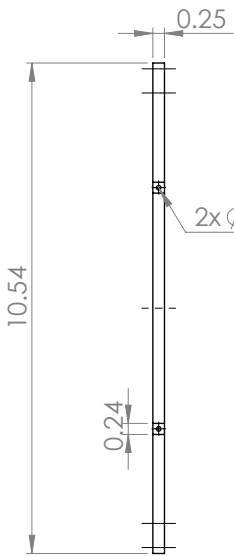
TITLE Palyload release mechanism top plate		
SIZE: <b>A4</b>	DATE: 4/27	DRAWN BY: Nathan Roy
MATERIAL: Al 6061		PART #: TRT2302002

DO NOT SCALE  
 SHEET 1 OF 1

6 5 4 3 2 1

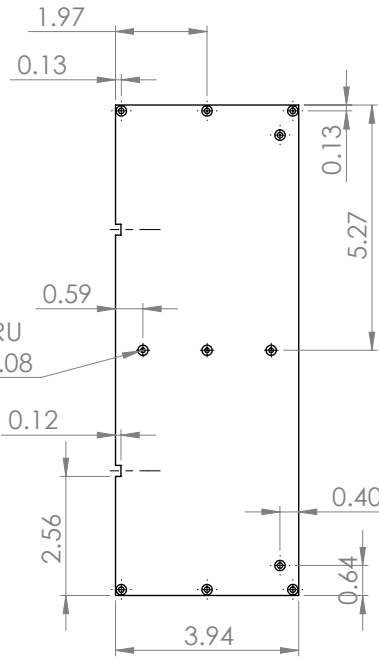


6 5 4 3 2 1



2x  $\phi$  M3x0.5  $\nabla$  0.59

11x  $\phi$  0.10 THRU  
 $\nabla$   $\phi$  0.22  $\nabla$  0.08



D  
C  
B  
A

UNLESS OTHERWISE SPECIFIED:  
DIMENSIONS ARE IN INCHES  
SURFACE FINISH:  
TOLERANCES:  
LINEAR:  
ANGULAR:



TERRAPIN ROCKET TEAM  
UNIVERSITY OF MARYLAND

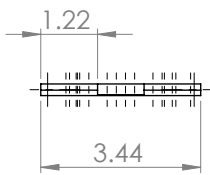
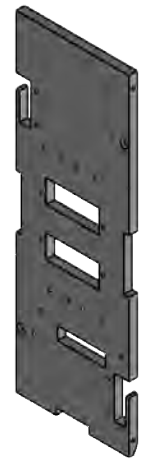
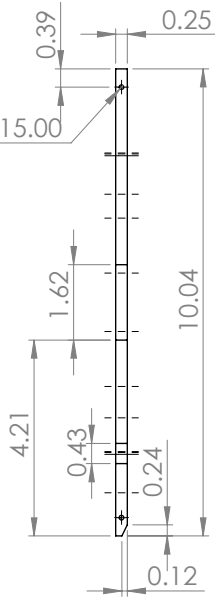
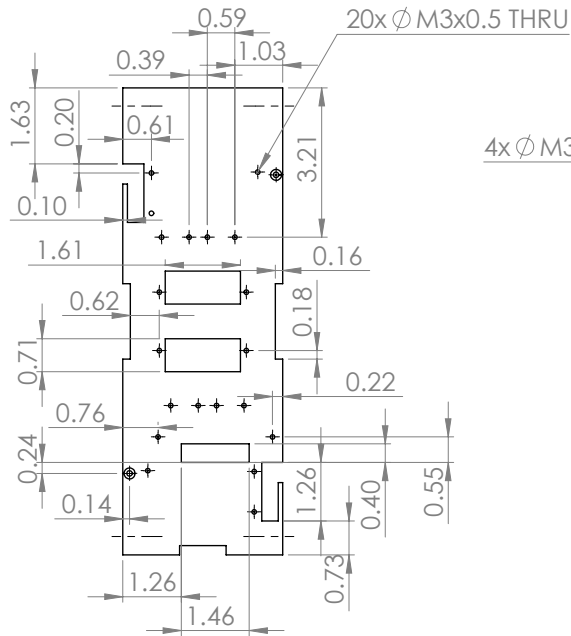
TITLE  
Payload release mechanism upper right plate

SIZE: <b>A4</b>	DATE: 4/27	DRAWN BY: Nathan Roy
--------------------	---------------	-------------------------

DO NOT SCALE SHEET 1 OF 1	MATERIAL: Al 6061	PART #: TRT2302004
------------------------------	----------------------	-----------------------

6 5 4 3 2 1

6 5 4 3 2 1



UNLESS OTHERWISE SPECIFIED:  
 DIMENSIONS ARE IN INCHES  
 SURFACE FINISH:  
 TOLERANCES:  
 LINEAR:  
 ANGULAR:



TERRAPIN ROCKET TEAM  
 UNIVERSITY OF MARYLAND

TITLE: Payload release mechanism upper back plate

SIZE: **A4** DATE: 4/27 DRAWN BY: Nathan Roy

MATERIAL: Al 6061 PART #: TRT2302005

DO NOT SCALE  
 SHEET 1 OF 1

6 5 4 3 2 1

D  
C  
B  
A

D  
C  
B  
A

6 5 4 3 2 1

D

D

C

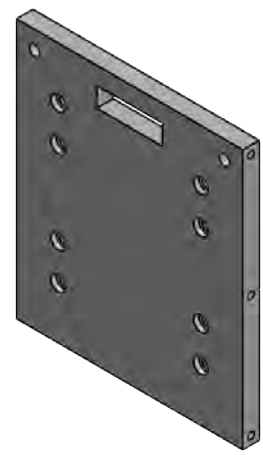
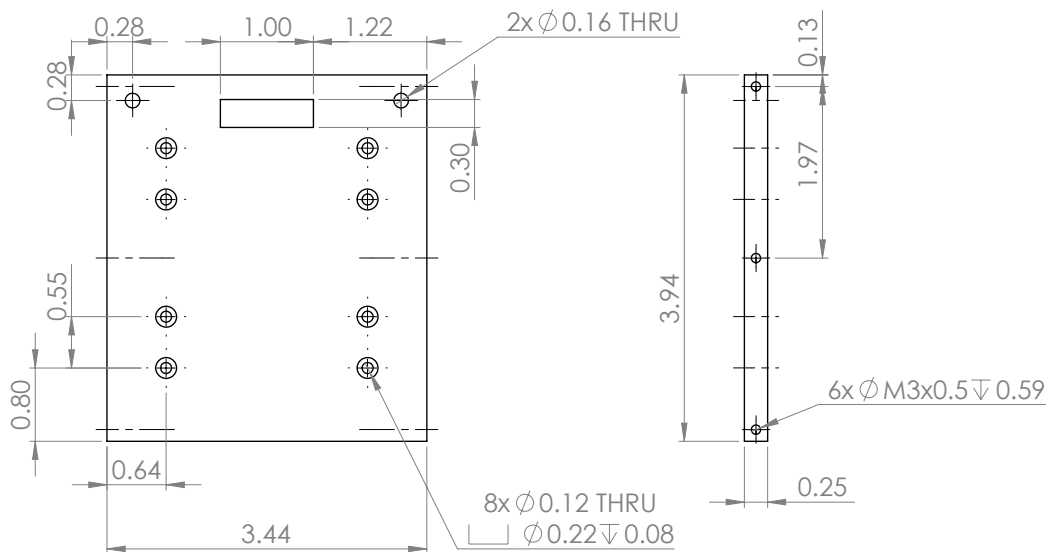
C

B

B

A

A



UNLESS OTHERWISE SPECIFIED:  
 DIMENSIONS ARE IN INCHES  
 SURFACE FINISH:  
 TOLERANCES:  
 LINEAR:  
 ANGULAR:

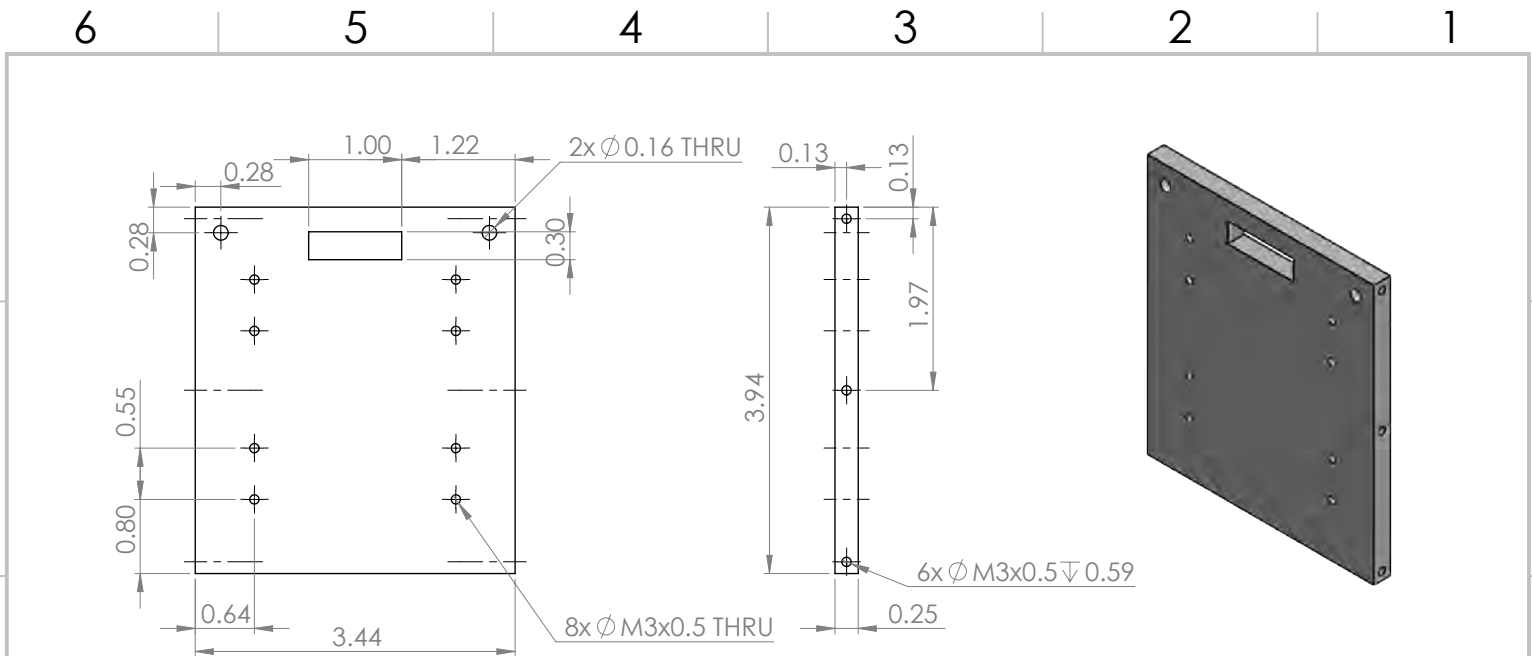


TERRAPIN ROCKET TEAM  
 UNIVERSITY OF MARYLAND

TITLE Payload release mechanism middle upper plate		
SIZE: <b>A4</b>	DATE: 4/27	DRAWN BY: Nathan Roy
MATERIAL: AL 6061		PART #: TRT2302006

DO NOT SCALE  
 SHEET 1 OF 1

6 5 4 3 2 1



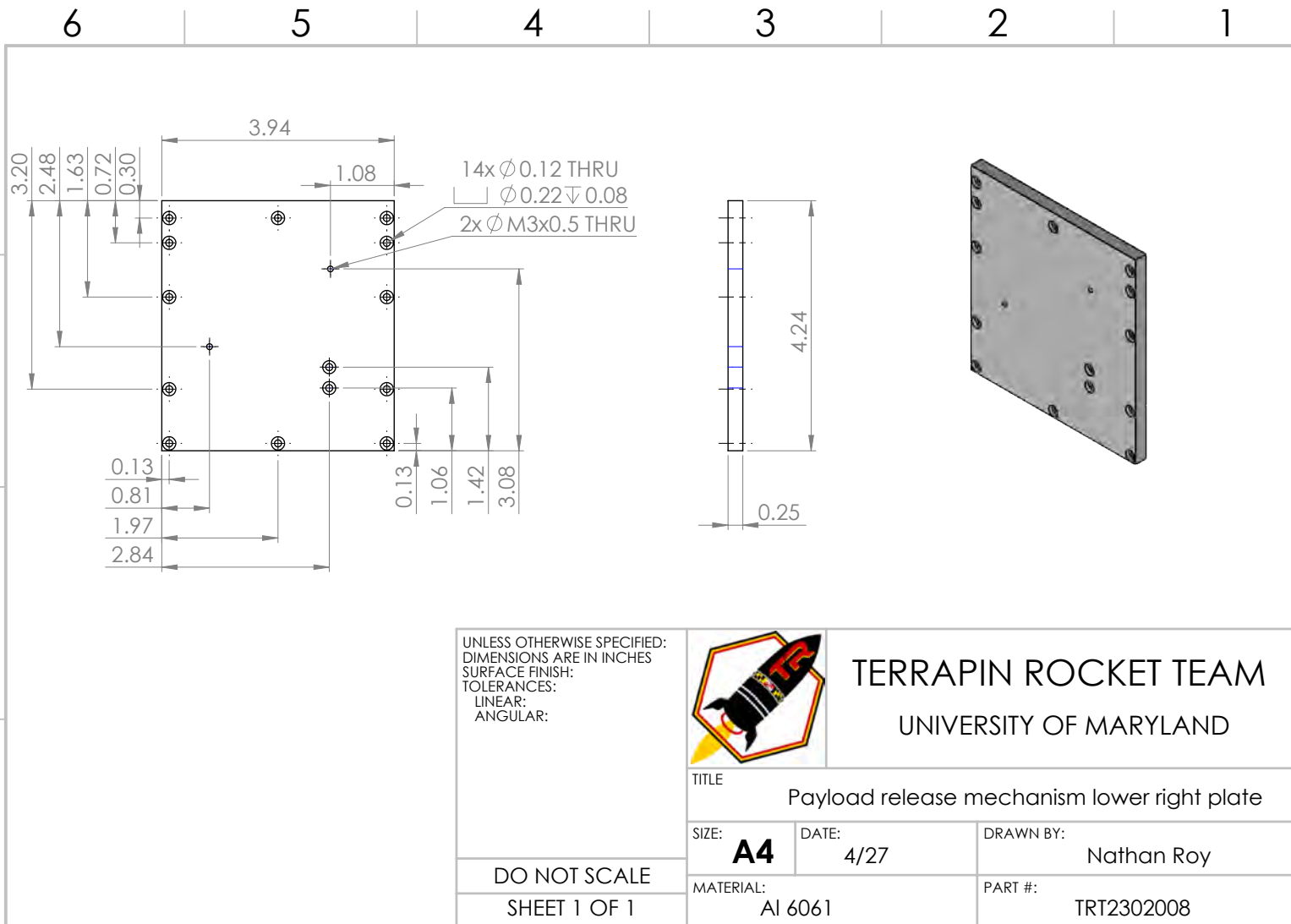
UNLESS OTHERWISE SPECIFIED:  
 DIMENSIONS ARE IN INCHES  
 SURFACE FINISH:  
 TOLERANCES:  
 LINEAR:  
 ANGULAR:



TERRAPIN ROCKET TEAM  
 UNIVERSITY OF MARYLAND

TITLE Payload release mechanism middle lower plate		
SIZE: <b>A4</b>	DATE: 4/27	DRAWN BY: Nathan Roy
MATERIAL: Al 6061		PART #: TRT2302007

DO NOT SCALE  
 SHEET 1 OF 1



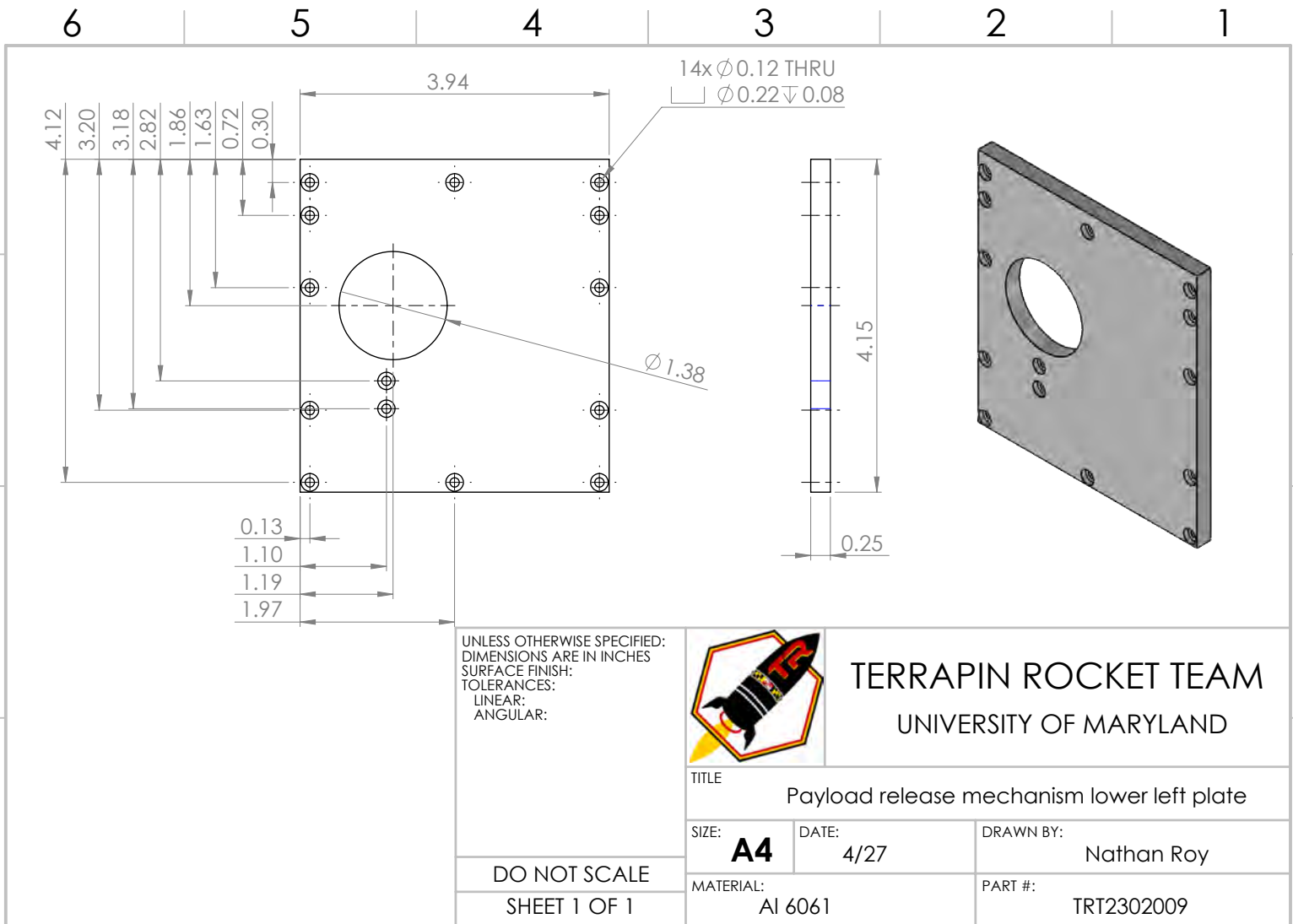
UNLESS OTHERWISE SPECIFIED:  
DIMENSIONS ARE IN INCHES  
SURFACE FINISH:  
TOLERANCES:  
LINEAR:  
ANGULAR:

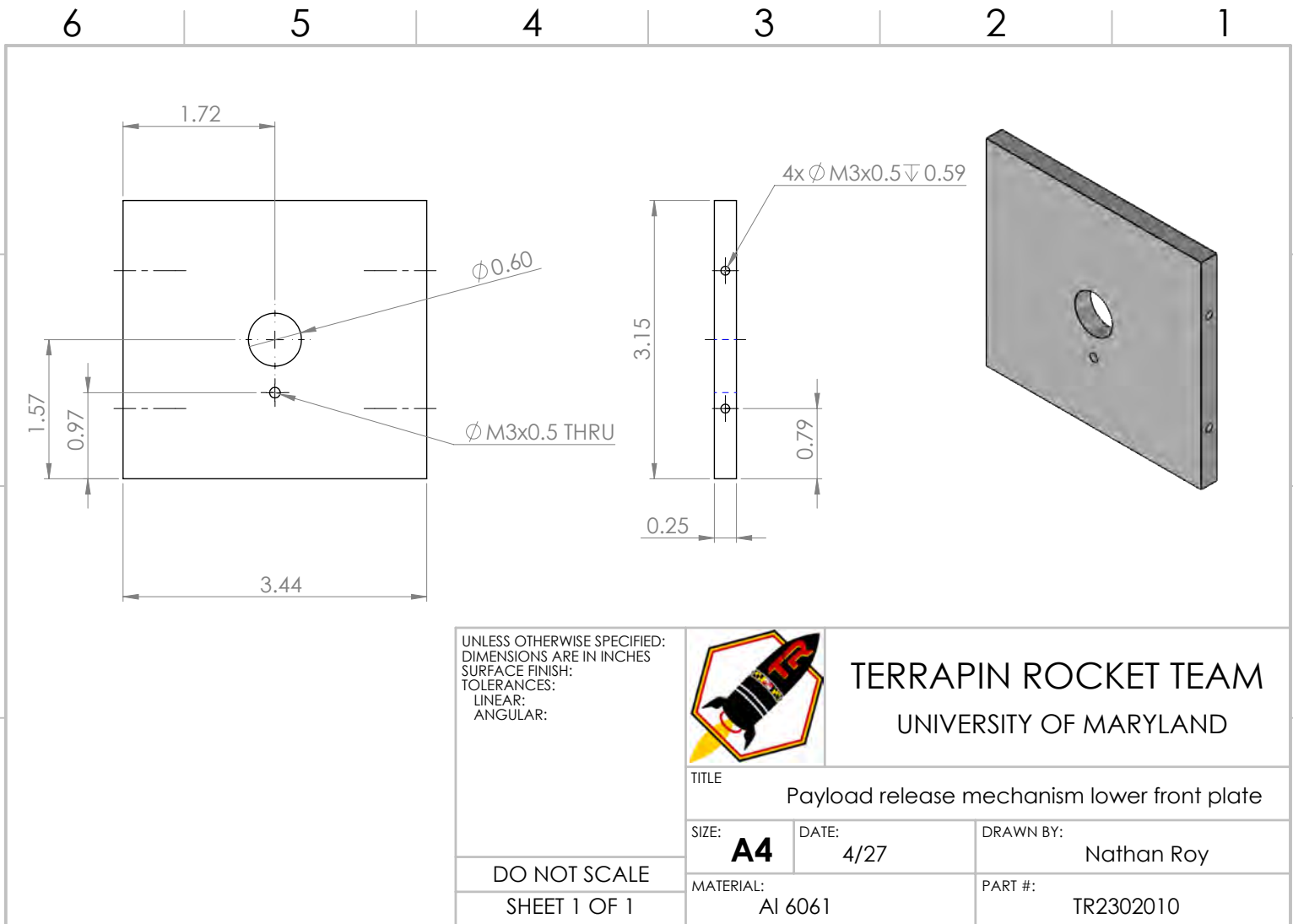


TERRAPIN ROCKET TEAM  
UNIVERSITY OF MARYLAND

TITLE Payload release mechanism lower right plate		
SIZE: <b>A4</b>	DATE: 4/27	DRAWN BY: Nathan Roy
MATERIAL: Al 6061		PART #: TRT2302008

DO NOT SCALE  
SHEET 1 OF 1





UNLESS OTHERWISE SPECIFIED:  
 DIMENSIONS ARE IN INCHES  
 SURFACE FINISH:  
 TOLERANCES:  
 LINEAR:  
 ANGULAR:



TERRAPIN ROCKET TEAM  
 UNIVERSITY OF MARYLAND

TITLE Payload release mechanism lower front plate		
SIZE: <b>A4</b>	DATE: 4/27	DRAWN BY: Nathan Roy
MATERIAL: Al 6061		PART #: TR2302010

DO NOT SCALE  
 SHEET 1 OF 1

6 5 4 3 2 1

D

D

C

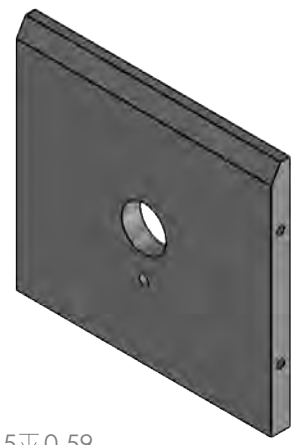
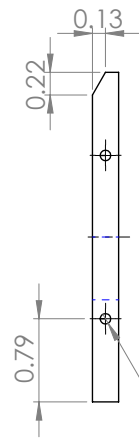
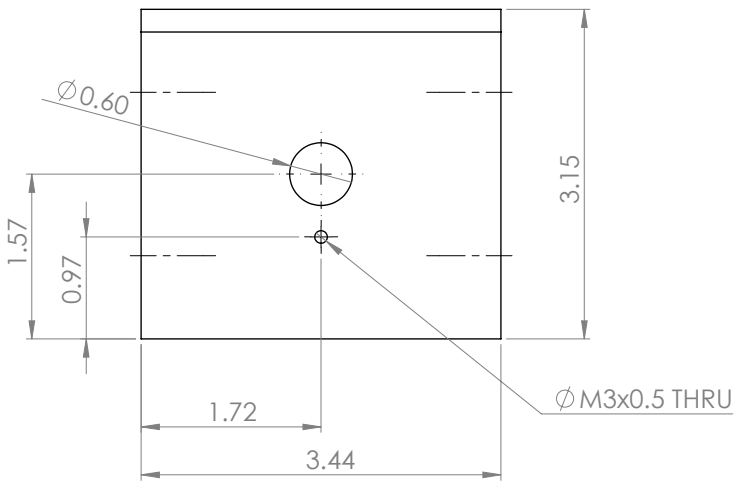
C

B

B

A

A



UNLESS OTHERWISE SPECIFIED:  
 DIMENSIONS ARE IN INCHES  
 SURFACE FINISH:  
 TOLERANCES:  
 LINEAR:  
 ANGULAR:



TERRAPIN ROCKET TEAM  
 UNIVERSITY OF MARYLAND

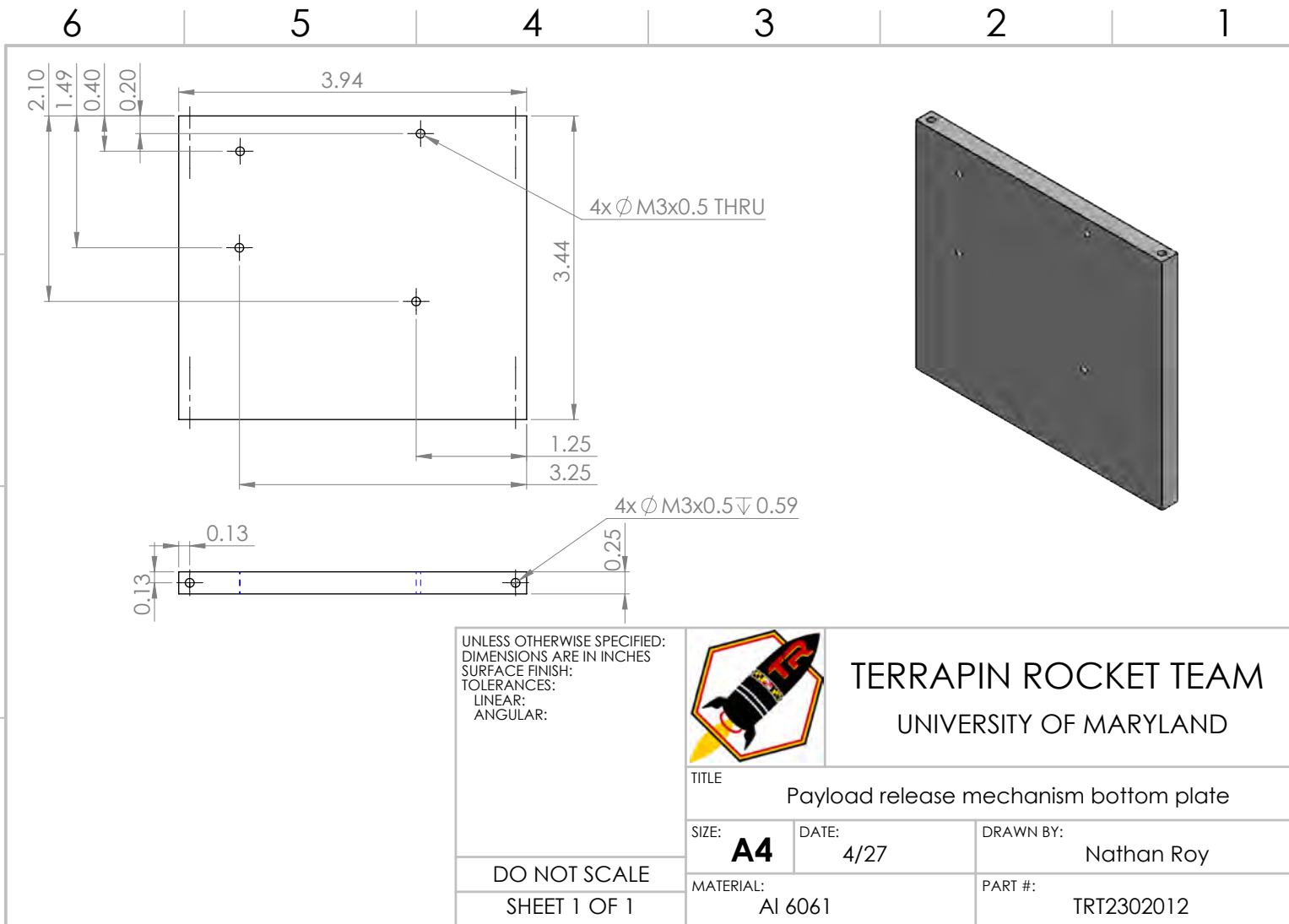
TITLE: Payload release mechanism lower back plate

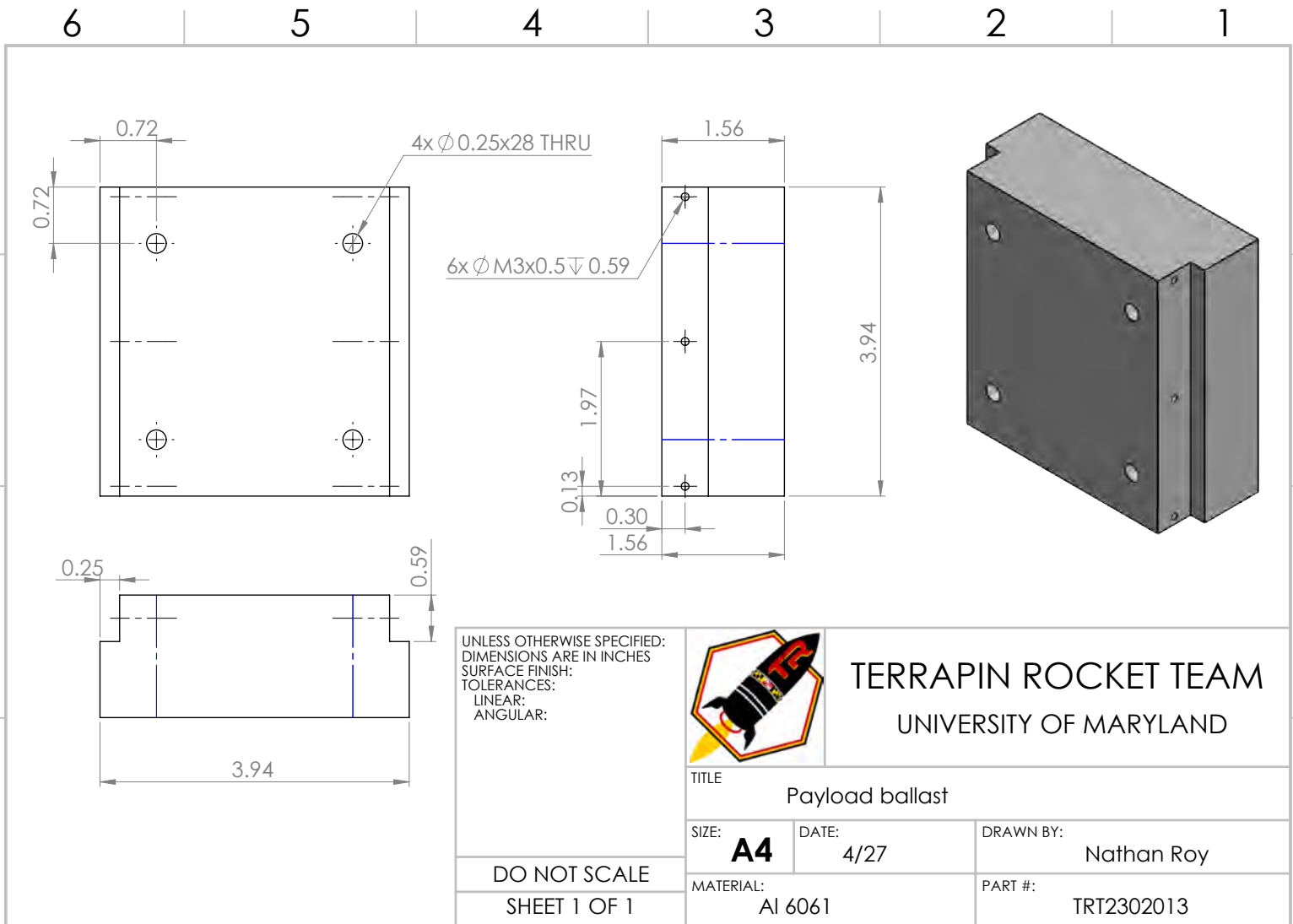
SIZE: **A4** DATE: 4/27 DRAWN BY: Nathan Roy

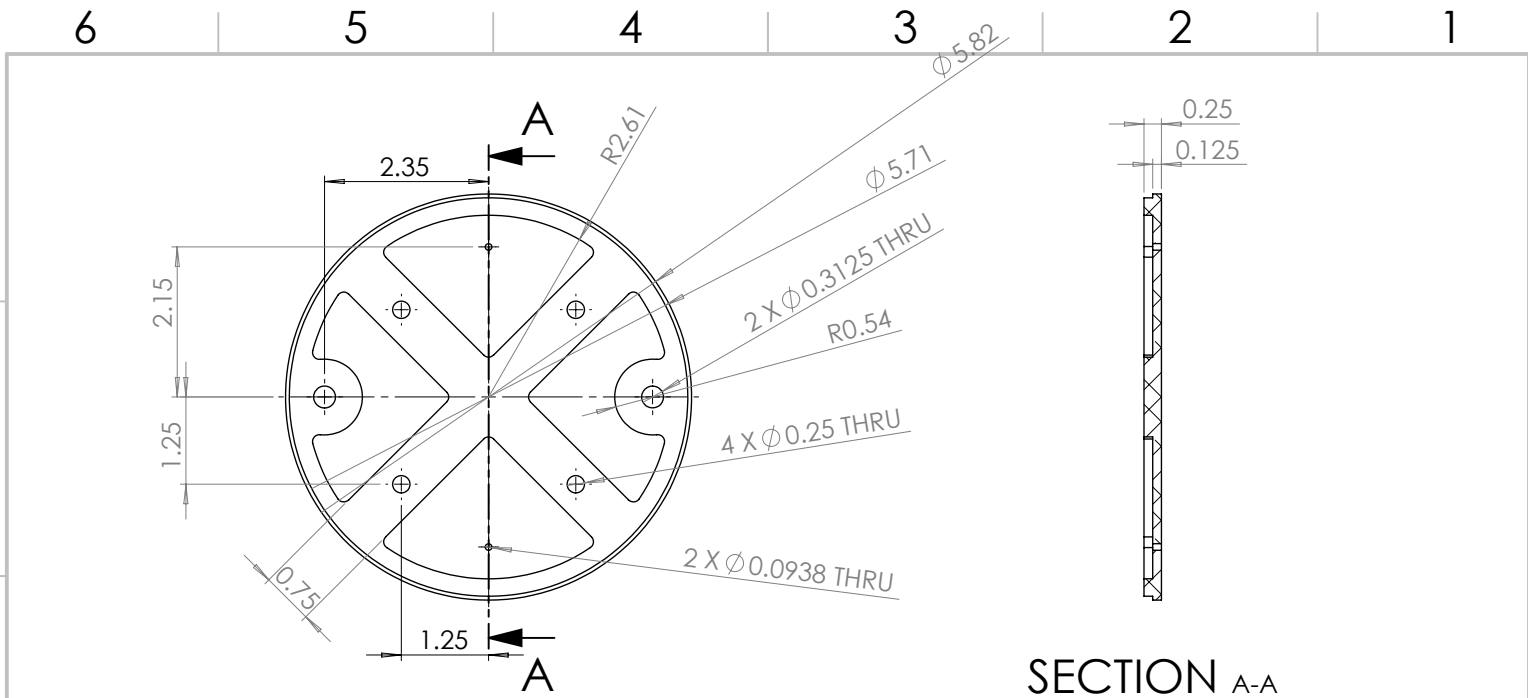
MATERIAL: Al 6061 PART #: TRT2302011

DO NOT SCALE  
 SHEET 1 OF 1

6 5 4 3 2 1







SECTION A-A

UNLESS OTHERWISE SPECIFIED:  
 DIMENSIONS ARE IN INCHES  
 SURFACE FINISH:  
 TOLERANCES:  
 LINEAR:  
 ANGULAR:



TERRAPIN ROCKET TEAM  
 UNIVERSITY OF MARYLAND

TITLE		
Payload Electronics Bay Forward Bulkhead		
SIZE:	DATE:	DRAWN BY:
<b>A4</b>	5/13/2023	Howard Zheng
MATERIAL:		PART #:
Aluminum 6061-T6		N/A

DO NOT SCALE  
 SHEET 1 OF 1

6 5 4 3 2 1

D

D

C

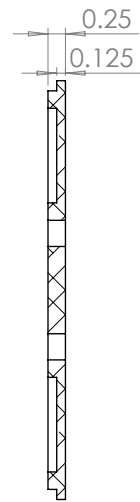
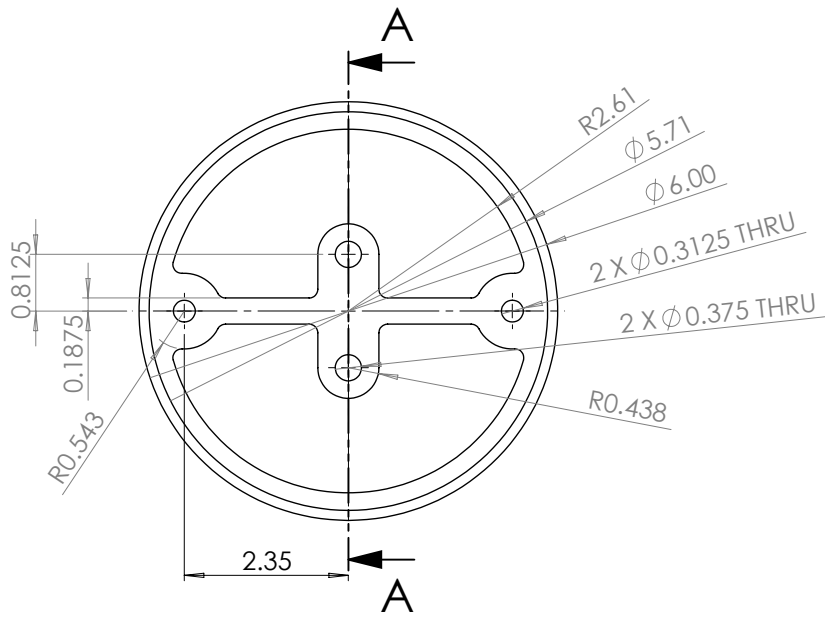
C

B

B

A

A



SECTION A-A

UNLESS OTHERWISE SPECIFIED:  
 DIMENSIONS ARE IN INCHES  
 SURFACE FINISH:  
 TOLERANCES:  
 LINEAR:  
 ANGULAR:



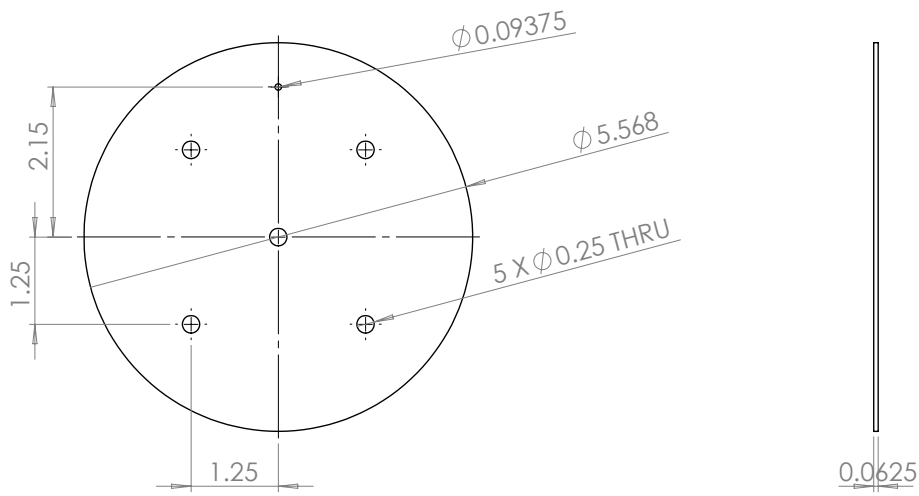
TERRAPIN ROCKET TEAM  
 UNIVERSITY OF MARYLAND

TITLE		
Payload Electronics Bay Aft Bulkhead		
SIZE:	DATE:	DRAWN BY:
<b>A4</b>	5/13/2023	Howard Zheng
MATERIAL:		PART #:
Aluminum 6061-T6		N/A

DO NOT SCALE  
 SHEET 1 OF 1

6 5 4 3 2 1

6 5 4 3 2 1



UNLESS OTHERWISE SPECIFIED:  
 DIMENSIONS ARE IN INCHES  
 SURFACE FINISH:  
 TOLERANCES:  
 LINEAR:  
 ANGULAR:



TERRAPIN ROCKET TEAM  
 UNIVERSITY OF MARYLAND

TITLE  
 Nosecone Bulkhead

SIZE: **A4**      DATE: 5/13/2023      DRAWN BY: Howard Zheng

MATERIAL: Aluminum 6061-T6      PART #: N/A

DO NOT SCALE  
 SHEET 1 OF 1

6 5 4 3 2 1

## Acknowledgments

This year would not have been possible without the support of our mentors, advisors, and donors. We have accomplished so much this year because of their generous support. First, we would like to thank our Tripoli Mentor Dennis Kingsley as well as the Maryland Delaware Rocketry Association (MDRA). Dennis has been working with us as our mentor for three years and has shared a great amount of experience with us. We'd also like to thank our solid propulsion mentor Scott Szympruch. He has provided lots of valuable advice, mixing facilities, and testing equipment for the team which has helped jumpstart our propulsion program. MDRA has been our primary launch site and our test flights would not have been possible without such a great organization and members close by. We'd also like to thank our faculty advisor Dr. Christopher Cadou as well as Dr. David Akin for their helpful reviews of our project.

We would like to thank the Maryland Space Grant Consortium for their generous donation. Their grant has supported the construction of *Karkinos* as well as our mission to create an inclusive environment for underrepresented groups and women.

Additionally, we would like to thank our generous donors and sponsors this year. The A. James Clark School of Engineering, The University of Maryland Student Government Association, The Maryland Robotics Center, Boeing, Northrop Grumman, Kratos Space and Missile Defense Systems, Inc., Blue Origin, and LaunchUMD supporters have all been critical in our successes this year. We would like to thank the team at Glenn Martin Wind Tunnel who allowed us to use their facility to test our Air Brake system in their wind tunnel.

## References

- [1] Rogers, C., "The Solid Rocket Motor - Part 6 Erosive Burning Design Criteria for High Power and Experimental/Amateur Solid Rocket Motors," 2005, pp. 33–34. URL <http://rasaero.com/dloads/Erosive%20Burning%20Design%20Criteria.pdf>.
- [2] "SkyAngle CERT-3™ Series," , 2023. URL <http://www.b2rocketry.com/Cert-3.htm>.
- [3] "Kevlar 3/8" Thick," , 2023. URL <https://macperformancerocketry.com/collections/tubular-kevlar/products/copy-of-top-flight-recovery-chute-harness-protectors>.
- [4] "7/16" Tubular Kevlar Booster Harness W/ 3 Sewn Loops," , 2023. URL <https://onebadhawk.com/716-tubular-kevlar--3-loop.html>.
- [5] "1/4" Eyenut," , 2023. URL <https://www.westmarine.com/wichard-1-4inch-stock-dia.-eye-nut-1-2inch-hole-dia.-1-4inch-20-thread-dia.-3750lb.-breaking-load-285199.html>.
- [6] "1/4" quicklink," , 2023. URL <https://www.mcmaster.com/3711T34/>.
- [7] "5/16" quicklink," , 2023. URL <https://www.mcmaster.com/8947T17/>.
- [8] "304 Stainless Steel U-Bolt," , 2023. URL <https://www.mcmaster.com/8896T77/>.
- [9] Becker, A., "Kalman Filter Tutorial," , 2023. URL <https://www.kalmanfilter.net/multiExamples.html>.
- [10] Unknown, "Euler Angle Formulas," , 1999. URL <https://www.geometrictools.com/Documentation/EulerAngles.pdf>.
- [11] Dellicker, S., Benney, R., LeMoine, D., Brown, G., Gilles, B., and Howard, R., *Steering a Flat Circular Parachute - They Said It Couldn't Be Done*, 2012. <https://doi.org/10.2514/6.2003-2101>, URL <https://arc.aiaa.org/doi/abs/10.2514/6.2003-2101>.